Addis Ababa University

Addis Ababa Institute of Technology

School of Graduate Studies

PhD Dissertation on:

Water Resource System Modeling and Hydro-economic Trade-off Analysis of Abbay River Basin, Ethiopia

BY:

Andargachew Melke Alemu

Supervisor:

Yilma Seleshi (Professor)

August 30, 2024
Addis Ababa, Ethiopia

DOCTORAL DISSERTATION APPROVAL SHEET

Addis Ababa University

Addis Ababa Institute of Technology

School of Civil and Environmental Engineering

This is to certify that the dissertation presented by Andargachew Melke entitled, **Water Resource System Modeling and Hydro-economic Trade-off Analysis of Abbay River Basin, Ethiopia**, and submitted in partial fulfillment of the requirements for the degree of Doctor of Philosophy in Civil Engineering (Hydraulic Engineering) complies with the regulation of the university and meets the accepted standards.

WATER RESOURCE SYSTEM MODELING AND HYDRO-ECONOMIC TRADE-OFF ANALYSIS OF ABBAY RIVER BASIN, ETHIOPIA

By:

Andargachew Melke _____ /_____/____/_____/

date

APPROVED BY BOARD OF EXAMINERS:

Proff. Yilma Seleshi _____ /_____/____/_____/

(Supervisor) date

Dr. Semu Ayalew _____ /_____/____/____/

(External Examiner) date

Dr. Belete Birhanu _____ /_____/____/____/

(Internal Examiner) date

Dr. Abraham Gebre _____ /_____/____/____/

(Dean, SCEE) date

_____ _____ /_____/____/____/

Chairperson date

Water Resource System Modeling and Hydro-economic Trade-off Analysis of Abbay River Basin, Ethiopia

By:

Andargachew Melke Alemu

Supervisor:

Yilma Seleshi (Professor)

(Professor of Water Resource Engineering)

A Dissertation Submitted to Graduate School of Addis Ababa University, Addis Ababa Institute of Technology, School of Civil and Environmental Engineering in partial fulfilment of the requirement for the degree of Doctor of Philosophy in Civil Engineering (Hydraulic Engineering).

August 30, 2024

Addis Ababa, Ethiopia

Declaration

By submitting this dissertation, I declare that the entirety of the work contained herein is my own, original work, that I am the sole author. The work contains no material that has been accepted for the award of any other degree or master in any university and, to the best of my knowledge and belief, contains no material previously published or written by another person, except where due reference has been made in the text. The reproduction and publication thereof by Addis Ababa University will not infringe to my knowledge any third party right and so that I have not previously in its entirety or in part submitted it for obtaining any qualification.

Andargachew Melke Alemu

Name of author Signature Date

Dedication

I dedicate this dissertation to my family, next to the Almighty God, the Virgin Mary, and the Holly Sprits, without whom I could not have written this chapter of my life.

Abstract

This study was aimed at analyzing the hydro-economic trade-off and synergy between water, hydropower, and irrigation in the Abbay River basin by considering multiple development scenarios. The study scoped in assessing the water potential of the basin and analyzing the trade-off and hydro-economic benefit between irrigation development and hydropower generation.

Multi-statistical performance criteria proved that the ArcSWAT model has the capacity to reproduce flows that agree with the measured flows and was found to be applicable over the Abbay River basin. The result revealed that the performance of the model improved as the basin was partitioned into sub-basins. The evaluation of different flow segments showed that the ArcSWAT model performed better for peak and high flows than mid and low flows. Overall, the model generates flow data that closely matches the measured flows in the Abbay River basin, which can be utilized as inputs to assess the trade-offs between hydropower and irrigation development.

The hydro-economic trade-off analysis was undertaken to provide insight regarding the benefits received from hydropower and irrigation development scenarios. The research demonstrated the holistic development of water resources for both energy generation and irrigation purposes, thereby maximizing economic benefits while ensuring sustainable water resource management. HEC-ResSim model was found to be adequate for evaluating the power generating capacity of multiple hydropower cascade systems under various irrigation water diversion scenarios. The findings revealed that by focusing solely on hydropower projects without incorporating irrigation development, the Abbay river basin would generate up to 38 TWh of annual energy from GERD, Karadobi, Bekoabo, and Mandaya cascades, with GERD accounting for 39% of the total output. Under full integration of irrigation development with four hydropower cascades, annual system energy generation was reduced by 12%.

The hydro-economic trade-offs between hydropower generation and irrigation development within the Abbay River basin. By analyzing various development scenarios, the study reveals how prioritizing one objective, either hydropower or irrigation, impacts the overall economic benefits. A key reference point is the absence of irrigation development, which serves as a baseline to assess the benefits of different scenarios.

The results demonstrate that as irrigation benefits increase, hydropower benefits decrease, and vice versa. For instance, with no irrigation development, annual benefits from a series of cascade hydropower projects range from $1.3 billion to $3.1 billion USD, depending on the number of projects.

However, expanding irrigation reduces hydropower benefits by approximately 5% for every unit increase in irrigation benefits.

When full irrigation development is achieved, annual irrigation benefits reach $3.6 billion USD, surpassing hydropower benefits by 17%. The analysis highlights that while trade-offs exist, pursuing both hydropower and irrigation concurrently results in greater combined benefits than focusing on either objective alone. The study concludes that integrated development of hydropower and irrigation within the Abbay River basin yields optimal economic outcomes, with combined annual benefits reaching nearly $6 billion USD, 94% higher than those from hydropower alone.

Assessing the long-term economic benefits of hydropower and irrigation development in the Abbay River basin, taking into account the variability in returns over time was another basic points addressed in this research. Four scenarios are explored, each involving different combinations of dams (GERD, Karadobi, Bekoabo, and Mandaya) and a consistent irrigation area of 1.2 million hectares.

The analysis shows a clear upward trend in economic benefits over time. Scenario 1, which includes only the GERD and 1.2 million hectares of irrigation, generates a present benefit of $4.5 billion USD, projected to rise to $26 billion USD by 2050. Scenarios with additional dams show progressively higher future benefits, with Scenario 4, incorporating all four dams and 1.2 million hectares of irrigation, yielding the highest returns of $34 billion USD by 2050.

The study underscores that while present economic benefits are modest, substantial gains are realized in the long term, particularly as more dams are added to the development plan. The findings suggest that comprehensive development of hydropower and irrigation in the Abbay River basin offers significant economic advantages, especially in the long run, with the full cascade of dams providing the greatest benefits. The study also revealed that simultaneous development of hydropower and irrigation is advisable rather than prioritizing hydropower projects exclusively over the Abbay River basin.

Key Words: Abbay River, Trade-off, hydro-economic, Water potential

List of Publication

- *Alemu, A. M., Seleshi, Y., & Meshesha, T. W., 2022. Modeling the spatial and temporal availability of water resources potential over Abbay river basin, Ethiopia. Journal of Hydrology: Regional Studies, 44, 101280. https://doi.org/10.1016/j.ejrh.2022.101280*

- *Alemu, A. M., & Seleshi, Y., 2024. Trade-off and synergy analysis between hydropower generation and irrigation development in the Abbay River Basin, Ethiopia. Journal of Hydrology: Regional Studies, 52, 101723. https://doi.org/10.1016/j.ejrh.2024.101723*

Acknowledgment

First and foremost, I want to thank God the Father, God the Son, and God the Holy Spirit for their love, grace, and unity throughout my life, which has enabled me to fulfil the objectives I established. I'd also like to thank Saint Merry, Holy Angels, Saints, and monks for their assistance throughout my life and for providing me with the fortitude, resources, and blessings I needed to finish my Ph.D. dissertation.

I am grateful to all my family members: my parents, brothers and sisters, and family members for their never-ending motivation and magnificent blessings.

I sincerely appreciate the inspiration, knowledgeable direction, patience, and support provided by my supervisors: Yilma Seleshi (Professor).

I want to express my sincere gratitude to the civil and environmental engineering faculty and staff of AAIT, Addis Ababa University, for their seamless support of my PhD. works throughout my study term. I would also want to express my gratitude to the Ethiopian National Meteorological Agency, the Ethiopian Ministry of Water and Energy, and Abbay Basin Authority, Eastern Nile Technical Regional Office, Ethiopian Meteorological agency for their kind assistance in providing data.

Last but not least, I'd like to take this opportunity to thank everyone who helped me finish this Ph.D. thesis.

Contents

List of Figures

List of Tables

List of Acronyms

ABA	Abbay Basin Authority
BCEOM	Bureau Central d'Etudes pour les Equipements d'Outre-Mer
BCM	Billion Cubic Meter
CK	Co-Kriging
DEM	Digital elevation Model
DSS	Decision support system
ENB	Eastern Nile Basin
FSL	Full Supply Level
EEPCO	Ethiopian Electric Power Corporation
ENTRO	Easter Nile Technical Regional Office
FDC	Flow Duration Curve
GERD	Grand Renaissance Dam
GIS	Geographic Information System
GWh	Giga watt hour
HEC-ResSim	Hydrologic Engineering Center-Reservoir Simulation
IDW	Inverse Distance Weighting
LULC	Land Use Land Cover
m.a.s.l	Meter Above Sea Level
MOL	Minimum Operation Level
MoWE	Ministry of water and energy
MW	Mega Watt
NBI	Nile basin Initiative
NSE	Nash-Sutcliff Efficiency
OK	Ordinary Kriging

PET	Potential Evapotranspiration
RMSE	Root Mean Square Error
SI	Seasonality Index
SWAT	Soil Water assessment Tool
TWh	Tera watt hour
UBNB	Upper Blue Nile Basin
WMO	World Metrology Organization

1. Introduction

1.1. Background of the study

Fresh water is essential for human well-being and social-economic sustainability (Yuan et al., 2016), the basis for life in terrestrial and freshwater ecosystems (Jackson et al., 2001). Quantifying the spatial and temporal availability of water potential is the most important objective for hydrologists (Gholamabbas et al., 2015). The demand for fresh water correlates with population growth, economic development, and changing the living habits of people. Water scarcity emerges from a combination of hydrological variability and high human use (WWAP 2016), and the imbalance between supply and demand of water resources not only restricts the balance of the ecosystem but also affects sustainable socio-economic development (Zhang et al., 2022). Modeling the spatial and temporal water resource potential and its variation is crucial for providing the strategic information needed for long-term planning, developing, managing, and utilizing the available potential in sustainable ways (Etefa, 2012). It is also vital to partly overcome problems due to data scarcity in the basin (Gebiyaw et al., 2021) since the spatial and temporal detailed information on freshwater availability is so far limited, especially for Africa (Schuol et al., 2008).

Concerns about environmental sustainability, poverty reduction, and rising inequitable utilization of resources are pressing issues that require attention and action (Siderius et al., 2022). Sustainable management of food, energy, and water (FEW) systems is crucial for human development and addressing the needs of a growing population (Torhan et al., 2022). In recent years, there has been significant attention given to the interaction between water availability, hydropower, and irrigation. Understanding and managing the complex interactions among these resource systems is essential for ensuring sustainable and efficient water use (Albrecht et al., 2018).

Hydropower production and irrigation development are intrinsically linked and have a significant influence on each other. Their interrelation is crucial for achieving sustainable economic development while meeting growing socioeconomic demands (Bazilian et al., 2011; Nhamo et al., 2018). Factors such as rising population, rapid urbanization, changing diets, and economic growth have led to an increased demand for energy and food, with significant implications for the

economy, environment, and well-being of communities. Without systemic management strategies, water resources may struggle to meet the increasing demand (Bassel and Rabi, 2015).

In Ethiopia, there is a focus on developing irrigation and hydropower in the Abbay River basin to address the demand for food and energy and promote sustainable development. The Abbay river basin, contributing more than 60% to the entire Nile flow (World Bank, 2006), is a potential water resource for Ethiopia, making it a potential basin for hydropower generation and irrigated agriculture (Mulat et al., 2018; Goor et al., 2010). Developing sustainable irrigation systems in Ethiopia, where salinity is not a major challenge, can enhance agricultural productivity and food security by providing a consistent water supply for irrigation purposes. This can lead to increased crop yields and income, contributing to poverty reduction. Harnessing the hydropower potential of the Abbay River can also generate clean and renewable energy, reducing reliance on fossil fuels and mitigating climate change. The generated energy will be accessible to the region that will earn foreign currency for Ethiopia, contributing to economic growth.

However, allocating water to different uses involves trade-offs between the benefits perceived (Hurford et al., 2014). Several research studies have been undertaken in the Nile Basin, addressing various aspects such as the assessment of irrigation expansion in the Abbay basin's impact on downstream flows (Allam and Eltahir, 2019), system performance evaluation (Geressu & Harou, 2015), evaluation of multi-storage hydropower development (Mulat et al., 2018), and the effects of large-scale multipurpose dam cascades on the downstream areas of the Eastern Nile river system (Tahani et al., 2014). Economic analyses of large-scale upstream river basins have been conducted by Paul and Kenneth (2010), along with studies on the optimal operation of multipurpose multi-reservoir systems, hydro-economic optimization of the Eastern Nile system (Goor et al., 2010; Digna et al., 2018), and sustainable reservoir management (Befekadu et al., 2015). Other research has explored the impact of upstream hydropower and irrigation development on downstream water availability (Murgatroyd et al., 2023) and simulation of water, energy, and food production (Tan et al., 2017). Despite these previous research efforts, there exists a gap in addressing the comprehensive consideration of full hydropower projects and potential irrigation development in the Abbay river basin.

1.2. Statement of the problem

The Abbay River basin is currently experiencing rapid demographic and economic development, leading to increased demands for food and energy. Several research studies have been conducted on the Abbay river basin related to hydrological processes and spatial distribution of the hydrological components (Gebiyaw et al. (2021), Tatenda et al. (2018), water budget (Abera et al., 2017), effects of climate change on water resources (Malede et al., 2022, Daniel et al., 2021, Vincent et al., 2018, Sintayehu and Fulco, 2015, etc.), evaluation of the expansion of irrigation over upper Blue Nile basin on down stream flows (Allam and Eltahir, 2019), evaluation of system performance (Geressu & Harou, 2015), multi-storage hydropower development (Mulat et al., 2018), impact of large scale multipurpose cascading of dams on downstream parts of the Eastern Nile river system (Tahani et al., 2014), economic analysis of large-scale upstream River basin (Paul and Kenneth, 2010), optimal operation of a multipurpose multi-reservoir system (Goor et al., 2010, Reem et al., 2018), sustainable management of reservoirs (Befekadu et al., 2015), impact of upstream hydropower and irrigation development on downstream water availability (Murgatroyd et al., 2023), modeling and simulation of water, energy and food production (Tan et al., 2017), hydro-economic optimization of the eastern Nile system (Digna et al., 2018) were among others.

The Abbay River Basin, a vital water resource in Ethiopia, plays a critical role in the country's socio-economic development, supporting hydropower generation, irrigation, and other water-dependent activities. However, the increasing demand for water due to population growth, agricultural expansion, and the development of hydropower projects has led to intensified competition for water resources. This competition has the potential to create significant trade-offs between various water uses, potentially leading to conflicts among stakeholders and unsustainable water management practices.

Despite the critical importance of the Abbay River Basin, the review of previous research indicated the gap in the research concerning the comprehensive assessment of hydro-economic trade-offs and synergy among water usage, hydropower generation, and irrigation, particularly within the context of the Abbay River basin. As a result, there is a need for a holistic approach that can inform more balanced and sustainable water resource management in the basin.

This research seeks to address these gaps by developing a water resource system model for the Abbay River Basin that integrates hydrological and hydro-economic analysis. The model was used to conduct a hydro-economic trade-off analysis, providing insights into the potential synergies and conflicts between different water uses. The ultimate goal is to inform policy and decision-making processes, ensuring that water resources in the Abbay River Basin are managed in a way that maximizes socio-economic benefits from hydropower and irrigation development.

1.2.1. General objective

The general objective of this study was to analyze the hydro-economic trade-off and synergy between water, hydropower and irrigation in the Abbay River basin by considering multiple development scenarios.

1.2.2. Specific objectives

This study aimed to achieve the following specific objectives.

- Modeling the spatial and temporal availability of water resources potential over Abbay river basin
- Trade-off and synergy analysis between hydropower generation and irrigation development in the Abbay River Basin
- Analyzing the hydro-economic trade-off between hydropower and irrigation with multiple development scenarios

1.3. Research questions

Based on the stated problems, this research expected to address the following research question

- How the implementation of new hydropower project affects the existed system-wide and individual energy generation capacity and system storage?
- How irrigation water withdraw affects the system-wide and individual energy generation capacity, system storage and reservoir operation?
- Which development alternative is better to maximize the benefit? Hydropower only? Combination of hydropower and irrigation?

1.4. Scope of the Study

This research aims to establish a foundation for sustainable water resource management, planning, and development. It involves analyzing water balance dynamics across different spatial and temporal scales within the Abbay river basin. The study further aims to create scenarios based on reservoir cascades for power generation and irrigation water withdrawal. Through this analysis, the study seeks to provide insights for informed decision-making regarding water resource management, efficient allocation strategies, and sustainable utilization of available water resources.

The scope of the research primarily focuses on conducting a comprehensive analysis of the trade-offs and synergies between hydropower generation and irrigation within the Abbay river basin. This involves utilizing a combination of hydrological modeling tools, such as ArcSWAT, to quantify the basin's water resource potential and HEC-ResSim to simulate power generation and reservoir operations under various development scenarios.

1.5. Organization of the dissertation

This dissertation paper comprises seven chapters, with the introduction serving as the first chapter and the concluding chapter as the final one. The structure follows a sequential flow mirroring the research journey, connecting the introduction, main body, and conclusion. Each chapter presents techniques, analysis, and results, except for chapters two and three, which stand independently as a comprehensive literature review and study area description, respectively. Additionally, every chapter concludes with its own remarks.

Chapter 1. Introduction

This section covered the general description and narration of water resource modeling and trade-off analysis. The introduction part also included the problem description, research objectives, research questions, work scope, and organization of the research paper.

Chapter 2. State-of-the-art literature review

This chapter covered reviewing previous research done in the Abbay river basin and identifying the potential gap. Moreover, the different hydrological modeling tools and reservoir operation simulation mechanisms were discussed in detail.

Chapter 3. Materials and Methods

In this chapter, the general description of the area, including the location, topography, land use type, soil type, hydro-meteorological characteristics, and slope classes, was included. The methodologies to achieve each specific objective was described in detail

Chapter 4: Result and discussion

This chapter covered the spatio-temporal availability and variability of water resource potential using a physically based hydrological model. The availability and spatial variability of water balance components were modeled for each sub-basin of the Abbay River basin. The modeled water potential was then used as input to analyse the second and third specific objectives.

The other major objectives dealt in this section was the evaluation of the trade-off and synergy between hydropower and irrigation under various development scenarios. The hydro-economic analysis was undertaken to provide insight regarding the benefits received from hydropower and irrigation development scenarios.

Chapter 5: Conclusion and Recommendations

This is the end part of the research paper focused on giving a summarized conclusion of the overall research results and giving recommendations for further research on the Abbay river basin.

2. Literature Review

2.1. Pervious research work and research gaps

Reservoir operation decisions often require balancing among objective bundles including hydropower generation, irrigation, water supply reliability, recreation, environmental flows, and flood control (Jose et al., 2016). Over the Nile River, numerous studies regarding modeling of the water resources system, reservoir operation, and hydrology have been made. Allam and Eltahir (2019) present a framework for optimal allocation of land and water resources in the upper Blue Nile (UBN) basin, which consists of two optimization models that aim to: (a) allocate land and water resources optimally to rain-fed and irrigated agriculture, and (b) allocate water to agriculture and hydropower production while maximizing the total net benefits. They consider eleven potential irrigation reservoirs identified from the Ethiopian master plan and the GERD hydropower plant for the optimization model. Trade-offs between agricultural expansion and hydropower generation were analyzed. The result revealed that the optimal agricultural expansion is expected to reduce the UBN flow by about 7.6 cubic kilometers, impacting the downstream countries Egypt and Sudan. Although large irrigation areas are considered in this research, from the side of the hydropower plant only GERD is considered, yet other proposed hydropower plants exist.

Multi-reservoir system design should consider the potential for coordinated operation of reservoirs. Geressu & Harou (2015) optimized the proposed upstream Blue Nile multi-reservoir system design considering Ethiopian hydropower and storage size of reservoirs using many objective evolutionary optimization techniques. They evaluated the proposed Blue Nile River reservoirs in Ethiopia with the objectives of minimizing the storage size of new infrastructures, maximizing firm monthly and average annual energy generation from the proposed dams, maximizing energy generation, and minimizing the water supply deficit for irrigation served by the existing two reservoir systems in Sudan. They found that a 4-reservoir system of GERD, Upper Mandaya, Karadobi, and Beko Abo Low achieves the highest average annual energy generation capacity of more than 39 TWh/yr, and Mandaya and GERD operated for firm energy and Upper Mandaya operated to maximize annual energy, which is most favorable to Sudanese system performance. This research tried to optimize the proposed hydropower plant with the perspective of firm and annual average energy generation and impacts to Sudan's energy and irrigation system

performance. The irrigation development with the Ethiopian part of the Blue Nile (Abbay Basin) and its trade-off with hydropower development are not included.

Mulat et al. (2018) evaluated the multi-storage hydropower development in the upper Blue Nile River (Ethiopia) to understand the future water development perspective in the Eastern Nile region by considering the current water use situation and proposed reservoirs in the upper Blue Nile (Abbay) River basin in Ethiopia using a simulation approach. The study was an indicative analysis of the potential benefit of upstream Nile development without significantly affecting existing development in the Nile Basin. The overall energy gain in the Eastern Nile region increases up to 258% due to the development of proposed hydropower reservoirs on the Ethiopian Blue Nile (Abbay). Moreover, the study result indicates that the regulation capacity of the reservoirs located in Ethiopia would increase irrigation water availability in Sudan. However, the implemented and proposed irrigation projects in Abbay River Basin are not considered in this research. Moreover, the author recommended further detail study by considering all proposed and implemented small and medium irrigation and water abstraction projects in the Abbay River basin. Ahmed (2012) simulated eastern Nile water resources using the HEC-ResSim model mainly to examine the impact of large-scale multipurpose cascading of dams on downstream parts of the Eastern Nile River system. Scenarios are considered to assess the availability of water in the basin at each of the source nodes and to evaluate the cascades on the downstream reservoir, considering all reservoirs proposed in the upper Blue Nile River, excluding all the existing and proposed irrigation areas and dams.

Tahani et al. (2014), in their study, Downstream Impact of Blue Nile Basin Development, assess the positive and negative impacts of Blue Nile projects on both national and regional levels to reach an optimal solution for an integrated development of the subbasin while minimizing the negative impact on the basin level downstream. The model simulations' results were assessed under different scenarios: baseline, Blue Nile projects (hydropower only), Blue Nile projects (irrigation only), Blue Nile projects (irrigation and hydropower), Equatorial Lakes' projects plus Baro-Akobo-Sobat plus Blue Nile projects (irrigation and hydropower). They applied a Mike Basin model to simulate the Nile Basin and Nile Basin Decision Support System (NBDSS) as a tool to evaluate scenarios based on the quantification of economic, environmental, and social indicators. The study showed that hydropower development in the Blue Nile is the best alternative

economically on the Blue Nile sub-basin level and downstream, while the baseline (current situation) is the best option for both social and environmental stakeholders in the Blue Nile. However, optimization exercise was not applied in this study, and they recommended that future studies include the application of optimization. Moreover, from the Ethiopian part of the Blue Nile basin, only the Grand Ethiopian Renaissance Dam (GERD), Mandaya Dam, and irrigation projects in Dinder, Tana Beles, and Anger-Didessa-Fincha sub-basins were considered, though additional proposed hydropower (e.g., Kara-dobi and Beko Abo) and irrigation projects exist.

Paul and Kenneth (2010) studied the economic analysis of large-scale upstream River basin development on the Blue Nile in Ethiopia, considering the transient, staggering, and implications of stochastic modeling of variable climate and climate change. The study focused on constructing and evaluating findings from a model able to assess the influence of the transient and long-term periods of the proposed development under varying economic, flow policy, construction, and climatic conditions. They applied the Investment Model for Planning Ethiopian Nile Development (IMPEND) model written with the General Algebraic Modeling System Software General Algebraic Modeling System (GAMS). The model encompasses the Blue Nile River from its inception at Lake Tana to the Rosaries Dam, just beyond the Sudan-Ethiopian border. Two transient scenarios are examined: (1) no stagger (dams are built simultaneously over a 7-year period with reservoirs initially full) and (2) stagger (dams built sequentially in 7-year increments) with reservoirs initially empty. The first scenario describes the situation in which all dams are immediately on-line and producing hydropower by ignoring the transient stage. The second scenario describes a more realistic approach, staggering construction due to financial constraints, and accounting for the filling stages of each reservoir. Three SRES scenarios (B2 from ECHam4, A2 from CGCM2, and the median case B2 from DOE PCM) are fully considered in this study.

For the hydropower and irrigation development projects specified, model results disregarding transient and construction stagger aspects demonstrate overestimations of $6 billion in benefits and 170% in downstream flows compared to model results accounting for these aspects. Benefit-cost ratios for models accounting for transient conditions and climate variability are found to range from 1.2–1.8 under historical climate regimes for the stream flow retention policies evaluated. The study mainly focused on the benefit-cost ratios under transient conditions, climate variability, and climate change and extended to Rosaries, which is not part of the Abbay basin. Irrigation

development in the Abbay basin is not considered. Moreover, the quantitative analysis of trade-offs between hydropower and irrigation development over the Abbay basin was not included, though it is essential for basin planning.

Goor et al. (2010) undertook research on optimal operation of a multipurpose multi-reservoir system in the Eastern Nile River Basin to examine the (re-)operation of infrastructures, in particular the proposed reservoirs in Ethiopia and the High Aswan Dam, and assess the economic benefits and costs associated with the storage infrastructures in Ethiopia and their spatial and temporal distribution. Stochastic dual dynamic programming was applied considering the hydrological uncertainty on management decisions and allocation policies. The analysis focused on two economic sectors: irrigation and hydropower generation. Four scenarios correspond to the current situation (baseline scenario), the most likely infrastructure to be built on the Blue Nile (Mandaya reservoir and hydropower plant), and full development of the basin was developed. The regulation capacity in Ethiopia was also considered. They revealed that building large new infrastructures in the upper part of the basin would have significant impacts on the operating strategies of the reservoirs. Due to the development of new infrastructure, the flood peak observed in the Blue Nile would be reduced while the low flows would be augmented. The main beneficiaries are hydropower in Ethiopia (production of hydroelectricity is boosted by 40 TWh) and irrigation in Sudan. Moreover, upstream storage in Ethiopia (and their regulation capacity) will generate positive externalities in Ethiopia and Sudan. In Sudan, the regulation capacity would increase irrigation water withdrawals by 5.5%. Due to new hydropower in Ethiopia and irrigation in Sudan, the annual basin-wide benefit increases by 3.48 billion US$ (for full development scenario of Ethiopian Blue Nile) and 1.29 billion US$ (if Mandaya reservoir and hydropower plant are built). However, this research considers the previous feasibility reports. For example, the border hydropower plant installed capacity is 1400 MW, which is 6000 MW currently. Moreover, the research focused on the hydropower potential of Ethiopian Blue Nile and its contribution for basin-wide benefits, yet there are potential irrigable lands over Ethiopian Blue Nile that are not considered in this study.

Befekadu et al. (2015) examined the potential for mutually beneficial and sustainable benefit sharing measures from the development and operation of the Grand Ethiopian Renaissance Dam while protecting baseline flows to the downstream countries, including flows into the Egyptian

High Aswan Dam. The approaches mainly construct, apply, and interpret findings from an empirical hydro-economic model developed for and applied to the Nile Basin. A dynamic optimization framework in General Algebraic Modeling System (GAMS) was used to formulate the model. They also consider two climate scenarios (baseline scenario and dry scenario). The result of this research is mainly dependent on policy (with and without GERD dam) and climate scenario. Moreover, with GERD dam implementation, only one fifth of its capacity is filled. They found that for the agricultural sector, Ethiopia's use of predicted annual average water for irrigated agriculture from the Nile River decreases from 2.87 BCM (base scenario) to 2.12 BCM (dry scenario). For midstream countries (South Sudan and Sudan), the construction of the GERD dam and climate scenario have no effects on water availability for irrigation and hydropower, while for downstream countries (Egypt), the impact is significant due to climate scenarios but not affected by reservoir policy. In economic value, due to the construction of GERD, Ethiopia will lose $1,218 million every year on average and a total of $15,130 million over the forecast 20-year period from reductions in irrigated agriculture. Due to climate scenario, Egypt will lose on average $5,467 million every year to native water supply shortages. Still, the proposed hydropower plants and irrigation area over the Abbay basin are not included. Moreover, the research did not address how the loss of benefit from irrigation due to GERD is offset by hydropower benefits.

Reem et al. (2018), in their work, Optimal Operation of the Eastern Nile System Using Genetic Algorithm and Benefits Distribution of Water Resources Development, analyzed the optimal scenarios for water resources management in the Eastern Nile regarding hydropower generation and irrigation development. A deterministic hydro-economic optimization model for the Eastern Nile Basin (ENOM) was applied to assess the distribution of benefits between the riparian countries from the optimal operation of the system. Cooperative and non-cooperative management scenarios were considered. The results showed there is no trade-off between hydro-energy and irrigation at the basin level when they are managed cooperatively (a 260 million $/year increase in hydro-generation would reduce irrigation returns by only 1 million $/year). A clear trade-off is shown in the case of non-cooperative system management, and a 70 million $/year increase in hydro-generation would result in a 155 million $/year reduction of irrigation returns. According to Reem et al. (2018), irrigation is more sensitive to the non-cooperative management scenario than hydro-energy because most of the irrigation lies in downstream countries, Sudan, and Egypt. The

results encourage the riparian countries to cooperate, as the benefit would be more than pursuing the non-cooperation option.

However, in this research only GERD is considered from planned large-scale infrastructures in the Ethiopian part of the Blue Nile. Large infrastructure developments in Ethiopia were assumed to operate mainly for hydropower. Large irrigation developments on the main stem of the Blue Nile were not considered. Only the Tana-Beles irrigation scheme was considered. Though the research result encourages a cooperative management scenario, it indirectly discourages Ethiopia from using water for irrigation development. On the other hand, this research limited Sudan's share as per the 1959 agreement, which seems controversial to the cooperative management and utilization of the Nile water and current negotiations among riparian countries. Moreover, the economic value of water was considered uniform for all countries yet not true in the actual situation. Diane et al. (2014) assessed the hydrologic and economic risks faced by the hydropower and agricultural sectors in Sudan and Egypt when the GERD will be online. A basin-wide, integrated hydro-economic model was applied to link the hydrologic, economic, and institutional components of the river basin and identify optimal allocation decisions in order to maximize the aggregated basin-wide net benefits. Stochastic dual dynamic programming (SDDP) was employed to solve multipurpose, multi-reservoir operation problems with stochastic inflows. Four development and management scenarios were considered, i.e., three scenarios (S1, S2, and S4) are based on full cooperation of developments (coordinated operation of all basin infrastructure to optimize the total basin-wide economic benefits), and one scenario (S4) corresponds to a situation in which the GERD would be operated to maximize energy revenues in Ethiopia only (unilateral operation of the GERD), regardless of downstream water demands. Except for S1, which is the base scenario, in all other scenarios the GERD is assumed online. Moreover, the irrigation expansion in Sudan and Ethiopia (around Lake Tana) was considered only in S4. Their study result showed with increased storage in Ethiopia, Egypt, and Sudan, they can expect greater net benefits from irrigation and hydropower and can also gain through reduced flooding and droughts. The main benefits lie in the ability of the GERD to remove the hydrological uncertainty inherent during periods of low flow. The researcher also encourages full cooperation between the 3 basin countries to realize these benefits. Though full cooperation is encouraged, it is also recommended that intermediate levels of cooperation be assessed since the ideal situation of fully cooperative riparian countries has been elusive in the Nile basin and will likely be difficult to reach in many

international river basins. This research, like many other research as reviewed above, did not give attention for expansion of irrigation in Ethiopian part of Blue Nile.

Table 2-1: some of water resources modeling research over Nile basin and their gaps

No	Author	Research Title	Research gap
1	Alam and Eltahir, 2019	Water-Energy-Food Nexus Sustainability in the Upper Blue Nile (UBN) Basin.	Only GERD was considered though other proposed reservoirs exists.
2	Geressu & Harou, 2015	Screening reservoir systems by considering the efficient trade-offs-informing infrastructure investment decisions on the Blue Nile	Irrigation development with Ethiopian part of Blue Nile (Abbay river basin) and its trade-off with hydropower development was not considered
3	Mulat et al, 2018	Evaluation of multi-storage hydropower development in the upper Blue Nile River (Ethiopia)	Existed and proposed irrigation projects in Abbay river basin were not considered
4	Ahmed, 2010	Eastern Nile Water Resources Simulation	Existed and proposed irrigation projects in Abbay river basin were not considered
5	Tahani et al, 2014	Downstream Impact of Blue Nile Basin Development.	All proposed hydropower and Irrigation projects were not considered.

6	Paul and Kenneth, 2010	Economic Analysis of Large-Scale Upstream River Basin Development on the Blue Nile in Ethiopia	Irrigation developments in Abbay basin were not considered
7	Goor et al, 2010	Optimal operation of a multipurpose multi-reservoir system in the Eastern Nile River Basin	Potential irrigable land on Ethiopian Blue Nile was not considered
8	Befekadu et al, 2015	Mutually beneficial and sustainable management of Ethiopian and Egyptian dams in the Nile Basin	Proposed hydropower plants and irrigation projects were not considered

2.2. Water Resources System Modeling

The basic concept of a system is that it relates two or more things. Out of the several definitions of a system, the simplest one states that it is a device that accepts one or more inputs and generates one or more outputs. The system can be classified as simple or complex. A simple system is one in which there is a direct relation between the input and the output of the system. A complex system is a combination of several sub-systems, each of which is a simple system. Therefore, a complex system may be subdivided into several simple systems. Each subsystem has a distinct relation between input and output. For example, a river basin system is a complex system comprising several subsystems (Vedula and Mujumdar, 2016).

Modeling provides a way, perhaps the principal way, of predicting the behavior or performance of proposed system infrastructure designs or management policies. Applications of models to real systems have improved our understanding of such systems and hence have often contributed to improved system design, management, and operation. Mathematical simulation and optimization models packaged within interactive computer programs provide a common way for planners and managers to predict the behavior of any proposed water resources system design or management

policy before it is implemented (Loucks and Beek, 2005). The basic techniques used in water resources systems analysis are optimization and simulation (Vedula and Mujumdar, 2016).

Optimization and simulation models can be advantageous for determining the best design and operating policy variable values in river basin systems. Optimization is often useful, not for finding the very best solution but for eliminating the worst alternatives from further consideration. The remaining ones can then be analyzed in greater detail using more detailed simulation models. Simulation by itself begs the question, 'What to simulate?' Optimization by itself begs the question, 'Is the solution really the best?' (Daniel and Eelco, 2005; Simonovic, 2009). Optimization determines the values of decision variables for optimizing the objective function (Vedula and Mujumdar, 2016). In optimization models, the objective function (or functions in multi-objective optimization) is the driving force. The term optimal solution essentially refers to the best from the solution of the mathematical model under all assumptions and constraints, whether explicitly stated or implicitly included in the formulation (Jain and Singh, 2003). Optimization models pose a more abstract question and challenge analysts to mathematically define their objective. This may be difficult for real resource systems that tend to be physically, economically, and politically complex. Because optimization models must search through a wide range of operational possibilities, they usually require simplifications that may be unacceptable or controversial to the real system operators (Faber and Harou, 2007).

Simulation models address 'what if' questions: What will likely happen over time and at one or more specific places if a particular design and/or operating policy are implemented? (Loucks and Beek, 2005). The essence of simulation is to reproduce the behavior of the system in every important aspect to learn how the system will respond to conditions that may be imposed on it or that may occur in the future. A simulation model of a water resource system duplicates its operation with a defined operational policy, using the parameters of physical and control structures, time series of flows, demands, and the variables describing water quality, etc. The main advantage of simulation models lies in their ability to closely describe reality. If a simulation model can be developed and is shown to represent the prototype system realistically, it can provide insight about how the real system might perform over time under varying conditions. Thus, proposed configurations of projects can be evaluated to judge whether their performance would be adequate or not before investments are made. In a like manner, operating policies can be tested before they

are implemented in actual control situations. Simulation is widely believed to be the most powerful tool to study complex systems (Jain and Singh, 2003). Questions answered by simulation models are more straightforward, focused, and occur naturally to those operating existing systems. Simulation is most useful for detailed analysis and development of existing and proposed operating rules (Faber and Harou, 2007) and development interventions. Various water resource models are currently available for simulation and optimization of water resource systems.

2.3. Type of modeling tools

Depending the area of application, Lund et al. (2010) organized/grouped the models as Precipitation climate models (e.g. GFDL, PCM, HadCM, local weather forecasting etc.) , Precipitation-runoff models (hydrological models) (e.g. HEC-HMS, SWAT, SWAP, SWMM, TOPMODEL, MIKE, local flood forecasting etc.), Stream models (e.g. HEC-RAS, DWOPER, FLDWAV, DAMBRK, MIKE 11, MIKE 21 etc.), Aquifer models (e.g. MODFLOW, MIKE SHE, IGSM etc.), Infrastructure operations models (e.g. HEC-ResSim, CALSIM, local system models etc.), Economic, agronomic, social, environmental demand and performance models (e.g. IWR-MAIN, HEC-FDA, various local and academic models) and Decision-making models (ESSA, Shared Vision Modeling, HEC-RPT, various hydro-economic models).

For this study, the hydrological model (ArcSWAT) and water resource model (HEC-ResSim Model) were applied, and further review was about the two models.

2.3.1. Hydrological modeling

Hydrological modeling is a powerful technique of hydrological systems investigation for both the research hydrologist and practicing water resources engineers involved in the planning and development of an integrated approach for the management of water resources. Lenhart et al. (2002, cited in Lijalem, 2006), Hydrological modeling is a great method of understanding hydrologic systems for the planning and development of integrated water resources management. The purpose of using a model is to establish baseline characteristics whenever data is not available and to simulate long-term impacts that are difficult to calculate, especially in ecological modeling.

Effective watershed management and ecological restoration require a thorough understanding of hydrologic processes in the watersheds. Spatial and temporal variations in soils, vegetation, and land use practices make a hydrologic cycle a complex system; therefore, mathematical models and geospatial analysis tools are needed for studying hydrologic processes and hydrologic responses to land use and climatic changes (Dilnesaw, 2006).

A hydrological model is a mathematical model used to simulate river or stream flow and calculate water quality calculations. Models often address individual steps modularly in the simulation process. Typically, subroutines for surface runoff include components for a land use type, topography, soil type, vegetation cover, precipitation, and land management practice (regular agricultural activities, e.g., pesticide or fertilizer application).

Many different types of hydrological models have been developed. Many of these models share structural similarities because of underlying assumptions, while some of the models are distinctly different. Therefore, these models are classified according to different criteria. Hypothesis traditionally proposed two kinds of modeling approaches with their strong points and limitations:

(1). physically based

(2). Conceptual lumped models

Physically based models (theoretical, white box) consist of formulation in terms of physical laws expressed in the form deterministic conservation equation for mass, momentum, and energy. The equations are solved numerically by dispraising the hydrological system into smaller entities on a square or polygonal mesh. However, accurately modeling of all processes of the hydrologic cycle becomes very complex, demands an eminent insight in hydrological behavior, and is very demanding for input data. Due to these properties, it is time-consuming and expensive (Abbott et al., 1986).

As an alternative to physically based distributed models, conceptual lumped models (grey box) are often used as robust tools at catchment scale. The model structures of these models are relatively simple and often are based on a series of interconnected reservoirs. Further, these models are invaluable instruments for operational water management (e.g., reservoir operation and flood

forecasting). Because the required input and output data are usually easily available, consequently, these models are mostly used in rainfall-runoff modeling (Ephrem, 2011).

2.3.2. Hydrological model selection

There are numerous criteria that can be used for selecting the appropriate hydrologic model. These criteria are project-dependent because every project has its own specific requirements and needs. Further, some criteria are also user-dependent, such as personal preference for computer operation system, input/output management, and structure.

Among the various project-depended selection criteria, Cunderlik (2003) lists out four main criteria that should be considered when selecting hydrological models. These are the required model outputs important for the needed purpose and therefore to be estimated by the model (does the model predict the variables required by the project such as peak flow, event volume and hydrograph, long-term flows, etc.?). Hydrologic processes that need to be modeled to estimate the desired outputs adequately (is the model capable of simulating regulated reservoir operation, snow accumulation and melt, single event or continuous processes, etc.?), availability of input data (can all the input data required by the model be provided within the time and cost constraints of the project?) and price (does the investment appear to be worthwhile for the objectives of the project?).

In this study, a spatially semi-distributed (ArcSWAT) model was used to assess the water resource potential of the Abbay River basin. The choice of these models depended on their moderate input data requirement (uses readily available inputs), ability to simulate the major hydrological processes, and their availability.

Over Abbay River basin, ArcSWAT was widely applied for hydrological model and water potential assessment (Tatenda et al., 2018, Abeyou et al., 2018, Meseret et al., 2020, Gebiyaw et al., 2021), sediment management analysis (Shimelis et al., 2010, Easton et al., 2010, Betrie et al., 2011, Yasir, 2014), climate and land use change impact assessment (Melke and Abegaz, 2017., Wakjira et al., 2020, Achenafi et al., 2020, Vincent et al., 2018), and is recommended as a permissible modeling tool. The model demonstrated good performance in producing the patterns and trend of the observed discharge, which assures the suitability of the SWAT model for future scenario analysis (Rebecca, 2019) for the basin. Moreover, SWAT has previously been applied in the highlands of Ethiopia and has given satisfactory results in the Lake Tana basin and upper Blue

Nile basin of Ethiopia (Setegn et al., 2009; Easton et al., 2010; Betrie et al., 2011). The SWAT model requires moderate input data, the ability to simulate the major hydrological processes, and its applicability and availability (Melke and Abegaz, 2017), making it suitable to apply for this study. The model structure and its description can be found in the following sections.

2.3.3. ArcSWAT model

SWAT is an acronym for soil water assessment tool, a river basin, or watershed, scale model. SWAT is a river basin scale, continuous time, spatially distributed model developed to predict the impact of land management practices on water, sediment, and agricultural chemical yields in large complex watersheds with varying soils, land use, and management conditions over a long period of time (Neitsch et al., 2009). SWAT requires specific information about weather, soil properties, topography, vegetation, and land management practices occurring in the watershed. The SWAT model uses readily available inputs: While SWAT can be used to study more specialized processes, the data required to make a run are commonly available from government agencies and are computationally efficient. Simulation of very large basins or a variety of management strategies can be performed without excessive investment of time or money and enables the user to study long-term impacts. Many of the problems currently addressed by the user involve the gradual buildup of pollutants and the impact on downstream water bodies. To study these types of problems, results are needed from runs with output spanning several decades.

2.3.3.1.SWAT model simulation Processes

SWAT allows number of different physical processes to be simulated in a watershed. For modeling purpose, a watershed may be partitioned into number of sub watersheds or sub basins. The use of sub basins in a simulation is particularly beneficial when different areas of the watershed are dominated land use or soils dissimilar enough in properties to impact hydrology. Input information for each sub basin is grouped or organized into the following categories: climate, hydrologic response unit (HRU), pond/wetlands, groundwater, and the main channel or reach draining the sub basin. Hydrologic response units are lumped land areas within the sub basin that are comprised of unique land cover, soil, and management combinations.

No matter what type of problem studied with SWAT, water balance is the driving force behind everything that happens in the watershed. To accurately predict the movement of pesticide, sediments or nutrients, the hydrologic cycle as simulated by the model must conform to what is

happening in the watershed. Simulation of the hydrology of a watershed can separated into two major divisions. The first division is the land phase of the hydrologic cycle which controls the amount of water, sediment, nutrient, and pesticides loading to the main channel in each sub basin. The second division is the water or routing phase of the hydrologic cycle which can be defined as the movement of water, sediment etc. through the channel network of the watershed to the outlet (Neitsch et al., 2009).

The hydrologic cycle simulated by SWAT is based on the water balance equation as follows.

$$SW_t = SW_0 + \sum_{i=1}^{t}(R_{day} - Q_{surf} - E_a - W_{seep} - Q_{gw}) \quad (2.1)$$

In which, SW_t is the final soil water content (mm water), SW_o is the initial soil water content in day i (mm water), t is the time (days), R_{day} is the amount of precipitation in day i (mm water), Q_{surf} is the amount of surface runoff in day i (mm water), Ea is the amount of evapotranspiration in day i (mm water), W_{seep} is the amount of water entering the vadose zone from the soil profile in day i (mm water), and Q_{gw} is the amount of return flow in day i (mm water).

The subdivision of the watershed enables the model to reflect differences in evapotranspiration for various crops and soils. Runoff is predicted separately for each HRU and routed to obtain the total runoff for the watershed. This increases accuracy and gives a much better physical description of the water balance.

Surface runoff occurs whenever the rate of precipitation exceeds the rate of infiltration. When water is initially applied to a dry soil, the infiltration rate is usually very high. However, it will decrease as the soil becomes wetter. When the application rate is higher than the infiltration rate, surface depressions begin to fill. If the application rate continues to be higher than the infiltration rate once all surface depressions have filled, surface runoff will commence.

SWAT provides two methods for estimating surface runoff: the SCS curve number procedure (USDA-SCS, 1972) and the Green & Ampt infiltration method (1911). Using daily or sub daily rainfall, SWAT simulates surface runoff volumes and peak runoff rates for each HRU (Ephrem, 2011).

2.3.4. Available water resources system models

HEC Models: A variety of models and decision support tools have been developed at the Hydrologic Engineering Centre (HEC), U.S. Army Corps of Engineers (USACE), in Davis, California. The reservoir system simulation packages (HEC-3, HEC-5, and HEC-ResSim) can perform network systems simulation analysis, including flood management, water supply, and hydropower operations. These programs are well documented and are publicly available. HEC-5 (USACE, 1998) is one of the most widely used reservoir systems operation simulation models, which can perform investigations of storage reallocations and other operational modifications at existing reservoirs as well as feasibility studies for proposed new projects. HEC-5 is an updated version of HEC-3, both software having similar capabilities, except that HEC-3 does not allow the comprehensive flood control capabilities of HEC-5 (Rani and Moreira, 2010).

HEC-ResSim (http://www.hec.usace.army.mil/software/hec-ressim/) is the successor of HEC-5, which is comprised of a window-based graphical user interface, a computer program to simulate reservoir operation, data management capabilities, and graphics and reporting features (Klipsch and Hurst, 2007). HEC-ResSim aids engineers and planners in predicting the behavior of reservoir systems in water management studies and to help reservoir operators plan releases in real time during day-to-day and emergency operations (Klipsch and Evans, 2007). HEC-ResSim uses an original rule-based approach to mimic the actual decision-making process that reservoir operators must use to meet operating requirements for flood control, power generation, water supply, and environmental quality. The graphical user interface makes HEC-ResSim easy to use, and the customizable plotting and reporting tools facilitate output analysis (Almohseen and Jalil, 2014).

HEC-ResSim is unique among reservoir simulation models because it attempts to reproduce the decision-making process that human reservoir operators must use to set releases. The program represents the physical behavior of reservoir systems with a combination of hydraulic computations for flows through control structures and hydrologic routing to represent the lag and attenuation of flows through segments of streams. It represents operating goals and constraints with an original system of rule-based logic that has been specifically developed to represent the decision-making process of reservoir operation. The generalized nature of HEC-ResSim, its flexible scheme for describing reservoir operations, and its powerful new features make it

applicable for modeling almost any single- or multi-purpose reservoir system (Klipsch and Evans, 2007).

The HEC-ResSim model has been applied in Ethiopia for water management and planning studies, i.e., Teshome (2015) used HEC-ResSim to model cascade dams and reservoir operations for optimal water use over Omo Gibe River Basin, Ethiopia; Ahmed (2010) applied for Eastern Nile Water Resources Simulation, Belachew and Mekonen (2014) also used the HEC-ResSim model for Eastern Nile Basin Water System Simulation, etc.

IRIS and IRAS: The Interactive River System Simulation (IRIS) package has been developed with support from the Ford Foundation, United Nations Environment Program, International Institute for Applied Systems Analysis, Austria, and Cornell University (Loucks et al., 1989, 1990). The model is developed with the intention to be used as a decision support and alternative screening tool for resolving conflicting issues associated with the management of international river basins (Salewicz, 2003). The Interactive River-Aquifer Systems (IRAS) model (Loucks and Bain, 2002; Loucks et al., 1996) is an extended version of IRIS. IRAS can address problems involving interactions between ground and surface waters and between water quality and quantity. The model is menu-driven, and the user defines the spatial and temporal resolution of the system being simulated. A variable computational time step can be used. The program provides a facility to interactively change operating rules during a simulation run.

WRAP Modeling System: Development of Water Rights Analysis Package (WRAP) at Texas A&M University began in the mid-1980s. WRAP simulates a river/reservoir system under a priority-based water allocation system. The model is designed for long-term monthly time step modeling assessments of hydrologic and institutional water availability and reliability for water supply diversions, environmental stream flow requirements, hydroelectric energy generation, and reservoir storage (Wurbs, 2005a). The public domain software and documentation of the model may be downloaded from the website (http://ceprofs.tamu.edu/rwurbs/wrap.htm).

MODSIM: MODSIM is a computer simulation model developed jointly by the Colorado State University (CSU) and the Bureau of Reclamation's Pacific Northwest Region. The model has been continuously used to simulate operations of reservoir systems throughout the world. MODSIM is designed for developing basin-wide strategies for short-term water management, long term

operational planning, drought contingency planning, water rights analysis, and environmental concerns. The graphical user interface of MODSIM allows users to create and link reservoirs in network objects (Rani and Moreira 2010). MODSIM can also be used with geographic information systems for managing the intensive spatial data base requirements of river basin management.

The software, along with the user's manual documentation, can be downloaded from the internet (http://modsim.engr.colostate.edu/beta.html).

RiverWare: RiverWare is in general a multi-objective river basin modeling tool, developed at the Center for Advanced Decision Support for Water and Environmental Systems (CADSWES) of the University of Colorado. The flexibility of RiverWare allows building and developing a wide variety of models to meet the diverse needs of many river basins. RiverWare is a proprietary software package, with more information about the software and documentation available at the CADSWES website (http://cadswes.colorado.edu). This system offers multiple solution methodologies that include simulation, simulation with rules, and optimization. RiverWare can accommodate a variety of applications, including daily scheduling, operational forecasting, and long-range planning.

CalSim: California Water Simulation Model (CalSim) is a simulation model for planning and management of the State Water Project (SWP) and Central Valley Project (CVP) of California, U.S.A. The model is developed by the California State Department of Water Resources (DWR) and the U.S. Bureau of Reclamation (USBR).

RIBASIM: RIBASIM (River Basin Simulation Model) is a generic model package for analyzing the behavior of river basins under various hydrological conditions (WL Deflt Hydraulics 2004). The model package is a comprehensive and flexible tool that links the hydrological water inputs at various locations with the specific water users in the basin (Van der, 2010).

WEAP: The Water Evaluation and Planning (WEAP) system is used to model the balance between water demand and supply at a range of spatial and temporal scales. WEAP models both water demand and its main drivers and water supply, simulating real-world policies, priorities, and preferences. It has been used to evaluate the impact of a wide range of potential water management measures, from conservation to wastewater reuse, and to plan for adaptation to climate change (SEI, 2012). WEAP is a user-friendly system that uses an object-based approach to allow the model

builder to represent the physical processes governing the availability and movement of water as well as interactions among all the water use and management activities in a watershed. The objects include such features as sub-catchments, surface water bodies, dams, and other infrastructure elements, as well as the location of specific water demands. WEAP can track the movement of water through a river basin, starting with exchanges with the atmosphere, i.e., precipitation and evapotranspiration, as well as interactions between groundwater and surface water systems (Yates and Miller, 2013). WEAP is applicable to municipal and agricultural systems, single sub-basins, or complex river systems. Moreover, WEAP can address a wide range of issues, e.g., sectoral demand analyses, water conservation, water rights and allocation priorities, groundwater and stream flow simulations, reservoir operations, hydropower generation and energy demands, pollution tracking, ecosystem requirements, and project benefit-cost analyses (SEI, 2015).

As a conclusive remark, for this study the pure simulation model (HEC-ResSim) was applied because it is better applicable for river basins with cascades of reservoirs.

2.4.Hydro-Economic Modeling

Economics and engineering are kindred disciplines that have frequently exchanged fundamental ideas over their long history (Lund et al., 2006). Water engineers continued to incorporate economic principles throughout the 19th and 20th centuries, increasingly in a system's analysis context. Often, optimization provided the mathematical link between economics and engineering. Economic engineering in the water field emphasizes the use of economic principles to support decision-making, flexible and integrated management, benefit valuation, plan design, alternative evaluation, finance, and institutional design (Braden, 2000; Lund et al., 2006). One manifestation of this mutually beneficial collaboration was the development of hydro-economic models (Julien et al., 2009). Hydro-economic models account for important connections and feedbacks between human systems (including the economy) and natural hydrologic systems. These frameworks can capture the key contributions that water resources and related natural systems can make to human activities and their well-being (Baker et al., 2021).

A hydro-economic model is both a computational method and a tool to analyze water resource management problems. As its name indicates, hydro-economic modeling combines economic management concepts with an engineering level of understanding of a hydrologic system. Hydro-

economic models integrate spatially distributed water resources, economic values, infrastructure, and management policies. The model optimizes water allocation between different uses across time and space, taking into account various physical, economic, environmental, and institutional constraints. Hydro-economic models have emerged as an effective tool for studying various water resources management problems around the globe: inter-sectoral water allocation, reservoir operation, transboundary water management, conjunctive management, water-food-energy nexus, climate change adaptation, investment planning (FAO, 2018).

Hydro-economic models (HEM) represent regional scale hydrologic, engineering, environmental, and economic aspects of water resources systems within a coherent framework. The idea is to operationalize economic concepts by including them at the heart of water resource management models. These models have emerged as a privileged tool for conducting integrated water resources management (IWRM) (Global Water Partnership, 2000; Cardwell et al., 2006). Hydro-economic models are solution-oriented tools for discovering new strategies to advance efficiency and transparency in water use. The goal is to look at a system in a fresh way to investigate promising water management schemes and policy insights (Julien et al., 2009).

Hydro-economic models are generally accepted as the most appropriate unit for integrated analysis since water-dependent production and environmental systems are strongly interconnected within river basins (Ringler et al., 2004). The main components of HEMs are mathematical representations of the hydrologic relationships in the water system and the water demand and production relationships of different water-using sectors (e.g., agriculture, industry, municipal sector, and hydropower production) (Bekchanov et al., 2015).

Globally, river basins and sub-catchments have applied different types of HEMs to solve various water management issues. Although some problems, such as increasing competition for water among economic sectors, are likely common for many water resource systems, each basin also has unique features that may generate specific problems that are different from the problems of other basins (Bekchanov et al., 2015). Jose et al. (2016) applied hydro-economic models to assess the economically optimal operation of a multi-purpose reservoir for hydropower and irrigated agriculture. In this study, conflicts in competing seasonal demands between agriculture and hydropower are the major issue. Salvador et al. (2009) developed hydro-economic modeling framework to determine optimal management of groundwater nitrate pollution from agriculture,

FAO (2018) developed hydro-economic model for the Senegal River basin to enhance cross-boundary water resource management and increase the understanding of the benefits of joint water resource management, Serkan and Frank (2009) applied hydro-economic model to analyze the competing water use among agriculture, urban, and environmental uses and assess the economic impacts of climate change. Applications of HEM encompass economic evaluations of both existing and proposed water projects, assessments of alternative water management strategies or policies, risk analysis related to hydro-climatic uncertainties (such as climate change), and the evaluation of costs and benefits associated with mitigation and adaptation efforts (Ortiz-Partida et al., 2023).

Hydro-economic models have been applied over the Nile basin at different spatial scales (the whole Nile basin, Eastern Nile basin, Blue Nile basin, Upper Blue Nile Basin) to solve/assess various water issues, i.e., Goor et al. (2010) applied a basin-wide integrated hydro-economic model to assess the economic benefits and costs associated with the storage infrastructures in Ethiopia and their spatial and temporal distribution. The model integrates essential hydrologic, economic and institutional components of the river basin in order to explore both the hydrologic and economic consequences of various policy options and planned infrastructural projects; Nile Economic Optimization Model (NEOM) was applied by Whittington et al. (2005) to assess the economic value of cooperation for the entire Nile Basin; Jeuland (2010) develops a hydro-economic modeling framework for integrating climate change impacts into the problem of planning water resources infrastructure development over Blue Nile; Diane et al. (2014) used an integrated, stochastic hydro-economic model of the entire Eastern Nile River basin to analyze various development and management scenarios particularly to analyze of the hydrologic and economic risks faced by downstream countries when the GERD will be online; Deterministic hydro-economic optimization model for the Eastern Nile Basin (ENOM) was applied by (Reem et al., 2018) to assess the distribution of benefits between the riparian countries from the optimal operation of the system under both cooperative and non-cooperative management.

2.4.1. Categories of Hydro-Economic Models

HEMs can be categorized into two general types. The first type is node-based river basin management models that include both simulation and optimization models (SIMOPT). The second type is economy-wide models that include Input-Output models (IOM) and Computable General Equilibrium (CGE) models.

In the node-based HEM, simulation and optimization are grouped together under the larger heading of node-based river management models. Within this group, simulation models are built and calibrated to reproduce the behavior of real water systems. Following this calibration, simulation HEMs can be used to assess different scenarios of physical or management-induced change. Optimization models, on the other hand, aim to determine a hypothetical best case (as determined by the objective function of the model) for a particular river basin; the optimal outcome may pertain to efficiency in water use, identify an optimal infrastructure development pathway, or minimize the costs of water allocation. Node-based HEMs can, therefore, be used descriptively to better quantify and understand the consequences of current institutions and management practices by asking 'what if' questions and testing their responses to different stressors or potential changes in management. Node-based HEMs can also be used to analyze the economic trade-offs among different water users or can be used to identify efficient or more equitable water allocations (e.g., by relaxing water sharing rules and institutions or testing the implications of institutions that aim to enhance equity). Node-based models also allow forecasting and assessment of the magnitude of various water management problems, such as flooding, droughts, or competition for water (e.g., upstream and downstream users, environmental water needs versus demand for production processes, or construction of new dams or irrigation projects that have adverse environmental impacts), and provide a framework for understanding how different solutions and interventions may serve to reduce them and mitigate conflicts. Economy-wide models differ substantially from these node-based river basin models in that they allow assessment not only of impacts in primary markets using water as an input to production. Instead, these approaches produce estimates of impacts on the broader economy (that are transmitted through secondary markets). Thus, they require a structure and data pertaining to the use of factors of production, including water and intermediate goods, and provide the basis for analyzing effects on income and its distribution to different economic sectors and agents. These models, however, do not thoroughly consider water systems since they are restricted by high-scale spatial and temporal aggregation of variables representing the water system. Economy-wide models consider simplified water use relationships by including water as one factor of production in addition to capital and labor resources. River basins or sub-catchments are considered single-nodes that can supply water to any economic sector that utilizes it. Such models typically emphasize economic relationships, intermediate uses, and

sectorial interlinkages and usually devote less attention to the spatial and temporal dynamics of water systems (Bekchanov et al., 2015).

3. Materials and Methods

3.1.General area description

The Upper Blue Nile Basin, known as Abbay in Ethiopia and originating from the Ethiopian plateau, is situated between 7.50 to 120 north and 340 to 400 east. This basin exhibits diverse topography, ranging from lowlands (nearly 500 masl) near the Ethio-Sudan border to mountainous regions (about 4250 masl) in the central highlands. Covering an area of around 177,000 km2 (excluding Rahad and Dinder), the basin consists of fourteen sub-basins, as depicted in Figure 3-2, and expands to nearly 199,000 km2 when including Rahad and Dinder. The Abbay River Basin constitutes 17% of Ethiopia's land mass and approximately 7% of the Nile Basin's total surface area.

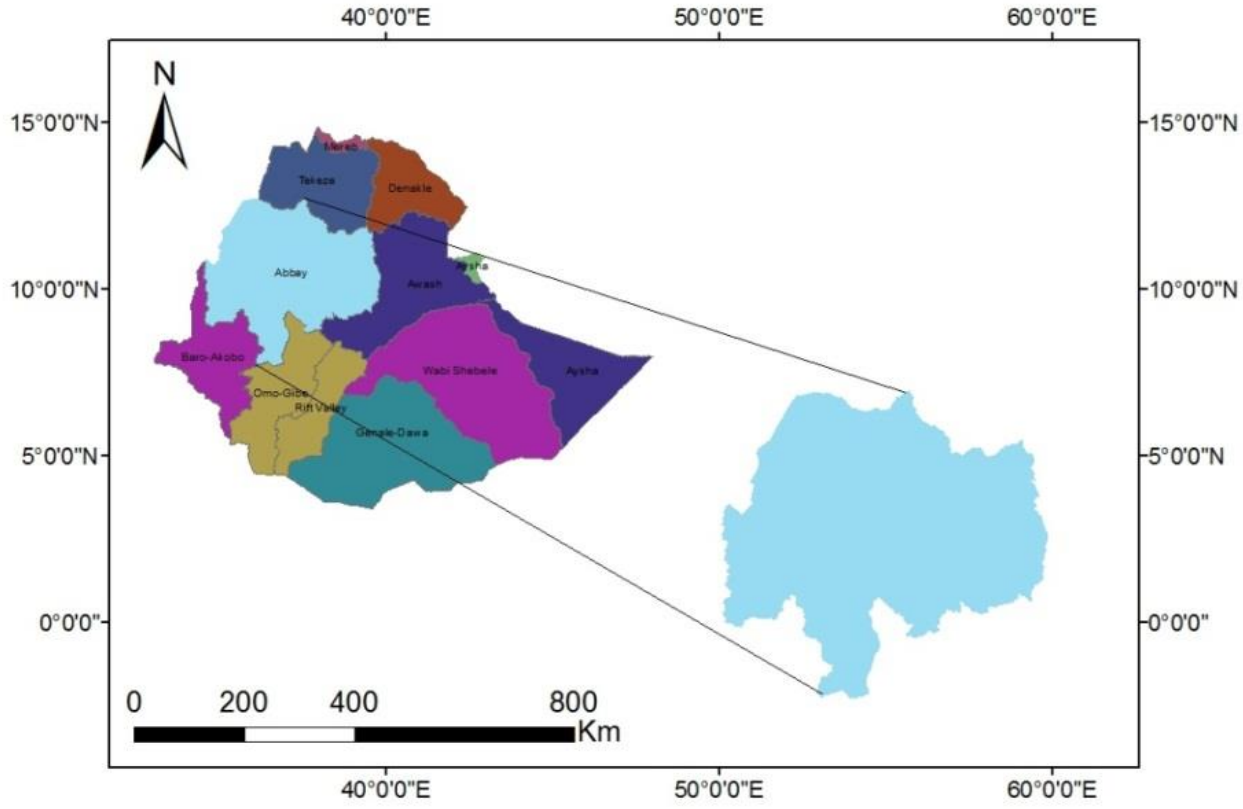

Figure 3.1: Location map of Upper Blue Nile Basin

3.1.1. Sub-basin of Abbay River basin

The Abbay River basin consists of fourteen sub-basins, as shown in Figure 3-2. The water resources of the basin are dominated by the Abbay River, which rises in the center of the catchment and develops its course in a clockwise spiral. It collects tributaries all along its 992 km length before reaching the Sudan border above the Rosaries dam. As the Gilgel Abbay, the main river flows north from its source near Sekela into Lake Tana. The lake also receives other tributaries from a catchment of 15,320 km2 (7.5% of the total), including the Megech, Ribb, and Gumara. After leaving the lake, the river reaches the celebrated Tis Abbay Falls, thereafter flowing in a deep and rugged gorge to the Sudan border. Tributaries acquired on the left bank include the Beshilo, Welaka, Jemma, Muger, Guder, Fincha, and Didessa. Right bank tributaries from the Gojam highlands tend to be smaller and include the Abeya, Suha, Chemoga, Birr, Fettam, and Dura. Two major tributaries join Abbay in the most lower parts, the Dabus on the left bank and the Beles, the only major right bank tributary. Rivers in the north-west are the Rahad and Dinder. These flow directly to Sudan, joining the Blue Nile below the Rosaries dam. They are semi-intermittent, remaining dry for months at a time despite catchments that account for 12% of the total basin (BCEOM, 1999).

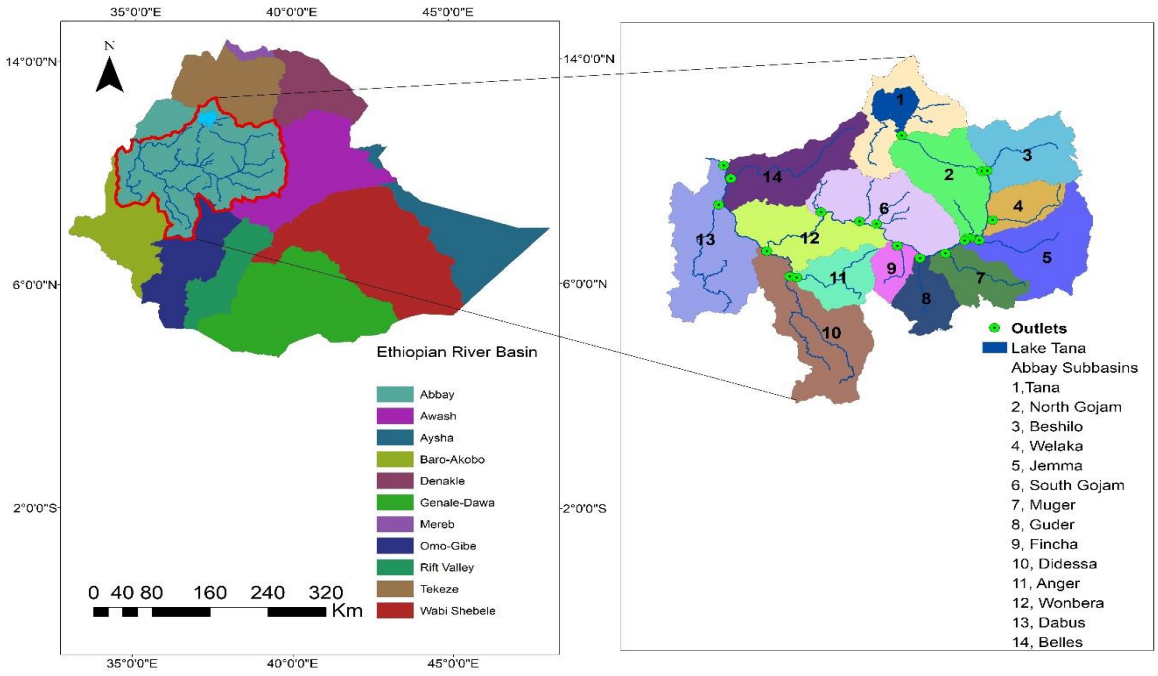

Figure 3.2: Sub-basin of Abbay River Basin

3.1.2. Hydro-meteorological characteristics

As the primary source of the Nile's water resources, it contributes over 60% to the overall flow of the river Nile. The basin plays a crucial role, with an annual average natural flow at the outlet from Lake Tana amounting to 3.5 BCM, representing about 7% of the total flow at the Sudan border. At the border, the average annual natural discharge is 49.4 BCM. Flow quantities in the basin exhibit variation, with the lowest and highest flows occurring in April and August, respectively (BCEOM, 1998).

The basin experiences three distinct seasons. From October to the end of February, it undergoes a dry season, followed by a short rainy season from March to May, and a major rainy season from June to September (Tesemma et al., 2010). The Abbay river basin is characterized by significant spatial and seasonal variations in rainfall. Spatially, the annual rainfall ranges from 904.51 mm to 2161.68 mm. In terms of seasonal distribution, 73.4%, 16.43%, and 10.21% of the total annual rainfall occur during the major rainy season, minor rainy season, and dry season, respectively (Alemu et al., 2022). Temperature variations in the basin are notable, with maximum and minimum temperatures ranging between 28°C and 38°C and 15°C and 20°C, respectively. In the headwaters of the basin, temperatures range from 12°C to 20°C, with minimum values dropping to −1°C and 8°C (Yimere & Assefa, 2022).

The Abbay River presents a substantial opportunity for the generation of hydropower and irrigation development. According to Awulachew et al. (2007), the Abbay river basin possesses a noteworthy gross hydroelectric potential of 78,820 GWh/year. This potential serves as a foundational resource for meeting the escalating energy and food requirements of millions of people within the basin, thereby contributing to the realization of comprehensive and sustainable development goals in the country.

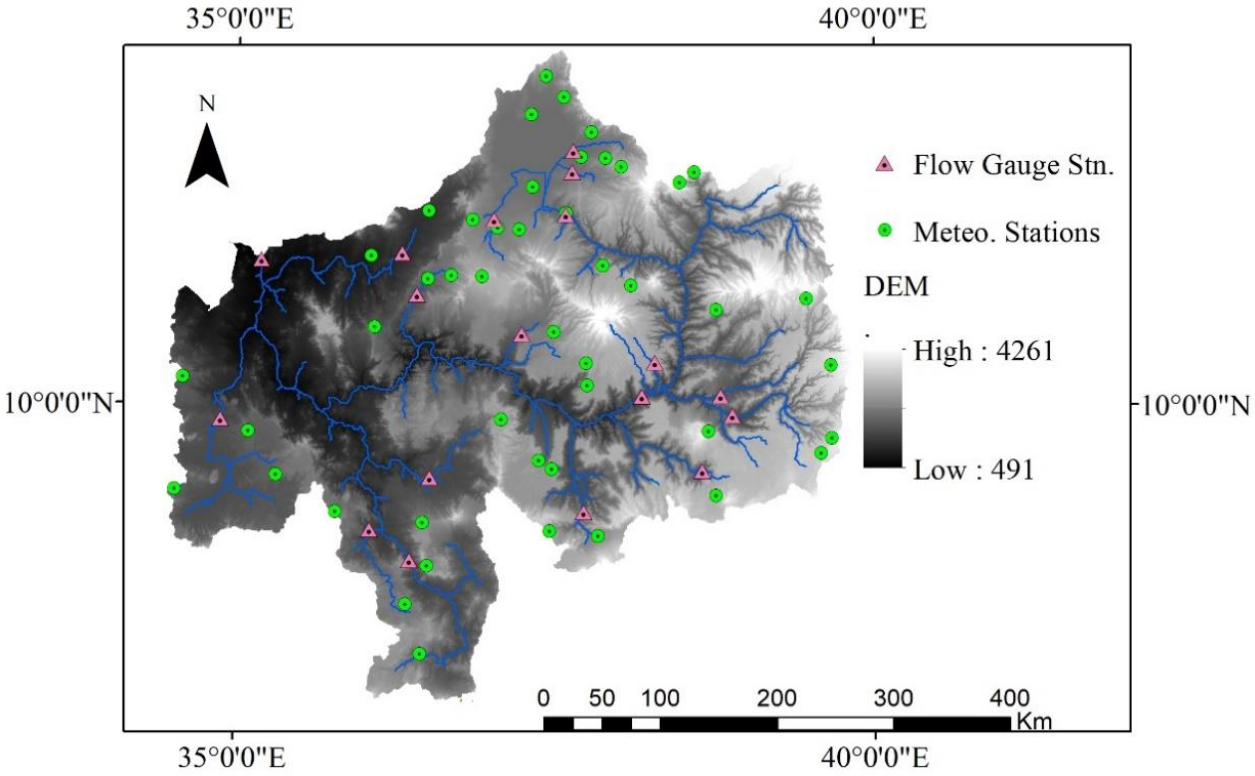

Figure 3.3: Abbay basin Digital Elevation Model (DEM_ 30m x 30m) Map, location of meteorological and Flow Gauge Stations (used as input for ArcSWAT modeling in this research)

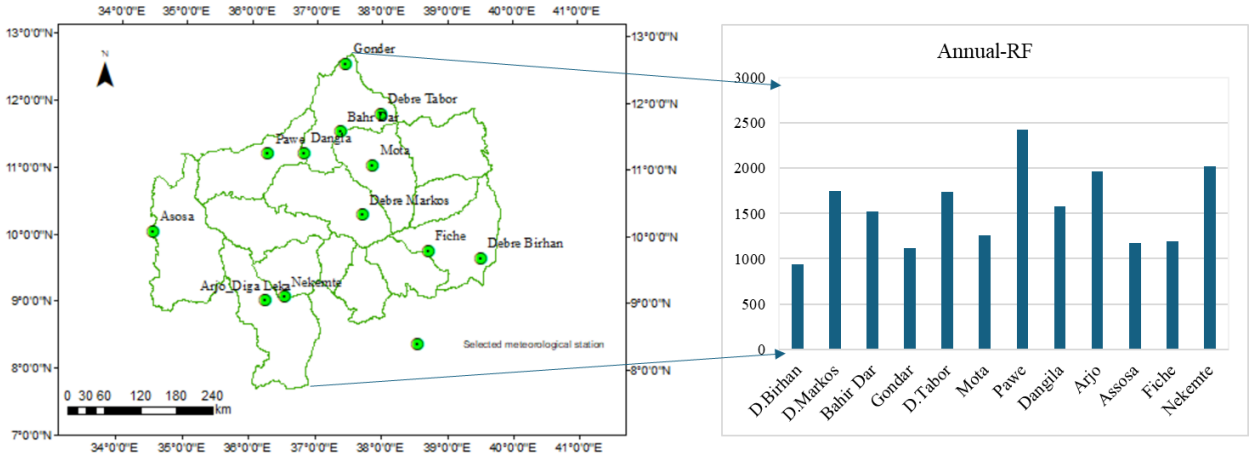

Figure 3.4: Long term annual average rainfall for selected stations over Abbay river basin

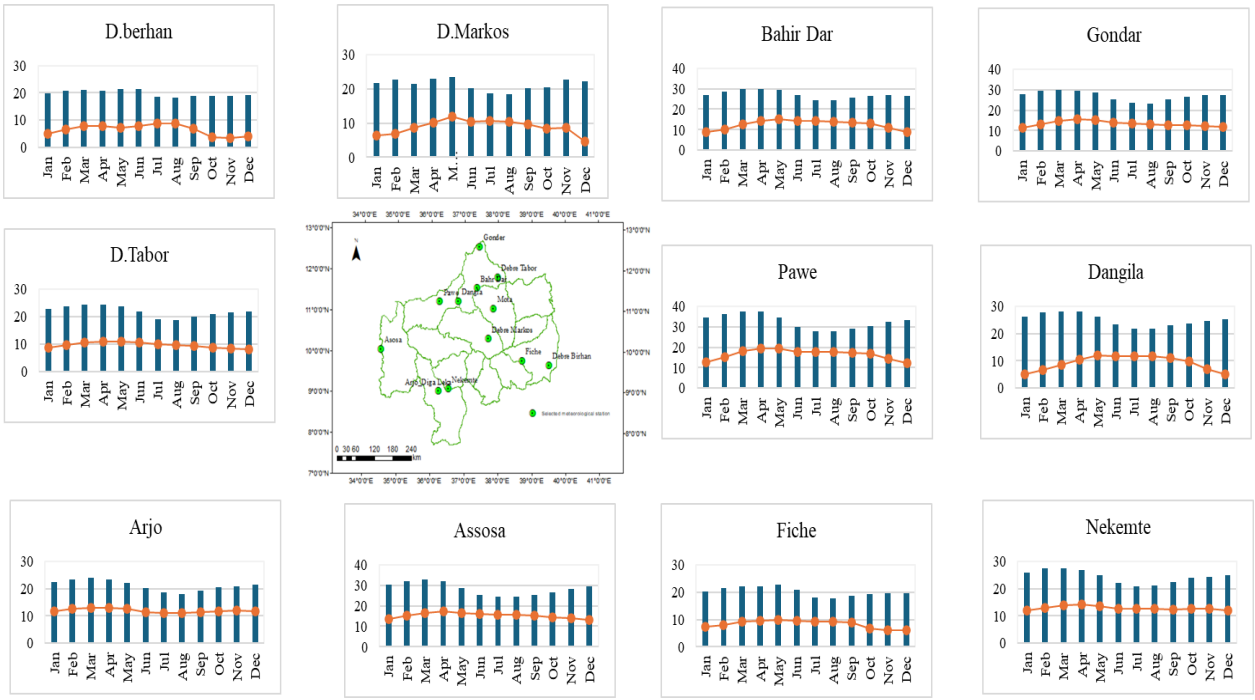

Figure 3.5: The long-term average monthly minimum and maximum temperature for selected sites over Abbay river basin. Blue: Maximum, Yellow: Minimum.

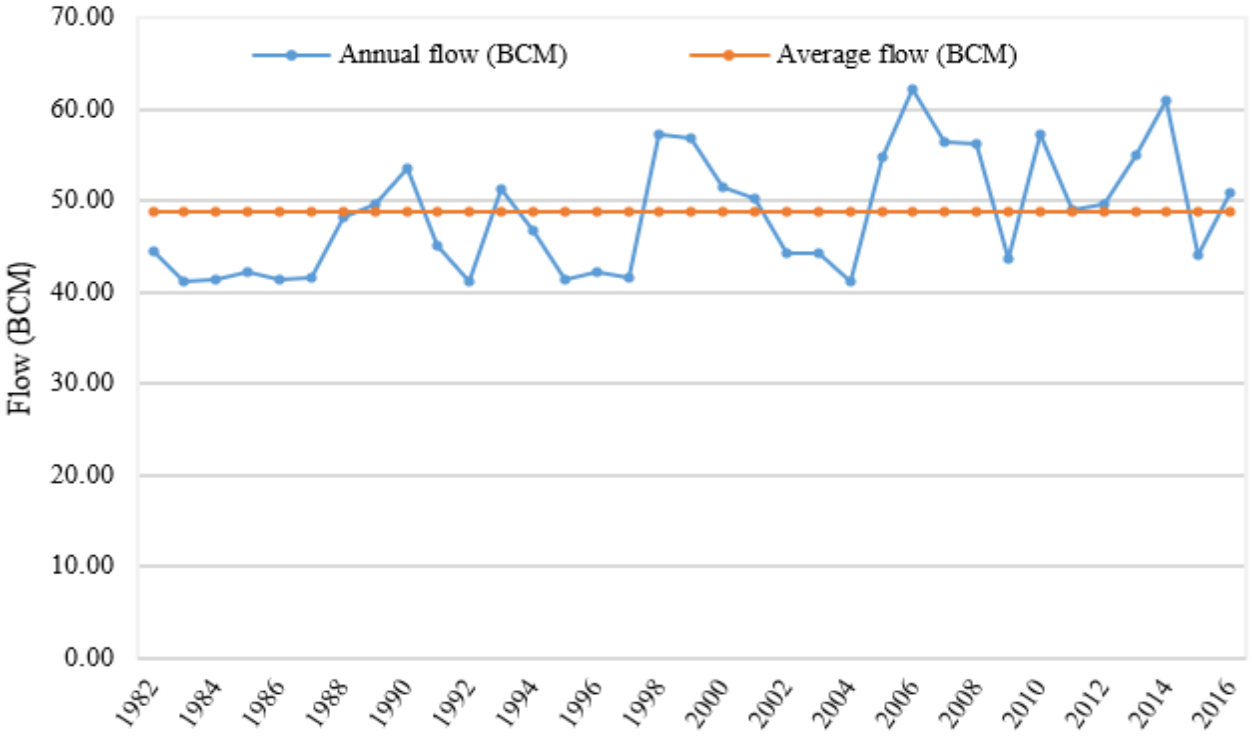

Figure 3.6: Annual flow of Abbay river basin at border gauge station

3.1.3. Land use and soil type

The Abbay River basin exhibits a diverse range of land use types. The majority of the basin is predominantly and extensively cultivated, with the upper region particularly recognized for its agricultural land use. In contrast, the western parts of the basin are noted for their forest cover alongside cultivation. Figures 3-7 and 3-8 illustrate the land use and soil types within the Abbay River basin, while Figure 3-9 depicts its slope classifications. These land use, soil type, and slope class data were utilized as inputs for the ArcSWAT modeling section of this study.

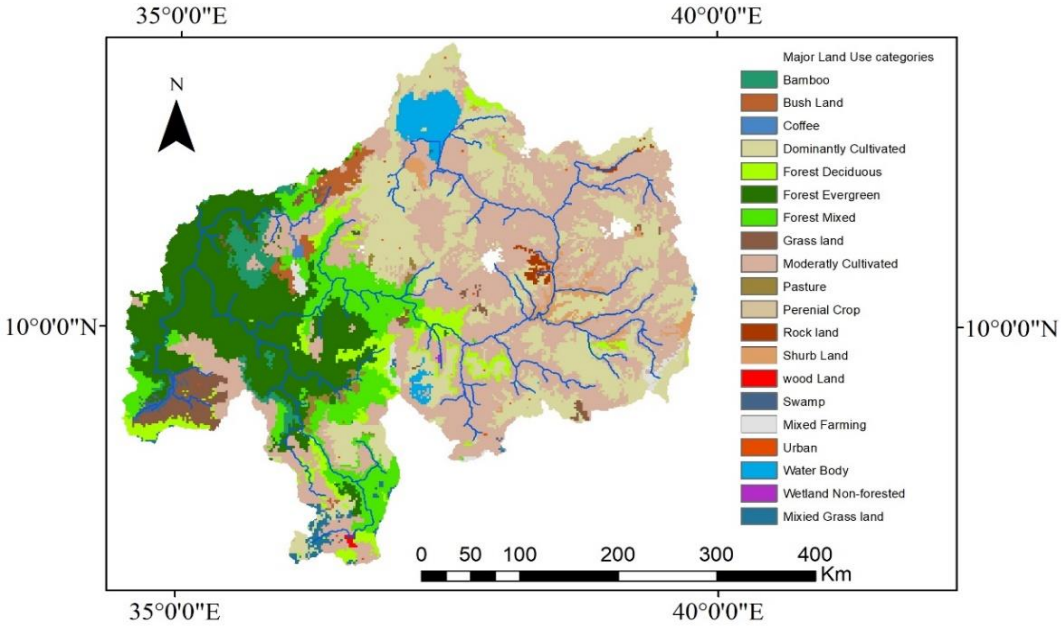

Figure 3.7: Land Use type of Abbay Basin (used as input for ArcSWAT modeling in this research)

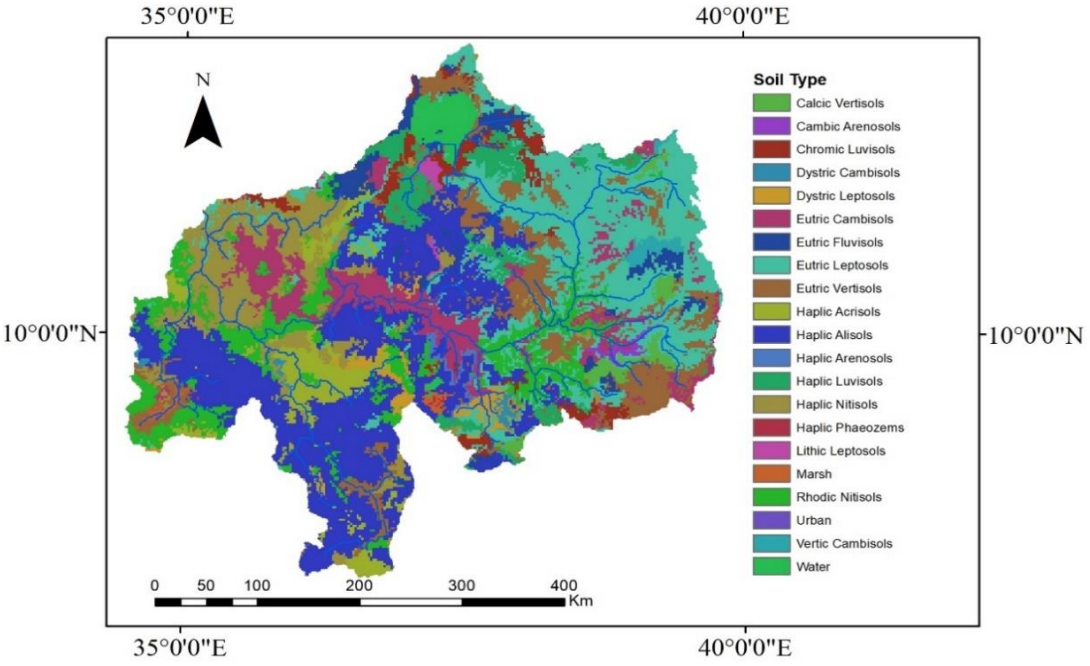

Figure 3.8: Major Soil Types of Abbay basin (used as input for ArcSWAT modeling in this research).

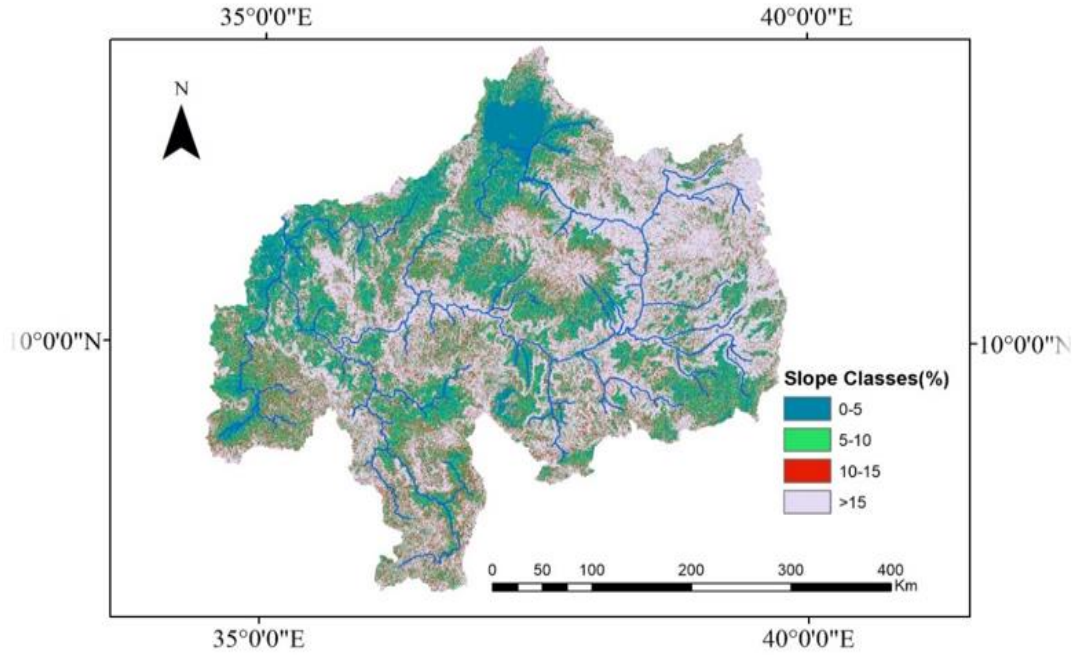

Figure 3.9: Abbay Basin Slope Classification ((used as input for ArcSWAT modeling in this research)

3.2. Hydrological modeling approach

For this study, the GIS interface Soil Water Assessment Tool (ArcSWAT-2012) was applied. SWAT (Soil and Water Assessment Tool) is a comprehensive, semi-distributed river basin model (Arnold et al., 2012), computationally efficient (Neitsch et al., 2011), and applied in addressing hydrologic and environmental issues (Gassman et al., 200; Akoko et al., 2021). The model was developed to assess water resources and predict the impacts of land use/cover changes and land management practices on soil erosion, sedimentation, and non-point source pollution on watersheds or large river basins (Gassman et al., 2007). The model has been applied in categories such as land use change, climate change, erosion, model development, and water quality.

Over Abbay River basin, ArcSWAT was widely applied for hydrological model and water potential assessment (Tatenda et al., 2018, Abeyou et al., 2018, Meseret et al., 2020, Gebiyaw et al., 2021), sediment management analysis (Shimelis et al., 2010, Easton et al., 2010, Betrie et al., 2011, Yasir, 2014), climate and land use change impact assessment (Melke and Abegaz, 2017., Wakjira et al., 2020, Achenafi et al., 2020, Vincent et al., 2018), and is recommended as a permissible modeling tool. The model demonstrated good performance in producing the patterns and trend of the observed discharge, which assures the suitability of the SWAT model for future scenario analysis (Rebecca, 2019) for the basin. Moreover, SWAT has previously been applied in the highlands of Ethiopia and has given satisfactory results in the Lake Tana basin and upper Blue Nile basin of Ethiopia (Setegn et al., 2009; Easton et al., 2010; Betrie et al., 2011). The SWAT model requires moderate input data, the ability to simulate the major hydrological processes, and its applicability and availability (Melke and Abegaz, 2017), making it suitable to apply for this study. Thus, it was expected that ArcSWAT is a powerful model to address our research objectives.

The hydrologic cycle simulated by SWAT is based on the water balance equation as follows.

The model is based on the water balance equation as follows:

$$SW_t = SW_0 + \sum_{t=i}^{t} \left(R_{day,i} - Q_{surf,i} - E_{a,i} - W_{seep,i} - Q_{gw,i}\right) \quad (3.1)$$

Where, SW_t is the final soil water content (mm), SW_o is the initial soil water content on day i (mm), t is the time (days), R_{day} is the amount of precipitation on day i (mm), Q_{surf} is the amount of surface runoff on day i (mm), Ea is the amount of evapotranspiration on day i (mm), W_{seep} is

the amount of water entering the vadose zone from the soil profile on day i (mm), and Q_{gw} is the amount of groundwater flow on day i (mm) (Neitsch et al., 2011).

For this research work SCS curve number method is used to estimate surface runoff because of the unavailability of sub daily data for Green & Ampt method. The SCS curve number equation is (SCS, 1972).

$$\mathbf{Q_{surf}} = \frac{(\mathbf{R_{day}} - \mathbf{I_a})^2}{(\mathbf{R_{day}} - \mathbf{I_a} + \mathbf{S})} \quad 3.2$$

Where, Q_{surf} the accumulated runoff or rainfall excess (mm H2O), R_{day}= is the rainfall depth for the day (mm H_2O), I_a is the initial abstractions which includes surface storage, interception, and infiltration prior to runoff (mm H_2O), S is the retention parameter (mm). The retention parameter varies spatially due to changes in soils, land use, management, and slope and temporally due to changes in soil water content.

3.2.1. ArcSWAT modeling processes

ArcSWAT modeling processes comprise a number of steps from watershed delineation to final model calibration and validation. The following subsection described the detail modeling process applied for the Abbay river basin.

3.2.1.1.Watershed delineation

Watershed delineation serves as the preliminary step in the ArcSWAT simulation process. To define the study area, a digital elevation model (DEM) with a resolution of 30 meters by 30 meters was employed. While it is possible to configure ArcSWAT for the entire basin, covering approximately 177,000 square kilometers (excluding Rahad and Dinder), this study opted to partition the basin into two distinct segments: the Upper Abbay basin and the Lower Abbay basin.

In this context, the Upper Abbay basin extends from the Lake Tana sub-basin to the Kessie gauge station, encompassing significant sub-basins such as Lake Tana, North Gojam, Jemma, Beshilo, and Weleka. The Kessie gauge station serves as the outlet for the Upper Abbay Basin. The Lower Abbay basin, on the other hand, stretches from Kessie to the border and includes major sub-basins like Beles, Didessa, Muger, Anger, Dabus, Fincha, Guder, Wonbera, and South Gojam.

The evaluation of ArcSWAT's performance involved multiple sites, including gauges situated at major tributaries and the main Abbay River. The simulation proceeded incrementally, with the outflow from the upper basin serving as the inflow for the lower basin. Notably, in the largest basin, enhancing the model's performance was achieved by increasing the number of partitioned sub-basins, as observed in previous work by Getachew et al. (2017). This partitioning approach is crucial for the Abbay River basin, characterized by its diverse physical attributes, as it allows for the incorporation of these characteristics into the simulation process.

Moreover, identifying the key parameters that significantly impact the rainfall-runoff process in each sub-basin contributes to improving ArcSWAT's performance. The model was configured to represent the basin under natural conditions, under the assumption that the few existing structures exerted minimal influence on the model's results. Notably, recent research conducted in the basin also omitted these limited hydraulic structures in their ArcSWAT model configurations.

The initial stream network and sub-basin outlets were determined using a drainage area threshold of 10,000 hectares. Subsequently, after establishing the initial stream networks and sub-basin outlets, the final stream network and outlet configuration for modeling were refined by adding and removing outlets. The final outlets, positioned at gauging stations, were used for the comparison of measured and simulated flows.

3.2.1.2.Hydrological response unit (HRU) analysis

The concept of Hydrologic Response Units (HRU) has risen as one of the most common approaches for semi-distributed hydrological modeling (Flügel, 1995). Many of the SWAT simulations occur at the HRU level, including impacts of agricultural management and conservation practices on crop production, hydrology, and water quality. The HRUs are normally defined by lumping similar land use, soil type, and optionally slope characteristics within a given sub-basin based on user-defined thresholds for each category. In this standard method, the user can control the number of HRUs by applying a threshold to the land area permitted for a given land use or soil type within a sub-basin (Kalcic et al., 2015). The subdivision of the watershed enables the model to reflect differences in evapotranspiration for various crops and soils. Runoff is predicted separately for each HRU and routed to obtain the total runoff for the watershed. This increases accuracy and gives a much better physical description of the water balance (Neitsch et al., 2011).

Thus, after watershed delineation of the Abbay basin, the Hydrologic Response Units (HRU) were defined in ArcSWAT by overlaying soils, land use, and slope classes. The HRUs were determined by assigning multiple HRUs for each sub- watershed by considering the sensitivity of the hydrologic processes based on a certain threshold value of soil/land use combinations, as it better describes the heterogeneity within the watershed and accurately simulates the hydrologic processes. The final HRU were defined based on a threshold percentage, i.e., only those land use classes, soil units, and slope classes in a sub-catchment were considered, which were larger than the respective threshold value.

For most applications, the default settings for land use threshold (20%), soil threshold (10%), and slope threshold (20%) are adequate (Winchell et al., 2013). Hence, in this research, the threshold values of 15% for land use, 10% for soils, and 15% for slope classes were used to reduce those very small HRU.

3.2.1.3.Weather statistics generation

After HRU for Abbay basin was defined, the next step for SWAT model setup is thus generating weather data. Weather data are the key drivers of hydrological modeling. However, available weather data can present gaps in data sequences and are often limited in their spatial coverage for use in hydrological models like the Soil and Water Assessment Tool (SWAT). To overcome this limitation, SWAT includes a weather generator algorithm that can complete this data based on long-term weather statistics (Javier et al., 2021).

SWAT includes the weather generator models developed by Sharpley and Williams (1990), to generate weather data. The SWAT Weather Database (Essenfelder, 2016) was applied to generate the SWAT WGEN statistics. SWAT Weather Database is designed to be a friendly tool to store and process daily weather data to be used with SWAT projects, which is capable of storing relevant daily weather information, easily creating.txt files to be used as input information during ArcSWAT project setup, and efficiently calculating the WGEN statistics of several weather stations in a one-step run (Essenfelder, 2016). The SWAT WGEN Statistics window allows the user to calculate the WGEN statistics based on the stored weather data and export it as an output file. The output format of such calculations is compatible with the SWAT WGEN database format.

Over the Abbay basin, there are several meteorological gauge stations with varied temporal and spatial resolution. The elements of such meteorological variables as daily precipitation, temperature, sunshine hour, wind speed, and relative humidity were, however, not available in all stations. Thus, those meteorological stations that have all meteorological elements were selected and used for SWAT WGEN statistics for the Abbay basin. Eight stations from the upper part of Abbay and eleven stations from the lower Abbay basin were selected based on the length of data and availability of meteorological elements such as daily precipitation, temperature, sunshine hour, wind speed, and relative humidity. The meteorological station data used for weather generator statistics was indicated in Appendix A-2.

Evapotranspiration is another element in the ArcSWAT water balance component. Penman-Monteith (Monteith, 1965), Priestley-Taylor (Priestley and Taylor, 1972), and Hargreaves (Hargreaves and Zohrab, 1985) are available methods in ArcSWAT to estimate evapotranspiration. These methods require different meteorological elements as input. The Hargreaves method requires air temperature only (Neitsch et al., 2009), and it was selected for this research. The Hargreaves method was mostly applied in several previous studies done on the Abbay basin. The second phase of the SWAT hydrologic simulation is the routing phase, which consists of the movement of water in the stream network. For this study, the variable storage method was used to route the flow of water in the channel, which is based on a simple continuity equation.

3.2.1.4.ArcSWAT model calibration and validation

Model calibration is a variable and model-specific set of processes that includes adjusting model parameters with directly measured values and tuning a set of model parameters that may not be able to be measured directly using overall model performance and an understanding of model sensitivities (VCS, 2020). Validation is the comparison of the model outputs with an independent data set without making further adjustments. Model validation confirmed the applicability of the watershed-based hydrologic parameters derived during the calibration process. In the validation process, the calibrated parameter ranges are applied to an independent measured data set. Validation is used to build confidence in the calibrated parameters (Karim et al. 2018).

Several calibration techniques have been developed for SWAT: the manual trial-and-error method, the automatic or numerical parameter optimization method, and a combination of both methods (Refsgaard and Storm, 1996). In addition, SWAT-CUP was recently developed and provides a

decision-making framework that incorporates a semi-automated approach (SUFI-2) using both manual and automated calibration and incorporating sensitivity and uncertainty analysis. In SWAT-CUP, users can manually adjust parameters and ranges iteratively between auto-calibration runs (Arnold et al., 2012). SUFI-2 accounts for all sources of uncertainties, such as uncertainty in the controlling variables, conceptual model, parameters, and measured data. In this method, the P factor represents the degree to which all uncertainties are accounted for and is computed as the percentage of measured data bracketed by the 95% prediction uncertainty (95PPU) (Hadi et al., 2014).

For the Abbay basin, the calibration and validation were performed at the daily time step using Sequential Uncertainty Fitting (SUFI2) in SWAT-CUP. The daily time resolution was applied to evaluate the model's ability to simulate at fine time resolution. Moreover, it is important to have daily simulated discharges that resemble the observed discharge and could be applied alternatively in areas where measured data are not available or missed data exists for any hydrology related analysis. The calibration and validation periods vary at each outlet location. This is mainly because of variations in the length of time series availability of discharge data in each gauge point. This variation occurred mainly for the lower Abbay basin since more than one outlet point was selected for calibration and validation. While for the upper part of the Abbay basin, where Kessie is the outlet point, the calibration period is from 1990-2005 and the validation is from 2006-2016. Whereas the lower part was calibrated and validated at Border, Didessa, Guder, Mugher, Beles, Anger, Fetam, and Birr gauge stations with various recorded lengths of time between 1990 and 2014. For both the lower and upper parts of SWAT simulation, two years warm-up period were considered.

The performance of the ArcSWAT model was also calibrated and validated at various flow quantiles. For this research, both simulated and measured flow data were discretized into four groups based on probability of exceedance (0%-2%, 2%-20%., 20%-70%, and 70%-100%), and evaluation was undertaken for each group. After the model was calibrated, validated, and checked for applicability, the ArcSWAT model was rerun using meteorological input data from 1980–2016, keeping physical model parameters constant. The simulation results from 1980-2016 were used for water balance component analysis and used as input for the HEC-ResSim model.

3.2.1.5.Model sensitivity analysis

Sensitivity analysis is a method of minimizing the number of parameters to be used in the calibration step by making use of the most sensitive parameters largely controlling the behavior of the simulation and used to identify the most influential parameters (Worqlula et al., 2018). Sensitivity analysis is the process of determining the rate of change in model output concerning changes in parameters (Arnold et al., 2012). In SUFI-2, there are two types of sensitivity analysis, i.e., global sensitivity analysis and one-at-a-time sensitivity analysis. For this study, global sensitivity analysis was applied. The Arc-SWAT model was run multiple times for each sub-basin to identify the most sensitive parameters, and then the final sensitive parameters that highly control the flow behavior were summarized into two major categories, the upper and lower parts of the Abbay basin. This is basically important to detect which parameters are most sensitive on a special basis over the Abbay River Basin.

Parameter sensitivities are determined by calculating the multiple regression system, which regresses the Latin hypercube generated parameters against the objective function values (Abbaspour, 2014).

$$g = \alpha + \sum_{i=1}^{m} \beta_i b_i \qquad 3.3$$

Where α and β are the intercept and the slope of the regression line, respectively; m defines the number of models runs; and g is the objective function.

The t-test and p-value were used to measure the sensitivity and significance of parameters. A *t*-test is then used to identify the relative significance of each parameter *bi*. The sensitivities given above are estimates of the average changes in the objective function resulting from changes in each parameter, while all other parameters are changing. This gives relative sensitivities based on linear approximations and, hence, only provides partial information about the sensitivity of the objective function to model parameters. The t-stat provides a measure of sensitivity (larger absolute values are more sensitive) and p-values determine the significance of the sensitivity, value close to zero has more significance (Abbaspour, 2014).

3.2.1.6.Input data for modeling

The ArcSWAT model relies on a variety of input data, encompassing soil, land use/cover, meteorological, and Digital Elevation Model (DEM) data. Soil, land use, and DEM data (featuring

a resolution of 30 m x 30 m) were sourced from the Ethiopian Ministry of Water and Energy (MWE), Abbay Basin Authority, and Eastern Nile Technical Regional Office (ENTRO).

Meteorological data, encompassing rainfall, temperature, relative humidity, wind speed, and sunshine hours, were collected from 49 meteorological stations (refer to Figure 3-3 and Appendix A-1) provided by the National Meteorology Agency (NMA). These meteorological data spanned from 1980 to 2016. For the calibration and validation of the ArcSWAT model, hydrological data were obtained from the Ethiopian Ministry of Water and Energy (MWE). The recorded periods of collected flow data varied across gauge stations and ranged from 1980 to 2016.

3.3. Trade-off and synergy analysis methods

3.3.1. HEC-ResSim modeling approach

Simulation models are distinct from mathematical programming techniques in which they provide the response of the system to specify inputs under given conditions or constraints. Hence, simulation models enable a decision maker to test discrete alternatives and evaluate the feasibility before implementing them.

For this research, simulation of the trade-offs between water-hydropower-irrigation-downstream flows under various development scenarios was undertaken using the HEC-ResSim model. The HEC-ResSim was applied to simulate reservoir operation and hydropower generation. HEC-ResSim uses a map-based schematic to represent the river and reservoir system, commonly used in water resource management, to assist modelers in performing reservoir project studies and to support reservoir regulators during real-time events for simulating and analyzing the operation of reservoir systems (Klipsch and Evans, 2007), to simulate reservoir operations for multiple objectives, including flood risk reduction, navigation, hydropower, and environmental support (Meshkat & Klipsch, 2018). HEC-ResSim was also applied in various reservoir simulation case studies, some of which have integrated it with hydrological models (Kim et al., 2020), simulating reservoir operation and conservation processes in hydropower and irrigation applications (Munir et al., 2022), and assessing the effects of development projects (Abdelkader et al., 2023). The generalized nature of HEC-ResSim, its flexible scheme for describing reservoir operations, and its powerful features make it applicable for modeling almost any single or multi-purpose reservoir system (Klipsch and Evans, 2007). It has been applied in Ethiopia for modeling cascade dams and reservoir operations (Teshome, 2015; Wondimagegnehu & Tadele, 2015; Dereje et al., 2020); water system simulation (Dereje et al., 2020; Belachew & Mekonen, 2014); and impact assessment of water development on downstream flow (Abdelkader et al., 2023).

HEC-ResSim offers three separate sets of functions called modules that provide access to specific types of data within a watershed. These modules are watershed set-up, reservoir network, and simulation. Each module has a unique purpose and an associated set of functions accessible through menus, toolbars, and schematic elements.

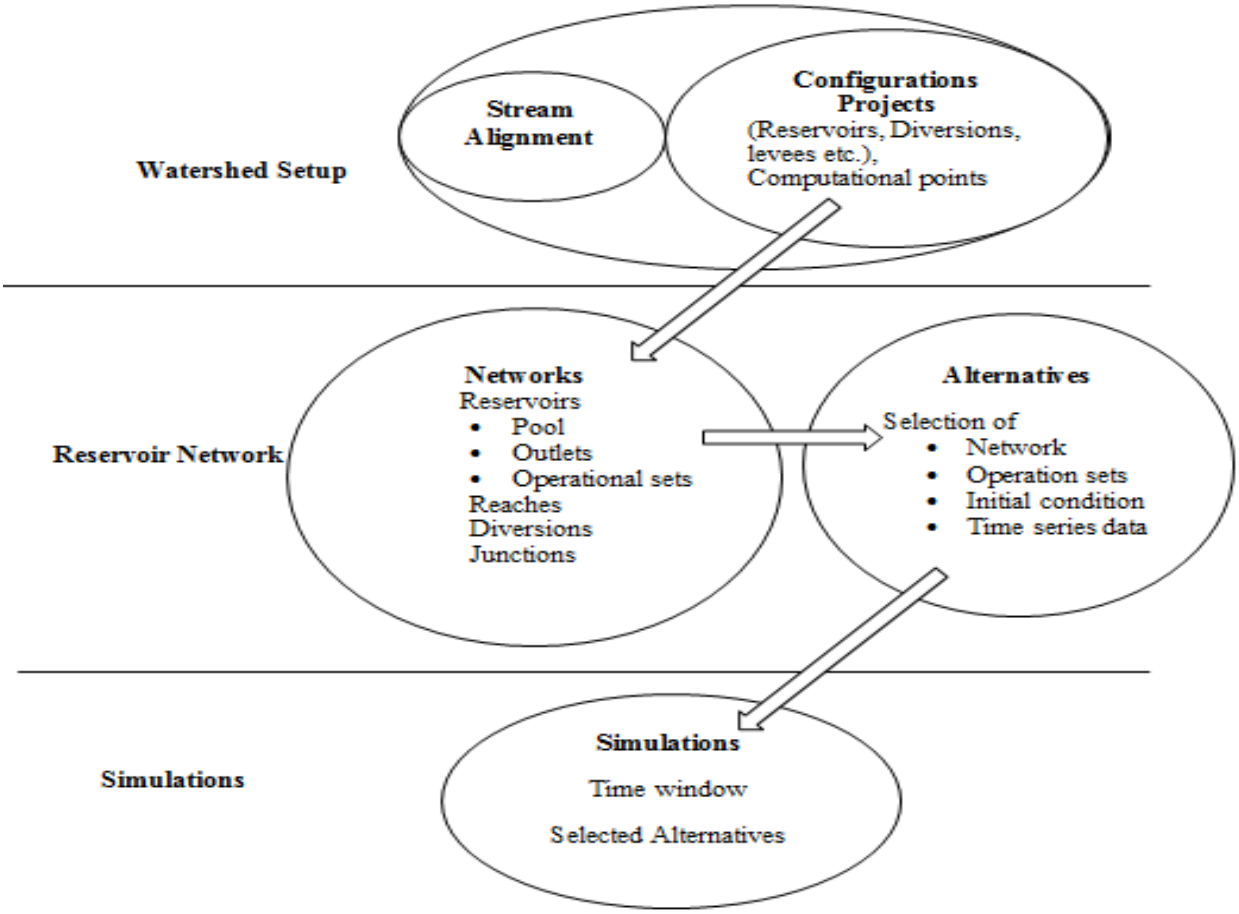

Figure 3.10: HEC-ResSim Module Concepts

3.3.1.1.Watershed setup module

The HEC-ResSim watershed for this study was named Abbay river basin. The purpose of the watershed setup module is to provide a common framework for watershed creation and definition.

A watershed is associated with a geographic region for which multiple models and area coverage's can be configured. The watershed setup involved creating a new watershed for the Abbay river basin. A shape file containing the basin boundary, Main River, and sub-basin boundary was imported into the module's main window as a background map. The stream alignment was established based on the mainstream and major tributaries. Computational points, reservoirs, and diversions were added to the watershed setup module and configured to accurately represent the physical features of the Abbay river basin.

3.3.1.2.Reservoir network

Once the configuration of the watershed was established, the next step was creating a schematic for the reservoir network. This schematic served as a guide, detailing the physical aspects and operational specifics of each reservoir. In the reservoir network module, the physical elements, such as the pool Elevation-Area-Storage (EVA), data on reservoir evaporation, dam elevation, length, and outlet capacity, as well as the installed capacity and efficiency of each cascade dam along the Abbay river basin, were carefully defined. Furthermore, operational data, including the formulation of rules and the delineation of zones such as flood control, conservation, and inactive, were carefully outlined. In the HEC-ResSim model, a range of operation rules are accessible, such as Tandem operation, hydropower schedule, and the power guide curve rule. For this research, the adequacy of these three reservoir operation rules was evaluated to identify the promising operation rules for cascade reservoirs in the Abbay river basin.

Following the configuration of the reservoir network, alternatives were defined. Each alternative included a reservoir network based on the initial layout of the Abbay river basin, accompanied by specific control specifications, operational settings for each reservoir, time-series inflows, and initial conditions for reference. HEC-ResSim allows the run control specification resolution from 30 minutes to daily ranges. For this study, the control specification was fixed at the daily level since the river flow time series data is obtained at daily resolution. The time-series flow data extracted from the simulation output of ArcSWAT was directly used as HEC-ResSim input. Given that the HEC-ResSim does not directly accept time-series flows from the SWAT simulation output folder, the creation of the HEC-DSS flow database from 1981 to 2016 was undertaken using the HEC-DSSVue (visual utility engine). The maximum release capacity and the upper elevation of the conservation zone were established as the initial (lookback) conditions. Independently, reservoir networks and alternatives were formulated for each scenario. Consequently, a total of ten distinct reservoir networks were generated for the purpose of this study. The first four reservoir network scenarios were formulated considering only hydropower projects to evaluate the monthly and annual energy generation potential of four major hydropower projects. Whereas the remaining six network scenarios were formulated by integrating hydropower projects and irrigation diversion to evaluate the trade-off and synergy between irrigation development and energy generation. The reservoir networks were configured considering the GERD reservoir (final construction stage) and three proposed reservoirs (Karadobi, Bekoabo, and Mandaya).

3.3.1.3.Routing reaches

Flow routing is the procedure to determine the time and magnitude of flow (i.e., the flow hydrograph) at a point on a watercourse from known or assumed hydrographs at one or more points upstream (Chow et al., 1988).

Routing reaches represent the natural streams in the system, and the lag and attenuation of flow is performed in HEC-ResSim using one of a handful of hydrologic routing methods such as Muskingum routing, Modified Puls routing, Coefficient routing, Muskingum-Cunge prismatic channel routing, Muskingum-Cunge 8pt channel routing, Stream flow Synthesis and Reservoir Regulation (SSARR) routing, or variable lag and K routing methods, each with its own set of parameters. Losses through seepage can be specified for each reach. For this study, due to the lack of a set of parameters for other hydrological routing methods, the Muskingum routing method was applied.

The Muskingum method is a commonly used routing method for handling a variable discharge-storage relationship (Chow et al., 1988). The Muskingum routing method requires three parameters: Muskingum K, Muskingum X, and the number of sub-reaches. The K parameter is the travel time of the flood wave through the reach, the X parameter is used to model the attenuation of the flood wave due to channel and overbank storage, and the number of sub-reaches is an additional parameter that affects the amount of attenuation through the reach. The X parameter is dimensionless and can vary from 0.0 to 0.5. A value of 0.0 maximizes attenuation of the flood wave, and a value of 0.5 does not attenuate the flood wave (direct translation of the hydrograph through the reach) (Klipsch et al., 2011). The Muskingum K parameter was determined by evaluating the time of peak flows at upstream and downstream gaged locations (observed inflow and outflow hydrograph) for the different historic events modeled in this study. One Muskingum K parameter was selected that provided the best estimate of travel time from all considered flood events. The Muskingum X parameter is typically set by calibrating the model to observed discharge.

This method models the storage volume of flooding in a river channel by a combination of wedge ($KX(I-Q)$) and prism storage (KQ) (Chow et al, 1988).

$$S = KQ + KX(I-Q) = K\big(XI + Q(1-X)\big) \qquad 3.4$$

$$S_j = K\left(XI_j + Q_j(1-X)\right) \quad 3.5$$

$$S_{j+1} = K\left(XI_{j+1} + Q_{j+1}(1-X)\right) \quad 3.6$$

$$S_{j+1} - S_j = \left(K\left(XI_{j+1} + Q_{j+1}(1-X)\right) - K\left(XI_j + Q_j(1-X)\right)\right) \quad 3.7$$

$$Q_{i+1} = C_1 I_{j+1} + C_2 I_j + C_3 Q_j \quad 3.8$$

$$C_1 = \frac{\Delta t - 2KX}{2K(1-X) + \Delta t} \quad 3.9$$

$$C_2 = \frac{\Delta t + 2KX}{2K(1-X) + \Delta t} \quad 3.10$$

$$C_3 = \frac{2K(1-X) - \Delta t}{2K(1-X) + \Delta t} \quad 3.11$$

3.3.1.4.Simulation module

The third module in the HEC-ResSim modeling process was the simulation module. This step involved performing computations and viewing results based on the established reservoir network, input data, and developed alternatives. The simulation window included parameters such as the starting time, lookback period (allowing the model to reach equilibrium or 'warm-up' before the starting simulation time), and end time of the simulation. In this research, the simulation was undertaken from 1981 to 2016, among which the first one year (1981) was used as a warm-up period. HEC-ResSim created a directory structure within the base folder of the watershed to represent the simulation. This simulation tree contained a copy of the watershed, including only the necessary files for the selected alternatives. Additionally, a simulation.dss file was generated within the simulation, which stored all the DSS records representing input and output data for the chosen alternatives. The simulation window also allowed for editing and saving of elements and alternatives for subsequent simulations. Figure 3.11 clearly shows the HEC-ResSim modeling framework.

3.3.1.5.Input data required for HEC-ResSim model

Generally, the model uses three types of data, i.e., hydrologic time series data that will be kept in HEC-DSSVue storage system and physical and operational data. Moreover, the GIS data as a shape file and layers, i.e., basin boundary, stream network, reservoir locations, lake locations, and other geo-referenced data, are required. Water demand (withdrawal) was considered at different existing and proposed irrigation demand sites. The irrigation water demands, including potential irrigable land, were collected from the Abbay river basin master plan, ENTRO toolkit.

Hydrologic time series data: Stream flows are mainly owned by the hydrology department of the Ethiopian Ministry of Water and Energy. Most hydrometric stations in the Abbay river basin are located on tributaries and secondary streams that have short recording periods with missing data (Conway, 2000; UNESCO, 2004). Considering data shortage, inadequacy, and missing data, hydrological simulation was undertaken using ArcSWAT (water potential assessment section). The simulated result, obtained after calibration and validation, was adopted as input for the HEC-ResSim model in areas where shortages of recorded periods and missing values are problems.

Physical and Operational Data: The physical and operational data of existing and proposed cascade dams and reservoirs were the other input data. These data included reservoir pool definition (elevation-area-storage), outlet capacity curves, hydropower plant data, operational zones, and minimum and maximum release requirements of each project. These data were extracted from their respective feasibility and detail engineering design documentations, Abbay river basin master plane study document, Eastern Nile Technical Regional Office (ENTRO), Ministry of Water and Energy (MoWIE), and Abbay River Basin Authority (ARBA). The elevation-area-storage curves (EAV), in addition to the collected data from the above-mentioned organization, were also generated using the ArcGIS tool.

The regulation planes for most reservoirs are described by a seasonally varying target pool elevation commonly called the guide curve (HEC, 2013). The storage of the reservoir above this target elevation is called the flood control pool. The storage below this guide curve is called a conservation pool. The guidelines for determining the release from the reservoir are then based on where the current pool elevation is in relation to the guide curve. Under basic operation, if the pool elevation is below the guide curve, then the basic objective of the regulator is to reduce the release to refill the pool; if the pool elevation is above the guide curve, the regulator will want to increase

the release to draw down the pool. Additional goals and constraints were then applied to temper such a rigid operation plan.

Operational set (operation plan/scheme upon release decision can be made) in HEC-ResSim network enables to determine the amount of water to be released at each time step of simulation run. The operational set consists of three basic features: zones, rules, and identification of guide curves.

Zones are the operational subdivision of the reservoir pool. These zones are flood control, conservation, and inactive. The flood control zone is storage that is reserved for unexpected floods due to extreme storms that occurred at the upstream catchment of the basin; the conservation zone holds water that is dedicated for the required purpose and downstream flow. The inactive zone is a special zone in the operation set. It represents the dead storage of the reservoir. The reservoir cannot be released from the inactive pool, and rules cannot be applied to this zone.

Rules represent the goal and constraints upon the release(s). Rules can be applied to selected zones of reservoir to describe the different factors influencing the release decision when the reservoir elevation is within each zone.

The guide curve concept is used as a basis for the release decision process in HEC-ResSim. Basic guide curve operation means “get the reservoir pool elevation to the current guide curve elevation as fast as possible, within the physical and operational constraint of the outlets (HEC, 2013). The guide curve was identified by selecting the top of the operational zones to represent the target elevation of the reservoir.

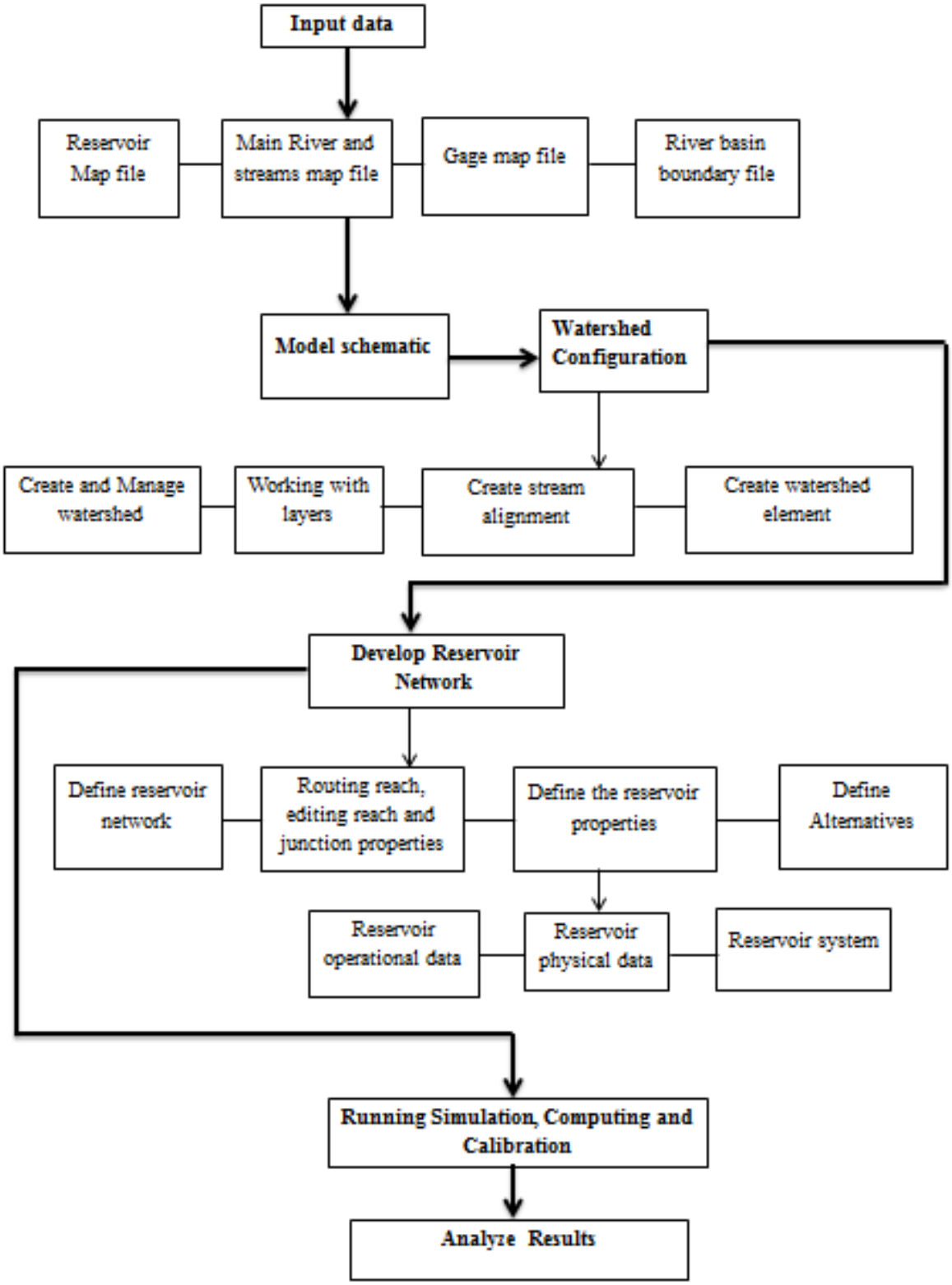

Figure 3.11: HEC-ResSim model framework (own source)

3.3.2. Scenario development

A scenario is a coherent, internally consistent, and plausible description of a possible future state. It is important to note that a scenario is not a forecast but rather a representation of one alternative image of how the future can unfold (Thornes, 2002). For this study, various scenarios were formulated, considering the current and proposed hydropower projects and irrigation expansion.

Abbay River Basin is home to several water resource development projects, each at different stages of progress. The basin could potentially generate up to 78,820 GWh/year gross hydroelectric potential (Awulachew et al. 2007), 38% of the country's total hydropower generation potential (ABA, 2016). As part of this study, three proposed hydropower dams upstream of GERD (Karadobi, Bekoabo, and Mandaya) have been taken into consideration for scenario development. In addition to hydropower potential, the Abbay basin has been assessed for its potential irrigable area. Research studies and feasibility reports have indicated different estimates for the potential irrigation areas in the basin, such as ENTRO (2006) (978,000 ha), WAPCOS (1990) (1,001,000 ha), MoWE recent study (815,581 ha), and Yimere & Assefa (2021) (738,183 ha). The previous research was depending on the land slope classes, method of irrigation, and economic viability at the time of the study. With the advancement of economy and technologies, the irrigation method and slope of agricultural land are expected to change. Thus, the potential irrigation area obviously will not be limited to the previous studies. Considering the future advancement in technology and irrigation methods, for this study, the irrigation area of 1.2 million ha was considered to capture the potential irrigation development scenario.

Two major scenarios with sub-scenarios were formulated. The first major scenario (S-1) focused on the Abbay river basin without irrigation water diversion. It ranged from the natural condition of the basin used for calibrating the HEC-ResSim model to assessing energy production in the full cascade of four major hydropower projects. Four sub-scenarios, i.e., S-1.1, S-1.2, S-1.3, and S-1.4, were developed. S-1.1 was formulated by considering only the GERD hydropower project. Sub-scenario S-1.1 evaluated the monthly and annual energy generation capacity and reservoir operation of the GERD hydropower project. It assumed that the diversion from Lake Tana for Beles HP would not affect GERD's hydropower production since the diverted water would eventually join the main Abbay River upstream of GERD. S-1.2, S-1.3, and S-1.4 were formulated by adding one additional hydropower project from the existing cascade system, as shown in Table

3.1. Thus, the first major scenario was aimed at assessing the energy generation capacity and reservoir operation of four hydropower projects both at the individual and system-wide level.

In the second major scenario (S-2), irrigation water diversion was included in the reservoir networks. The irrigation water requirement for the Abbay river basin was collected from the Eastern Nile Technical Regional Office (ENTRO) and the Ministry of Water and Energy (MoWE). The volume of irrigation water was then estimated using the irrigation area, and the computed annual irrigation water was indicated in Figure 3-12. This allowed for the assessment of water availability in the cascade reservoirs and the trade-off between energy generation and irrigation development. Subsequently, six sub-scenarios (S-2.1, S-2.2, S-2.3, S-2.4, S-2.5, and S-2.6) were developed under S-2 by considering the progressive expansion of irrigation development. From S-2-2.1 to S-2.4, the irrigation area considered was based on their respective current status (under construction, design phase, feasibility study completed and prefeasibility study). In the last three sub-scenarios (S-2.4, S-2.5, and S-2.6), the cascade of hydropower projects is similar, while irrigation development is in an incremental trend. The last three scenarios were aimed at assessing how the energy production from four cascade hydropower projects was affected by the progressive expansion of irrigation, reaching the potential irrigable area of the basin. Generally, the main objective of S-2 was to evaluate the trade-off and economic synergy between hydropower generation and irrigation development.

Table 3.1: Cascade of hydropower and considered irrigation areas in each stage of scenario

S-1	Reservoir cascade					
S-1.1					Tana	GERD
S-1.2				Tana	Karadobi	GERD
S-1.3			Tana	Bekoabo	Karadobi	GERD
S-1.4		Tana	Mandaya	Bekoabo	Karadobi	GERD

S-2	Reservoirs cascade					Irrig. area (*10^3 ha)
S-2.1				Tana	GERD	230
S-2.2			Tana	Karadobi	GERD	313
S-2.3		Tana	Bekoabo	Karadobi	GERD	424
S-2.4	Tana	Mandaya	Bekoabo	Karadobi	GERD	526
S-2.5	Tana	Mandaya	Bekoabo	Karadobi	GERD	800
S-2.6	Tana	Mandaya	Bekoabo	Karadobi	GERD	1,200

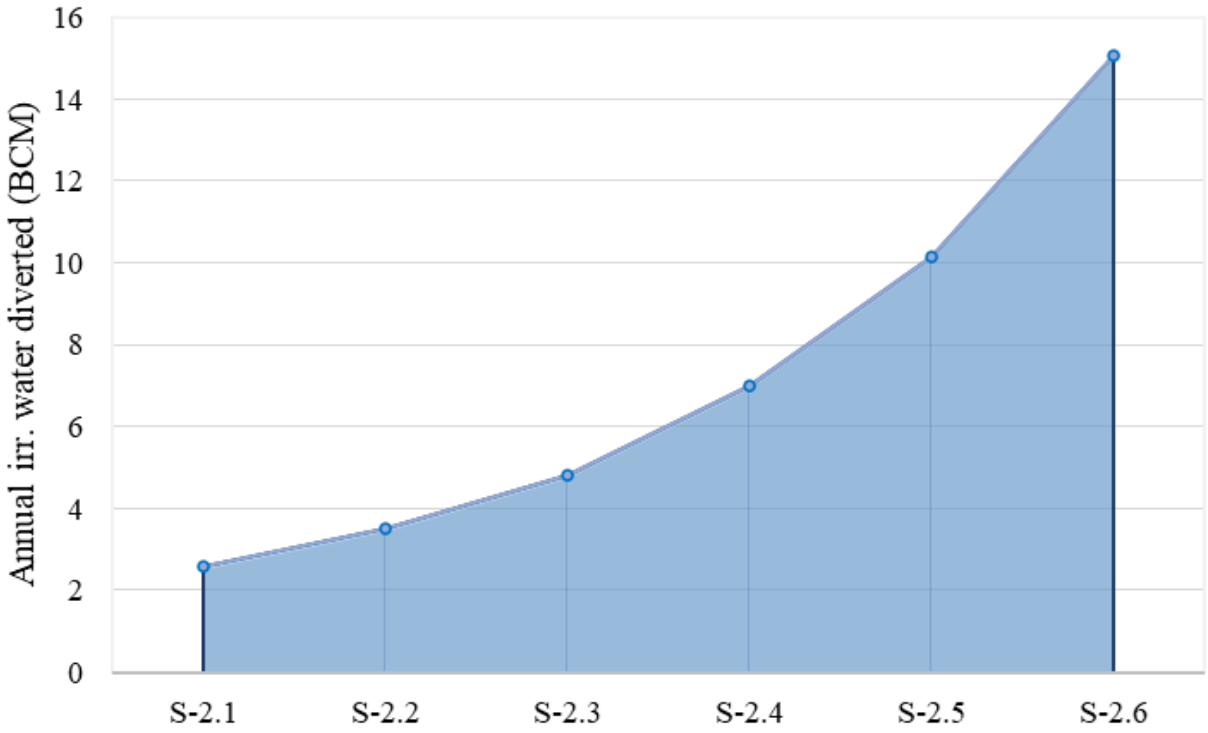

Figure 3.12: Annual irrigation water requirement for each proposed irrigation area as shown in Table 3.1

3.3.3. Hydro-economic trade-off analysis

Hydro-economic analysis serves the purpose of evaluating the impacts of infrastructure and policy measures created to address challenges in water management (Kahil et al., 2015) and identifying prospects for enhancing and optimizing overall benefits within a basin (Hossen et al., 2021). It is crucial to consider economic benefit assessments of both current and upcoming water initiatives, as well as different strategies for managing water resources (Ortiz-Partida et al., 2023). Understanding the economic trade-offs between the development of hydropower and irrigation in the Abbay river basin is thus crucial in understanding how the value of one objective can be augmented at the expense of the other. This evaluation aimed at the fundamental analysis of the combined benefits derived from the quest of these two objectives.

The hydro-economic trade-off analysis was achieved by formulating various development scenarios as shown in Table 3.2. The first scenario focused solely on GERD hydropower, integrated with six progressive irrigation development scenarios. This scenario emphasizes the

implications of different scales of irrigation expansion alongside the GERD energy generation. The second scenario encompasses two hydropower projects, namely the GERD and Karadobi, in conjunction with five irrigation development scenarios. This comparison sheds light on the trade-offs between multiple cascade hydropower projects and varying scales of integrated irrigation development. The third scenario extends the scope further by incorporating three hydropower projects, namely the GERD, Karadobi, and Bekoabo, coupled with five irrigation development scenarios. This extension enables a more comprehensive understanding of the hydro-economic dynamics associated with a combination of multiple hydropower projects and varying scales of irrigation development. The last scenario presents a holistic view encompassing the potential development of four major hydropower projects (GERD, Karadobi, Bekoabo, and Mandaya) and four irrigation development scenarios. The detailed analysis captures the trade-offs and synergies arising from the combined development of multiple hydropower projects integrated with a significant scale of irrigation development.

Table 3.2: Hydropower and irrigation development scenario for hydro-economic trade-off analysis

Hydropower cascade scenario				Irrigation development scenario (*10^3 ha)					
				S-1	S-2	S-3	S-4	S-5	S-6
GERD				230	313	424	526	800	1,200
GERD	Karadobi				313	424	526	800	1,200
GERD	Karadobi	Bekoabo			313	424	526	800	1,200
GERD	Karadobi	Bekoabo	Mandaya			424	526	800	1,200

Different previous research over the basin considered various values of water for irrigation and hydropower. Digna et al. (2018) utilized the price of hydropower generation at 0.08 USD/kWh and the value of water released for irrigation at 0.05 USD/m^3. Whittington et al. (2005) assumed the economic value of irrigation between 0.01-0.25 USD/m^3 depending on the crop typologies. Bashe et al. (2022) estimated the economic value of irrigation water for the upper Blue Nile basin, specifically for Koga large-scale irrigation, as 0.074 USD/m3. Similarly, Jeuland et al. (2010) have also employed values of 0.07 and 0.1 USD/kWh for hydropower prices, without and with power trade between countries, respectively. In NBI (2020) and NBI (2022), it is reported that the

irrigation value of water typically varied from crop to crop between 0.09 and 0.89 USD/m3 in the Nile basin countries.

For this study, the present price of hydropower at 0.08 USD/kWh was considered. However, the economic return of irrigation water was considered based on the current price of agricultural products. Over the basin, different crops have been growing, and the return per hectare also varied from crop to crop. As this study mainly focused on evaluating the trade-off and synergy between water-hydropower and irrigation, the economic return of irrigation was determined by considering wheat as the dominant crop. Thus, the economic return of irrigation water was estimated based on the yield of wheat (ton/ha) and its present sale price. In Ethiopia, the average wheat yield in 2021 was 3 tons/ha (CSA, 2021), and Zegeye et al. (2020) estimated an average potential of 5 tons/ha in highland areas of the country.

Thus, to be concise, for this study, the economic return of irrigation water was estimated by considering average wheat production of 4 tons/ha. The average price of wheat in 2022 was 0.75 USD/kg (https://www.tridge.com/intelligences/wheat/ET/price), which was applied as the present price in this research. Accordingly, the value of irrigation was found to be 0.27 USD/m3 which is consistent with the previous research.

Therefore, the benefits of irrigation development were assessed using the economic value of irrigation water based on crop prices, and the hydropower benefits were calculated using the price per energy unit (price/Kwh). Initially, the hydropower benefits for each cascade scenario were calculated without accounting for irrigation development. These calculations provided a baseline for understanding how energy production and corresponding benefits decrease with the expansion of irrigation areas. Subsequently, the energy generation for each hydropower project was simulated under various irrigation water diversion scenarios, as presented in Table 3.2. The volume of water diverted for irrigation corresponding to each scenario is illustrated in Figure 3.12. The decrease in HP benefit for each irrigation area development was then calculated to assess the trade-off.

The combined benefits were then assessed by summing the benefits obtained from the simultaneous development of hydropower and irrigation.

$$B(1) = P_e \sum_{t,j}^{T,J} KWH_{t,j} \quad 3.12$$

$$B(2) = P_w * Q_w \quad 3.13$$

$$Benefit\{B(1), B(2)\} = \left(P_e \sum_{t,j}^{T,J} KWH_{t,j} + P_w * Q_w \right) \quad 3.14$$

Where, $B(1)$ and $B(2)$ are returns from hydropower generation and irrigation developments respectively. P_e = The price of energy (US$/kwh), P_w (US$/m^3) is the value of irrigation water, $KWH_{t,j}$ is energy generated from reservoir (j) at time (t), J is the total number of dams in the system, Q_w is the total volume of irrigation water (bcm).

This study presents the notion of future value, acknowledging the planned implementation of numerous irrigation and hydropower projects in the Abbay River basin. Additionally, the returns from existing operational projects are not expected to remain constant over time. To accurately assess the future hydro-economic benefits in the basin, it is essential to consider future value. Therefore, future values of irrigation and hydropower were calculated based on the present value, interest rate, and the time periods involved. To be consistent with Ethiopia's 10-year strategic development plan, future periods of 2030, 2040, and 2050 were considered. The interest rate depends on the institution, country, or context in which the rate is applied; it usually varies between 2% and 12% (Baker et al., 2021). In Ethiopia, the ordinary interest rate is 7% (https://tradingeconomics.com/ethiopia/interest-rate), which was applied for this research.

$$FV = PV * (1 + r)^n \quad 3.15$$

Where, FV is the future value, PV is the present value, r is interest rate per period and n is number of periods.

Thus, for this research we have four price values for each development objectives. Present value (P1) and future values P2 (2030), P3 (2040) and P4 (2050). Based on equation 3.15, the future values were calculated. The prices of energy (USD/kwh) of 0.08, 0.12, 0.24, and 0.46 were used for P1, P2, P3 and P4 respectively while the values of irrigation water (USD/m^3) 0.27, 0.41, 0.80

& 1.57 for P1, P2, P3, and P4 were used. These prices were applied for full irrigation development scenario (S-6 as shown in Table 3.2) integrated with different hydropower cascade scenarios.

3.4. SWAT Model performance evaluation

To evaluate the model's performance relative to the observed data, the following performance measures were mostly used: Percent difference between simulated and observed data (P_{bias}), Correlation coefficient (R^2), Nash and Sutcliffe simulation efficiency (E_{ns}) (Nash and Sutcliffe, 1970) and Kling-Gupta Efficiency (KGE).

The percentage difference measures the average difference between the simulated and measured values for a given quantity over a specified period (usually the entire calibration or validation period in the study). The percentage difference can be calculated using the following equation.

$$P_{bias} = 100\left[\frac{\sum_{i=1}^{n} q_{si} - \sum_{i=1}^{n} q_{oi}}{\sum_{i=1}^{n} q_{oi}}\right] \quad 3.15$$

Where,$\mathbf{P_{bias}}$ is the percent of difference, q_{si} is the simulated values in each model time step, q_{oi} is the measured values in each model time step.

The correlation coefficient (R^2) is the square of the Pearson product–moment correlation coefficient and describes the proportion of the total variance in the observed data that can be explained by the model. The closer the value of R^2 to 1, the higher is the agreement between the simulated and the measured flows. It is calculated as using the following equation:

$$R^2 = \frac{[(\sum_{i=1}^{n} q_{si} - \overline{q_s})(\sum_{i=1}^{n} q_{oi} - \overline{q_o})]^2}{\sum_{i=1}^{n}(q_{si} - \overline{q_s})^2 \sum_{i=1}^{n}(q_{oi} - \overline{q_o})^2} \quad 3.16$$

Where, R^2 is the correlation coefficient, q_{si} is the simulated values, $\overline{q_s}$ is the average simulated value, q_{oi} is the measured value, $\overline{q_o}$ is the average measured value, n is the number of computed values.

Nash and Sutcliffe simulation efficiency (E_{Ns}) indicates the degree of fitness of observed and simulated data. The value of E_{NS} ranges from 1.0 (best) to negative infinity. E_{NS} value of 0.0 means the model predictions are just as accurate as using the measured data average to predict the measured data. E_{NS} values less than 0.0 indicates the measured data average is a better predictor

of the measured data than the model predictions while a value greater than 0 indicates the model is a better predictor of the measured data than the measured data average (Dilnesaw, 2006). It is calculated as follows with the same variables defined above:

$$E_{NS} = 1 - \frac{\sum_{i=1}^{n}(q_{oi} - q_{si})^2}{\sum_{i=1}^{n}(q_{oi} - \overline{q_o})^2} \quad 3.17$$

Where, E_{NS} is the Nash and Sutcliffe simulation efficiency, q_{si} is the simulated values, q_{oi} is the measured value, $\overline{q_o}$ is the average measured value, n is the number of computed values.

Calibration for hydrology at a D<15%, R^2 >0.6 and E_{NS}> 0.5 is acceptable (Santhi et al., 2001).

The Kling-Gupta Efficiency (KGE) proposed by Gupta et al. (2009) was also applied since it addresses several shortcomings in NSE and is increasingly used for model calibration and evaluation (Wouter et al., 2019). It was applied to evaluate the performance of the model in reproducing flows at different flow quantiles.

$$KGE = 1 - \sqrt{(\beta - 1)^2 + (\alpha - 1)^2 + (\Upsilon - 1)^2} \quad 3.18$$

Where β is the bias error, α represents the flow variability error, and r shows the linear correlation between simulations and observations.

$$KGE = 1 - \sqrt{\left(\frac{\mu_{sim}}{\mu_{obs}} - 1\right)^2 + \left(\frac{\sigma_{sim}}{\sigma_{obs}} - 1\right)^2 + (\Upsilon - 1)^2} \quad 3.19$$

Where σ_{obs} and σ_{sim} are the standard deviation of observations and simulations respectively.

Table 3.3: Statistics for performance evaluation adopted from Moriasi et al., (2015)

R^2	NSE	P_{bias}	Temporal Scale	Performance Rate
$R^2 > 0.85$	NSE > 0.80	PBIAS < ±5	D-M_A	Very Good
$0.75 < R_2 \leq 0.85$	$0.70 < NSE \leq 0.80$	$\pm5 \leq PBIAS < \pm10$	D-M_A	Good
$0.60 < R^2 \leq 0.75$	$0.50 < NSE \leq 0.70$	$\pm10 \leq PBIAS < \pm15$	D-M_A	Satisfactory
$R^2 \leq 0.60$	$NSE \leq 0.50$	$PBIAS \geq \pm15$	D-M_A	Not Satisfactory

D-M_A denotes Daily, Monthly, and Annual temporal scales, respectively.

In addition to the above-mentioned model performance criteria, the capability of the model to capture uncertainty was also evaluated based on the P-factor and R-factor. In SUFI-2, all sources of uncertainty (i.e., uncertainty due to driving variables, conceptual model, parameter, and measured data) are considered and are quantified by p-factor and R-factor (Abbaspour et al., 2007). The P-factor is the percentage of the measured data bracketed by the 95PPU. This index provides a measure of the model's ability to capture uncertainties. As all the "true" processes are reflected in the measurements, the degree to which the 95PPU does not bracket the measured data indicates the prediction error. Ideally, the P-factor should have a value of 1, indicating 100% bracketing of the measured data, hence capturing or accounting for all the correct processes. The R-factor, on the other hand, is a measure of the quality of the calibration and indicates the thickness of the 95PPU. Its value should ideally be near zero, hence coinciding with the measured data. The combination of P-factor and R-factor together indicates the strength of the model calibration and uncertainty assessment, as these are intimately linked (Arnold et al., 2012). Statistically, the P-factor and R-factor therefore indicate the quality of measured data and the model's capability to capture uncertainties related to data quality. Ideally the range of values as P-factor ~100% and R-factor ~0 indicates good quality of data and the model's ability to capture uncertainty; under less stringent model quality requirements, the P-factor > 0.5 and R-factor < 1.3 are still sufficient (Schuol et al., 2008).

3.5. HEC-ResSim model performance evaluation

The model's performance was assessed by comparing the simulated flow at gauged stations with observed flow data. In this study, the HEC-ResSim model was calibrated for unregulated flows, meaning that the model simulated flow without accounting for reservoir operations in the main channel and tributaries. The unregulated flow was generated by the model using input flood routing parameters, producing outflows as a simulation output. HEC-ResSim automatically simulates unregulated flows by routing inflows through the stream network as if no reservoirs exist, enabling calibration and validation of the model parameters that influence local flows downstream of the reservoirs.

The model's performance was evaluated at two key gauging stations located in the middle (Kessie) and lower (Border) sections of the Abbay River. The calibration period used daily observed and simulated flows averaged on a monthly basis from 1990 to 2007, while the validation period

covered data from 2008 to 2016. To assess the model's accuracy in replicating observed data, three performance metrics were employed: percent bias (Pbias), the correlation coefficient (R^2), and the Nash-Sutcliffe efficiency (Ens) (Nash and Sutcliffe, 1970). Further details on these performance evaluation methods are provided in Section 3.4.

4. Results and discussion

4.1. Water potential Assessment results

In this section, the detailed results regarding the water resource potential in the Abbay river basin were analyzed.

4.1.1. Spatial rainfall distribution

Rainfall across Ethiopia is very seasonal. There are three seasons locally named major rainy season (June–September), which is dominated by major rainfall; Belg (Feb–May) (short rainy season) and Bega (October–January) bring generally dry weather to central and northern Ethiopia (GGU, 2016). These classifications, however, slightly vary in the southern parts of the country, characterized by a bimodal rainfall pattern with rainfall periods from March to May and from September to November (Wogayehu et al., 2018).

For this study, seasons were classified as major rainy season (June-September), minor rainy season (February-May), and dry season (October-January) since the local terms are not repeatable to the international reader. The long-term daily rainfall (1980-2016) from 49 meteorological stations (Figure 3-3) over the basin was averaged on a monthly, seasonally, and annual basis and interpolated by the Inverse Distance Weighting (IDW) method to make spatial surfaces and assess its distribution as shown in Figure 4-1. The annual rainfall varied from 904.51mm to 2161.68mm. Sub-basins such as Didessa, the eastern part of Dabus, Wonbera, the southern part of Anger, the upper part of Beles, the southern and south-eastern part of the Tana basin, and the western part of Gojam received from mid- to high rainfall depth. Central parts (lower part of north Gojam, Welaka, Beshilo, and Jemma), most downstream parts of the basin (near the Ethio-Sudan border), and the south-east parts (Guder and Mugher) are relatively defined by low to mid-rainfall depth. In the major (JJAS) rainy season, the rainfall depth varied from 722.91 mm to 1761.19 mm, while in the minor (FMAM) rainy season it varied from 82.12 mm to 400.19 mm. Regarding percentage of occurrence, from 53.78% to 88.72% of the total annual rainfall occurred from June to September, and the remaining fractions occurred during minor rainy and dry seasons. The long-term average rainfall depicted that 73.4%, 16.43%, and 10.21% of the total annual rainfall occurred in major rainy, minor rainy, and dry seasons, respectively. The results of this research strongly coincide with previous research results (Getachew et al., 2021; Abeer et al., 2019; Erwin et al., 2017).

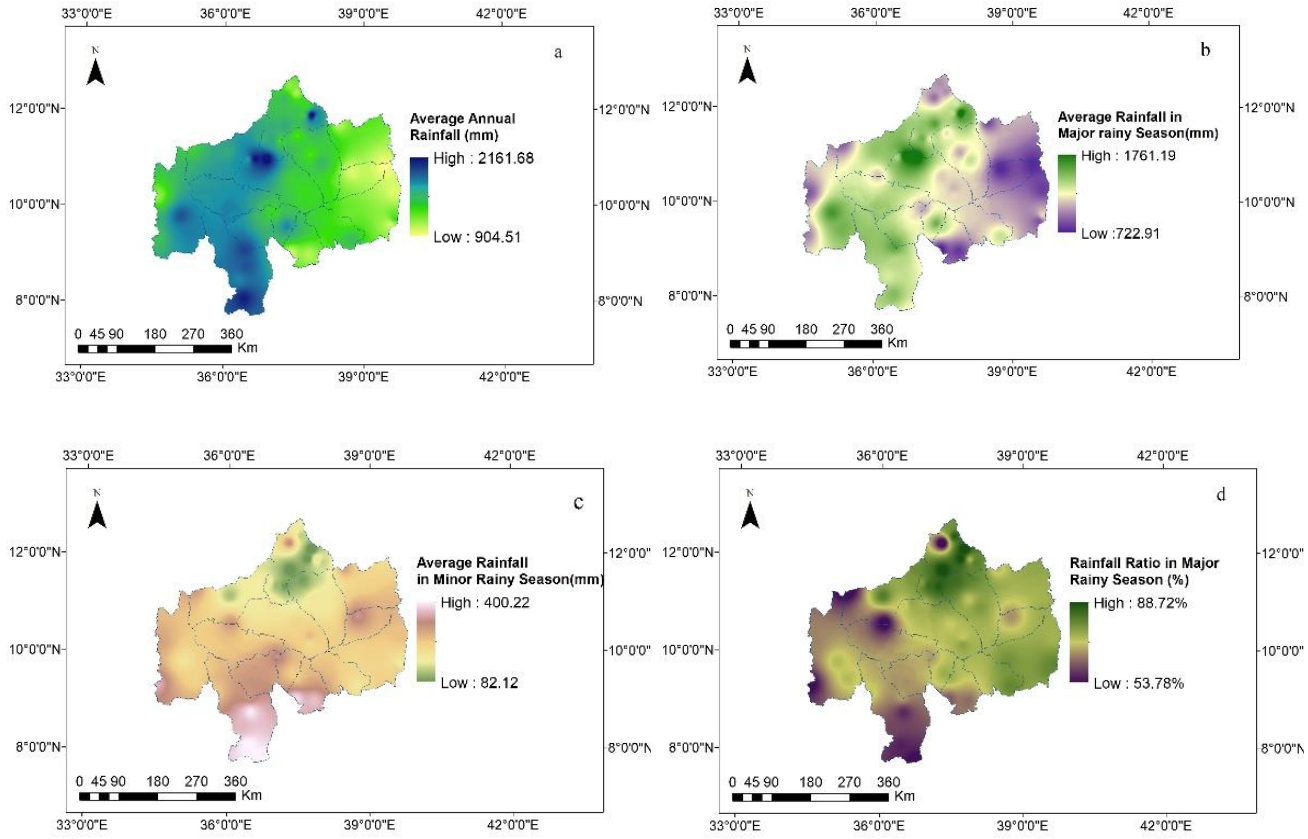

Figure 4.1: Rainfall distribution of Abbay basin (Annual, Seasonal). Major Rainy season (Jun to September), Minor/short rainy season (February to May)

4.1.2. Sensitivity analysis results

There are about 23 physical parameters that control the rainfall-runoff process in the ArcSWAT model (Ashraf and Ahmet, 2013). For the Abbay basin, those 23 parameters were included to identify the most influential ArcSWAT parameters on predicting flow components. Based on the t-test (the larger the absolute value, the more sensitive) and P-value (a value close to zero is more significant), 11 parameters were found to be sensitive for the upper part of the Abbay basin (Table 5-2). Soil Conservation Service (SCS) runoff curve number (A__CN2.mgt) was the most sensitive parameter that affects the simulation result. Available water capacity of the soil layer (SOL_AWC.sol) and surface runoff lag time (V__SURLAG.bsn) were the second and third sensitive parameters controlling the flow simulation. Generally, Table 4.1 indicates the rank of sensitivity of parameters from up to downward.

Table 4. 1: Sensitive parameter and final optimized parameter values for upper part of Abbay basin. The prefix A, R and V indicates the method of adjusting the given values. A_ indicates adding the given values to the existing Values, R_ indicates multiplying the existing Value and V_ indicates the Replacing the existing value with the given value.

Parameter Name	Sensitivity result		Range and optimized values		
	t-Stat	P-Value	Fitted Value	Min	Max.
A__CN2.mgt	5.74	0.01	0.93	-6	10
R_SOL_AWC.sol	-5.44	0.01	0.08	-0.15	0.15
V__SURLAG.bsn	-4.67	0.01	12.67	1	15
V__REVAPMN.gw	4.55	0.02	127	10	400
V__CH_K2.rte	4.03	0.03	172.17	5	300
V__GW_REVAP.gw	-3.66	0.04	0.05	0.02	0.2
V__ESCO.hru	-3.35	0.04	0.56	0	0.8
V__RCHRG_DP.gw	-3.18	0.05	0.21	0	0.9
V__GWQMN.gw	-2.95	0.06	2850	500	3000
V__CH_N2.rte	-2.59	0.08	0.25	0.01	0.3
V__EPCO.bsn	-2.55	0.08	0.51	0	0.8

For the lower part of the Abbay river basin before calibration and validation at each gauge point was undertaken, sensitivity analysis was done for the entire basin from Kassie to the border by considering border gauge station. Table 4.2 indicated the sensitivity analysis results ranked with their level of sensitivity and significance. Like the upper parts of the basin, 11 parameters were found to be sensitive for the lower parts of the basin. SCS runoff curve number (A__CN2.mgt) and available water capacity of the soil layer (SOL_AWC.sol) were the first and second most sensitive parameters. From both the upper and lower parts of the sensitivity analysis result, the final fitted value for effective channel hydraulic conductivity (CH_K2.rte) seems high. According to Arnold et al. (2012), the result of this research revealed that the riverbed over the Abbay basin is characterized by moderate to very high loss rates. Tables 4.1 and 4.2 illustrated that sensitive parameter types were found to be similar in both the upper and lower parts of the Abbay River basin. However, their sensitivity ranks varied from upper to lower, except for the first and last two

parameters. Those sensitive parameters (Table 4.2) were used for calibration and validation at Didessa, Beles, anger, Birr, Guder, Muger, and Fetam gauge stations. The final fitted values of parameters for seven sub-basins are shown in Table 4.3. The result confirmed that though similar sensitive parameter types were used for calibration, their final fitted values were different across seven sub-basins. This indicates the various characteristics of sub-basins such as topography, land management practices, or rainfall patterns.

Table 4. 2: Sensitivity analysis results for lower part of Abbay (Border as outlet). The prefix A, R and V indicates the method of adjusting the given values. A_ indicates adding the given values to the existing Values, R_ indicates multiplying the existing values and V_ indicates the replacing the existing value with the given value.

Parameter Name	t-Stat	P-Value
A__CN2.mgt	5.89	0.00
R_SOL_AWC.sol	-2.59	0.01
V__RCHRG_DP.gw	-2.53	0.02
V__GWQMN.gw	2.45	0.03
V__SURLAG.bsn	-2.43	0.05
V__REVAPMN.gw	-2.41	0.80
V__CH_K2.rte	-1.39	0.13
V__GW_REVAP.gw	1.38	0.15
V__ESCO.hru	-1.33	0.16
V__CH_N2.rte	1.27	0.25
V__EPCO.bsn	1.24	0.30

A_ indicates adding the given values to the existing Values, **R_** indicates multiplying the existing Value and **V_** indicates the Replacing the existing value with the given value

Table 4. 3: Sensitive parameter and final optimized parameter values for lower part of Abbay basin. The prefix A, R and V indicates the method of adjusting the given values. A_ indicates adding the given values to the existing Values, R_ indicates multiplying the existing Value and V_ indicates the Replacing the existing value with the given value.

	Range		Fitted Value							
Parameter Name	Min.	Max.	Border	Didessa	Beles	Birr	Fetam	Anger	Guder	Muger
A__CN2.mgt	-15.00	15.00	-6.25	-11.50	-5.15	6.18	10.75	-12.75	-2.95	-5.25
R_SOL_AWC.sol	-0.15	0.15	0.09	0.10	0.08	-0.11	0.12	0.07	-0.10	0.11
V__RCHRG_DP.gw	0.00	0.90	0.34	0.20	0.13	0.09	0.52	0.06	0.73	0.52
V__GWQMN.gw	1000.00	4000.00	2750.00	2100.00	2400.80	1800.00	1750.55	2045.35	1965.56	2345.72
V__SURLAG.bsn	1.00	20.00	9.67	7.67	3.67	6.50	5.52	11.54	6.54	4.67
V__REVAPMN.gw	10.00	400.00	253.75	353.75	162.50	52.45	102.05	122.30	63.20	73.80
V__CH_K2.rte	10.00	200.00	130.76	135.76	35.76	102.40	82.68	167.65	107.78	57.78
V__GW_REVAP.gw	0.02	0.20	0.05	0.01	0.03	0.12	0.14	0.15	0.05	0.07
V__ESCO.hru	0.00	0.80	0.18	0.20	0.09	0.45	0.51	0.03	0.32	0.16
V__CH_N2.rte	0.01	0.30	0.19	0.11	0.10	0.02	0.08	0.14	0.17	0.07
V__EPCO.bsn	0.00	0.80	0.06	0.08	0.04	0.20	0.09	0.03	0.23	0.56

A_ indicates adding the given values to the existing Values**, R_** indicates multiplying the existing Value and **V_** indicates the Replacing the existing value with the given value.

4.1.3. Calibration and validation result

The performance of the ArcSWAT model at border gauge station indicated R^2 (0.79) and NSE (0.76), and the validation result verified R^2 (0.72) and NSE (0.71), while at Kessie gauge station R^2 (NSE) was 0.74 (0.69) during calibration and 0.73 (0.69) during validation. The model was also calibrated and validated at various major tributaries where measured gauge data are available. This is important to assess the spatial water potential availability throughout the entire Abbay basin, starting from the most upstream sub-basin (Lake Tana sub-basin) to the border. Thus, the ArcSWAT model's applicability was assessed at seven sub-basins (Beles, Anger, Didessa, Birr, Guder, Mugher, and Fetam). As indicated in Table 4.4, the performance of the model varied between sub-basins. At the calibration stage, R^2 varied from 0.71 (Birr) to 0.82 (Didessa) and NSE from 0.61 (Guder) and 0.8 (Didessa and Mugher), while at the validation stage, R2 varied from

0.69 (Guder) to 0.8 (Didessa) and NSE from 0.63 (Guder) and 0.75 (Beles, Birr, and Mugher). The least model performance was shown at the Guder subbasin. In some calibration points, nonetheless, the input parameters were similar; the model was better performed at the validation stage than at the calibration stage, and the reverse was true for other gauge points. This performance variation may possibly be due to differences in quality of data, mainly the rainfall and measured flows, in the calibration and validation stages. The meteorological and hydrological data quality may be subject to several errors, such as incorrect or inaccurate data entered, mistyped data, malfunctioning of instrumentation, inadequate documentation, human errors, and anomalies in the field data collection, periodic malfunctioning of sensors, abnormal values, and data gaps (Faybishenko et al., 2021). The performance of the ArcSWAT model was also evaluated based on its capability to capture uncertainties with 95PPU using p_factor and r_factor. For the upper part of the Abbay basin, the p-factor and r-factor were 0.73 (73%) and 0.81, respectively. For the lower part of the Abbay basin, the p-factor and r-factor were 0.74 (74%) and 1.03, respectively. Based on Schuol et al. (2008), in which p-factor > 0.5 and r-factor 1.3 are sufficient, the ArcSWAT model achieved the acceptable range.

Table 4. 4: Calibration and Validation Statistics of various gauge locations. The negative and positive P_{bias} (%) value indicates overestimation and underestimation of flows respectively.

Gauge	Cal-Daily		Val-Daily		Cal-Monthly		Val-Monthly		
	R^2	NSE	R^2	NSE	R^2	NSE	R^2	NSE	P_{bias}
Border	0.79	0.76	0.72	0.71	0.83	0.80	0.77	0.75	-10.09
Kessie	0.74	0.69	0.73	0.69	0.86	0.82	0.87	0.85	-9.70
Beles	0.75	0.73	0.76	0.75	0.89	0.85	0.88	0.86	-11.32
Didessa	0.82	0.80	0.80	0.71	0.90	0.81	0.89	0.88	-3.50
Birr	0.71	0.70	0.79	0.75	0.86	0.84	0.93	0.89	-8.56
Fetam	0.73	0.72	0.74	0.70	0.88	0.86	0.88	0.84	-13.00
Anger	0.79	0.73	0.76	0.69	0.88	0.84	0.86	0.78	-12.59
Guder	0.72	0.61	0.69	0.63	0.88	0.79	0.89	0.83	-10.17
Mugher	0.81	0.80	0.79	0.75	0.85	0.83	0.82	0.81	-10.46

The model efficiency was also evaluated based on the percentage of difference between simulated and measured values. The graphical visualization (Figure 4.2, Figure 4.3) showed that the ArcSWAT model was both underestimated and overestimated in various calibration and validation periods. The model particularly lacks the ability to capture peak flows in some periods and overestimate the peak flow in some other period. However, the aggregated differences between measured and simulated values over the entire calibration and validation period revealed overestimation of flow (Table 4.4). Pbias values oscillated between -3.5% and -13%. The negative values showed the overestimation of the model. The minimum absolute value (3.5%) was for Didessa while the maximum absolute value (13%) was for Lower Fetam gauge station. Overall, the model performed well, falling within the tolerable ranges defined by Moriasi et al. (2015). Previous researches done over the Abbay River basin using the ArcSWAT model (Meseret et al., 2020; Wakjira et al., 2020; Belay et al., 2021; Gemechu et al., 2021; Gebiyaw et al., 2021) were also within the acceptable ranges. The calibration and validation of this research at a daily time scale also showed good performances after being evaluated with multiple criteria. Generally, from the statistical performance criteria and graphical visualization, it can be concluded that the ArcSWAT model has the capacity to simulate flows that agree with the measured values and is applicable over the Abbay River basin at different spatial scales. The simulated discharge may be used as an alternative data source in areas where measured flow is not available or a high missed value is a problem for the intended purpose.

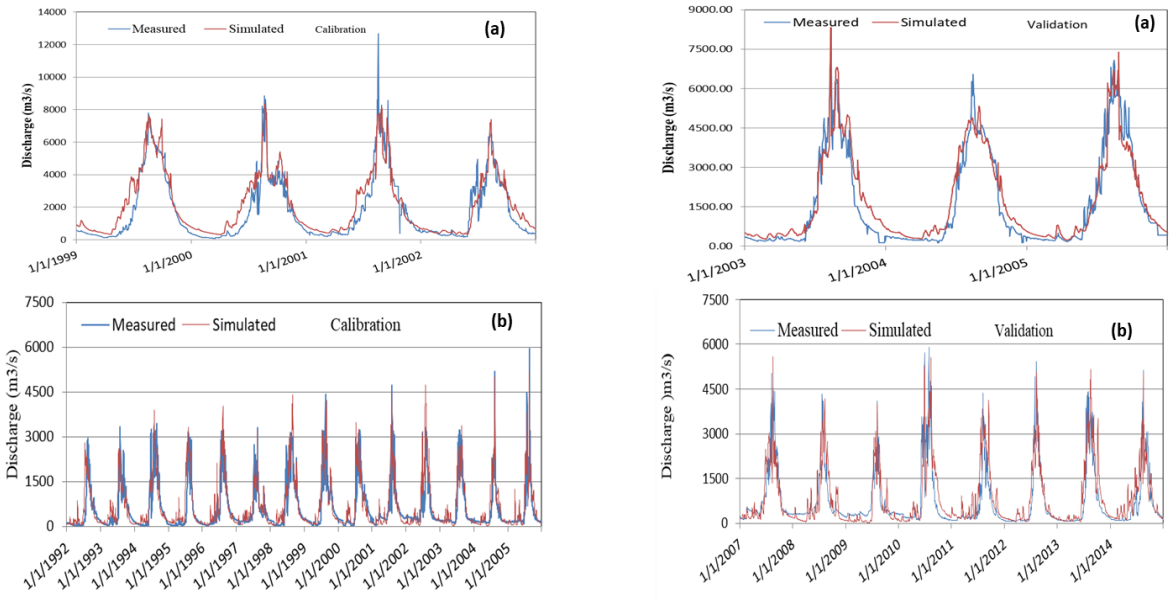

Figure 4.2: Daily Calibration and Validation at Border (a) and Kessie (b) gauge station

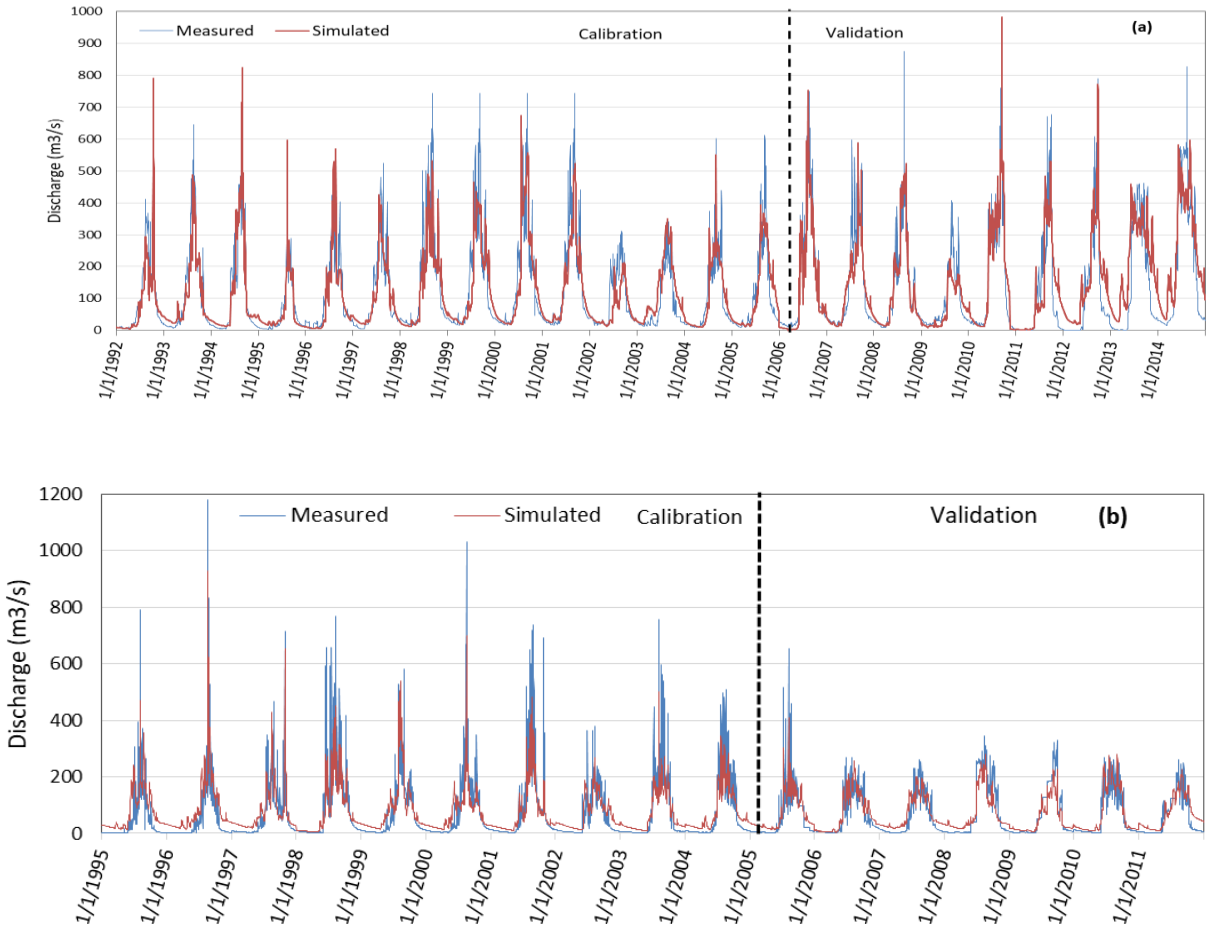

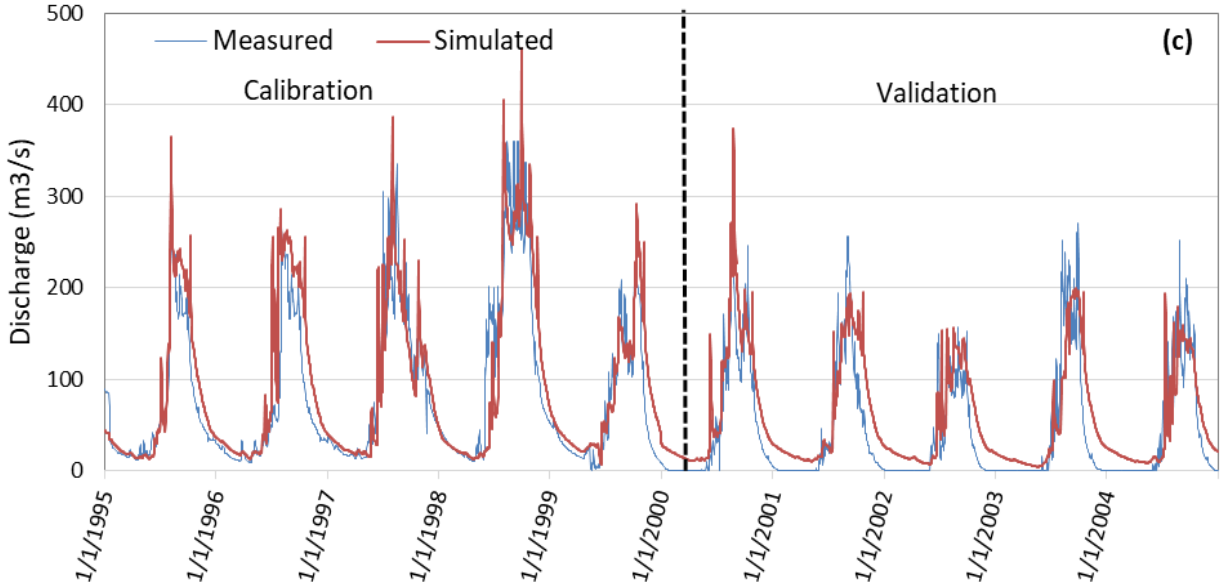
Measured
Simulated
Calibration
Validation
(c)
Discharge (m3/s)
500
400
300
200
100
0
1/1/1995
1/1/1996
1/1/1997
1/1/1998
1/1/1999
1/1/2000
1/1/2001
1/1/2002
1/1/2003
1/1/2004

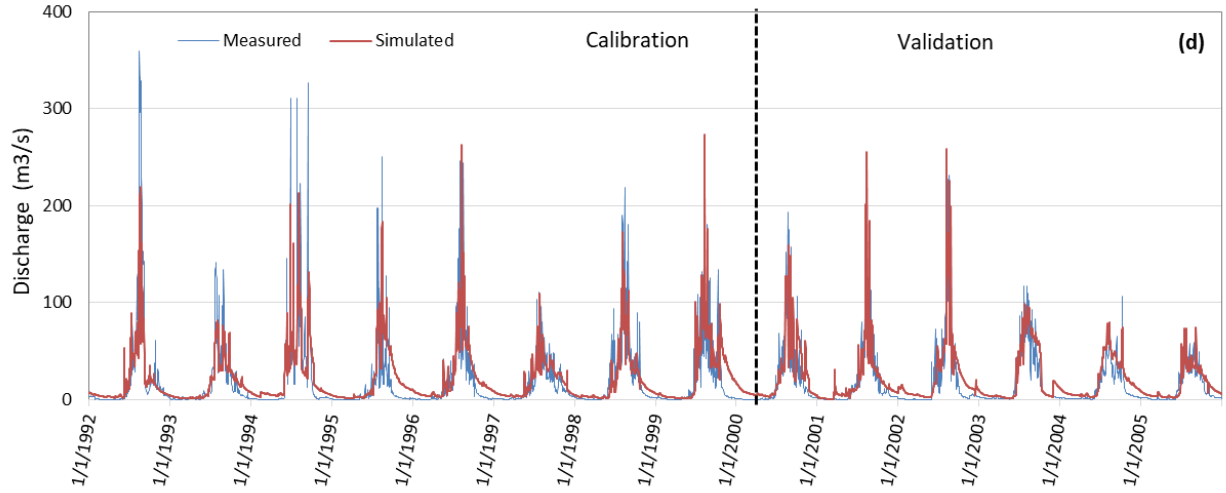
Measured
Simulated
Calibration
Validation
(d)
Discharge (m3/s)
400
300
200
100
0
1/1/1992
1/1/1993
1/1/1994
1/1/1995
1/1/1996
1/1/1997
1/1/1998
1/1/1999
1/1/2000
1/1/2001
1/1/2002
1/1/2003
1/1/2004
1/1/2005

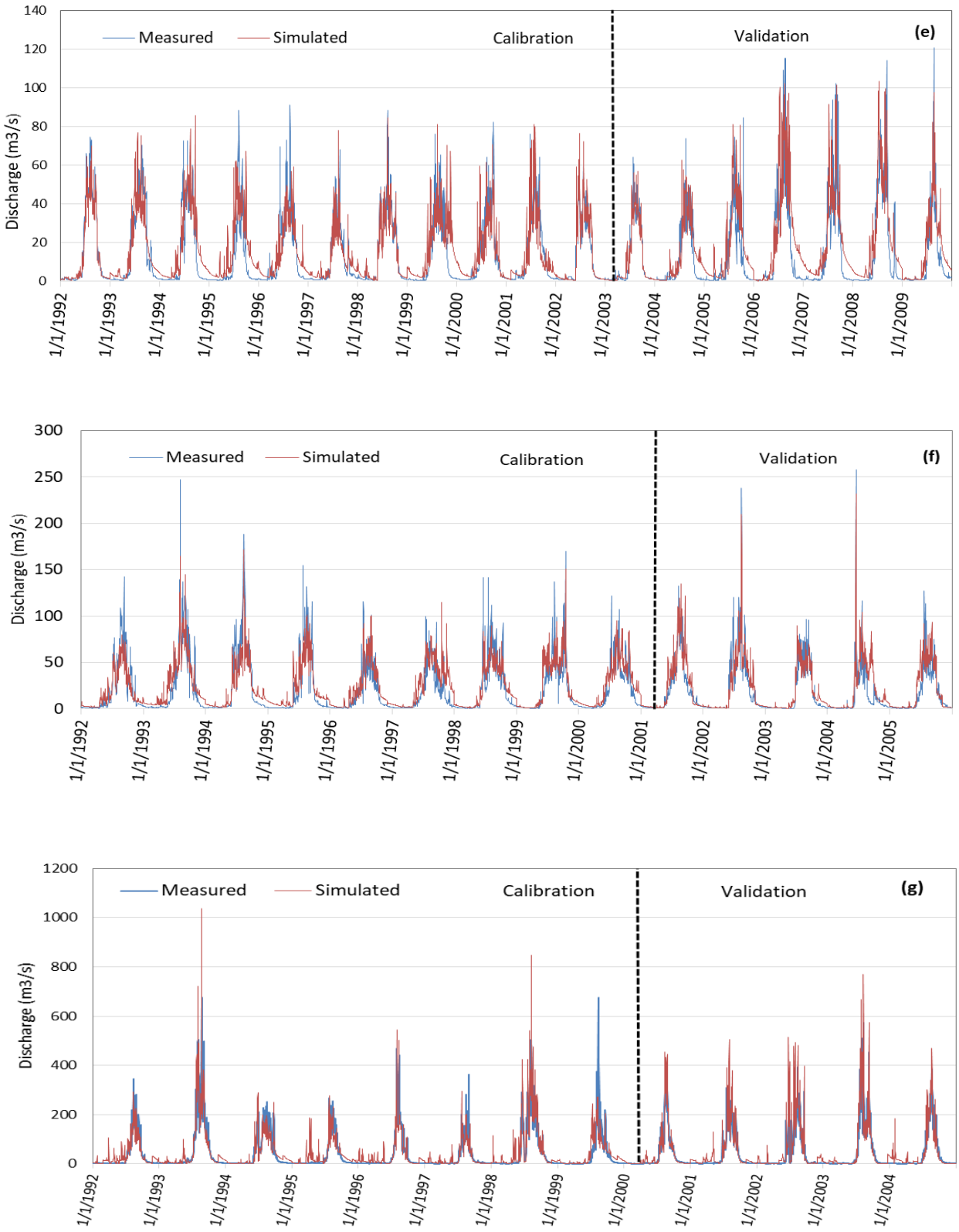

Figure 4.3: Calibration and Validation at different Gauge Stations located on Major Tributaries. Didessa (a), Beles (b), Anger (c), Birr (d), Guder (e), Fetam (f), Mugher (g)

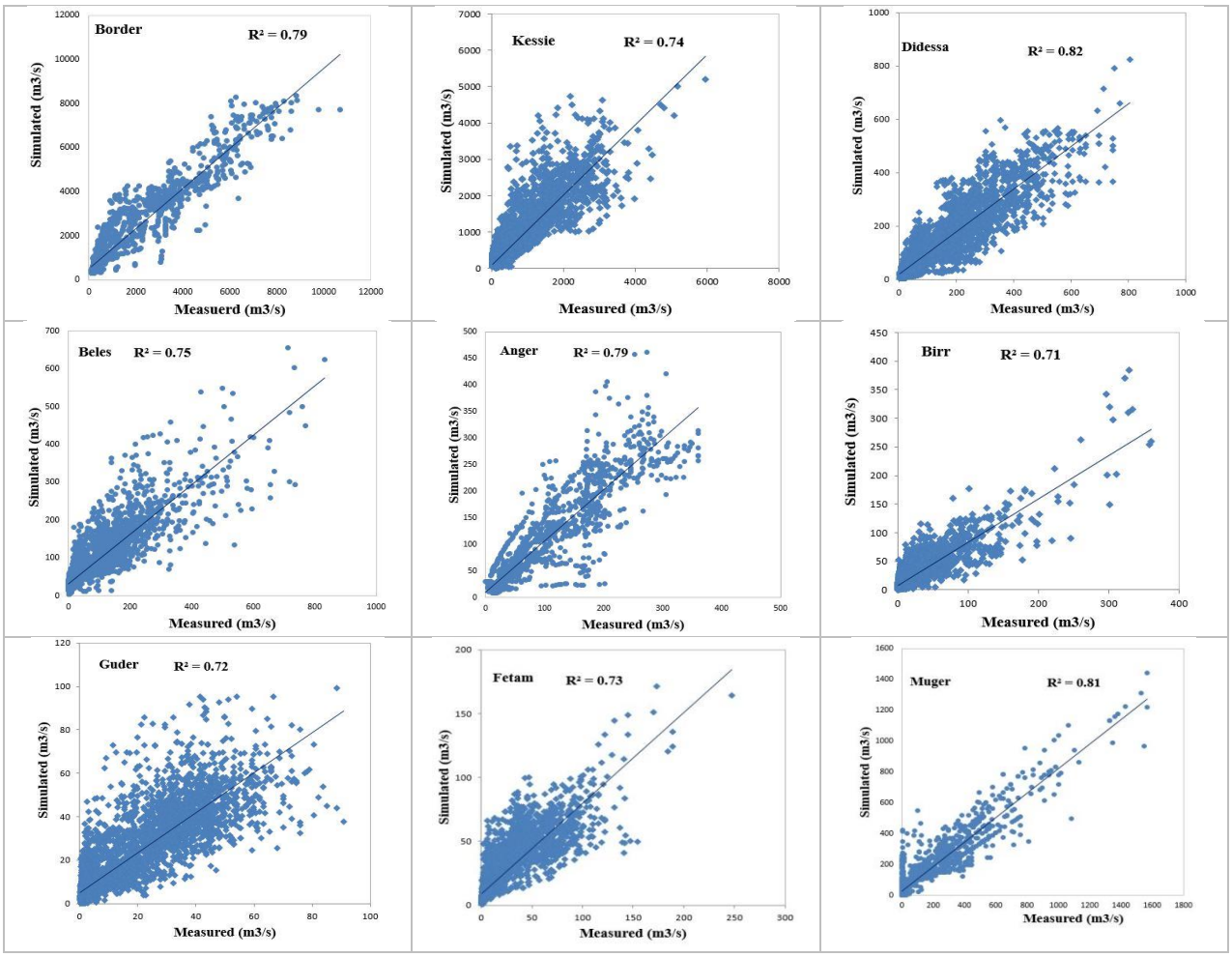

Figure 4. 4: Scatter Plots of Measured and Simulated flow at Calibration Stages.

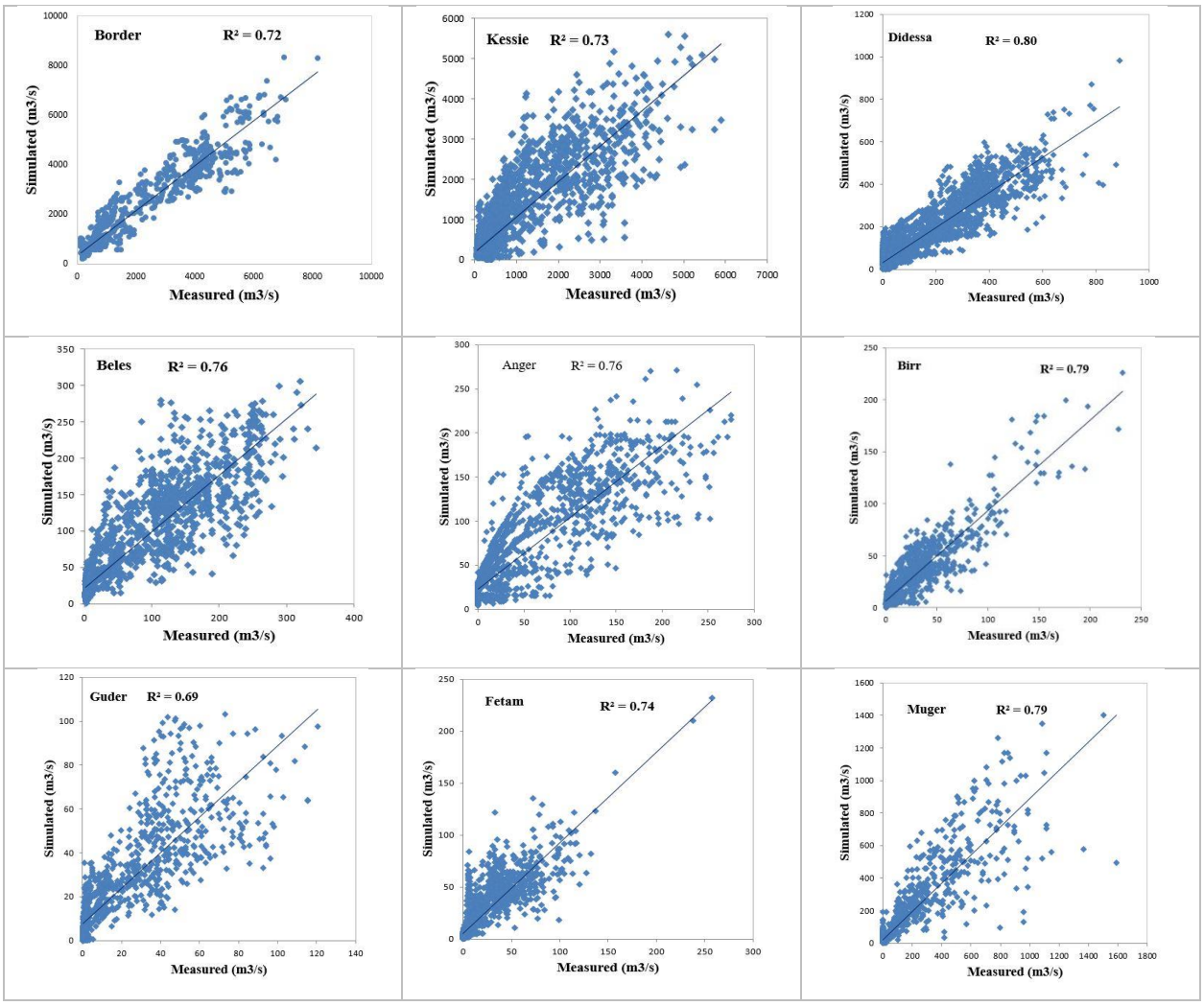

Figure 4.5: Scatter plots of measured and simulated flow at validation stage.

4.1.4. ArcSWAT performance at different quantile domain

The previous performance evaluation (Table 4.4) was based on aggregated simulated and measured flows for the entire calibration and validation periods. Evaluating the performance of the ArcSWAT model with various quantile domains is essential. This allowed us to evaluate the model's ability to simulate various segments of the hydrograph governed by different hydrological processes (Vinod et al., 2018). Flow-duration curve (FDC) is an important tool for evaluating model performance since it assists in evaluating the reproduction of discharges of different magnitudes (Yokoo and Sivapalan 2011) and is used for hydrological behavior interpretation (Thalli et al., 2020). Figure 4.6 showed the Flow Duration curve (FDC) of various simulations and measured flow combinations at two major gauge points (Kessie and border gauge stations). The

flow duration curve covers the daily data from 1999-2005 (Border) and 1992-2014 (Kessie), which is similar for the data period used in Figure 4.2. From graphical visualization, it can be concluded that in most flow segments, the model overestimates as compared to the measured value. The percent of bias (Pbias) indicated in Table 4.5 also supported the graphical visualization regarding overestimation of the model.

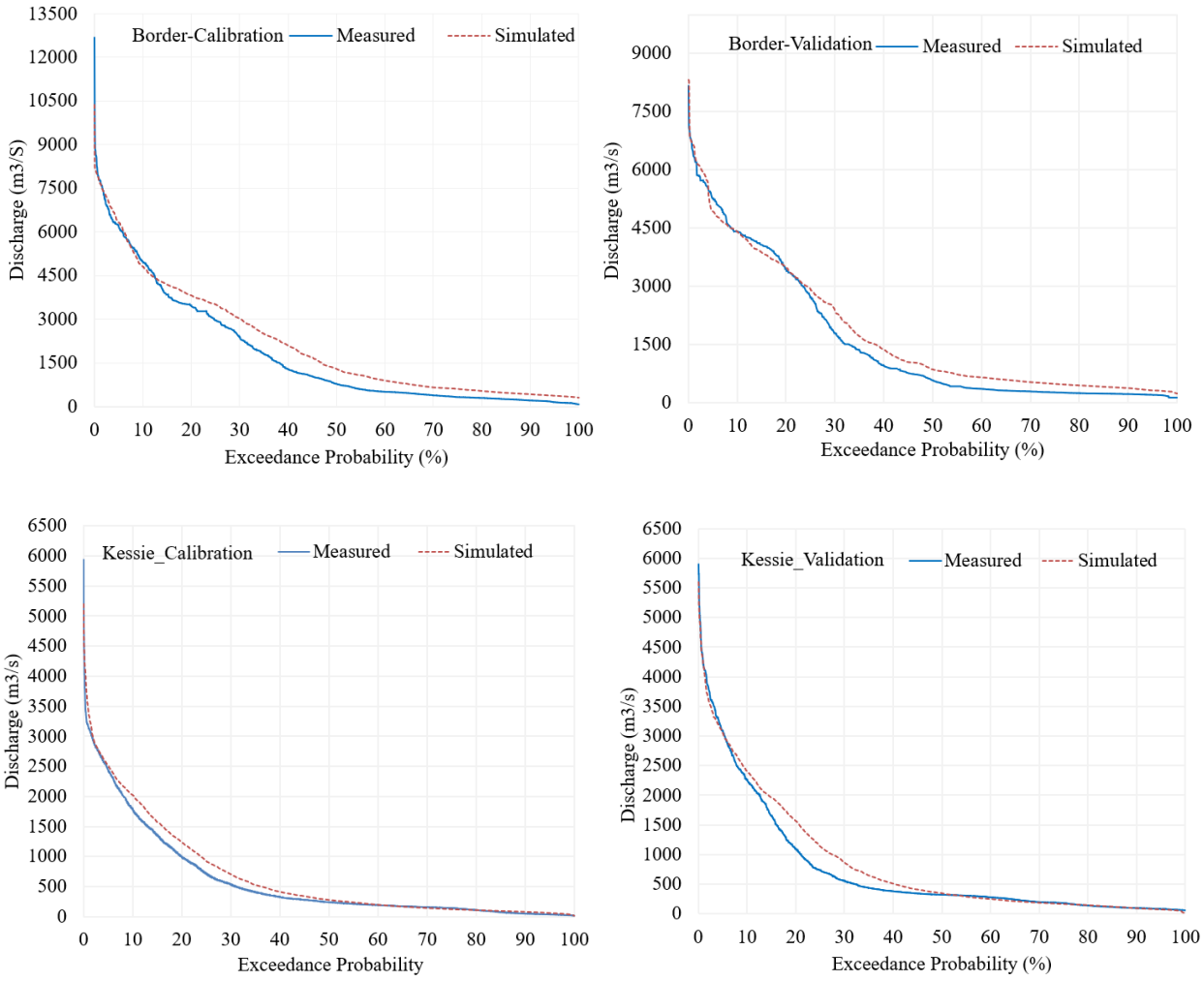

Figure 4. 6: Flow duration curves of the observed and simulated flow at two main gauge points (Border and Kessie)

The performance of the ArcSWAT model was evaluated at different flow magnitudes. In this section, Kling-Gupta Efficiency (KGE) proposed by Gupta et al. (2009) was also applied since it addresses several shortcomings in NSE and is increasingly used for model calibration and evaluation (Wouter et al., 2019). The results of the evaluation were shown in Table 4.5. For peak

and high flow segments, the ArcSWAT model performed very well within the acceptable range of evaluation criteria both at the calibration and validation stages. For the two flow segments R^2, KGE and NSE values were from 0.83-0.98, 0.62-0.95, and 0.64-0.94, respectively. The results of performance for mid- and low-flow segments, however, indicated some inconsistency.

Table 4. 5: Performance of ArcSWAT model at various quantile ranges. Peak Flow: 0-2%, High flow: 2%-20%, Mid flow: 20%-70% and Low Flow: 70%-100%. Numbers in Bold are model performance criteria out of acceptance ranges as stated in Table 3.3. The negative and positive Pbias (%) value indicates overestimation and underestimation of flows respectively.

		Border		Kessie	
Flow Quantile	Evaluation Method	Cal.	Val.	Cal.	Val.
Peak Flow	R^2	0.95	0.83	0.84	0.96
	KGE	0.62	0.81	0.87	0.95
	NSE	0.67	0.64	0.66	0.91
	Pbias (%)	3.50	-3.28	-6.72	2.70
High Flow	R^2	0.96	0.95	0.98	0.97
	KGE	0.93	0.92	0.84	0.75
	NSE	0.94	0.89	0.86	0.85
	Pbias (%)	-3.40	2.70	-9.96	-8.06
Mid Flow	R^2	0.98	0.98	0.99	0.98
	KGE	0.60	0.70	0.62	**0.30**
	NSE	0.66	0.80	0.71	**0.46**
	Pbias (%)	**-28.70**	-14.79	**-23.17**	**-22.21**
Low Flow	R^2	0.97	0.91	0.92	0.94
	KGE	**0.35**	**0.21**	0.88	0.95
	NSE	**0.41**	**0.45**	0.78	0.94
	Pbias (%)	**-48.06**	**-31.86**	-12.01	1.85

As shown in Table 4.5, for mid-range flows, the R^2, KGE, and NSE values were within acceptable ranges at the two gauge points, except at the Kessie gauge point during validation, where the KGE and NSE values were notably low (0.3 and 0.46, respectively). For low flows (70%-100%) at the border gauge point, both KGE and NSE values were low during both calibration and validation. However, the inconsistencies in evaluation results for mid and low flows do not necessarily indicate that the model is unable to capture these flows. This conclusion is supported by the fact that similar flow segments produced contradictory evaluation results between calibration and validation stages. Additionally, the overall aggregated evaluation results during both stages (see Table 4.4) demonstrated reasonable model performance. Therefore, the low KGE and NSE values could likely be attributed to the quality of the input data, such as rainfall and measured flow data. The poor data quality may stem from various factors, as described by Chao et al. (2015).

4.1.5. Water balance results

Modeling the spatial dynamics of water balance components is essential for effective water resource management (Gabriel et al., 2009). This study analyzed the water balance components of the Abbay basin for each sub-basin, using model simulation results from 1980 to 2016. The key components examined included precipitation (PRECIPmm), actual evapotranspiration (ETmm), and water yield (WYLDmm). Figure 4.7 illustrated distribution of these components across sub-basins in the Abbay river basin

Annual average rainfall across the basin varied significantly, ranging from 904.52 mm in the Welaka sub-basin to 2161.68 mm in the Anger sub-basin. The southern sub-basins (Guder, Didessa, Fincha, and Anger) and the northern (Tana sub-basin) experienced higher annual rainfall, between 1600 mm and 2200 mm. In contrast, the Beshilo, North Gojam, Mugher, Beles, Wonbera, and South Gojam sub-basins received between 1000 mm and 1550 mm annually. The Welaka, Jemma, and Dabus sub-basins recorded the lowest annual rainfall, ranging from 900 mm to 950 mm.

Annual actual evapotranspiration (ET) varied between 443.87 mm and 1051.01 mm. The highest ET was observed in the Tana sub-basin, located in the most upstream part of the basin, while the lowest ET occurred in the eastern sub-basins (Welaka, Jemma, and parts of Beshilo). The ET trend showed a decrease from north to south (excluding the Anger sub-basin) and from west to east. These findings are consistent with previous studies (Allam et al., 2016; Gebiyaw et al., 2021). The

ratio of ET and water yield (WYLD) to rainfall is depicted in Figures 4.8 (e) and (f), respectively. The ET percentage ranged from 30.23% to 66.34%, with an average of 55.20% of total rainfall lost as ET. These results closely align with earlier research by Abera et al. (2017), Khairy (2021), and Abebe et al. (2022).

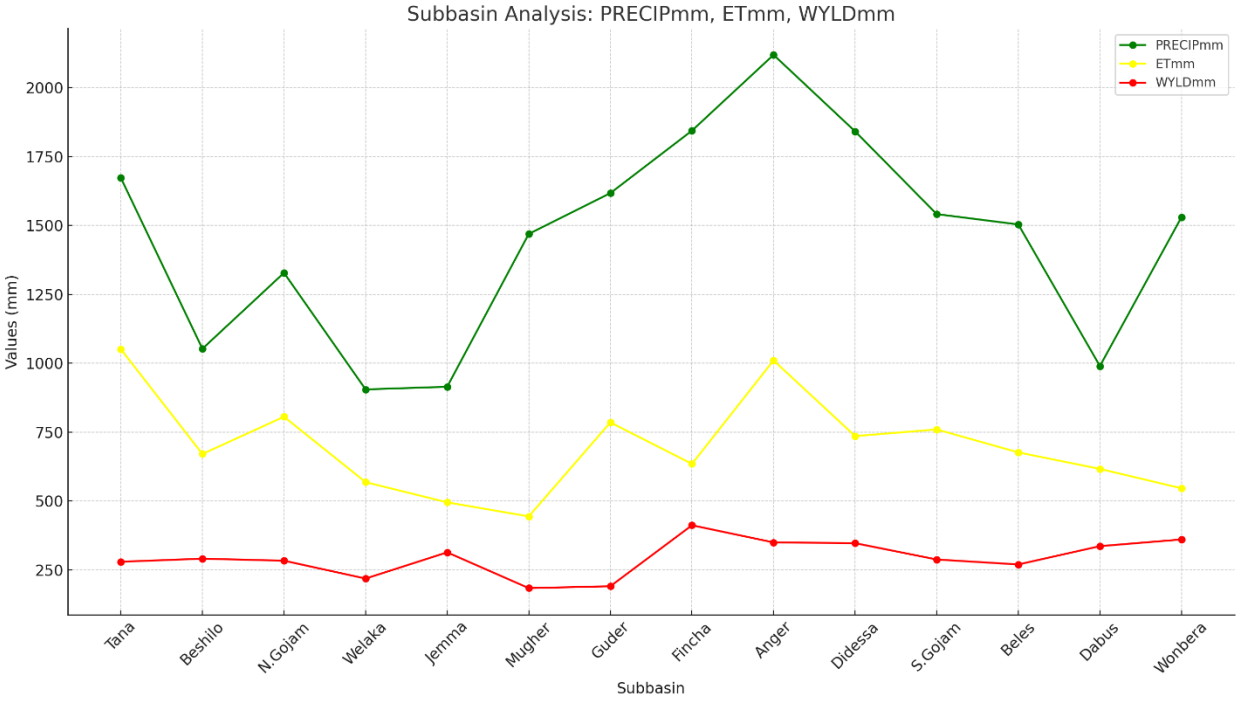

Figure 4.7: Annual water balance components for each sub-basin

The data presented in Figure 4.7 also illustrates the water yield (WYLDmm) across various sub-basins, shedding light on the distribution of water resources within each region. The values range from 183.68 mm to 411.79 mm, indicating significant variability in water availability. This variation is likely influenced by factors such as precipitation patterns, land use, and soil characteristics.

The ratio of water yield (WYLD) to precipitation (PRECIP) expressed as a percentage, serves as a critical indicator of how much precipitation contributes to river flows in a given area. The water yield varies from 11.79% to 34.28%, as shown in Figure 4.8(f), suggesting considerable differences in hydrological responses among the sub-basins. The average annual water yield (WYLD) for the entire Abbay river basin was found to be 21.73% of the annual rainfall, consistent with previous studies by Allam et al. (2016) and Gebiyaw et al. (2021). Furthermore, the annual

volume of water contributed by each sub-basin, as depicted in Figure 4.10, aligns with findings from earlier research by FDRE-ABDO (2020) and McCartney et al. (2012), underscoring the reliability of the current data in accurately reflecting regional water potential.

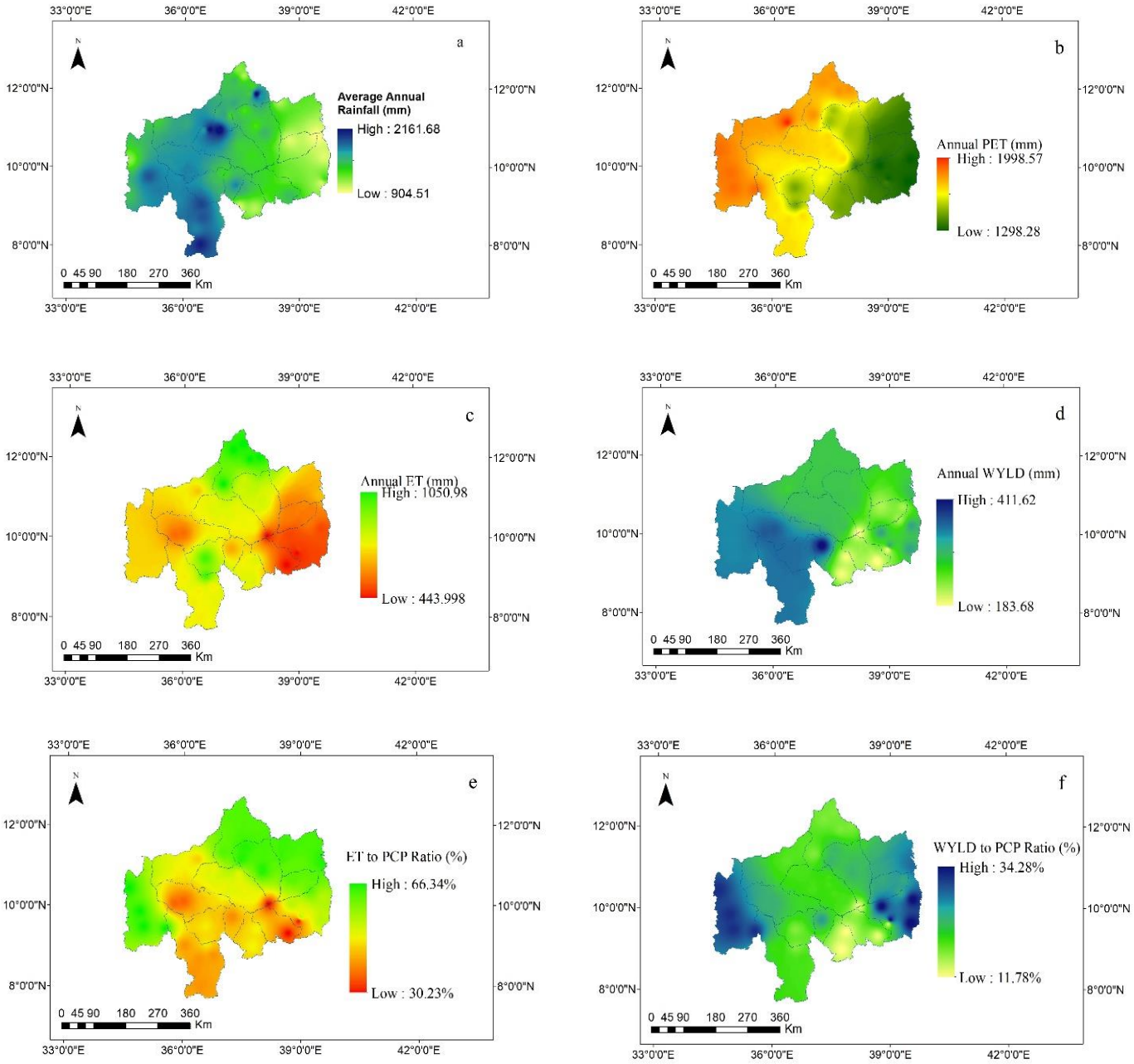

Figure 4.8: Annual Water balance components, spatial distribution, and ratio of the components. a) PCP (mm), b) PET (mm), c) ET (mm), d) WYLD (mm), e) ET ratio (%), f) WYLD ratio (%)

Understanding the seasonal variation of water balance components throughout the year is essential for grasping hydrological dynamics. Figure 4.9 presents the seasonal distribution of key water balance components. The analysis covers different seasons: the major rainy season, the minor rainy season, and the dry season. During the major rainy season, SURQmm contributions ranged from 5.64% to 39.16%. In the minor rainy season, these contributions varied between 0.65% and 7.36%, while during the dry season, they fluctuated from 0.2% to 4.53% (Figure 4.9 (a)-(c)). Surface runoff contributions are significantly higher in the eastern regions and parts of the Abbay basin, particularly in Beshilo, Welaka, Jemma, and North Gojam, during both the major and minor rainy seasons. However, during the dry season, this pattern shifts. The topography of the eastern Abbay basin, characterized by highlands, rugged mountainous terrain, and predominantly cultivated land (Denekew and Bekele, 2009), encourages greater surface runoff as rainfall is less likely to infiltrate into the subsurface. The smallest proportion of SUR_Q relative to WYLD_Q was observed in the Tana sub-basin during the major rainy season. The presence of lakes can influence flow regimes by altering the magnitude of streamflow, typically by attenuating flows (Zuzanna et al., 2017).

Various studies have examined the contribution of groundwater to the total streamflow in the Upper Blue Nile Basin, with differing results. For instance, Gebiyaw et al. (2021) found that groundwater contributes 40.15% of the annual water yield in the basin. Similarly, Mengistu et al. (2021) reported that groundwater's contribution to the annual water yield varies between 25% and 41%. Gemechu et al. (2021) found the groundwater contribution to be the highest (65%) in the Guder sub-basin.

In the present study, the groundwater contribution to water yield was assessed on a seasonal basis. The findings indicate that groundwater contributes the most to the total water yield during the wet season, with spatial contributions ranging from 28.56% to 59.76%. During the rainy season, the soil becomes more saturated, which reduces the capacity of the soil to absorb more water. Excess water, therefore, percolates down to recharge groundwater aquifers, raising the water table and increasing the availability of groundwater. The maximum contribution (59.76%) shown in some parts of the basin seems unrealistic. This may occur due to the high sensitivity of groundwater parameters in that area.

During the dry season and minor rainy season, the groundwater contribution remains significant in the northern parts (Tana basin), with a maximum value of 37.31%. Whereas, the average value was found to be 19%.

The Tana sub-basin exhibits the highest groundwater contribution to total water yield (GW_Q to WYLD_Q) during the dry season. This finding is consistent with Tigabu et al. (2020), who observed that groundwater discharge is the primary contributor to streamflow in the major tributaries of the Lake Tana basin. Their study reported that the Gilgel Abbay, Gumara, and Ribb catchments receive 77.6%, 68%, and 58.4% of their streamflow from groundwater, respectively. Similarly, Abiy et al. (2015) estimated the average groundwater contribution in the Tana sub-basin to be around 60%. The third component of water yield is lateral flow. The LAT_Q to WYLD ratio in major and minor rainy seasons varied from 3.46% to 10.95% and 0.16% to 5.40%. The lateral flow seems low compared to the previous research by Gebiyaw et al. (2021).

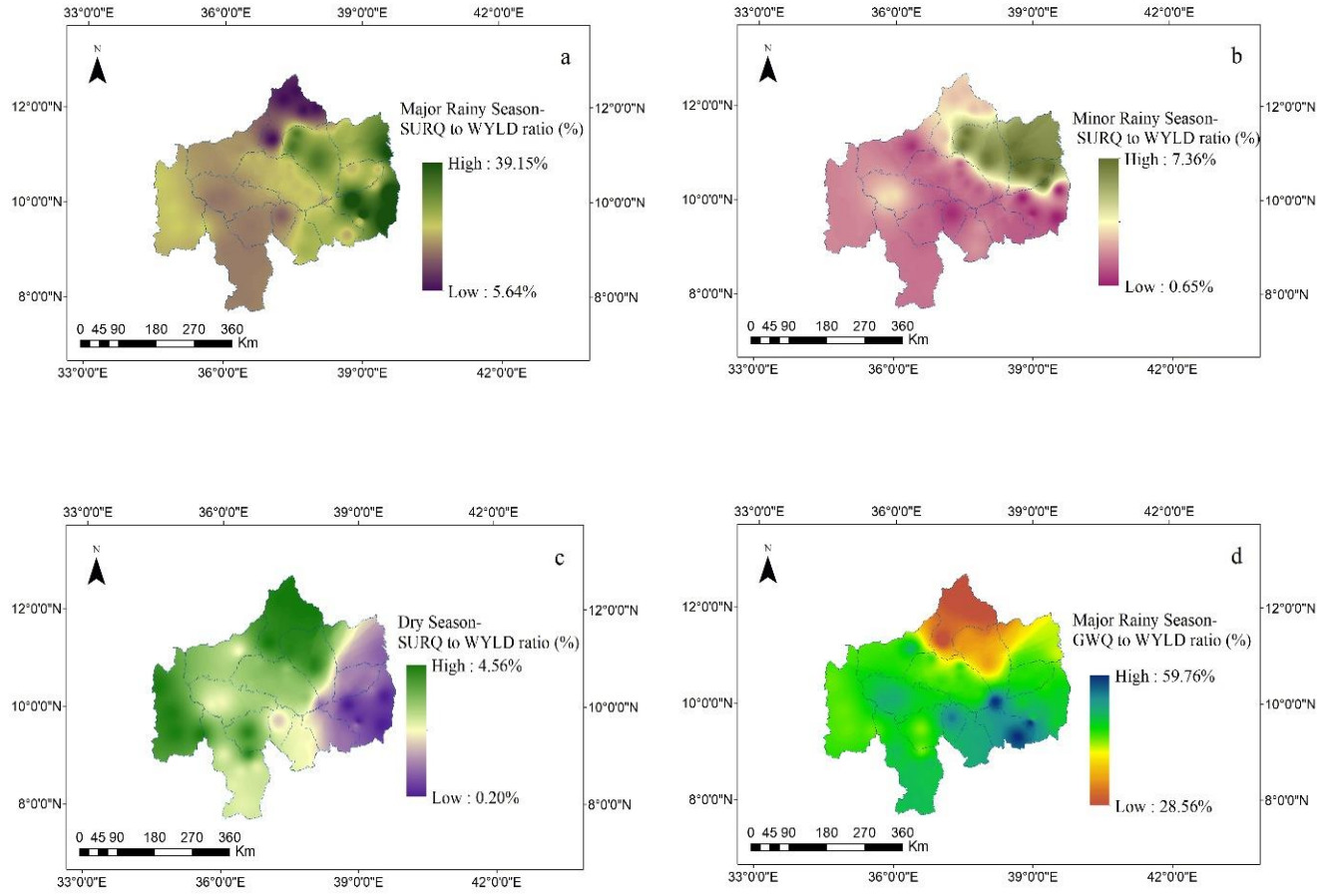

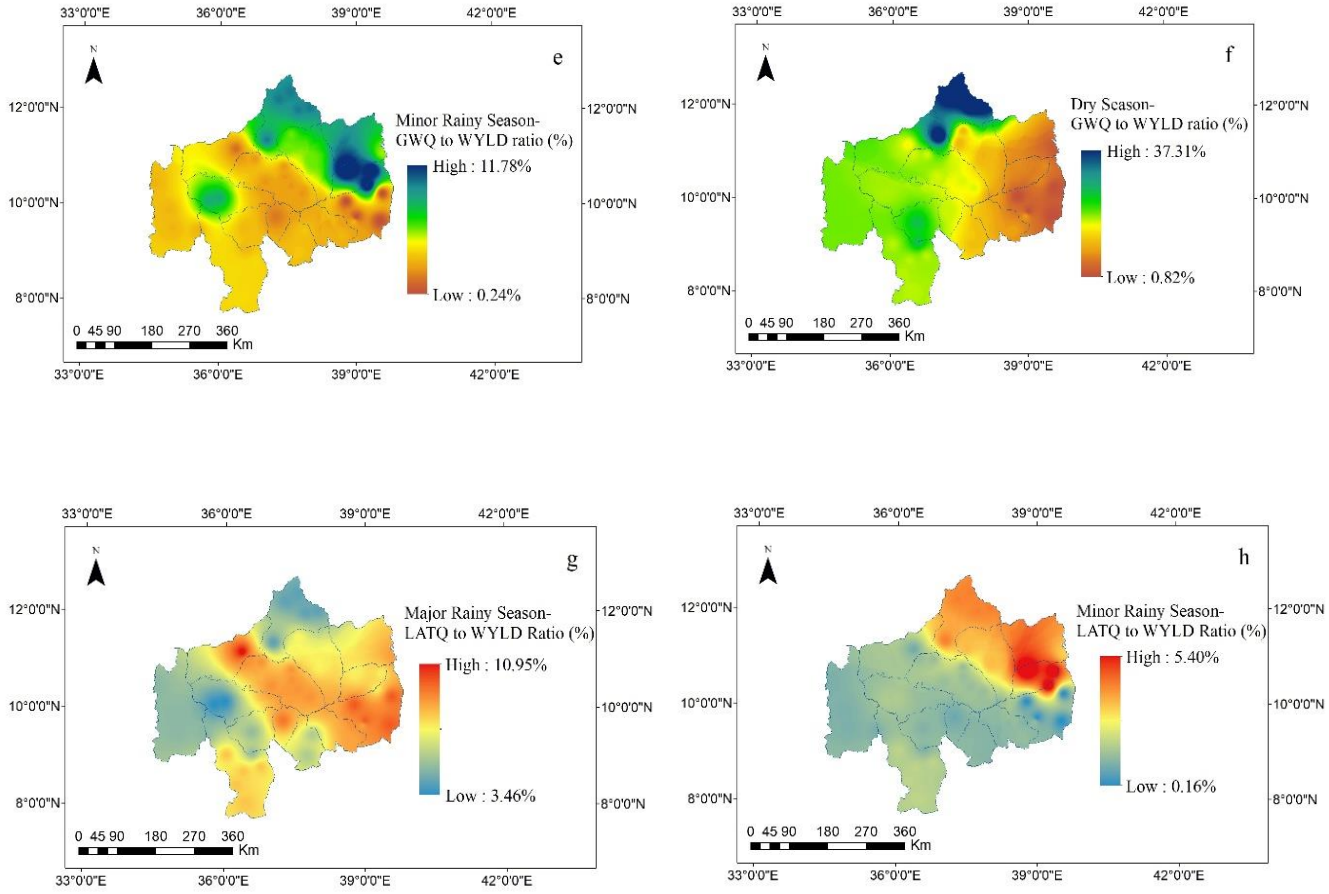

Figure 4.9: Seasonal distribution of water balance components over Abbay basin. Major rainy season (JJAS), minor rainy season (FMAM) and dry season (ONDJ)

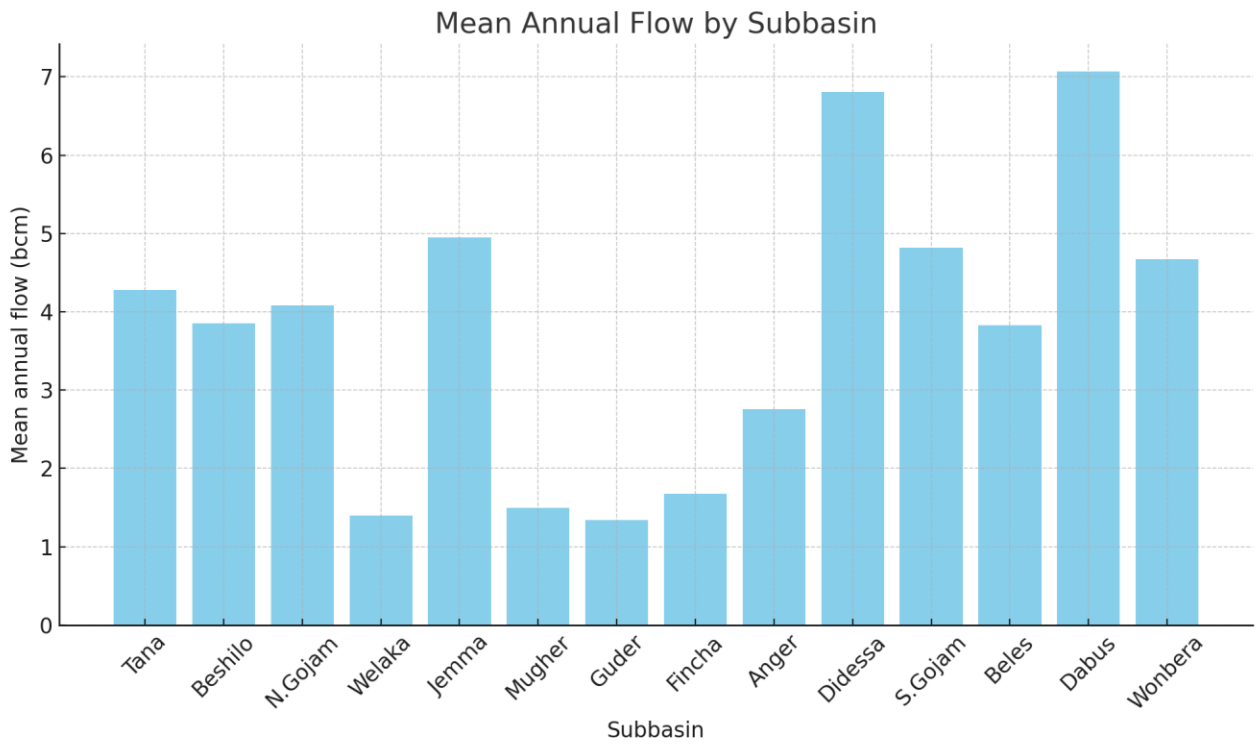

Figure 4.10: mean annual flow for each sub-basin (bcm)

4.2. Water potential assessment conclusion

This study provided a comprehensive assessment of water resource potential and its components over the Abbay river basin using the ArcSWAT model. The aggregated calibration and validation result revealed that the ArcSWAT model has the capacity to simulate flows that agree with the measured values and is applicable over the Abbay river basin at different spatial scales. The result also revealed that the performance of the model well improved as the basin was partitioned into sub-basins. The identified sensitive parameters that highly affect the rainfall-runoff process for each sub-basin can be used as the basis for future reaches on the Abbay river basin using the SAWT model. The calibration and validation of the model at different flow segments using FDC also showed a reasonable model efficiency. The independent evaluation of different flow segments showed that the ArcSWAT model performed better for peak and high flows than mid and low flows.

The model successfully generates flow data that closely matches the measured flows in the Abbay River basin. Therefore, it can be utilized in areas with no or limited measured data, periods with missing data, or to extend flow records for gauges with short measurement periods. In this research, the model results were used as inputs to assess the trade-offs between hydropower and irrigation development.

Furthermore, the model can be applied to assess the water balance components. It provides insights into the relationships between precipitation, evapotranspiration, runoff, and storage, helping to quantify the availability of water resources. By accurately modeling these components, decision-makers can assess the sustainability of water use, plan for efficient water allocation, and predict the impacts of climate change and human activities on water resources. This is particularly important for managing competing demands, such as agriculture, hydropower, and domestic water supply, ensuring that water resources are used efficiently and sustainably.

Finally, this research was based on considerations that exclude climate change impacts. The soil moisture storage component was not also considered. Thus, we suggest doing research considering climate change impacts and soil moisture storage to capture comprehensive analysis of the water balance components in the Abbay river basin.

4.3. Trade-off and synergy analysis Results

In this second major objective of the research, a comprehensive analysis was conducted on the trade-offs and synergies between hydropower and irrigation. The analysis ranged from evaluating the hydropower generation of various cascade projects in the Abbay River basin to assessing the associated hydro-economic benefits.

The first step in HEC-ResSim modeling was configuring the basin stream alignment, junctions, impact areas, stream nodes, reservoirs, diversion, and computational points and then followed by reservoir networking. For this study the watershed configuration and reservoir network configuration were done step by step depending on the scenario developed and objectives. Thus Figure 4.11 and Figure 4.12 showed the watershed configuration and reservoir networking respectively.

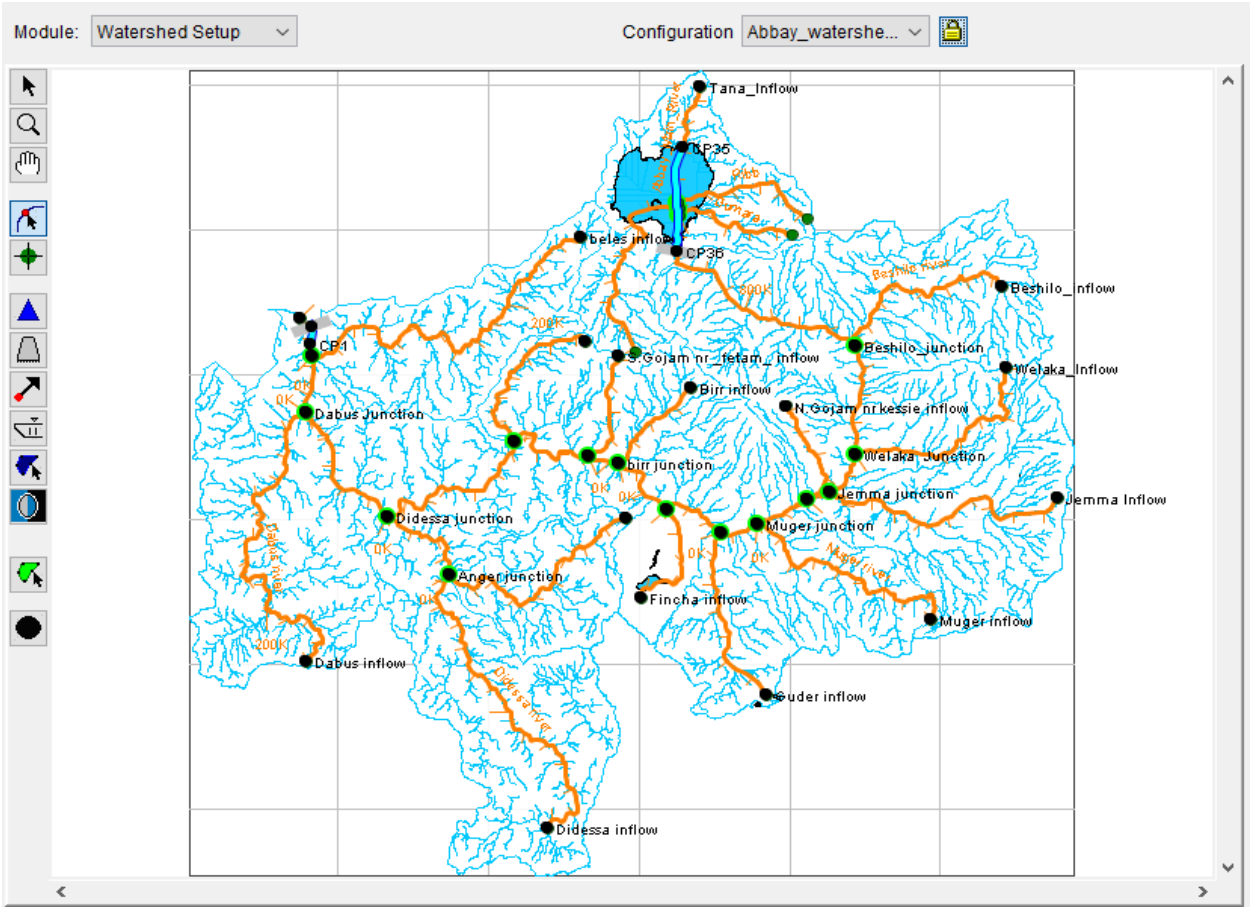

Figure 4.11: Abbay watershed configuration (Stream Alignment, nodes, and computational points)

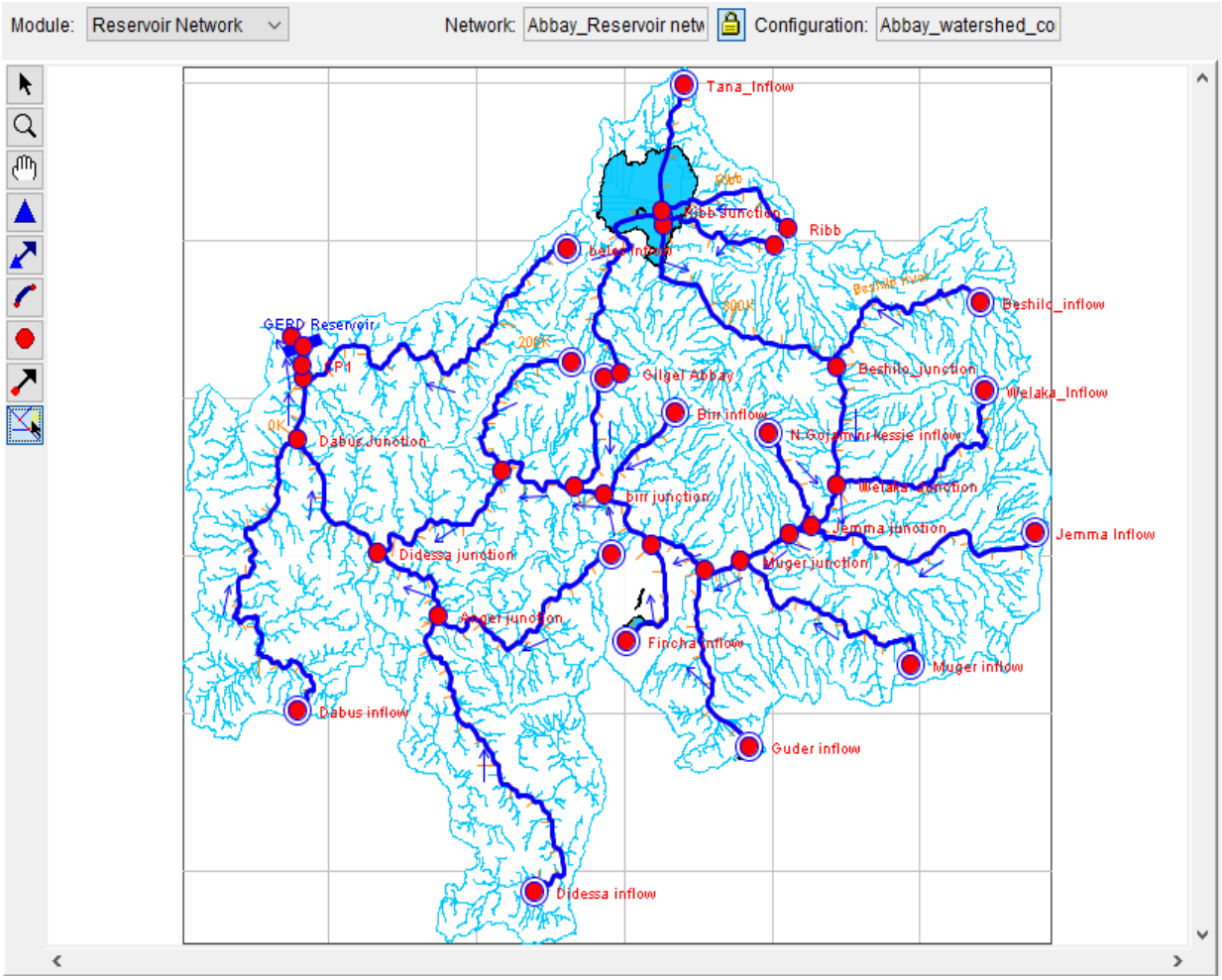

Figure 4.12: Reservoir network configuration (routing reaches, junctions)

4.3.1. Calibration and validation of HEC-ResSim model

The HEC-ResSim model was calibrated and validated to assess its ability to direct flows within natural river channels. Figure 4.13 illustrates the graphical visualization and statistical results between measured and simulated flows at two main gauge stations. The correlation coefficient (R^2) was found to be between 0.93 and 0.96, and Nash and Sutcliffe simulation efficiency (NSE) was between 0.91 and 0.93 for calibration and validation both at Border and Kessie gauge stations. The percent of bias, on the other hand, lied between 5% and 6%. The statistical results generally fall within the acceptable ranges specified by Moriasi et al. (2015). The simulated flow results closely matched the measured flows at both gauge stations. Thus, based on the statistical measure and evaluation through graphical visualization, it can be concluded that the HEC-ResSim model effectively simulates the flows that agreed with measured flows in the Abbay river basin.

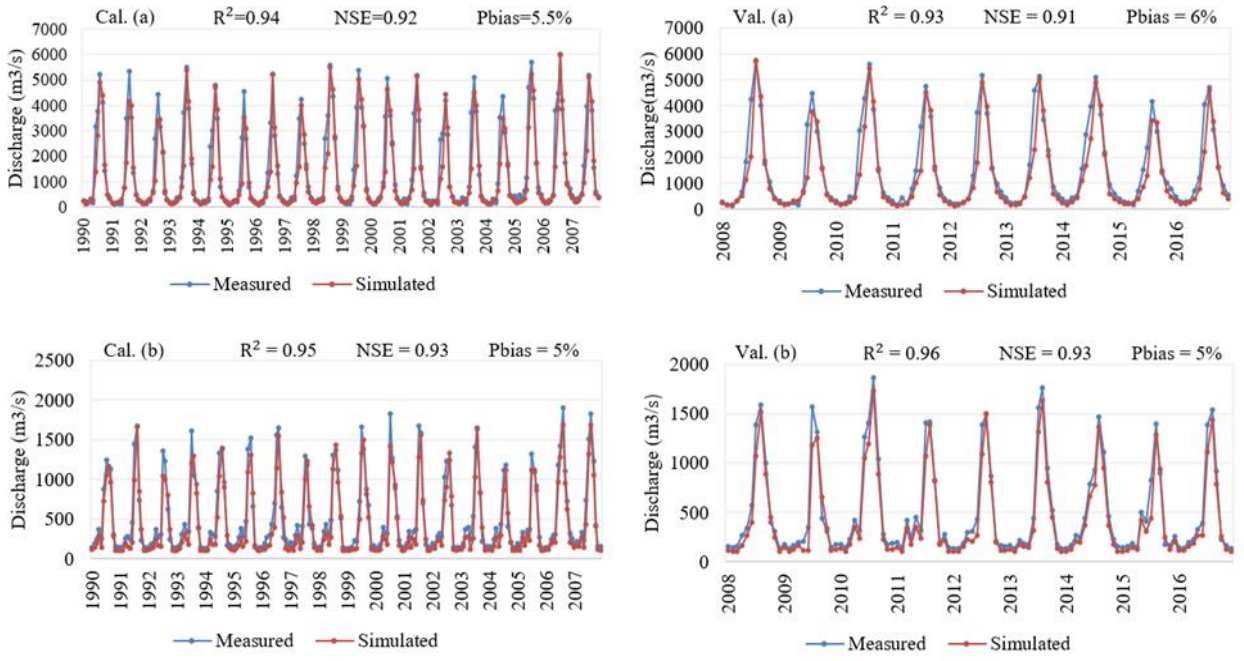

Figure 4.13: Calibration of HEC-ResSim Model at Border (a) and Kessie (b)

4.3.1.1.Energy generation under three reservoir operation rules

These scenarios (S-1.2, S-1.3, and S-1.4) focused on evaluating energy production at both the system-wide and individual project levels, assessing the available water in the system-wide and individual reservoirs, and analyzing reservoir operation without considering irrigation diversion in the river system. The assessment involved three reservoir operation rules: tandem operation, hydropower guide curve, and hydropower schedule to determine the most optimal operation rule that would maximize energy production in the cascade reservoirs. In S-1.2, the analysis included GERD and Karadobi projects. S-1.3 expanded to include GERD, Karadobi, and Bekoabo, while S-1.4 represented the full cascade of four major projects, including GERD, Karadobi, Bekoabo, and Mandaya. The cascade scenarios were formulated based on the assumption that the construction sequence would progress from GERD to the most remote projects, namely Karadobi, Bekoabo, and Mandaya.

Figure 4.14 presents the monthly energy generated for each scenario and reservoir operation rule. Tandem operation (TO) and hydropower schedule (HPS) showed higher variation in monthly energy generation compared to the power guide curve rule (PGC). In S-1.2, tandem operation resulted in monthly energy variation ranging from 507.63 GWh to 5001.76 GWh, with an average energy generated of nearly 1702 GWh and a standard deviation of 1823 GWh. The application of

the power guide curve rule led to monthly energy variation between 1360.8 GWh and 3198.20 GWh, with an average energy of 1866 GWh and a standard deviation of 574.6 GWh. The hydropower schedule rule yielded energy generation ranging from 495.86 GWh to 4590.95 GWh, with an average value of 2215 GWh and a standard deviation of 1565.67 GWh. S-1.3 and S-1.4 showed similar patterns in monthly energy generation as S-1.2, but with increased energy production. In S-1.3, tandem operation resulted in a minimum of 580.5 GWh and a maximum of 6410.2 GWh, while the hydropower schedule rule produced a minimum of 640 GWh and a maximum of 6034 GWh. In contrast, the power guide curve rule showed less variation, with a minimum of 1752 GWh and a maximum of 4560 GWh. The standard deviations for the three reservoir operation rules in S-1.3 were 2263 GWh (TO), 944 GWh (PGC), and 1708 GWh.

In the case of S-1.4, which included four major hydropower projects, the monthly energy generated varied from 723.4 GWh to 7591.61 GWh for tandem operation, 2094.62 GWh to 5700.6 GWh for the power guide curve, and 825 GWh to 7208.44 GWh for the hydropower schedule. The standard deviations were 2688 GWh (TO), 1259 GWh (PGC), and 2041 GWh (HPS). The simulation results indicated that monthly energy variations were higher for TO and HPS compared to PGC. The fluctuation in energy generation for TO and HPS led to rapid rises and falls in the energy curve, resulting in deficits and surpluses of energy supply. On the other hand, the PGC rule showed lower standard deviations for all scenarios, indicating less fluctuation in monthly energy generation and enabling a more even distribution of energy throughout the year to meet energy demands.

Figure 4.15 illustrates annual energy production for three reservoir operation rules. Hydropower schedule (HPS) resulted in the maximum energy output for all scenarios, reaching 26.15 TWh (S-1.2), 40.35 TWh (S-1.3), and 51.16 TWh (S-1.4). Tandem operation (TO) produced the least annual energy generation for all scenarios, with values of 20.42 TWh (S-1.2), 27.37 TWh (S-1.3), and 33.82 TWh (S-1.4). The power guide curve operation (PGC) generated average energy production between TO and HPS, with values of 22.40 TWh (S-1.2), 30.56 TWh (S-1.3), and 38.83 TWh (S-1.4).

The total storage capacity (BCM) in the reservoir system for all scenarios and operation rules followed the reverse trend of energy generation, as shown in Figure 4.16. Tandem operation resulted in the maximum system storage, indicating an emphasis on maintaining reservoir storage balance rather than maximizing hydropower production.

The annual energy production achieved (38.83 TWh) through the operation of the full cascade of reservoirs following the power guide curve is consistent with prior research results reported by Mulat et al. (2018) and Geressu & Harou (2015). The hydropower schedule exhibited a peculiar pattern where the maximum energy generation coincided with the lowest recorded reservoir storage and an uneven monthly distribution of energy generation was reflected. This uneven distribution resembled tandem operation. Consequently, a power guide curve has been identified as the ideal operational guideline for generating energy in a cascade reservoir system, ensuring optimal storage utilization and energy generation. Ayenew et al. (2020) also evaluated the adequacy of these three reservoir operation rules and identified the hydropower guide curve rule as a promising approach for modeling cascade reservoirs in the basin to optimize the utilization of available water resources for hydropower generation, environmental conservation, and flood control within the cascade reservoir system.

Additionally, the performance of the multiple reservoir operation rules (TO, PGC, and HPS) was evaluated for individual hydropower projects. Figure 4.18 displays the annual energy production for each power plant. The energy generated varied across projects for each reservoir operation rule. For Karadobi, Bekoabo, and Mandaya, the maximum energy generation coincided with the hydropower schedule rule, while the minimum was observed under tandem operation. The power guide curve operation produced average energy between TO and HPS for these three projects. Interestingly, for GERD, both PGC and HPS showed almost equal energy generation, while TO result the minimum energy output. Evaluating the performance of the multi-reservoir operation rules for the entire cascade system as well as individual projects is crucial for achieving optimal energy generation capacity and maintaining optimal water storage levels. Figure 4.17(a-i) also illustrated the monthly variation of energy production for each hydropower project across different scenarios and reservoir operation rules.

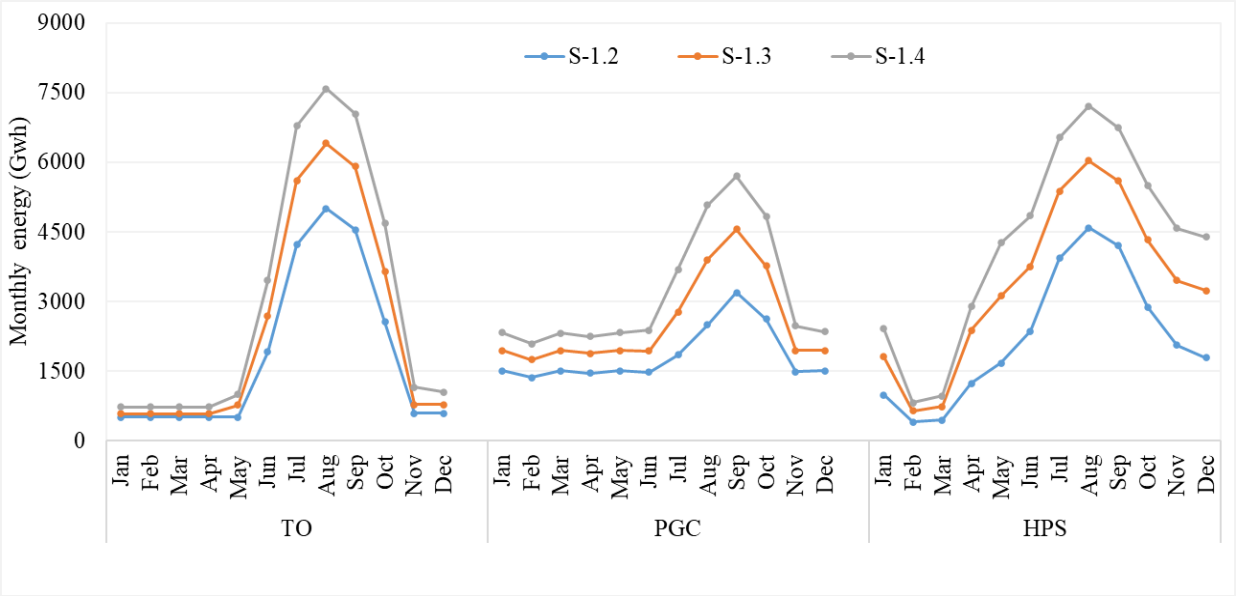

Figure 4.14: Monthly energy generation for each scenario and operation rule (S-1.2: monthly total energy generated from GERD and Karadobi, S-1.3: monthly total energy generated from GERD, Karadobi and Bekoabo, S-1.4: monthly total energy generated from GERD, Karadobi, Bekoabo and Mandaya). TO: Tandem Operation, PGC: Power Guide Curve, HPS: hydropower schedule

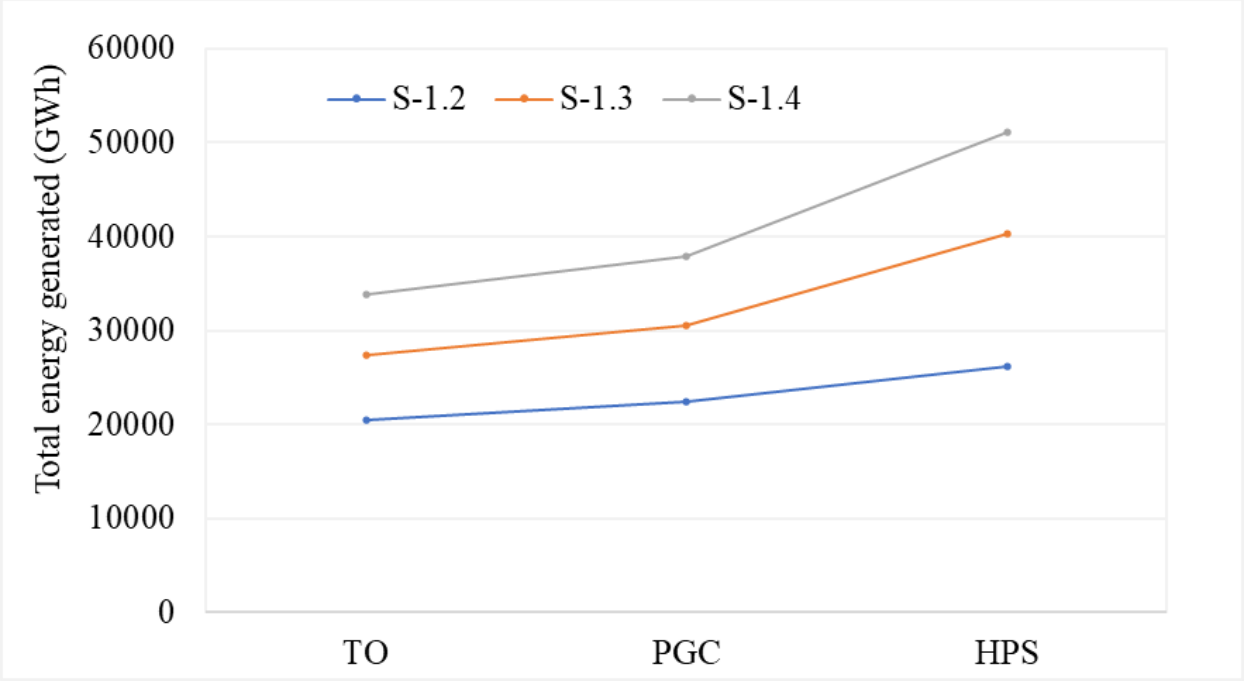

Figure 4.15: Annual total energy generated (GWh) for each cascade scenario and reservoir operation rule

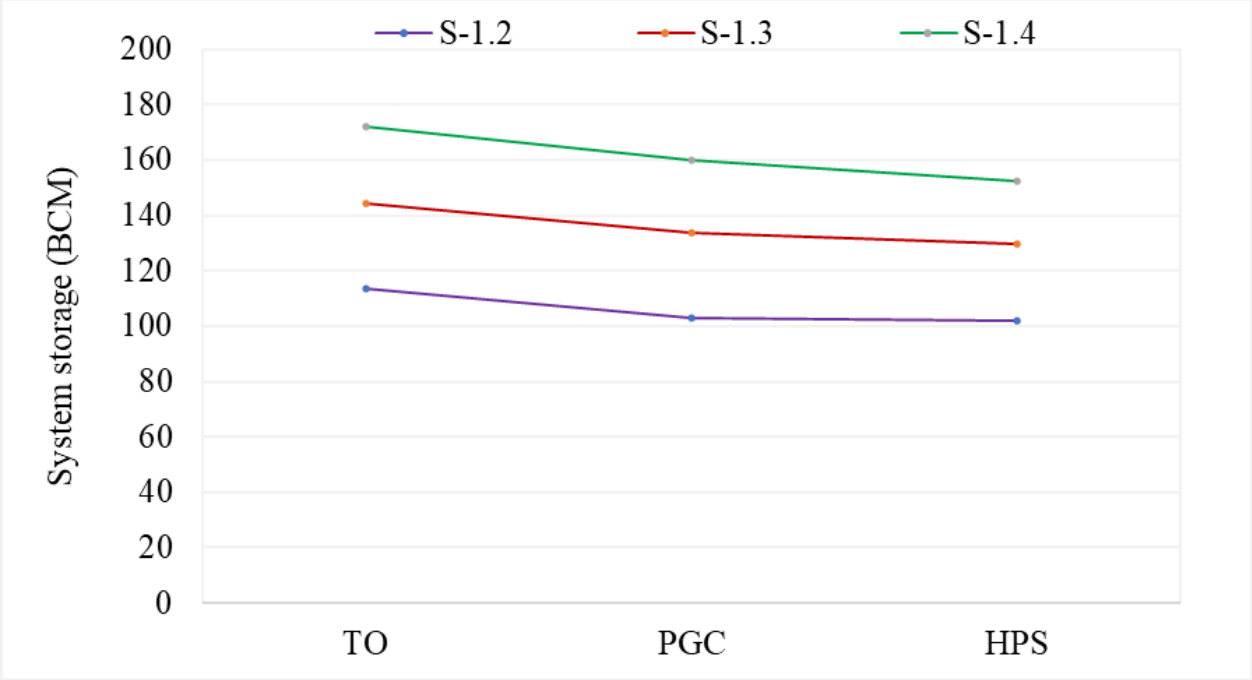

Figure 4.16: The total available reservoir storage (BCM) for each cascade scenario and reservoir operation rule

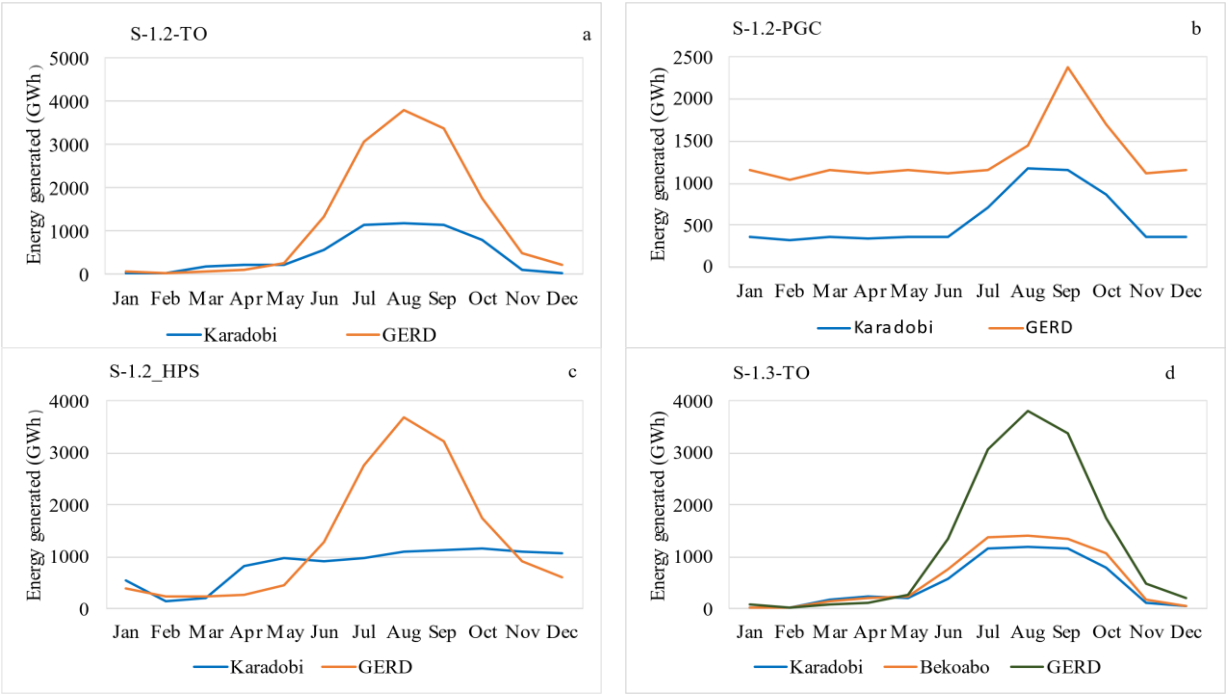

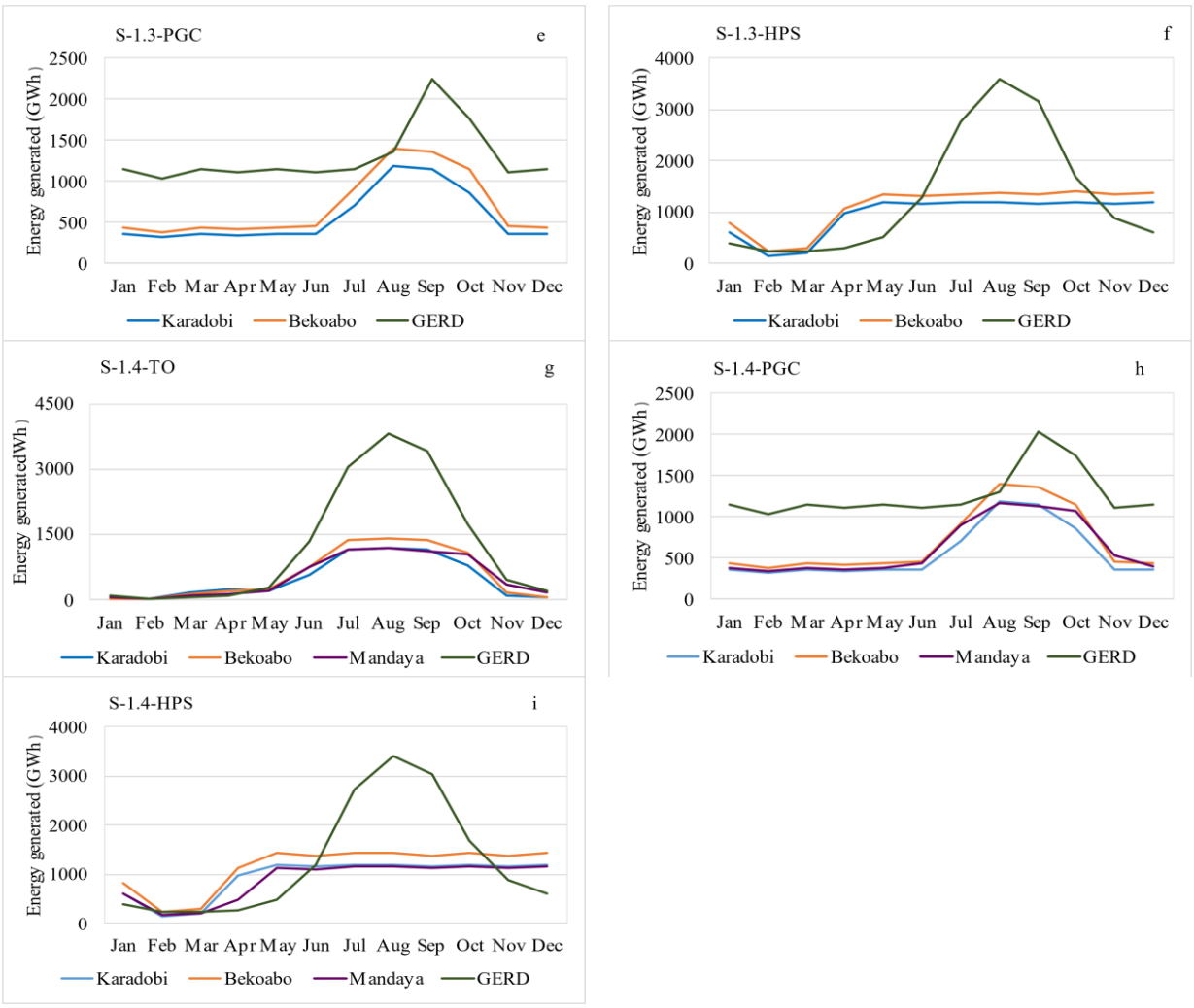

Figure 4.17: Energy generated (GWh) for each cascade scenarios and reservoir operation rule. TO: Tandem Operation, PGC: Power Guide Curve and HPS: hydropower Schedule. S-1.2, S-1.3 and S-1.4 are sub-Scenarios for the first Major scenario (S-1).

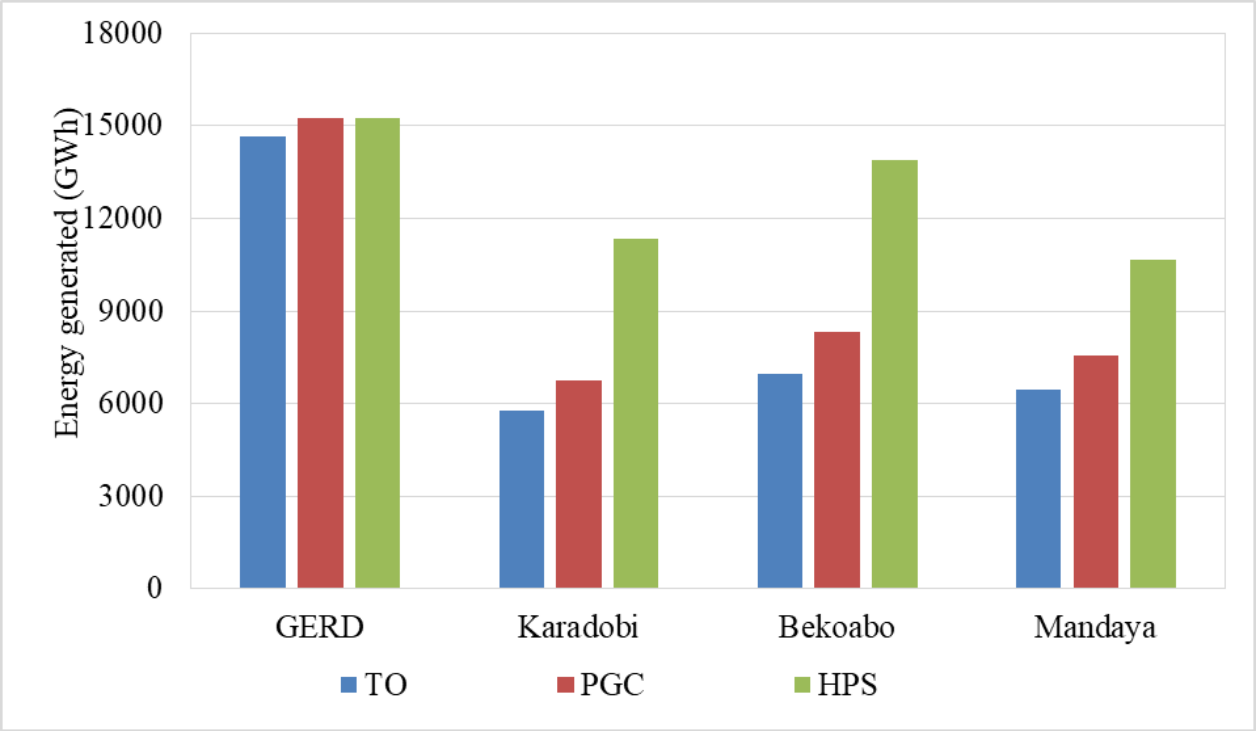

Figure 4.18: Annual Energy generated (GWh) from each hydropower project under different reservoir operation rules.

Table 4. 6: Summary of simulated power reports for each cascade scenario and reservoir operation rules (TO: Tandem operation, PGS: Power Guide Curve, HPS: hydropower Schedule)

	S-1.2			S-1.3			S-1.4		
	TO	PGC	HPS	TO	PGC	HPS	TO	PGC	HPS
GERD Reservoir-Power Plant									
Energy Generated per Time Step (MWh)	40136.98	42923.42	43514.76	39716.65	42535.37	42979.68	38990.40	41773.70	41739.42
Power Generated (MW)	1672.37	1788.48	1813.12	1654.86	1772.31	1790.82	1624.60	1740.57	1739.14
Plant Factor	0.32	0.35	0.35	0.32	0.34	0.35	0.32	0.34	0.34
Flow Power (cms)	1335.05	1476.26	1485.72	1321.06	1465.47	1482.65	1296.90	1445.47	1471.06
Karadobi Dam-Power Plant									
Energy Generated per Time Step (MWh)	15777.27	18440.60	28099.76	15778.17	18440.60	28099.76	15780.56	18440.60	28099.76
Power Generated (MW)	657.39	768.36	1170.82	657.42	768.36	1170.82	657.52	768.36	1170.82
Plant Factor	0.41	0.48	0.67	0.41	0.48	0.68	0.41	0.48	0.68
Flow Power (cms)	274.53	323.91	508.32	274.55	323.91	508.32	274.60	323.91	508.32
Beko Abo Dam-Power Plant									
Energy Generated per Time Step (MWh)				19036.50	22739.25	36475.42	19036.59	22739.25	36475.42
Power Generated (MW)				793.19	947.47	1519.81	793.19	947.47	1519.81
Plant Factor				0.41	0.49	0.69	0.41	0.49	0.69
Flow Power (cms)				323.42	386.98	625.81	323.43	386.98	625.81
Mandaya Dam-Power Plant									
Energy Generated per Time Step (MWh)							17650.13	20674.50	29242.42
Power Generated (MW)							735.42	861.44	1218.43
Plant Factor							0.43	0.51	0.65
Flow Power (cms)							492.87	579.36	823.32

4.3.2. Trade-off between hydropower generation and irrigation development

In this context, the HEC-ResSim model was developed with a focus on hydropower projects integrated with various extent of irrigation development. Its primary purpose was to assess various aspects, including the energy generation of individual and system wide project, availability of water within the system and individual reservoir and evaluating the trade-off between energy generation and irrigation development. Within the scope of this study, the power guide curve rule, defining the hydropower generation requirement in relation to the available storage within the power pool, was utilized.

4.3.2.1.Scenario-1 (S-1) results

In this phase of the scenario (S-1), the analysis focused on assessing the energy generated at both the system-wide and individual levels without considering irrigation development. Moreover, the impact of implementing new hydropower projects on existing energy production, reservoir operation, and downstream flow availability was evaluated. The analysis was focused on four sub-scenarios (S-1.1 to S-1.4).

In the case of S-1.1, the HEC-ResSim model was used to simulate the GERD hydropower project and Lake Tana reservoir exclusively. The reservoir's full supply level (FSL) was set at 640m, and the minimum operating level (MOL) was 590m. The gated spillway sill level was fixed at 624.9 m. During periods when the pool elevation fell below the MOL or during the initial filling phase, only two turbines served by the bottom outlets positioned at 542 m were operational (Eldardiry & Hossain, 2021).

The reservoir's volume at FSL was 74 BCM, while at MOL it was 14.8 BCM (water below this level was considered dead storage). Consequently, the active storage volume amounted to 59.2 BCM. This section primarily focuses on the variations in reservoir elevation, operation, and power/energy generation over the long-term inflow period from 1982 to 2016. The simulation results for this period were presented in Figures 4.19, 4.20, 4.21, and 4.22. The reservoir elevation fluctuated between 622.8 m and 640.74 m (Figure 4.19), with an average elevation of 634.87 m being maintained.

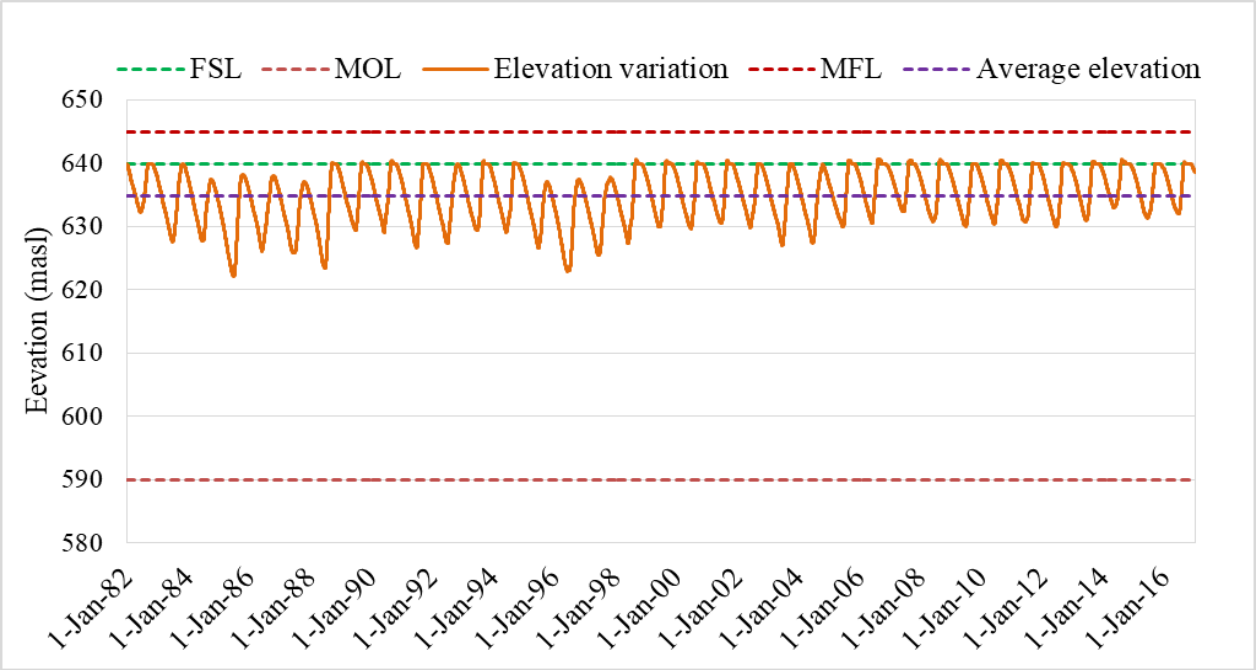

Figure 4.19: Daily GERD reservoir water level and operating levels (S-1.1)

During the period of inflow from 1982 to 2016, the daily storage of the GERD reservoir fluctuated between 45.30 BCM and 75.34 BCM (Figure 4.20). On average, the volume was measured at 64.9 bcm. The lowest storage occurred in May 1985, corresponding to an elevation of 622.8 m. Severe drought years in the Abbay river basin were identified as 1984 and 2002 (Bayissa et al., 2021), while Abera and Gebeyehu (2022) classified 1983, 1984, 2001, and 2010 as the most extreme hydrological drought years. The minimum storage observed in June 1985 was a result of the previous year's drought. The reservoir's storage volume within the specified years, 1982 to 2016, remained within the active storage zone (above the minimum operating level), indicating that GERD will continue to operate without interruption despite hydrological variability.

Based on Figure 4.22, the long-term monthly average storage indicates that May experienced the lowest storage levels, while September reached the highest storage levels. In February, the storage volume reached 64.91 BCM, equivalent to the average storage of 64.9 BCM. Generally, from March to July, monthly storage levels were below average. From August to January, monthly storage levels were above the average value. Notably, throughout the 35-year period from 1982 to 2016, the GERD reservoir never fell below the minimum operating level (MOL) of 590 meters, demonstrating its ability to function properly even under severe hydrological conditions.

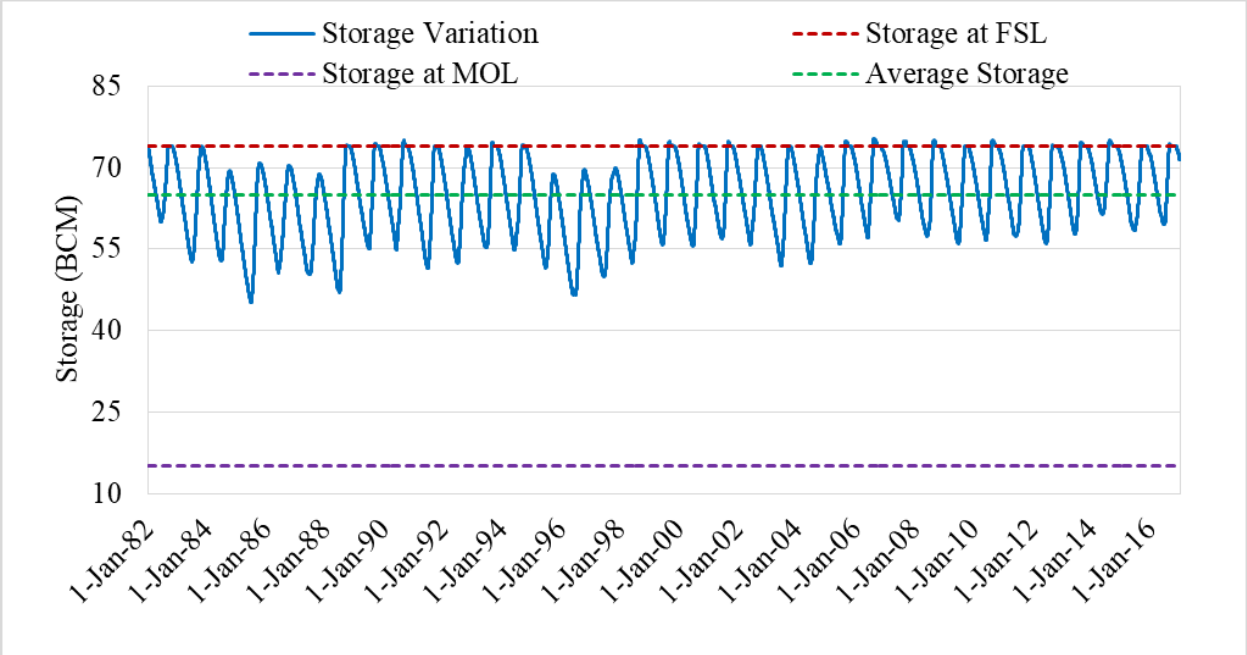

Figure 4.20: Daily GERD reservoir storage variation and average storage (S-1.1)

Regarding the spilling of excess water above the full supply level, it was observed that the maximum storage reached 75.34 billion cubic meters (BCM), exceeding the storage at the full supply level (FSL) of 74 BCM by 1.34 BCM. Therefore, over a period of 35 years, 1.34 BCM of water was spilled as excess flow.

The average inflow (48.76 BCM) and outflow (48.12 BCM) volumes during full operations showed no significant variation (Figure 4.21). The presence of the GERD reservoir enabled consistent downstream flows. During periods of high flow, it mitigated damage caused by severe floods, while during dry periods, additional water released from the reservoir for power generation compensated for low flows. By referring to Figure 4.21, we can understand that the presence of GERD reduced peak flows during high flow years (e.g., 1998 and 2006), whereas the total outflow from GERD increased during low flow periods (e.g., 1984 and 1995).

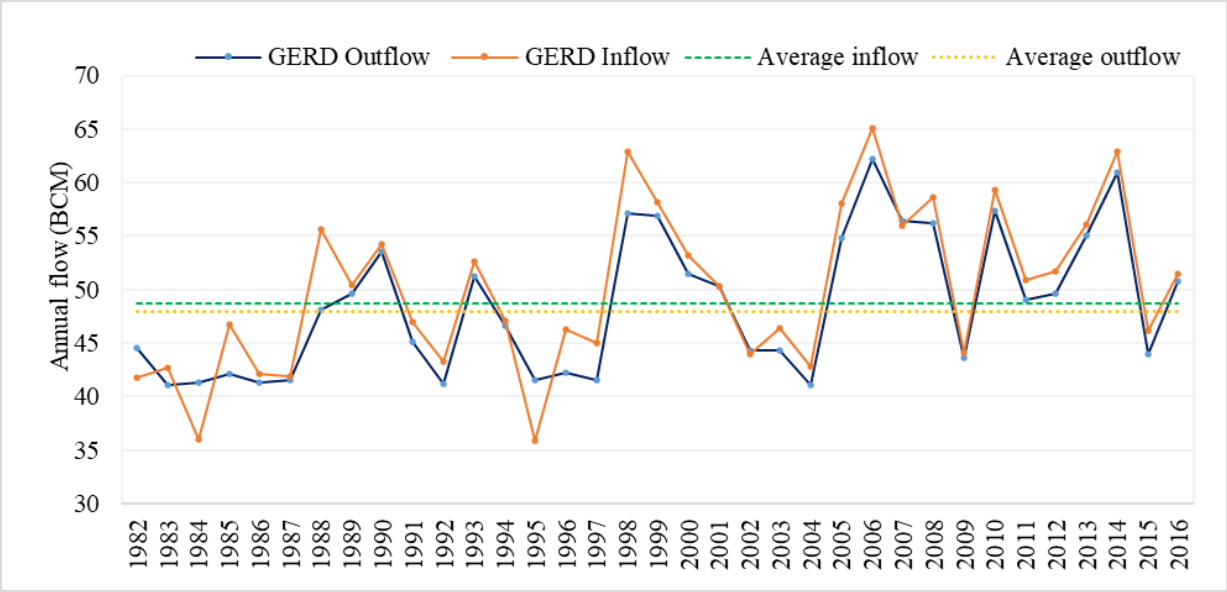

Figure 4.21: GERD reservoir inflow, outflow, and average flow (S-1.1)

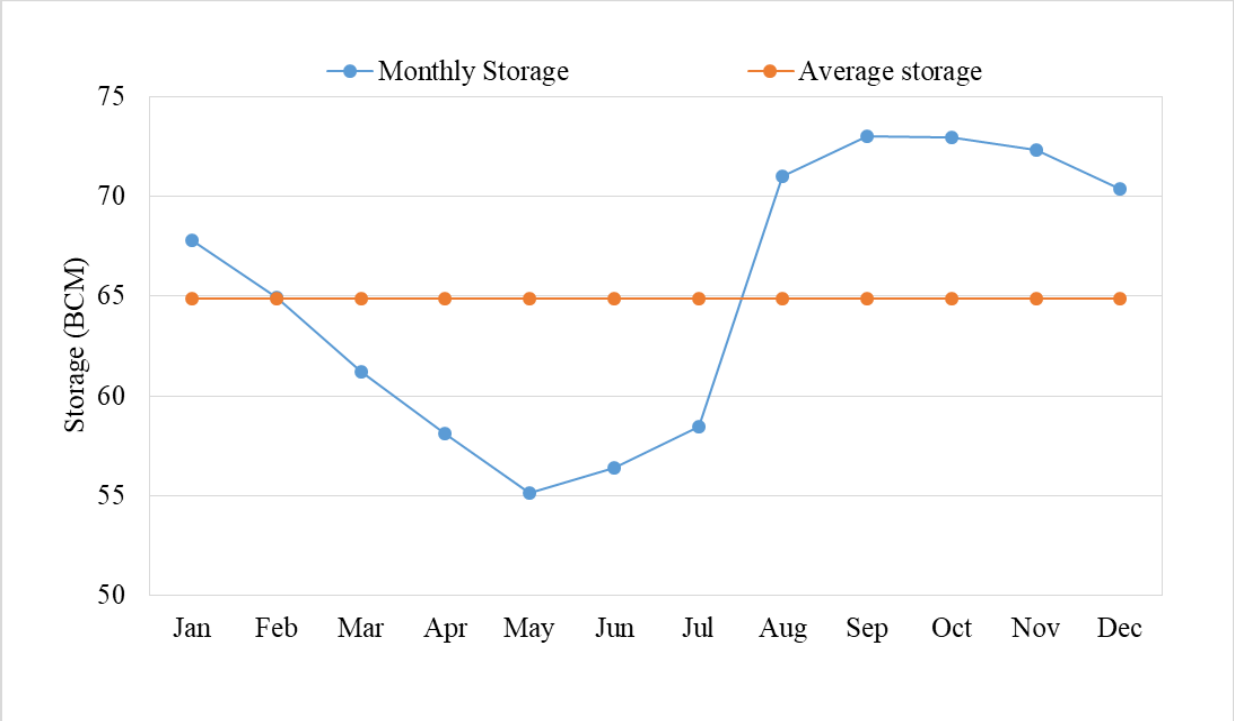

Figure 4.22: Long term monthly average of GERD Reservoir (BCM) (S-1.1)

The installed capacity of the GERD has undergone several amendments over time. Initially, it was designed to have an installed capacity of 6450 MW (EEPco, 2019). Abtew and Dessu (2019) raised concerns about GERD's ability to operate at this design capacity, leading to a reduction to 5250

MW. Eventually, the installed capacity was further adjusted to 5150 MW, which is the value considered in this research.

For the simulation of GERD hydropower under S-1.1, the average power generated during daily time steps was 1810 MW. This resulted in an annual energy production of 15865 GWh, with an average capacity factor of 0.32. These findings align well with a previous study by Dereje et al. (2020). Eldardiry and Hossain (2021) applied a deterministic dynamic programming (DDP) optimization scheme to evaluate GERD's hydropower potential and estimated an annual energy production of 13629 GWh, with a capacity factor of 0.30. This estimate appears to be underestimated compared to the results of this research. The underestimation could be attributed to the highly constrained optimization system and/or could stem from differences in modeling approaches or variations in the time frame of input flow data.

Figure 4.23 illustrates the monthly variation in energy production and capacity factor. The minimum energy production occurred in May (1062 GWh), while the maximum was observed in September (2452 GWh). On average, the monthly energy production amounted to 1322 GWh. These variations in energy production corresponded to the fluctuations in reservoir storage, as depicted in Figure 4.12.

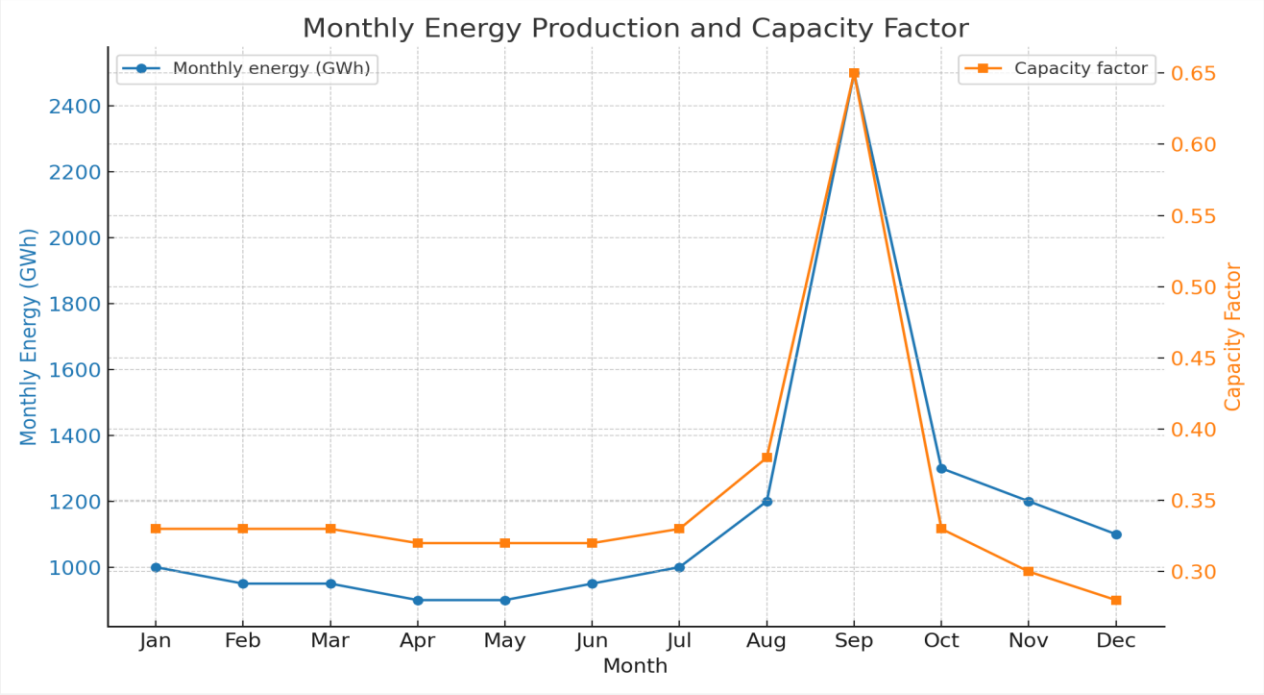

Figure 4.23: GERD Monthly energy production and corresponding capacity factor (S-1.1)

The capacity factor exhibited monthly variations, ranging from 0.31 in May to 0.65 in September, with an average value of 0.32 across all months. The energy production capacity of GERD gradually decreased from January (1085 GWh) to May (1062 GWh), with a standard deviation of 8 GWh. During the flood season (June to September), there was a sharp increase in energy production, characterized by a high standard deviation of 540 GWh. Subsequently, from September to December, there was a sharp decrease in energy production, accompanied by a standard deviation of 550 GWh. Figure 4.23 also indicated high monthly variations in GERD's energy production, particularly in the immediate periods before and after the peak energy production month (September). This observation highlights the high sensitivity of GERD's energy production to reservoir storage and inflow discharges. The overall energy production of GERD exhibited month-to-month variations, with a standard deviation of 404 GWh.

As the new hydropower project added to the cascade, the system-wide energy generation capacity also increased. Figure 4.24 (b) illustrates the monthly system energy generation for various scenarios. In S-1.2, the inclusion of the Karadobi hydropower project into the cascade system led to a notable 41% increase in the average monthly energy generation of the entire system, rising from 1322 GWh to 1866 GWh. The operation of three cascade reservoirs (S-1.3) contributed to a further boost, elevating the system-wide average monthly energy generation to 2546 GWh. This signifies a 36% increase in the system's energy generation capacity compared to S-1.2, with the Bekoabo hydropower project playing a significant role in this enhancement. With the operation of four cascades of hydropower projects (S-1.4), the system-wide average monthly energy generation reached 3152 GWh, showing a 24% increase compared to S-1.3.

The system energy generation capacity was also evaluated based on percentile curves, as illustrated in Figure 4.24(d). The energy generated at the 25^{th} percentile ranged from 1050 GWh to 2200 GWh. Similarly, the 75th percentile yielded energy values ranging from 1500 GWh to 4120 GWh for the respective scenarios. While the median values (50^{th} percentile) were found to be 1200 GWh for S-1.1 and 2500 GWh for S-1.4. Figure 4.24(c) also illustrated the monthly energy generation pattern and percentile of an individual project. Analyzing the energy generation pattern of independent projects is crucial to assessing the impact of new projects on existing operational ones. Although system-wide energy generation increased as the cascade of hydropower increased, results of individual energy generation capacity revealed that with the integration of new

hydropower projects into the system, notable effects were observed for GERD hydropower, which experienced a reduction of energy generation, especially in the peak energy generation period (August and September) (Figure 4.24(a)). In August, the energy generation capacity of GERD decreased by 5%, 10%, and 14% in S-1.2, S-1.3, and S-1.4 compared to S-1.1. Similarly, in September, the reductions were 3%, 5%, and 13% in the respective scenario.

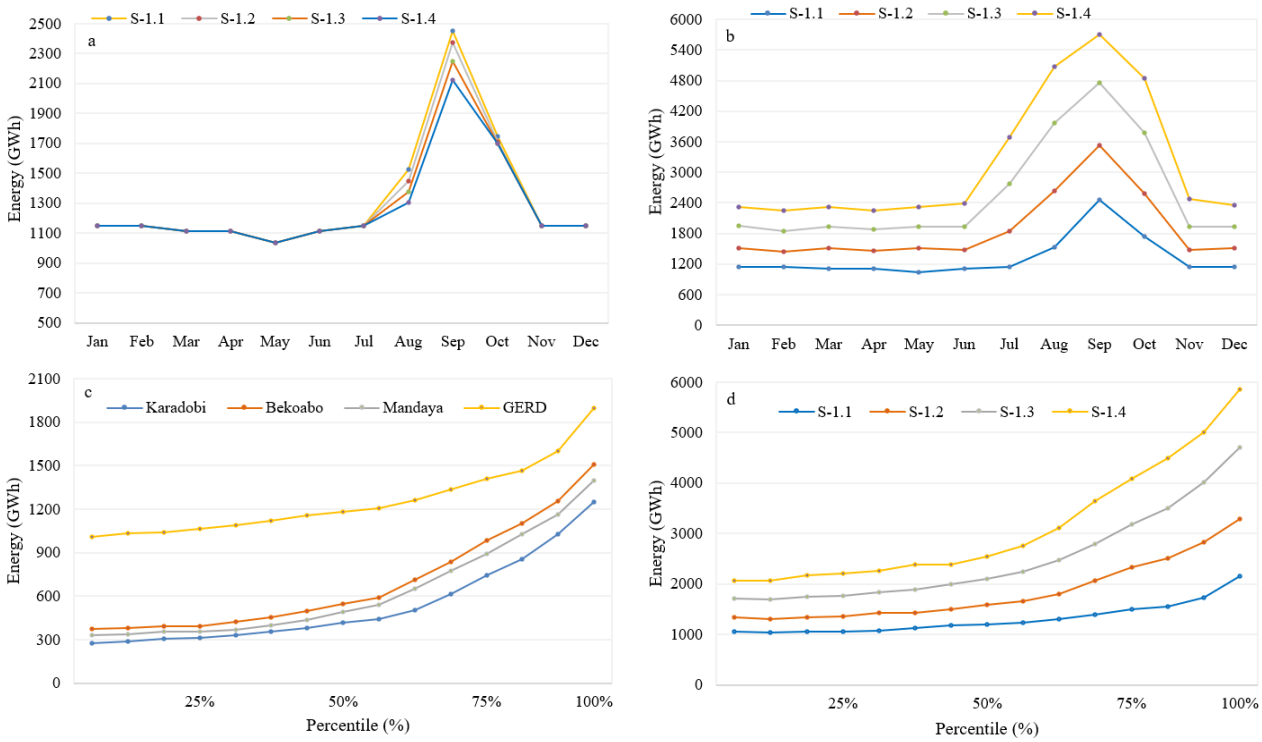

Figure 4.24: Energy generated from various cascade scenarios. GERD energy generation trend for every addition of one project upstream (a), system energy generation (b), monthly individual energy generation percentile when four projects are cascaded (c) and monthly system energy generation percentile from four cascade projects (d)

In terms of annual energy output, the system energy generation capacity for S-1.2, S-1.3, and S-1.4 has reached 22 TWh, 31 TWh, and 38 TWh, respectively, as shown in Figure 4.25(b). Despite a significant increase in annual system-wide energy generation from four cascade reservoirs (S-1.4), the independent energy generation result revealed that GERD annual energy generation capacity reduced by 4.2%. Figure 4.25(a) also showed the average system storage available in the reservoirs for each cascade scenario.

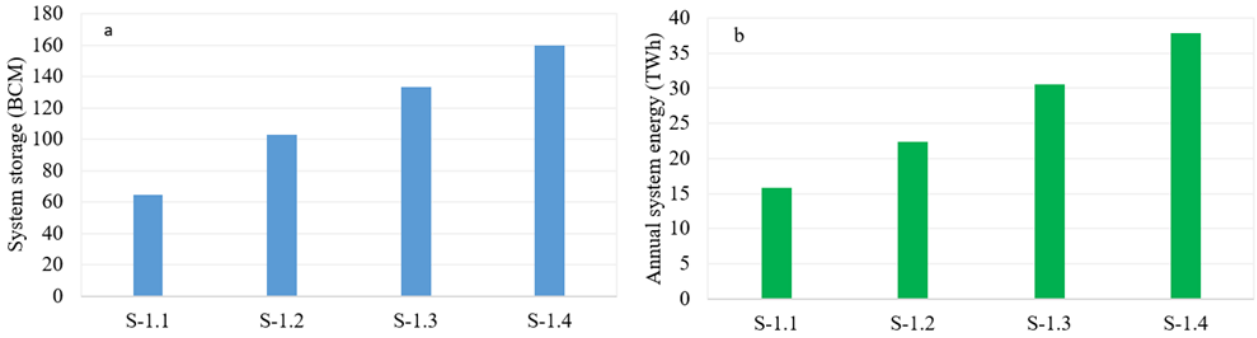

Figure 4.25: Average annual available system storage (a) and annual system energy generated (b)

4.3.2.2.Scenario-2 (S-2) Results

This scenario was focused on evaluating the impact of an irrigation development on the system and individual energy generation capacity in the Abbay river basin. Within the major scenario (S-2), six sub-scenarios (S-2.1 to S-2.6) were formulated, representing various combinations of hydropower projects and irrigation water diversion. Thus, the results in S-2 were analyzed by taking S-1 as a baseline to quantify the change in energy generation when irrigation development is progressively expanded to the maximum potential area.

The diversion of water for agricultural purposes upstream resulted in changes in hydrological conditions downstream, subsequently affecting the inflows and operation of the hydropower reservoir. Figure 4.26 illustrates the change in energy generation for each irrigation development scenario. The graphical visualization revealed that across all scenarios, there was a noticeable decline in monthly energy production, particularly in the wet season from June to November, whereas less impact was observed in the dry season. To quantify the extent of impacts on seasonal basis, the generated energy was described as percentile values. Figure 4.27 described the 25^{th}, 50^{th}, and 75^{th} percentiles of monthly system energy generation under the consideration of various extents of irrigation development. Comparing the percentile of monthly system energy generation without irrigation (Figure 4.24(d)) and with irrigation (Figure 4.27) provides clear images on the impact of irrigation development on the energy generation capacity of hydropower projects. The results revealed that the more decline in energy generation occurred in the 75^{th} percentile ranges, which were generated in the wet season. For S-1.1, S-1.2, and S-1.3, the 75^{th} percentile was 1500 GWh, 2300 GWh, and 3300 GWh, respectively (Figure 4.24 (d)). However, in S-2.1, S-2, and S-2.3, it was found to be 1400 GWh, 2100 GWh, and 2950 GWh (Figure 4.27), showing 7%, 9%,

and 11% decline, respectively. However, a significant effect was not observed on energy generated in the dry season, described as 25^{th} and 50^{th} percentile ranges. S-2.4, S-2.5, and S-2.6 were aimed at evaluating the effect of increased potential irrigation development on the energy generation capacity of four hydropower plants. Thus, the result of these three scenarios was compared with S-1.4. The 50^{th} and 75^{th} percentile values in S-1.4 were 2550 GWh and 4120 GWh, respectively (Figure 4.24 (d)). However, in S-2.4, S-2.5, and S-2.6 (Figure 4.27), the 50^{th} percentile value decreased by 5%, 6%, and 8%, and the 75^{th} percentile value was decreased by 10%, 12%, and 15%, respectively, due to potential irrigation development. During the dry season, diverting irrigation water upstream decreases the inflow into downstream reservoirs, thereby diminishing the active storage level of the reservoir. Consequently, this alteration affects the refilling process, unable to reach the full supply level. As a result, there was a notable reduction in the peak energy generation capacity. The 25^{th} percentile range was, however, not significantly affected. This revealed that the development of irrigation over the Abbay river basin would not severely affect the energy generation capacity, particularly for 75^{th} percent of exceedance.

Figure 4.28, on the other hand, depicted the change in annual system energy and reservoir storage. Compared to S-1.1, S-1.2, and S-1.3, the annual energy generation in S-2.1, S-2.2, and S-2.3 declined by 4%, 5%, and 6%, respectively. Subsequent assessments from S-2.4 to S-2.6 analyzed the hydropower generation capacity of full cascade projects, including GERD, Karadobi, Bekoabo, and Mandaya, integrated with potential irrigation development. This hydropower cascade system exhibited similarities to the S-1.4 configuration. Thus, using S-1.4 as a baseline, the trade-offs results revealed that the annual system energy generation capacity of four major hydropower plants decreased by 8%, 9%, and 12% for S-2.4, S-2.5, and S-2.6, respectively. The research also gave emphasis to evaluating the individual hydropower generation capacity to identify the most affected hydropower plants. This is important to set up optimal reservoir operation. Accordingly, the trade-off between full irrigation development and individual energy generation capacity revealed that GERD experienced the highest decrease in annual energy generation capacity, with a decline of 16%, followed by Bekoabo and Mandaya with equal reductions of 8%, and Karadobi with a 7% reduction (Table 4.7).

Table 4. 7: Change of annual energy production capacity (GWh) for individual projects due to irrigation intervention

Scenario combination	GERD		Change (%)	Karadobi		Change (%)	Bekoabo		Change(%)	Mandaye		Change(%)
S-1.1 (S-2.1)	15866	15301	4%									
S-1.2 (S-2.2)	15666	14869	5%	6732	6401	5%						
S-1.3 (S-2.3)	15524	14522	6%	6732	6371	5%	8301	7917	5%			
S-1.4 (S-2.4)	15246	13776	10%	6732	6299	6%	8301	7769	6%	7548	7090	6%
S-1.4 (S-2.5)	15246	13283	13%	6732	6283	7%	8301	7671	8%	7548	7080	6%
S-1.4 (S-2.6)	15246	12631	16%	6732	6262	7%	8301	7596	8%	7548	6939	8%

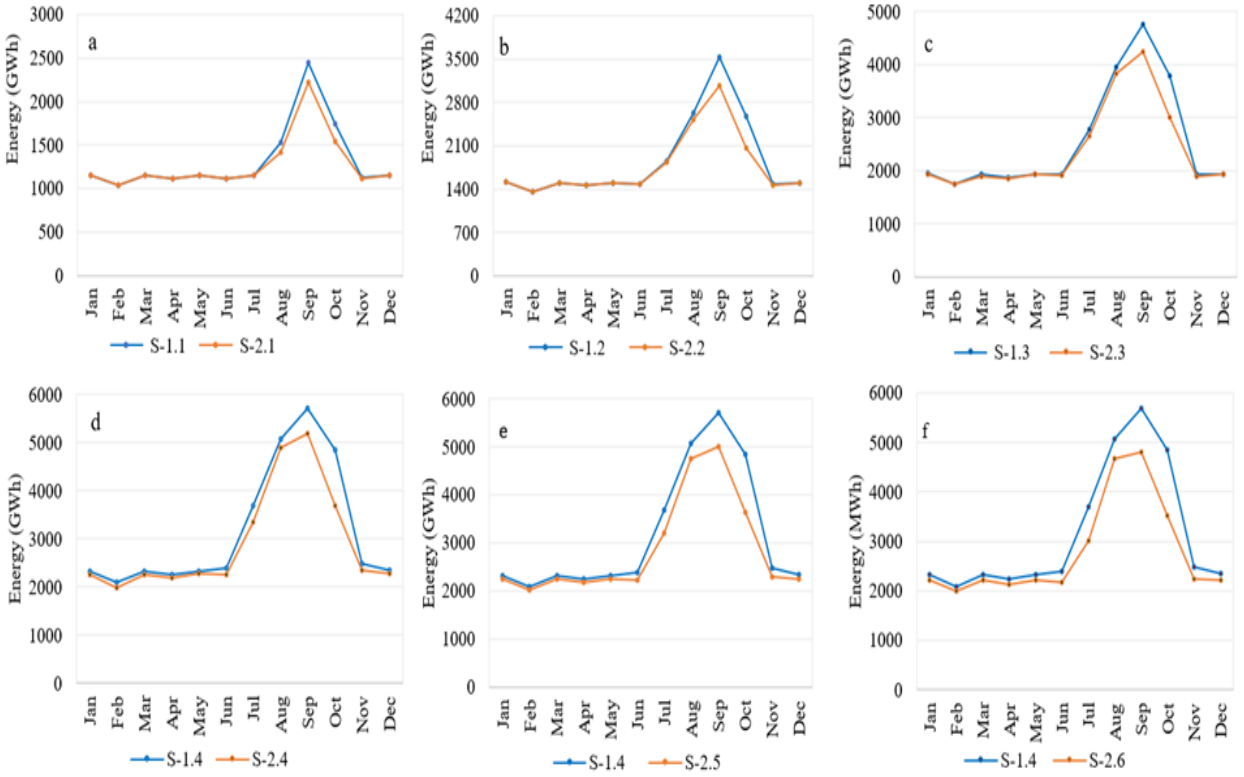

Figure 4.26: Monthly system wide energy generation (GWh) for each combination of scenarios.

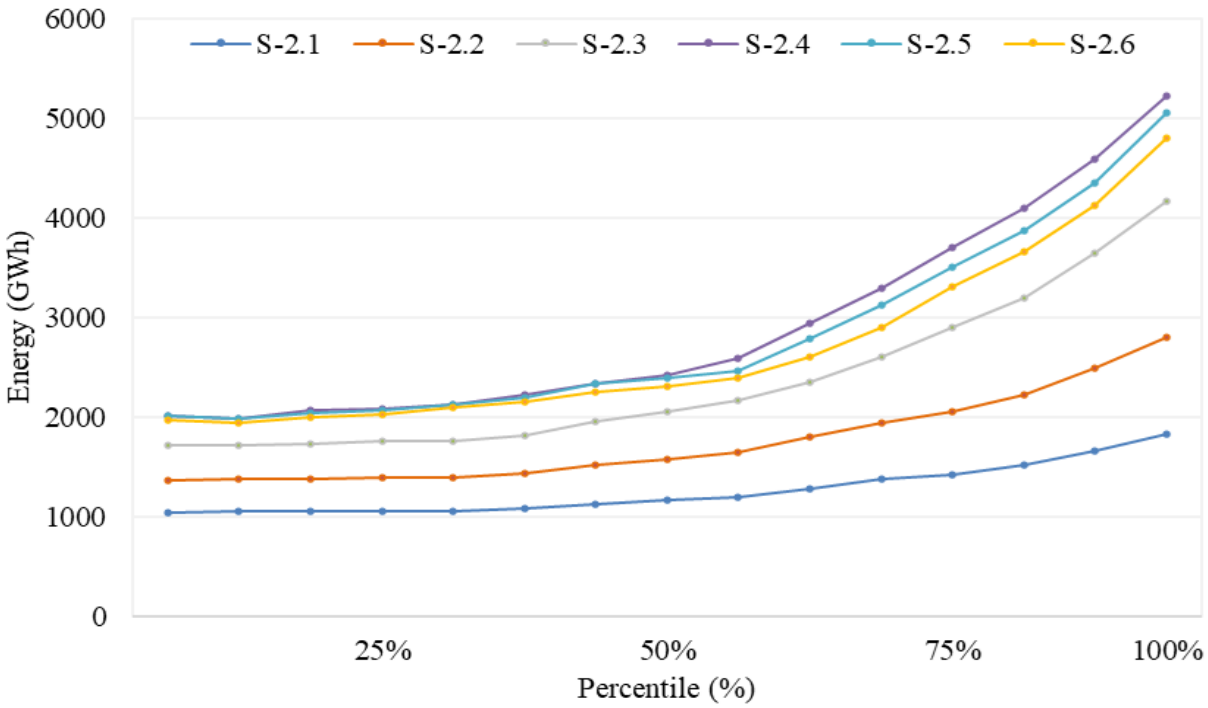

Figure 4.27: Percentile of monthly system energy generation (GWh) considering irrigation development.

The diversion of irrigation also affects both the operation of the reservoir system and the availability of water. In Figure 4.28(b), the reservoir system storage is illustrated for various scenarios, comparing situations with and without irrigation intervention. It is evident that storage without irrigation exceeded that with irrigation. For scenario S-2.1, the average storage decreased by 3%. In scenarios S-2.2 and S-2.3, the system storage declined by 4% and 6% compared to S-1.2 and S-1.3, respectively. The average system water availability in the reservoirs for scenarios S-2.4, S-2.5, and S-2.6 were evaluated by taking S-1.4 as a baseline. It was observed that the average system storage in S-1.4 was 160 BCM (Figure 4.28 (b)). However, with potential irrigation development, the system storage decreased in each scenario by 8%, 12%, and 16% for S-2.4, S-2.5, and S-2.6, respectively. Figure 4.29 also showed the average storage of individual reservoirs. For S-2.6, representing full irrigation development, the results showed that the most significant storage decline was observed in the GERD reservoir, with a 21% decrease compared to individual storage in S-1.4. Following GERD, the storage in Mandaya, Bekoabo, and Karadobi decreased by 19%, 14%, and 6%, respectively. The percentage decrease in individual reservoir storage corresponds to the extent of irrigation development upstream of each reservoir. The more

downstream the reservoir, the greater the impact of irrigation development upstream, leading to more pronounced effects on reservoir storage due to increased irrigation water diversion. Table 4.8 and Table 4.9 also showed the power summary and reservoir operation for each scenario and time step.

Increasing irrigation diversion leads to a corresponding decline in both energy production and storage capacity, emphasizing the trade-off between irrigation development and energy generation. The finding of the scenario analysis revealed that though the energy production and reservoir operation show a decline trend as irrigation expands, it is noticed that irrigation expansion is not a severe threat, especially for average energy generation of hydropower projects over the Abbay river basin. Instead, diverted water for irrigation purposes could boost productivity, leading to improved food security. Additionally, it could facilitate the export of agricultural goods, generating foreign income and offsetting the losses incurred from reduced energy production.

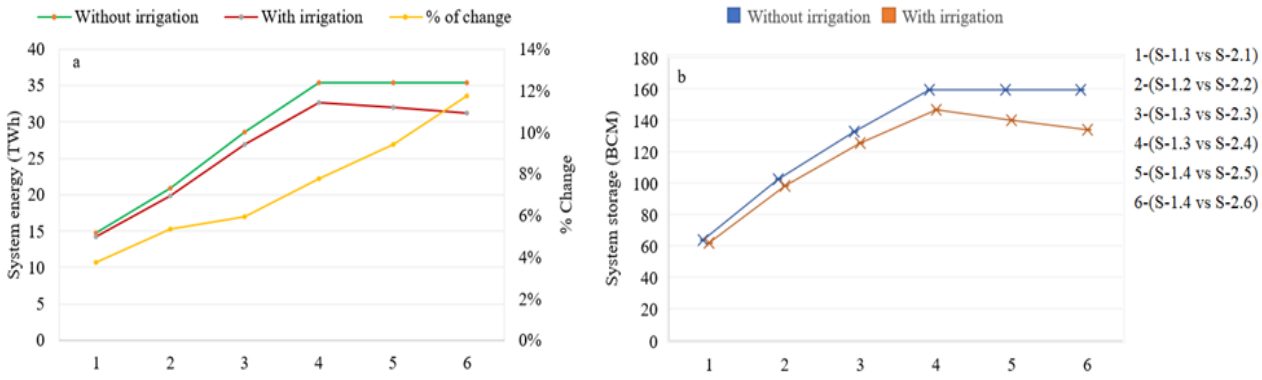

Figure 4.28: Annual system wide energy generation (a) and average system storage (b) for each scenario.

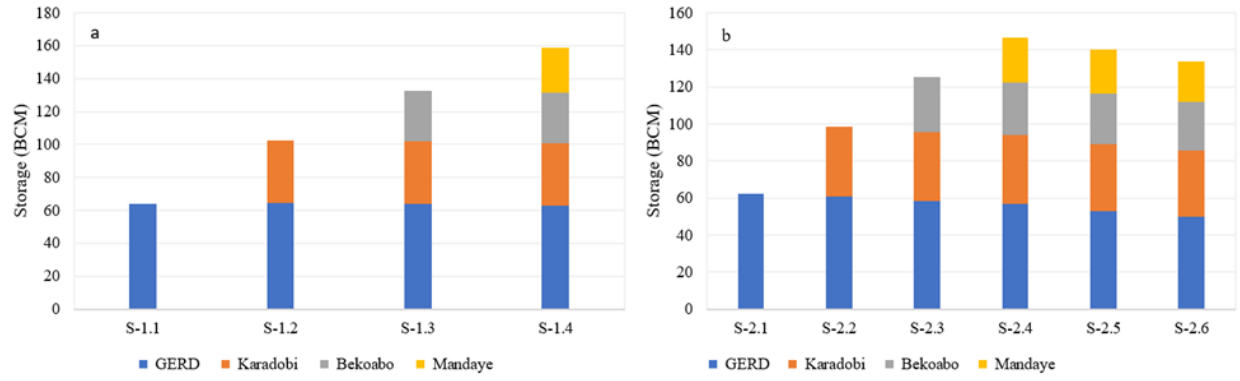

Figure 4.29: Independent Storage for each scenario without irrigation (a) and with irrigation (b)

Table 4. 8: Summary of simulated power reports for each cascade scenario with intervention of irrigation projects for each time step (daily for this study)

HP Project	S-2.1	S-2.2	S-2.3	S-2.4	S-2.5	S-2.6
GERD Reservoir-Power Plant						
Energy Generated per Time Step (MWh)	41923.7	40740.5	39790.1	37747.6	36397.8	34610.8
Power Generated (MW)	1746.82	1697.52	1657.92	1572.82	1516.57	1442.12
Plant Factor	0.34	0.33	0.32	0.31	0.29	0.28
Karadobi Dam-Power Plant						
Energy Generated per Time Step (MWh)		17535.2	17648.3	17254.5	17212.5	17153.3
Power Generated (MW)		730.63	735.35	718.94	717.19	714.72
Plant Factor		0.45	0.44	0.41	0.37	0.36
Beko Abo Dam-Power Plant						
Energy Generated per Time Step (MWh)			21688.2	21455.3	21288.5	21054.2
Power Generated (MW)			903.68	893.97	887.02	877.26
Plant Factor			0.42	0.41	0.38	0.37
Mandaya Dam-Power Plant						
Energy Generated per Time Step (MWh)				19686.3	19393.8	19009.6
Power Generated (MW)				820.26	808.07	792.07
Plant Factor				0.44	0.42	0.4

Table 4. 9: Summary of reservoir operation for each cascade scenario with intervention of irrigation projects for each time step (daily for this study)

HP Project	S-2.1	S-2.2	S-2.3	S-2.4	S-2.5	S-2.6
GERD Reservoir						
Storage (m3)	62.85	61.43	59.07	57.62	53.51	50.38
Elevation (m)	633.63	632.68	631.11	630.10	627.19	624.68
Karadobi Dam						
Storage (m3)		37.71	36.50	36.00	35.00	34.55
Elevation (m)		1142.58	1139.63	1138.38	1135.82	1134.64
Beko Abo Dam						
Storage (m3)			29.00	27.00	26.42	25.53
Elevation (m)			1061.50	1061.49	1061.37	1061.15
Mandaya Dam						
Storage (m3)				24.31	23.52	22.22
Elevation (m)				798.85	798.55	798.03

4.3.3. Hydro-economic trade-off analysis

Through this analysis, a clearer understanding of the development options emerges, be it the exclusive emphasis on hydropower, a single focus on irrigation, or the pursuit of a combined approach, all with the overarching goal of maximizing overall benefits. A vital point of reference within this framework is the zero (0.00) irrigation benefit, which serves as a benchmark indicating the absence of any irrigation development. Considering the present value (P1), Figure 4.30 illustrated the hydro-economic trade-offs between hydropower and irrigation across various development scenarios, providing a detailed overview of the interplay between the two critical components. Whereas Figure 4.31 presented a comprehensive illustration of the individual and combined benefit obtained from hydropower and irrigation development. It is apparent that as the benefits of irrigation grow, the benefits from hydropower diminish, and conversely, as the benefits from hydropower increase, the benefits from irrigation decrease. Initially, assuming no development in irrigation, the accrued annual benefit from four distinct cascade hydropower projects was found as 1.3 billion USD (GERD), 1.8 billion USD (GERD and Karadobi), 2.5 billion USD (GERD, Karadobi, and Bekoabo), and 3.1 billion USD (GERD, Karadobi, Bekoabo, and Mandaya), as shown in Figure 4.30 (a, b, c, and d).

However, as irrigation expanded and more water was diverted from the system, the benefits derived solely from hydropower decreased by a second-order polynomial function in all scenarios (Figure 4.30). The trade-off analysis result revealed that with a unit increase in irrigation benefit, the hydropower benefit decreases by 5%. Unlike the decrease in hydropower benefits, the benefits arising from irrigation witnessed a rise concurrent with the expansion of irrigation. Upon achieving full irrigation development (S-2.6), the annual irrigation benefit reached 3.6 billion USD, surpassing the benefits obtained solely from full hydropower development by 17%. To the right of the pins (Figure 4.30), the trade-off curves showed steeper slopes, which revealed a greater reduction of hydropower benefits with further irrigation development.

The research underscored the importance of not just assessing the trade-offs but also considering the synergies between hydropower and irrigation returns. This approach aims to promote the formulation of development scenarios that optimize overall benefits. Remarkably, while the enhanced focus on one objective came at the cost of the other, the overall benefit derived from both objectives underscores the importance of concurrently pursuing irrigation and hydropower

development. Figure 4.31 illustrates the individual and combined annual benefit of hydropower and irrigation for each scenario. In all scenarios, the combined benefits derived from both hydropower and irrigation outweigh the benefits of pursuing a single objective, such as focusing solely on hydropower. Despite the inherent conflict between the two objectives, their combined benefits are substantial. Evaluating the situation from this perspective, the results of this study revealed that, across various instances of irrigation expansion, the combined benefit of hydropower and irrigation surpasses the benefits derived solely from hydropower. Investigating into a comprehensive assessment of full irrigation development integrated to four cascade hydropower projects, it is revealed that the total annual benefit reaches nearly 6 billion USD, which exceeded those of hydropower benefit alone by 94%. At the point of intersection between the hydropower benefit and irrigation benefit curve, the total benefit obtained was 5 billion USD. Above S-2.4, the hydropower benefit curve showed downward deflection, indicating more trade-off in benefits. However, the total benefit was still at its increasing trend, revealing that the irrigation benefit was more outweighed than the benefit of hydropower. The trade-off curve for the future values (P2-P4) follows the same patterns like Figure 4.30 except the change in amount of benefits. The graphical visualization is found in the appendix section (Figure E-2, Figure E-3 & Figure E-4).

The findings underscore the importance of understanding the trade-offs and synergy between hydropower and irrigation development in the context of the Abbay Basin. The result would provide insights to formulate sustainable strategies that balance the benefits of both objectives, ensuring the optimal utilization of water resources for economic and environmental sustainability. The result generally indicates that over the Abbay river basin it is encouraged to develop both hydropower and irrigation concurrently rather than focusing solely on hydropower only.

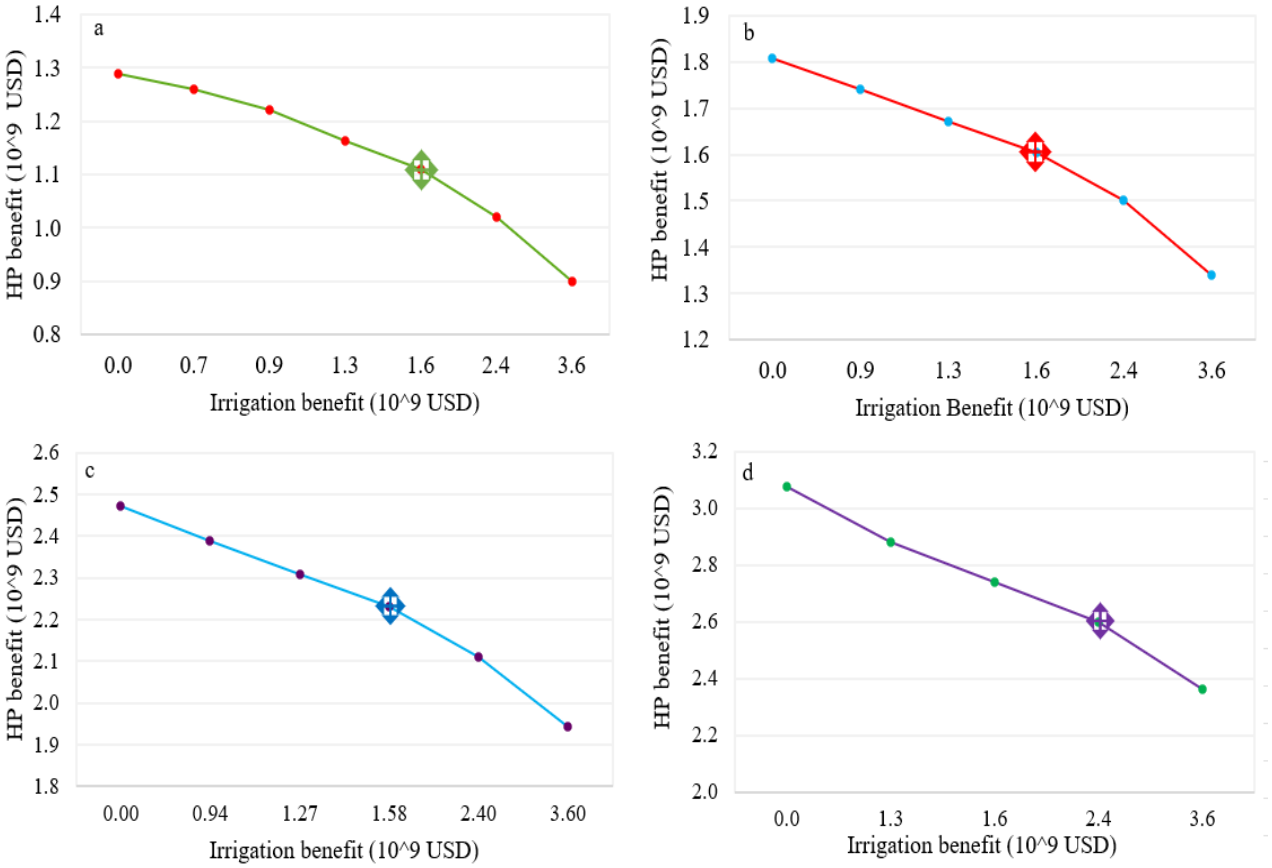

Figure 4.30: Hydro-economic trade-off between hydropower and irrigation development (P1). a) GERD plus six irrigation scenarios, b) GERD and Karadobi plus five irrigation scenarios, c) GERD, Karadobi and Bekoabo plus five irrigation scenarios, d) GERD, Karadobi, Bekoabo and Mandaya plus four irrigation Scenarios (as shown in Table 3.2).

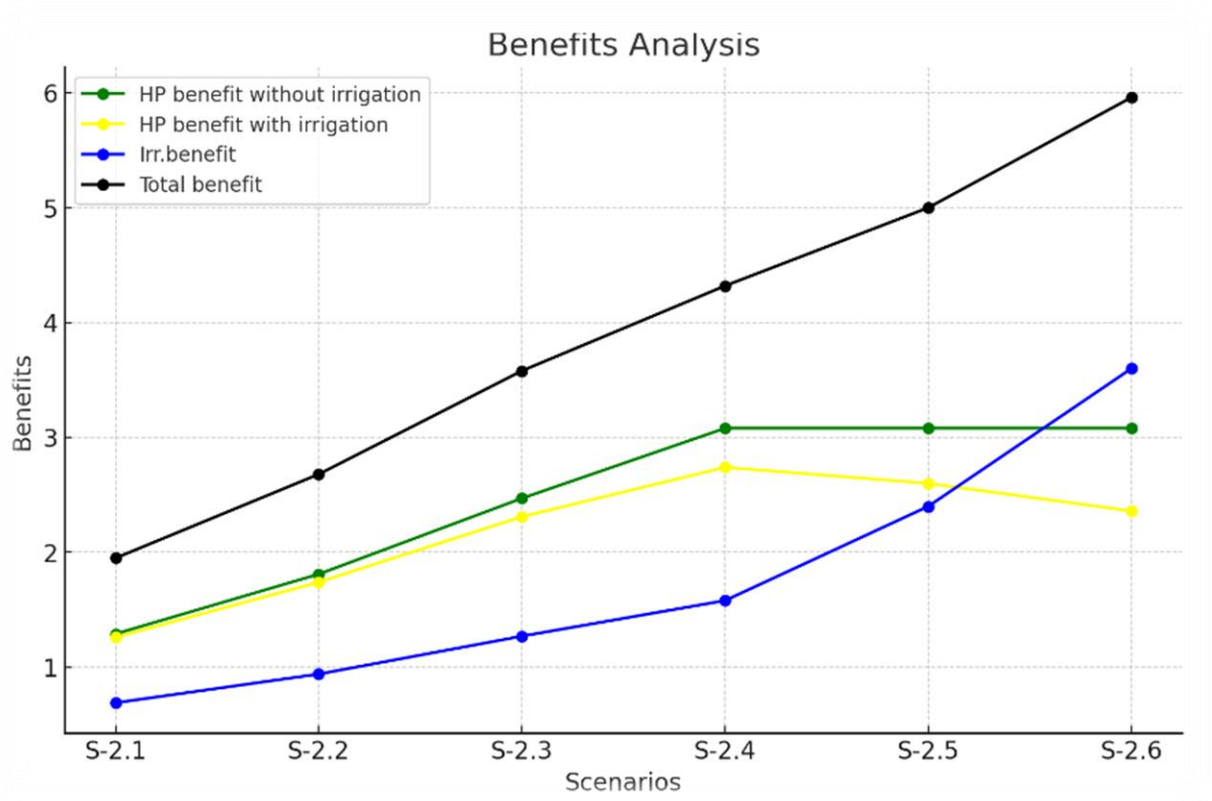

Figure 4.31: Summary of Hydro-economic benefit (billion US$) from hydropower and irrigation development in each stage of scenario (as shown in Table 3.1).

4.3.4. Hydro-economic benefits considering future values

In large-scale projects designed to generate long-term benefits, the expected returns are unlikely to remain constant over time. The perceived benefits fluctuate with changes in returns over the years. To account for this variability, this research examines the concepts of present value and future value within the context of the Abbay River basin.

The Figure 4.32 describes the hydro-economic benefits in billion USD from hydropower generation and irrigation development within the Abbay River basin, across four different scenarios of dam and irrigation development. Each scenario represents a combination of dams GERD, Karadobi, Bekoabo, and Mandaya and a consistent irrigation area of 1.2 million hectares.

In Scenario 1, where only the GERD is coupled with 1.2 million hectares of irrigation, the present value (P1) is estimated at 4.5 billion USD. This value is projected to increase significantly in the future, reaching 7 billion USD by 2030 (P2), 13 billion USD by 2040 (P3), and 26 billion USD by

2050 (P4). This shows a clear upward trend, reflecting the growing benefits of hydropower and irrigation over time.

Scenario 2, which includes the GERD and Karadobi dams alongside 1.2 million hectares irrigation area, starts with the present benefit of 5 billion USD but sees slightly higher future benefits: 7 billion USD in 2030, 15 billion USD in 2040, and 29 billion USD in 2050. The inclusion of Karadobi appears to enhance the benefits, particularly in the later years.

Scenario 3 further adds the Bekoabo dam to the previous two dams and maintains the irrigation area. This scenario shows a higher present value of 5.5 billion USD. The future benefits also increase progressively, reaching 8 billion USD in 2030, 16 billion USD in 2040, and 32 billion USD by 2050. The inclusion of Bekoabo contributes to a more substantial increase in economic benefits, particularly noticeable from 2040 onwards.

Finally, Scenario 4, which incorporates all four dams (GERD, Karadobi, Bekoabo, and Mandaya) along with the 1.2 million hectares of irrigation, starts with the benefit of 6 billion USD but shows the highest future benefits: 9 billion USD by 2030, 18 billion USD by 2040, and 34 billion USD by 2050. This scenario demonstrates the most significant economic benefits, indicating that the full development of the basin's hydropower potential, coupled with irrigation, yields the highest returns in the long term.

Overall, the analysis reveals that while the present economic benefits are modest, the future benefits increase substantially with each additional dam, particularly in the long-term horizons of 2040 and 2050. This suggests that the combined development of hydropower and irrigation infrastructure in the Abbay River basin can lead to considerable economic gains, with the full cascade of dams providing the most substantial returns.

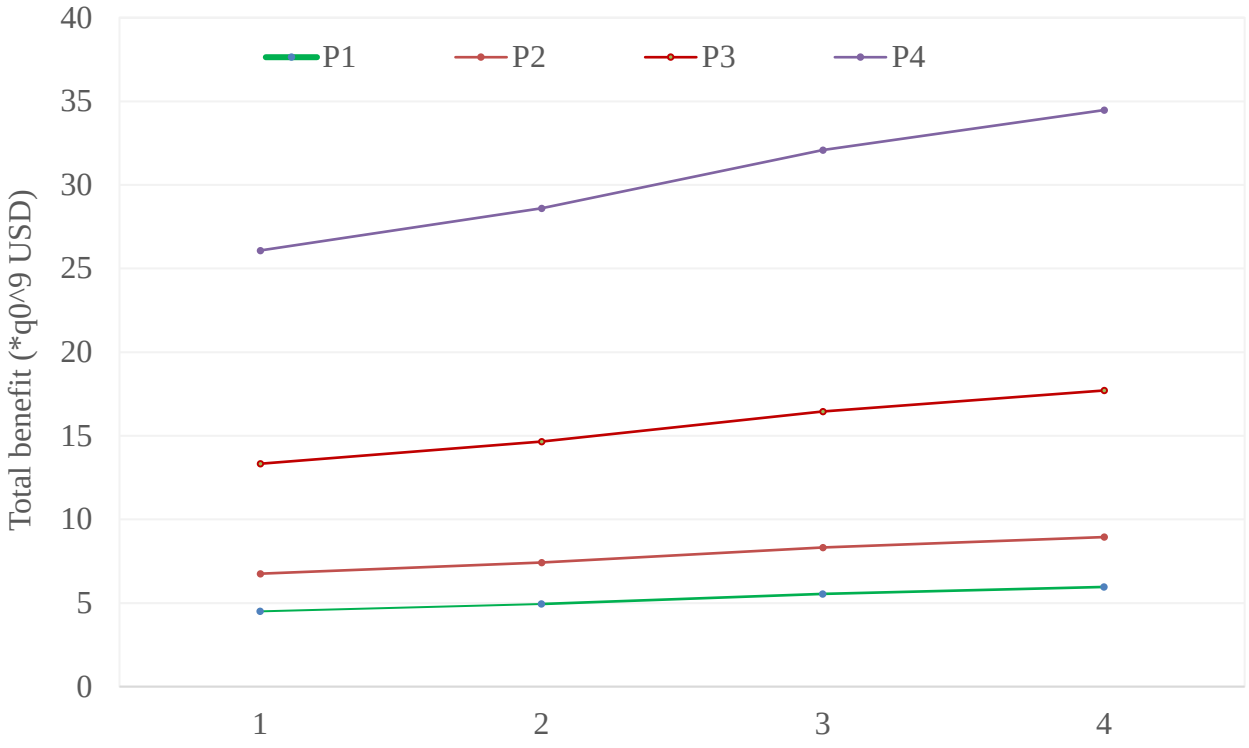

Figure 4.32: Total benefits (US$) for different return rates. P1 is the present value, P2-P4 are future values corresponding to 2030, 2040 and 2050. 1 indicates GERD plus 1.2 million hectares of irrigation, 2 indicates GERD, Karadobi plus 1.2 million hectares of irrigation, 3 indicates GERD, Karadobi and Bekoabo plus 1.2 million hectares of irrigation, 4 indicates GERD, Karadobi, Bekoabo and Mandaya plus 1.2 million hectares of irrigation

4.4. Trade-off and synergy analysis conclusion

This study conducted a thorough assessment of the hydropower and irrigation trade-off and synergy in the Abbay river basin. The combination of the hydrological model (ArcSWAT) to quantify the water resource potential of the basin and HEC-ResSim to simulate the power generation and reservoir operation with various development scenarios was applied.

The successive developments of hydropower projects and the operation of multiple cascades contributed to the substantial growth in average monthly and annual energy generation, reflecting the enhanced energy generation capacity of the system. The enhanced energy generation capacity resulting from the operation of multiple cascades in the Abbay river basin has significant implications for increasing energy demand. It enables the country to meet growing energy needs, drive economic development, improve energy access, explore regional energy export opportunities, and advance its renewable energy transition. Irrigation is, on the other hand, essential to increase agricultural productivity, achieve food security, and export agricultural products. Analyzing the trade-off and synergy between hydropower and irrigation under various development scenarios is crucial for making informed decisions regarding water resource management, efficient water allocation strategies, sustainable development, and utilization of available water resources. By considering different development scenarios and their associated trade-offs and synergy, policymakers can make informed decisions that maximize the overall benefits while minimizing potential negative consequences.

The result of this research generally revealed that the total benefit gained from hydropower and irrigation underscores the individual benefit, though the two objectives are conflicting with each other. Thus, it is encouraged to develop both hydropower and irrigation concurrently rather than giving emphasis only to hydropower.

To provide full insight into the management, planning, and development of water resources, we suggest further research on water-energy-food nexus modeling by considering climate change and ecological consequences of hydropower and irrigation projects.

5. Conclusion and recommendation

5.1. Conclusion

Given that the Abbay River basin serves as a potential water source for the entire Nile flow, the spatio-temporal assessment of water balance components holds significant importance for various purposes. The quantitative results obtained for the water balance components are crucial for planning, development, and management processes concerning these resources.

This study also conducted a thorough assessment of the water-hydropower-irrigation trade-off and synergy in the Abbay river basin. The reservoir simulation model (HEC-ResSim) was applied to simulate different combinations of hydropower reservoirs and irrigation diversions. The calibration results, evaluated through regression coefficients and a comparison with previous research, demonstrated that the HEC-ResSim model was a suitable tool for this study.

The successive additions of hydropower projects and the operation of multiple cascades contributed to the substantial growth in average monthly and annual energy generation, reflecting the enhanced energy generation capacity of the system. The enhanced energy generation capacity resulting from the operation of multiple cascades in Ethiopia has significant implications for increased energy demand. It enables the country to meet growing energy needs, drive economic development, improve energy access, explore energy export opportunities, and advance its renewable energy transition.

Analyzing the trade-off and synergy between hydropower and irrigation under various development scenarios is crucial for making informed decisions regarding water resource management, efficient water allocation strategies, and sustainable and equitable utilization of available water resources. Hydropower, as a renewable energy source, offers the potential for clean electricity generation and reducing greenhouse gas emissions. Irrigation is, on the other hand, essential to increase agricultural productivity and achieve food security. Therefore, the trade-off analysis is essential to strike a balance between energy generation and sustainable water use. By considering different development scenarios and their associated trade-offs, policymakers can make informed choices that maximize the overall benefits while minimizing potential negative consequences.

5.2. Recommendation

With this research, it was tried that the modeling of water resources, evaluation of trade-offs, and synergy among conflicting water needs for the Abbay river basin have been addressed. However, the conducted analysis can be improved or expanded in several ways, including:

- To provide full insight into the management, planning, and development of water resources, we suggest further research on water-energy-food nexus modeling by considering climate change and ecological consequences of hydropower and irrigation projects.
- In this research, the hydro-economic analysis was done considering only wheat as a dominant crop. Other crops were not considered. Thus, further research is recommended by considering other crops into the system.
- In this research, the hydro-economic analysis was done considering the present value. Thus, future research is recommended by considering the future value of return.
- Climate change impacts hydrology and reservoir inflows and operations. Therefore, future research should concentrate on assessing how climate change affects reservoir operations and the energy generation of hydropower plants.
- Over the Abbay river basin, different irrigation potential areas were identified. However, due to irrigation technology advancement, agricultural land use change, and economic growth of the country, the potential irrigable area is expected to be more than previously estimated. Research on the potential assessment of irrigable area is thus needed for the future. This would be important for policymaking and informed decision making.
- The land use change is obviously affecting the rainfall-runoff dynamics. This research didn't consider the land use changes to model the water resource potential. Thus, future research is highly recommended considering the land use change.
- Improving irrigation efficiency and its implication on the trade-off between hydropower and irrigation is recommended in future research.
- Evaluating the catchment management impacts on reservoir sedimentation is also recommended in future research.

References

Abbay Basin Authority (ABA, 2026). The Federal Democratic Republic of Ethiopia, Abbay Basin Authority, booklet

Abbaspour, K.C., 2014. User manual for SWAT-CUP12, SWAT calibration and uncertainty analysis programs. Swiss Federal Institute of Aquatic Science and Technology, Eawag, Dübendorf, Switzerland. Available from: http://www.eawag.ch/forschung/ siam/software/swat/index

Abbaspour, K.C., Yang J., Maximov I., Siber R., Bogner K., Mieleitner J., Zobrist J., Srinivasan R., 2007. Modelling hydrology and water quality in the pre-alpine/alpine Thur watershed using SWAT. Journal of Hydrology, 333:413-430.

Abbott, M., Bathurst, J., Cunge, J., O'Connell, P., & Rasmussen, J., 1986. An introduction to the European Hydrological System -Systeme Hydrologique Europeen, "SHE", 1: History and philosophy of a physically-based, distributed modelling system. Journal of Hydrology, 87(1–2), 45–59. https://doi.org/10.1016/0022-1694(86)90114-9

Abdelkader, A., Haggag, M., Hamed, K., & Radwan, H. G., 2023. Assessment of the Impacts of Proposed Water Resource Development Projects in Baro-Akobo-Sobat Basin on Nile Inflows at High Aswan Dam. Journal of Hydrology: Regional Studies, 46, 101335.

https://doi.org/10.1016/j.ejrh.2023.101335

Abebe, S. A., Qin, T., Zhang, X., Li, C., & Yan, D., 2022. Estimating the Water Budget of the Upper Blue Nile River Basin With Water and Energy Processes (WEP) Model. *Frontiers in Earth Science, 10*. https://doi.org/10.3389/feart.2022.923252

Abeer, S., Mona G. I., Wael, E.M., Manabu F., Amr, E., Waled, D., 2019. Statistical Assessment of Rainfall Characteristics in Upper Blue Nile Basin over the Period from 1953 to 2014. Water, 11, 468; doi:10.3390/w11030468

Abera Tareke, K., & Gebeyehu Awoke, A., 2022. Hydrological and Meteorological Drought Monitoring and Trend Analysis in Abbay River Basin, Ethiopia. Advances in Meteorology, 2022, 1–18. https://doi.org/10.1155/2022/2048077

Abera, W., Formetta, G., Brocca, L., & Rigon, R. (2017). Modeling the water budget of the Upper Blue Nile basin using the JGrass-NewAge model system and satellite data. Hydrology and Earth System Sciences, 21(6), 3145–3165. https://doi.org/10.5194/hess-21-3145-2017

Abeyou, W. W., Essayas K. A., Haw, Y., Jaehak J., Charlotte M., Robin T., Thomas J. G., Tammo S. S., 2018. Evaluating hydrologic responses to soil characteristics using SWAT model in a paired-watersheds in the Upper Blue Nile Basin. www.elsevier.com/locate/catena https://doi.org/10.1016/j.catena.2017.12.040

Abtew W. and Dessu S. B., 2019. The Grand Ethiopian Renaissance Dam on the Blue Nile, Springer Geography, https://doi.org/10.1007/978-3-319-97094-3_1

Abiy, A. Z., Demissie, S. S., MacAlister, C., Dessu, S. B., & Melesse, A. M. (2015). Groundwater Recharge and Contribution to the Tana Sub-basin, Upper Blue Nile Basin, Ethiopia. In Springer geography (pp. 463–481). https://doi.org/10.1007/978-3-319-18787-7_22

Achenafi G., Yihun D. T., Dereje H., Haimanote K. B., Kibruyesfa S., 2020. Impact of climate and Land Use Change on Hydrological Response in Gumara Watershed, Ethiopia. Authorea. DOI: 10.22541/au.159863388.81259725

Ahmed M. R., 2012. Eastern Nile Water Resources Simulation. Eastern Nile Technical Regional Office – Entro.

Akoko, G., Le T.H., Gomi,T., Kato, T., 2021. A Review of SWAT Model Application in Africa. Water, 13, 1313. https://doi.org/10.3390/w13091313

Albrecht, T. R., Crootof, A., & Scott, C. A., 2018, April 1. The Water-Energy-Food Nexus: A systematic review of methods for nexus assessment. Environmental Research Letters, 13(4), 043002. https://doi.org/10.1088/1748-9326/aaa9c6

Alemu, A. M., Seleshi, Y., & Meshesha, T. W., 2022. Modeling the spatial and temporal availability of water resource potential over Abbay river basin, Ethiopia. Journal of Hydrology: Regional Studies, 44, 101280. https://doi.org/10.1016/j.ejrh.2022.101280

Allam, M. M., & Eltahir, E. A. B., 2019. Water-Energy-Food Nexus Sustainability in the Upper Blue Nile (UBN) Basin. Frontiers in Environmental Science, 7. https://doi.org/10.3389/fenvs.2019.00005

Allam, M. M., Jain Figueroa, A., McLaughlin, D. B., & Eltahir, E. A. B., 2016. Estimation of evaporation over the upper Blue Nile basin by combining observations from satellites and river flow gauges. Water Resources Research, 52(2), 644–659. https://doi.org/10.1002/2015wr017251

Almohseen K., Jalil S., 2014. Simulation Models for Bekhma Reservoir Operation System (Comparison Study). Journal of University of Duhok, Vol. 17, No.1 (Pure and Eng. Sciences)

Annys, S., Adgo, E., Ghebreyohannes, T., Van Passel, S., Dessein, J., & Nyssen, J., 2019. Impacts of the hydropower-controlled Tana-Beles interbasin water transfer on downstream rural livelihoods (northwest Ethiopia). Journal of Hydrology, 569, 436–448. https://doi.org/10.1016/j.jhydrol.2018.12.012

Apaydin, H., Sonmez, F., & Yildirim, Y., 2004. Spatial interpolation techniques for climate data in the GAP region in Turkey. Climate Research, 28, 31–40. https://doi.org/10.3354/cr028031

Arnold J. G., Moriasi D. N., Gassman P. W., Abbaspour K. C., White M. J., Srinivasan R., Santhi C., Harmel R. D., Griensven A. van, Van Liew M. W., Kannan N., Jha M. K., 2012. SWAT: Model Use, Calibration, and Validation. The ASABE, 55(4), 1491–1508. https://doi.org/10.13031/2013.42256

Arnold J.G., Kiniry J.R., Srinivasan R., Willimas J.R.,Heney E.B., Neitsch S.L., 2012. SWAT Input/Output Documentation. Texas water Resources Institute.

Arnold, J. G., Allen, P. M., Muttiah, R., & Bernhardt, G., 1995. Automated Base Flow Separation and Recession Analysis Techniques. Ground Water, 33(6), 1010–1018. https://doi.org/10.1111/j.1745-6584.1995.tb00046.x

Ashraf EL-S., Ahmet I., 2013. Evaluating the impact of land use uncertainty on the simulated stream flow and sediment yield of the Seyhan River basin using the SWAT model. TURKISH JOURNAL OF AGRICULTURE AND FORESTRY, 38, 515–530. https://doi.org/10.3906/tar-1309-89

Asitatikie, A. N., & Nigussie, E. D., 2020. Modeling on naturalization of inflow and outflow nutrients sources of Blue Nile River at the Lake Tana in Basaltic Plateau of Ethiopia. Modeling Earth Systems and Environment, 7(4), 2283–2295. https://doi.org/10.1007/s40808-020-00972-x

Awulachew, S. B., Yilma, A. D., Loulseged, M., Loiskandl, W., Ayana, M., Alamirew, T., 2007. Water Resource and Irrigation Development in Ethiopia. Colombo, Sri Lanka: International Water Management Institute. 78p. (Working Paper 123).

https://www.iwmi.cgiar.org/Publications/Working_Papers/working/WP123.pdf

Baker, J. S., Van Houtven, G., Cai, Y., Moreda, F., Wade, C., Henry, C., Redmon, J. H., & Kondash, A. J. (2021). A Hydro-Economic Methodology for the Food-Energy-Water Nexus: Valuation and Optimization of Water Resources.

https://doi.org/10.3768/rtipress.2021.mr.0044.2105

Bashe, T., Alamirew, T., & Dejen, Z. A. (2022, October 12). Estimating the economic value and economic return of irrigation water as a sustainable water resource management mechanism. Sustainable Water Resources Management, 8(6). https://doi.org/10.1007/s40899-022-00764-4

Bassel T. D. and Rabi H. M., 2015. Water–energy–food (WEF) Nexus Tool 2.0: guiding integrative resource planning and decision-making. Water International, vol. 40, Nos. 5–6, 748–771, http://dx.doi.org/10.1080/02508060.2015.1074148

Bayat, B., Zahraie, B., Taghavi, F., Nasseri, M., **2012**. Evaluation of spatial and spatiotemporal estimation methods in simulation of precipitation variability patterns. Theor. Appl. Climatol. 113, 429–444.

Bayissa, Y., Moges, S., Melesse, A., Tadesse, T., Abiy, A. Z., & Worqlul, A., 2021. Multi-Dimensional Drought Assessment in Abbay/Upper Blue Nile Basin: The Importance of Shared Management and Regional Coordination Efforts for Mitigation. Remote Sensing, 13(9), 1835. https://doi.org/10.3390/rs13091835

Bazilian, M., Rogner, H., Howells, M., Hermann, S., Arent, D., Gielen, and D., 2011.Considering the energy, water and food nexus: towards an integrated modelling approach. Energy Policy 39,7896–7906.http://dx.doi.org/10.1016/j.enpol.2011.09.039

BCEOM. 1998. Abbay River Basin Integrated Development Master Plan, Section II, Volume V, Water Resources Development, Part 1: Irrigation and Drainage, Ministry of Water Resources, Addis Ababa, Ethiopia.

BCEOM, 1999. Abbay River Basin integrated master plan, main report. Ministry of Water Resources, the Federal Democratic Republic of Ethiopia, Addis Ababa.

BCEOM, 1998. Abbay River Basin master plan, phase-2, section I- main report. Ministry of Water Resources, the Federal Democratic Republic of Ethiopia, Addis Ababa.

Befekadu G. H., Harb A.E., Saud A. A., Verne R.S, Frank A. W., 2015. Mutually beneficial and sustainable management of Ethiopian and Egyptian dams in the Nile Basin. Journal of Hydrology 529, 1235–1246. http://dx.doi.org/10.1016/j.jhydrol.2015.09.017

Bekchanov, M.; Sood, A.; Jeuland, M., 2015. Review of hydro-economic models to address river basin management problems: structure, applications and research gaps. Colombo, Sri Lanka: International Water Management Institute (IWMI). 60p. (IWMI Working Paper 167). doi: 10.5337/2015.218

Belay B. B., Mamaru A. M., Berhanu G. S., Mulu S. K., 2021. SWAT and HBV models' response to streamflow estimation in the Upper Blue Nile Basin, Ethiopia. Water-Energy Nexus, 41–53, https://doi.org/10.1016/j.wen.2021.03.001

Belachew A. and Mekonen Z., 2014. Eastern Nile Basin Water System Simulation Using Hec-ResSim Model. CUNYAcademic Works. http://academicworks.cuny.edu/cc_conf_hic/373

Belete B., Yilma S., Solomon S. D. and Assefa M. M. (2016). Bias correction and characterization of climate forecast system re-analysis daily precipitation in Ethiopia using fuzzy overlay. Meteorol. Appl.(2016). DOI: 10.1002/met.1549

Betrie, G. D., Mohamed, Y. A., van Griensven, A., & Srinivasan, R. (2011, March 8). Sediment management modelling in the Blue Nile Basin using SWAT model. Hydrology and Earth System Sciences, 15(3), 807–818. https://doi.org/10.5194/hess-15-807-2011

Braden, J.B., 2000. Value of valuation: introduction. Journal of Water Resources Planning and Management 126 (6), 336–338.

Cardwell, H.E., Cole, R.A., Cartwright, L.A., Martin, L.A., 2006. Integrated water resources management: definitions and conceptual musings. Journal of Contemporary Water Research and Education (35), 8–18.

Chao L., Zhou H., and Zhou X., 2015. Data quality assessment in hydrological information systems. Journal of Hydroinformatics 17(4):640. DOI: 10.2166/hydro.2015.042

Chow W. T., Maidment D. R., Mays L. W., 1988. Applied Hydrology, New York, McGraw-Hill: 572.

Clever M., 2018. The Value of Green Water Management in Sub-Saharan Africa: A Review. Journal of Contemporary Water Research & Education, 165(1), 67–75. https://doi.org/10.1111/j.1936-704x.2018.03294.x

Conway, D., Hulme, M., 1993. Recent fluctuations in precipitation and runoff over the Nile sub-basins and their impact on main Nile discharge. Clim. Change 25, 127–151. https://doi.org/10.1007/BF01661202

Conway D., 1997. A water balance model of the Upper Blue Nile in Ethiopia, Hydrological Sciences Journal, 42:2, 265-286, DOI: 10.1080/02626669709492024

CONWAY, D., 2000. The Climate and Hydrology of the Upper Blue Nile River. The Geographical Journal, 166(1), 49–62. https://doi.org/10.1111/j.1475-4959.2000.tb00006.x

CSA, 2021. The Federal Democratic Republic of Ethiopia Central Statistical Agency (CSA). Agricultural Sample Survey, Volume I, Addis Ababa

Cunderlikm Juraj, 2003. Hydrologic model selection fort the CFCAS project: Assessment of Water Resources Risk and Vulnerability to Changing Climatic Conditions, Project Report I

Daniel M., Woldeamlak B., Alessasandro D., Hans J.P., 2021. Climate change impacts on water resources in the Upper Blue Nile (Abay) River Basin, Ethiopia. Journal of Hydrology, https://doi.org/10.1016/j.jhydrol.2020.125614

Daniel P., Eelco V.B., 2005. Water Resource System Planning and Management: an Introduction to Methods, Models and Applications. UNESCO, WL/ Delft Hydraulics, the Netherlands.

Denekew, A. Y. and Bekele, S. A., 2009. Characterization and Atlas of the Blue Nile Basin and its Sub basins. International Water Management Institute.

https://publications.iwmi.org/pdf/H042502.pdf

Dereje M. A., Mamaru A. M., Fasikaw A. Z., Asegdew G. M., 2020. Multi-purpose Reservoir Operation Analysis in the Blue Nile Basin, Ethiopia. Advances of Science and Technology: 7th EAI International Conference, ICAST 2019, Bahir Dar, Ethiopia, August 2–4, 2019, Proceedings. https://doi.org/10.1007/978-3-030-43690-2_1

Dessie M., Verhoest N. E. C., Pauwels V. R. N., Admasu T., Poesen J., Adgo E., Deckers J., and Nyssen J., 2014. Analyzing runoff processes through conceptual hydrological modeling in the Upper Blue Nile Basin, Ethiopia. Hydrol. Earth Syst. Sci., 18, 5149–5167, www.hydrol-earth-syst-sci.net/18/5149/

Diekkrüger, B., Kapangaziwiri, E., Badou, D.F., Mbaye, M.L., Yira, Y.,. Lawin, E.A, Afouda, A., 2018. Modelling Blue and Green Water Availability Under Climate Change in the Beninese Basin of the Niger River Basin, West Africa, (April), 2526–2542. Doi:10.1002/hyp.13153

Dilnesaw Alamirew, 2006. Modeling of Hydrology and soil Erosion of Upper Awash River Basin. PhD Thesis, University of Bonn.

Digna, R. F., Castro-Gama, M. E., der Zaag, P. V., Mohamed, Y. A., Corzo, G., & Uhlenbrook, S., 2018. Optimal Operation of the Eastern Nile System Using Genetic Algorithm, and Benefits Distribution of Water Resources Development. MDPI.

https://doi.org/10.3390/w10070921

Digna, R. F., Castro-Gama, M. E., der Zaag, P. V., Mohamed, Y. A., Corzo, G., & Uhlenbrook, S., 2018. Optimal Operation of the Eastern Nile System Using Genetic Algorithm, and Benefits Distribution of Water Resource Development. MDPI.

https://doi.org/10.3390/w10070921

Eastern Nile Technical Regional Office (ENTRO), 2006. Water Atlas of the Blue Nile Sub-Basin, Draft Report Eastern Nile Technical Regional Office (ENTRO) Ethiopia.

Easton, Z. M., Fuka, D. R., White, E. D., Collick, A. S., Biruk Ashagre, B., McCartney, M., Awulachew, S. B., Ahmed, A. A., & Steenhuis, T. S. (2010, October 11). A multi basin SWAT model analysis of runoff and sedimentation in the Blue Nile, Ethiopia. Hydrology and Earth System Sciences, 14(10), 1827–1841. https://doi.org/10.5194/hess-14-1827-2010

EEPCo (Ethiopian Electric Power Corporation). 2019, last accessed 5 November 2019. See: http://www.eepco.gov.et/abouttheproject. “Grand Ethiopian Renaissance Dam”

Eldardiry, H., & Hossain, F., 2021. Evaluating the hydropower potential of the Grand Ethiopian Renaissance Dam. Journal of Renewable and Sustainable Energy, 13(2), 024501. https://doi.org/10.1063/5.0028037

Ephrem Alemu, 2011. Effects of Watershed characteristics on River Flow for the Case of Rib and Catchments, Upper Blue Nile Basin. MSc thesis.

Erwin I, P., Amr F., Ralf L., Markus D., 2017. Improving SWAT model performance in the upper Blue Nile Basin using meteorological data integration and subcatchment discretization. Hydrol. Earth Syst. Sci., 21, 4907–4926. https://doi.org/10.5194/hess-21-4907

Essenfelder A. H., 2016. SWAT Weather Database: A Quick Guide. Version: v.0.16.07. doi: 10.13140/RG.2.1.4329.1927

EtefaTilahun Ashine, 2021. Modeling Surface Water Potential of Somodo Watershed. Irrigat Drainage Sys Eng 10. https://www.hilarispublisher.com/open-access/

Ethiopian Technical Experts, 1996. Nile Basin Integrated Water Resource Management: a strategy for cooperation. In: M.A. Abu-Zeid and A.K. Biswas, eds, River Basin planning and management. Calcutta: Oxford University Press, 67.

FAO, 2018. Hydro-economic modelling for basin management of the Senegal River.

Faber B.A., Harou J.J., 2007. Multi-objective Optimization of Reservoir Systems using HEC-ResPRM. World Environmental and Water Resources Congress: Restoring Our Natural Habitat.

Faybishenko B., Versteeg R., Pastorello G., Dwivedi D., Varadharajan, C., Agarwal D., 2021. Challenging problems of quality assurance and quality control (QA/QC) of meteorological

time series data. Stoch. Environ Res Risk Assess 36, 1049–1062. https://doi.org/10.1007/s00477-021-02106-w

Federal Democratic Republic of Ethiopia Abbay Basin Development Office (FDRE-ABDO), 2020. State of the Abbay Basin. https://aba.gov.et/wp-content/uploads/2023/01/State-of-the-Abbay-Basin-2013-2.pdf

Gabriel, B. S., Kwabena A., Guleid A., 2009. Water balance dynamics in the Nile Basin. Hydrological process. https://doi.org/10.1002/hyp.7364

Gassman, P. W., Reyes, M. R., Green, C. H., and Arnold, J. G., 2007. The Soil and Water Assessment Tool: Historical Development, Applications, and Future Research Directions. Transactions of the ASABE, 50(4), 1211–1250. https://doi.org/10.13031/2013.23637

Gebiyaw S.T., Geremew S.G., Azage G.G.,Agizew N. E., 2021. Hydrological modeling in the Upper Blue Nile basin using soil and water analysis tool (SWAT). Modeling Earth Systems and Environment, https://doi.org/10.1007/s40808-021-01085-9

Gemechu, T.M., Zhao, H., Bao, S., Yangzong, C., Liu, Y., Li, F., Li, H., 2021. Estimation of Hydrological Components under Current and Future Climate Scenarios in Guder Catchment, Upper Abbay Basin, Ethiopia, Using the SWAT. Sustainability, 13(17), 9689. https://doi.org/10.3390/su13179689

Geressu, R. T., & Harou, J. J., 2015. Screening reservoir systems by considering the efficient trade-offs—informing infrastructure investment decisions on the Blue Nile. *Environmental Research Letters*, *10*(12), 125008. https://doi.org/10.1088/1748-9326/10/12/125008

Getachew T.A., Tsgegaye T., Berhan G.A., 2021. Spatial and temporal trends and variability of rainfall using long-term satellite product over the Upper Blue Nile Basin in Ethiopia. Remote Sensing in Earth Systems Sciences, 4(3), 199–215. https://doi.org/10.1007/s41976-021-00060-3

Getachew T., Dong K. P., Young-Oh K., 2017. Comparison of hydrological models for the assessment of water resources in a data-scarce region, the Upper Blue Nile River Basin. Journal of Hydrology: Regional Studies, https://doi.org/10.1016/j.ejrh.2017.10.002

Gholamabbas S., Lida V., Ali A. B., Bahram G., Golmar G., 2015. Modeling Blue and Green Water Resources Availability in an Iranian Data Scarce Watershed Using SWAT. Journal of water management Modeling. DOI: https://doi.org/10.14796/JWMM.C391

Global Guidance Unit (GGU), 2016. Seasonal Weather Assessment for Ethiopia during March – July. Met Office. https://reliefweb.int/report/ethiopia/seasonal-weather-assessment-ethiopia-during-march-july

Global Water Partnership, 2000. Integrated Water Resources Management. Global Water Partnership TAC Background Paper 4. Stockholm, Sweden.

Goor, Q., Halleux, C., Mohamed, Y., & Tilmant, A. (2010, October 12). Optimal operation of a multipurpose multi-reservoir system in the Eastern Nile River Basin. Hydrology and Earth System Sciences, 14(10), 1895–1908. https://doi.org/10.5194/hess-14-1895-2010

Gragne A. S. , Uhlenbrook S., Mohammed Y., and Kebede S.. 2008. Catchment modeling and model transferability in upper Blue Nile Basin, Lake Tana, Ethiopia. Hydrol. Earth Syst. Sci. Discuss., 5, 811–842, www.hydrol-earth-syst-sci-discuss.net/5/811

Gupta, H. V., Kling, H., Yilmaz, K. K., and Martinez, G. F., 2019. Decomposition of the mean squared error and NSE performance criteria: Implications for improving hydrological modelling. J. Hydrology, 377, 80–91, https://doi.org/10.1016/j.jhydrol.2009.08.003

Hadi M., Siva K. B., Karim C. A., Jamal B. T., Christopher T. B. S. and Alias M. S., 2014. SWAT-based hydrological modelling of tropical land-use scenarios. Hydrological Sciences Journal, 59(10), 1808–1829. https://doi.org/10.1080/02626667.2014.892598

Hargreaves, G. H. and Zohrab, A. S., 1985. Reference Crop Evapotranspiration from Ambient Air Temperature. Applied Engineering in Agriculture, 1(2), 96–99. https://doi.org/10.13031/2013.26773

HEC (Hydrologic Engineering Center), 2009. HEC-DSSVue Data Storage System Visual Utility Engine. User's Manual. U.S. Army Corps of Engineer , Davis, CA 95616-4687. CPD-79.

HEC (Hydrologic Engineering Center), 2013. HEC-ResSim Reservoir System Simulation, User's Manual, Version 3.1, US Army Corps of Engineers: Hydrologic Engineering Center.

Hossen, M. A., Connor, J., & Ahammed, F., 2021. Review of hydro-economic models (HEMs) which focus on transboundary river water sharing disputes. Water Policy, 23(6), 1359–1374. https://doi.org/10.2166/wp.2021.114

Hurford, A. P., Huskova, I., & Harou, J. J., 2014. Using many-objective trade-off analysis to help dams promote economic development, protect the poor and enhance ecological health. Environmental Science & Policy, 38, 72–86. https://doi.org/10.1016/j.envsci.2013.10.003

Irit Eguavoen, 2009. The Acquisition of Water Storage Facilities in the Abbay River Basin, Ethiopia. ZEF Working Paper Series, ISSN 1864-6638. http://www.zef.de/workingpapers.html.

Jackson, R. B., Carpenter, S. R., Dahm, C. N., McKnight, D. M., Naiman, R. J., Postel, S. L., & Running, S. W., 2001. WATER IN A CHANGING WORLD. Ecological Applications, 11(4), 1027–1045. http://dx.doi.org/10.1890/1051-0761(2001)011[1027:wiacw]2.0.co;2

Jacquin, A.P.; Soto-Sandoval, J.C., 2013. Interpolation of monthly precipitation amounts in mountainous catchments with sparse precipitation networks. Chil. J. Agric. Res. 73, 406–413

Jain S.K., V.P. Singh V.P., 2003. Water Resource Systems Planning and Management. Book (1st edition). Elsevier Science B.V, The Netherlands

Jeuland, M., 2010. Economic implications of climate change for infrastructure planning in transboundary water systems: An example from the Blue Nile. Water Resources Research, 46(11). https://doi.org/10.1029/2010wr009428

Johnston, K., Ver Hoef, J.M., Krivoruchko, K., Lucas, N., 2001. Using ArcGIS geostatistical analyst, 380. Esri Redlands.

Jose M.G., Marcelo A.O., Josué M.A., Rodrigo M. and Marques G. 2016. Multi-Purpose Reservoir Operation: A Tradeoff Analysis between Hydropower Generation and Irrigated Agriculture Using Hydro-Economic Models. World Environmental and Water Resources Congress.

Julien J. H., Manuel P.V., David E. R., Josue M.A., Jay R. L., Richard E. H., 2009. Hydro-economic models: Concepts, design, applications, and future prospects. Journal of Hydrology 375, 627–643

Junchao J., Leting L.,Yuechi H., Caizhi S., 2021. Effect of Climate Variability on Green and Blue Water Resources in a Temperate Monsoon Watershed, Northeastern China. Sustainability. Sustainability , 13, 2193. https://doi.org/10.3390/su13042193

Kahil, M. T., Dinar, A., & Albiac, J., 2015. Modeling water scarcity and droughts for policy adaptation to climate change in arid and semiarid regions. Journal of Hydrology, 522, 95–109. https://doi.org/10.1016/j.jhydrol.2014.12.042

Khairy, W. M. (2021). Spatial Analysis of Base Flow and Stream Flow from the Abbay River Basin after Watershed Management Interventions. International Journal of Environmental Science and Development, 12(11), 316–325.

https://doi.org/10.18178/ijesd.2021.12.11.1356

Kim, J., Read, L., Johnson, L. E., Gochis, D., Cifelli, R., & Han, H., 2020. An experiment on reservoir representation schemes to improve hydrologic prediction: coupling the national water model with the HEC-ResSim. Hydrological Sciences Journal, 65(10), 1652–1666. https://doi.org/10.1080/02626667.2020.1757677

Klipsch J.D., Evans, T.A., 2007. Reservoir Operations Modeling with HEC-RESSIM, Hydrologic Engineering Center, U.S. Army Corps of Engineers, Davis, CA. 530-756-1104.

Klipsch J.D., Hurst M.B., 2007. HEC-ResSim: reservoir system simulation, user's manual version 3.0. CPD-82. USACE, Institute of Water Resources.

Klipsch J.D. Hurst M.B., Fleming M., 2011. Reservoir Operations and Stream flow Routing Component, Delaware River Basin Flood Analysis Model. U.S. Army Corps of Engineers, Hydrologic Engineering Center, Davis, CA 95616.

Klipsch J.D, Hurst M.B., 2013. HEC - ResSim Reservoir System Simulation Version 3.1 User Manual (Computer Program Documentation). https://doi.org/10.1109/jstars.2021.3051103

Kurtzman, D., Navon, S., Morin, E (2010). Improving interpolation of daily precipitation for hydrologic modelling: Spatial patterns of preferred interpolators. Hydrol. Process, 23, 3281–3291

Lenhart, T., Eckhardt, K., Fohrer, N., & Frede, H. G., 2002. Comparison of two different approaches of sensitivity analysis. Physics and Chemistry of the Earth, Parts a/B/C, 27(9–10), 645–654. https://doi.org/10.1016/s1474-7065(02)00049-9

Loucks D.P., Stedinger J.R., Haith D.A., 1981. Water resource systems planning and analysis. Prentice-Hall, Englewood Cliffs.

Loucks D.P., Salewicz K.A., Taylor MR. 1989. IRIS an interactive river system simulation model, general introduction and description. Cornell University, Ithaca, New York, and International Institute for Applied Systems Analysis, Laxenburg, Austria

Loucks D.P., Salewicz K.A., Taylor M.R., 1990. IRIS an interactive river system simulation model. User's manual. Cornell University, Ithaca, New York, and International Institute for Applied Systems Analysis, Laxenburg, Austria

Loucks D.P., Taylor M.R., French P.N., 1996. IRAS-Interactive river-aquifer simulation. Program description and operating manual. Cornell University

Loucks D.P. and Beek E., 2005. Water Resource Systems Modeling: It's Role in Planning and Management. United Nations Educational, Scientific and Cultural Organization. Book (Chapter-2), ISBN 92-3-1 03998-9. DOI 10.1007/978-3-319-44234-1_2

Loucks D.P., Bain MB., 2002. Interactive river-aquifer simulation and stochastic analyses for predicting and evaluating the ecologic impacts of alternative land and water management policies. In: Bolgov M.V. et al (eds) Proceedings of hydrological models for environmental management. Kluwer, Dordrecht, pp 169–194

Lund J.R., Scheierling S. M., Milne G., 2010. Modeling for Watershed Management: A Practitioner's Guide. Water Work notes. http://www.worldbank.org/water.

Ly S., Charles, C., Degré, A., 2013. Different methods for spatial interpolation of rainfall data for operational hydrology and hydrological modeling at watershed scale. A review. Biotechnol. Agron. Soc. Environ. 17, 392–406.

Li J., Heap A.D., 2014. Spatial interpolation methods applied in the environmental sciences: A review. Environ. Model. Softw. 53, 173–189.

Lund, J.R., Cai, X., Characklis, G.W., 2006. Economic engineering of environmental and water resource systems. Journal of Water Resources Planning and Management 132 (6), 399–402.

Malede, D.A., Agumassie, T.A., Kosgei, J.R., Andualem T,G., Diallo I., 2022. Recent Approaches to Climate Change Impacts on Hydrological Extremes in the Upper Blue Nile Basin, Ethiopia. Earth Syst Environ 6, 669–679. https://doi.org/10.1007/s41748-021-00287-6

Mair A., Fares, A., 2011. Comparison of rainfall interpolation methods in a mountainous region of a tropical island. J. Hydrol. Eng. 16, 371–383

Marye B., Jinsong D., Mengmeng Z., Ke W., Shixue Y., Yang H., Melanie W., 2018. A New Approach to Modeling Water Balance in Nile River Basin, Africa. Sustainability 2018, 10, 810; doi:10.3390/su10030810.

McCartney, Matthew; Alemayehu, T.; Easton, Z. M.; Awulachew, Seleshi Bekele. 2012. Simulating current and future water resources development in the Blue Nile River Basin. https://hdl.handle.net/10568/34731

Matheron G., 1971. The theory of regionalized variables and its applications. Paris: École Nationale Supérieure des Mines de Paris

McCartney, M., Alemayehu, T., Shiferaw, A., Awulachew, S. B., 2010. Evaluation of current and future water resources development in the Lake Tana Basin, Ethiopia. Colombo, Sri

Lanka: International Water Management Institute. 39p. (IWMI Research Report 134). doi:10.3910/2010. 204.

Melke, A, Abegaz, F., 2017. Impact of climate change on hydrological responses of Gumara catchment, in the Lake Tana Basin - Upper Blue Nile Basin of Ethiopia. international Journal of Water Resources and Environmental Engineering, 9(1), 8–21. https://doi.org/10.5897/ijwree2016.0658

Mengistu, D., Bewket, W., Dosio, A., & Panitz, H. J. (2021). Climate change impacts on water resources in the Upper Blue Nile (Abay) River Basin, Ethiopia. Journal of Hydrology, 592, 125614. https://doi.org/10.1016/j.jhydrol.2020.125614

Meseret D., Bilisummaa D., Fiseha B.M., 2020. Assessment of Surface Irrigation Potential of the Dhidhessa River Basin, Ethiopia. Hydrology, 7(3), 68. https://doi.org/10.3390/hydrology7030068

Meshkat, M., & Klipsch, J. D., 2018. Modeling Interconnected Reservoirs with HEC-ResSim. World Environmental and Water Resource Congress 2018. https://doi.org/10.1061/9780784481424.024

Moges, M. A., Zemale, F. A., Alemu, M. L., Ayele, G. K., Dagnew, D. C., Tilahun, S. A., & Steenhuis, T. S., 2016. Sediment concentration rating curves for a monsoonal climate: upper BlueNile. SOIL, 2(3), 337–349. https://doi.org/10.5194/soil-2-337-2016

Monteith, J. L., 1965. Evaporation and Environment. In: The state and movement of water in living organism. 19th Symp. Soc. Exptl. Biol. P. 205-234

Moriasi, D.N., Gitau, M.W., Pai, N., Daggupati, P., 2015. Hydrologic and water quality models: Performance measures and evaluation criteria. Transactions of the ASABE, 58(6), 1763–1785. https://doi.org/10.13031/trans.58.10715

Moriasi D.N., Arnold J.G., Van Liew M.W., Binger R.L., Harmel R.D., Veith T.L., 2007. Model Evaluation Guidelines for Systematic Quantification of Accuracy in Watershed Simulations. Transactions of the ASABE, 50(3), 885–900. https://doi.org/10.13031/2013.23153

Mulat, A. G., Moges, S. A., & Moges, M. A., 2018. Evaluation of multi-storage hydropower development in the upper Blue Nile River (Ethiopia): regional perspective. Journal of Hydrology: Regional Studies, 16, 1–14. https://doi.org/10.1016/j.ejrh.2018.02.006

Mulat, A.G., Moges, S.A., 2014. Assessment of the impact of the Grand Ethiopian Renaissance Dam on the performance of the high Aswan Dam. J. Water Resour. Prot.6, 583–598. http://dx.doi.org/10.4236/jwarp.2014.66057

Munir, M. M., Shakir, A. S., Rehman, H. U., Khan, N. M., Rashid, M. U., Tariq, M. A. U. R., & Sarwar, M. K., 2022. Simulation-Optimization of Tarbela Reservoir Operation to Enhance Multiple Benefits and to Achieve Sustainable Development Goals. Water, 14(16), 2512. https://doi.org/10.3390/w14162512

Murgatroyd, A., Wheeler, K., Hall, J., & Whittington, D., 2023. Trade-offs between hydropower and irrigation in transboundary river systems: the implications of further development on the Blue Nile in Ethiopia. https://doi.org/10.21203/rs.3.rs-2820888/v1

NBI, 2022. Hydro-economic analysis for the Nile Basin Collaborative Water Resources Assessment. http://134.213.39.163/sites/default/files/WRM-2022 01_HEM%20Results%20Techncial%20Report.pdf

Neitsch, S.L., Arnold, J.G. Kiniry, J.R., Williams, J.R., 2011. Soil & Water Assessment Tool: Theoretical Documentation Version 2009. Texas A & M University, USA

NBI, 2012. Chapter 2, The Water Resources of the Nile Basin, State of the River Nile Basin Report. Nile Basin Initiative, pp. 28.

Nash, J.E., Sutcliffe, J.V., 1970. River flow forecasting through conceptual models part I—A discussion of principles. J. Hydrol. 10, 282–290

Neitsch, S.L., Arnold, J.G. Kiniry, J.R., Williams, J.R., 2009. Soil and Water Assessment Tool (SWAT) Theoretical Documentation, Version 2009, Grassland Soil and Water Research Laboratory, Agricultural Research Service, Black land Research Center, Texas Agricultural experiment Station.

Nhamo, L., Ndlela, B., Nhemachena, C., Mabhaudhi, T., Mpandeli, S., & Matchaya, G. (2018, April 27). The Water-Energy-Food Nexus: Climate Risks and Opportunities in Southern Africa. Water, 10(5), 567. https://doi.org/10.3390/w10050567

Ortiz-Partida, J. P., Fernandez-Bou, A. S., Maskey, M., Rodríguez-Flores, J. M., Medellín-Azuara, J., Sandoval-Solis, S., Ermolieva, T., Kanavas, Z., Sahu, R. K., Wada, Y., & Kahil, T., 2023. Hydro-Economic Modeling of Water Resources Management Challenges: Current Applications and Future Directions. Water Economics and Policy, 09(01). https://doi.org/10.1142/s2382624x23400039

Padowski J.C., Jawitz, J.W., 2012. Water availability and vulnerability of 225 large cities in the United States. Water Resour. Res. 48, W12529.

Paul B. and Kenneth S., 2010. Economic Analysis of Large-Scale Upstream River Basin Development on the Blue Nile in Ethiopia Considering Transient Conditions, Climate Variability, and Climate Change. Journal of Water Resources Planning and Management, 136(2), 156–166. https://doi.org/10.1061/(asce)wr.1943-5452.0000022

Penman, H., 1956, February. Evaporation: an introductory survey. Netherlands Journal of Agricultural Science, 4(1), 9–29. https://doi.org/10.18174/njas.v4i1.17768

Priestley C. H. B. and Taylor R. J., 1972. On the Assessment of Surface Heat Flux and Evaporation Using Large-Scale Parameters. Monthly Weather Review, 100(2), 81–92. http://dx.doi.org/10.1175/1520-0493(1972)100<0081:otaosh>2.3.co;2

Rani D., Moreira M.M., 2010. Simulation–Optimization Modeling: A Survey and Potential Application in Reservoir Systems Operation. Water Resources Management, 24(6), 1107–1138. https://doi.org/10.1007/s11269-009-9488-0

Reem F. D., Mario E. C.G., Pieter Z., Yasir A. M., Gerald C. and Stefan U., 2018. Optimal Operation of the Eastern Nile System Using Genetic Algorithm, and Benefits Distribution of Water Resources Development. Water, 10(7), 921. https://doi.org/10.3390/w10070921

Rebecca S., Shashwan D. and Nimnee B., 2019. Application of SWAT Model for Estimating Runoff in Upper Blue Nile River Basin. Conference: International Conference on Advanced Research in Applied Science and Engineering.

https://www.researchgate.net/publication/334559558

Ringler, C., Von Braun, J., Rosegrant, M.W., 2004. Water policy analysis for the Mekong River basin. Water International 29(1): 30-42.

Sahlu, D., Moges, S. A., Nikolopoulos, E. I., Anagnostou, E. N., & Hailu, D., 2017. Evaluation of High-Resolution Multisatellite and Reanalysis Rainfall Products over East Africa. Advances in Meteorology, 2017, 1–14. https://doi.org/10.1155/2017/4957960

Salewicz K.A., 2003. Building the bridge between decision-support tools and decision-making. In: Nakayama M (ed) Proceedings of international waters in Southern Africa, water resources management and policy series. United Nations University Press, Tokyo, pp 114–135

Salman, M., Casarotto, C., Tilmant, A., Piña, J., 2018. Hydro-economic modelling for basin management of the Senegal River. Food and Agriculture Organization of the United Nations.

Salvador P.H., Manuel P.V., Andres S., 2009. A hydro-economic modelling framework for optimal management of groundwater nitrate pollution from agriculture. Journal of Hydrology 373, 193–203. doi:10.1016/j.jhydrol. 04.024.

Santhi, C., Arnold, J. G., Williams, J. R., Dugas, W. A., Srinivasan, R., & Hauck, L. M., 2001. Validation Of The Swat Model On A Large Rwer Basin With Point and Nonpoint Sources. Journal of the American Water Resources Association, 37(5), 1169–1188. https://doi.org/10.1111/j.1752-1688.2001.tb03630.x

Satti, S., Zaitchik, B., & Siddiqui, S., 2015. The question of Sudan: a hydro-economic optimization model for the Sudanese Blue Nile. Hydrology and Earth System Sciences, 19(5), 2275–2293. https://doi.org/10.5194/hess-19-2275-2015

Sayl, K.N., Muhammad, N.S. & El-Shafie, A., 2017. Optimization of area–volume–elevation curve using GIS–SRTM method for rainwater harvesting in arid areas. Environ Earth Sci 76. https://doi.org/10.1007/s12665-017-6699-1

Schuol, J., Abbaspour, K. C., Yang, H., Srinivasan, R., & Zehnder, A. J. B., 2008. Modeling blue and green water availability in Africa. Water Resources Research, 44(7). https://doi.org/10.1029/2007wr006609

SEI, 2012. Integrating the WEAP and LEAP systems to support planning and analysis at the water-energy nexus. Sei-international.org. Factsheet.

SEI, 2015. WEAP: Water evaluation and planning system user guide. USA Center

Serkan G., Frank A. W., 2009. Hydro-economic modeling for water resources management: The Nilufer Basin, Turkey. Ecological Economics 68, 2666–2678

Setegn, S. G., Srinivasan, R., Melesse, A. M., & Dargahi, B. (2009). SWAT model application and prediction uncertainty analysis in the Lake Tana Basin, Ethiopia. Hydrological Processes, n/a-n/a. https://doi.org/10.1002/hyp.7457

Siderius, C., van Walsum, P., & Biemans, H., 2022. Strong trade-offs characterize water-energy-food related sustainable development goals in the Ganges–Brahmaputra–Meghna River basin. Environmental Research Letters, 17(10), 105005. https://doi.org/10.1088/1748-9326/ac94e9

Simonovic S P., 2009. Managing Water Resources: Methods and Tools for a Systems Approach. UK: UNESCO.

Sintayehu L. G., Fulco L., 2015. Hydrological Response to Climate Change of the Upper Blue Nile River Basin: Based on IPCC Fifth Assessment Report (AR5). Journal of Climatology & Weather Forecasting, 03(01). https://doi.org/10.4172/2332-2594.1000121

Shimelis G. S., Bijan D., Ragahavan S., and Assefa M. M., 2010. Modeling of Sediment Yield from Anjeni-Gauged Watershed, Ethiopia Using SWAT Model1. JAWRA Journal of the

American Water Resources Association, 46(3), 514–526. https://doi.org/10.1111/j.1752-1688.2010.00431.x

Smedema, L. K., & Rycroft, D. W. (1983, August 1). *Land Drainage: Planning and Design of Agricultural Drainage Systems*. https://doi.org/10.1604/9780801416293

Sutcliffe and Park, 1999. The Hydrology of the Nile, IAHS Special Publication No. 5. IAHS Press, Institute of Hydrology, Wallingford, Oxford shire OX10 8BB, UK.

Tahani M. S., Mohamed E. S. and Abbas S., 2014. Downstream Impact of Blue Nile Basin Development. Nile Basin Water Science & Engineering Journal, Vol.7.

Tan, C., Erfani, T., & Erfani, R., 2017. Water for Energy and Food: A System Modelling Approach for Blue Nile River Basin. Environments, 4(1), 15.

https://doi.org/10.3390/environments4010015

Tassew, B. G., Belete, M. A., & Miegel, K. (2019, March 10). Application of HEC-HMS Model for Flow Simulation in the Lake Tana Basin: The Case of Gilgel Abay Catchment, Upper Blue Nile Basin, Ethiopia. Hydrology, 6(1), 21. https://doi.org/10.3390/hydrology6010021

Tatenda L., Vincent R., Gete Z., Alemtsehay S., 2018. Spatial and Temporal Variability in Hydrological Responses of the Upper Blue Nile basin, Ethiopia. Water, 11(1), 21. https://doi.org/10.3390/w11010021

Teegavarapu R.S.V., Meskele T., Pathak C.S., 2012. Geo-spatial grid-based transformations of precipitation estimates using spatial interpolation methods. Comput. Geosci-UK.

Tesemma Z.K., Mohamed Y.A., Steenhuis T.A., 2010. Trends in rainfall and runoff in the Blue Nile Basin: 1964–2003. Hydrol Process 24:3747–3758. https://doi.org/10.1002/hyp.7893

Teshome S. G., 2051. Modeling of Cascade Dams and Reservoirs Operation for Optimal Water Use: Application to Omo Gibe River Basin, Ethiopia. PhD Dissertation Submitted to the Faculty of Civil & Environmental Engineering of the University of Kassel, Germany

Thalli M. S., Nadhir Al-A., S. D. B., Amai M., 2020. Evaluation of Satellite Precipitation Products in Simulating Streamflow in a Humid Tropical Catchment of India Using a Semi-Distributed Hydrological Model. Water, 12, 2400; doi:10.3390/w12092400., www.mdpi.com/journal/water

Tigabu, T. B., Wagner, P. D., Hörmann, G., & Fohrer, N. (2020). Modeling the spatio-temporal flow dynamics of groundwater-surface water interactions of the Lake Tana Basin, Upper Blue Nile, Ethiopia. *Hydrology Research*, *51*(6), 1537–1559. https://doi.org/10.2166/nh.2020.046

Thornes, J. E., 2002. IPCC, 2001: Climate change 2001: impacts, adaptation and vulnerability, Contribution of Working Group II to the Third Assessment Report of the Intergovernmental Panel on Climate Change, edited by J. J. McCarthy, O. F. Canziani, N. A. Leary, D. J. Dokken a. International Journal of Climatology, 22(10), 1285–1286. https://doi.org/10.1002/joc.775

Torhan, S., Grady, C. A., Ajibade, I., Galappaththi, E. K., Hernandez, R. R., Musah-Surugu, J. I., Nunbogu, A. M., Segnon, A. C., Shang, Y., Ulibarri, N., Campbell, D., Joe, E. T., Penuelas, J., Sardans, J., & Shah, M. A. R., 2022. Tradeoffs and Synergies Across Global Climate Change Adaptations in the Food-Energy-Water Nexus. Earth's Future, 10(4). https://doi.org/10.1029/2021ef002201

United Nations Educational, Scientific and Cultural Organization (UNESCO)., 2004. National Water Development Report for Ethiopia. UN-WATER/WWAP/2006/7, World Water Assessment Program, Report, MOWR, Addis Ababa, Ethiopia, pp.273.

USACE, 1998. HEC-5: Simulation of flood control and conservation systems. User's manual, version 8.0. Hydrological Engineering Centre

USBR (United States Bureau of Reclamation), 1964. Land and Water Resources of the Blue Nile Basin. Main Report. United States Dept. of Interior Bureau of Reclamation, Washington, DC, USA.

Van der K., 2010. Ribasim Version 7.00, User manual. Delft Hydraulics, the Netherlands

Vedula S., Mujumda P.P., 2016. Water Resources Systems: Modelling Techniques and Analysis. Book. https://www.researchgate.net/publication/308961191.

Vincent, R., Tatenda, L., Gete, Z., Alemtsehay T. S., Tibebu, K. N., Hans Hurni., 2018. Effects of climate change on water resources in the upper Blue Nile Basin of Ethiopia. Heliyon, 4(9), e00771. https://doi.org/10.1016/j.heliyon.2018.e00771

Vinod C., Tirupati B., Ram B., 2018. Multi-objective autocalibration of SWAT model for improved low flow performance for a small snowfed catchment. Hydrological Sciences Journal, 63(10), 1482–1501. https://doi.org/10.1080/02626667.2018.1505047

Wakjira T. D., Tamene A. D. and Konrad M., 2020. Watershed Hydrological Response to Combined Land Use/Land Cover and Climate Change in Highland Ethiopia: Finchaa Catchment. Water, 12(6), 1801. https://doi.org/10.3390/w12061801

Walsh RPD, Lawler DM., 1981. Rainfall seasonality spatial patterns and change through time.Weather36: 201–208.

WAPCOS (Water & Power Consultancy Services (I) Ltd.), 1990. Preliminary Water Resources Development for Master Plan for Ethiopia Final Report, prepared for EVDSA, Addis Ababa, Ethiopia.

Winchell M., Srinivasan R., Di Luzio M., Arnold J., 2013. ArcSWAT Interface for Swat2012, User Guide. Black land Research and Extension Center Texas Agrilife Research

WL Deflt Hydraulics. 2004. RIBASIM, Version 6.32. WL Deflt Hydraulics, Delft, Holland.

Whittington, D., Wu, X., & Sadoff, C., 2005. Water resources management in the Nile basin: the economic value of cooperation. Water Policy, 7(3), 227–252. https://doi.org/10.2166/wp.2005.0015

Wogayehu, L., Deriba K., Kassahun T., 2018. Characteristics of Seasonal Rainfall and its Distribution Over Bale Highland, Southeastern Ethiopia. Journal of Earth Science & Climatic Change, 09(02). https://doi.org/10.4172/2157-7617.1000443

World Bank, 2006. Ethiopia: managing water resource to maximize sustainable growth. World Bank Agriculture and Rural Development Department. Washington D.C. http://documents.worldbank.org/curated/en/947671468030840247

Worqlula A., Ayanab E., Yena H., Jeonga J., MacAlisterc C., Taylor R., Greik T.J., Steenhuis T.S., 2018. Characteristics of Seasonal Rainfall and its Distribution Over Bale Highland, Southeastern Ethiopia. Journal of Earth Science & Climatic Change, 09(02). https://doi.org/10.4172/2157-7617.1000443

Wouter J. M. K., Jim E. F., Ross A. W., 2019. Technical note: Inherent benchmark or not? Comparing Nash-Sutcliffe and Kling-Gupta efficiency scores. https://doi.org/10.5194/hess-2019-327

Wurbs R.A., 2005a. Modeling river/reservoir system management, water allocation, and supply reliability. J Hydrol 300(1–4):100–113

WWAP (United Nations World Water Assessment Programme), 2016. The United Nations World Water Development Report: Water and jobs Facts and Figures. Paris, UNESCO

Xu, W., Zou, Y., Zhang, G., Linderman, M. A., 2015. Comparison among spatial interpolation techniques for daily rainfall data in Sichuan province, China. Int. J. Climatol. 35, 2898–2907

Yasir Salih Ahmed Ali, 2014. The Impact of Soil Erosion in the Upper Blue Nile on Downstream Reservoir Sedimentation. PhD dissertation, published by CRC Press/Balkema, Netherlands

Yasuda, H., Fenta, A., Berihun, M., Inosako, K., Kawai, T., & Belay, A., 2022. Water level change of Lake Tana, source of the Blue Nile: Prediction using teleconnections with sea surface temperatures. Journal of Great Lakes Research, 48(2), 468–477. https://doi.org/10.1016/j.jglr.2022.01.006

Yates, D.N., Miller, K.A., 2013. Integrated decision support for energy/water planning in California and the Southwest. Int. J. Clim. Change Impacts Responses 4, 49–64

Yimere, A., & Assefa, E., 2022. Current and Future Irrigation Water Requirement and Potential in the Abbay River Basin, Ethiopia. Air, Soil and Water Research. https://doi.org/10.1177/11786221221097929

Yimere, A., & Assefa, E., 2021. Assessing and mapping irrigation potential in the abbay river basin, ethiopia. Russian Journal of Agricultural and Socio-Economic Sciences, 114(6), 97–109. https://doi.org/10.18551/rjoas.2021-06.11

Yihun T. D.., Sirak T., Essayas A. Kaba., Solomon G. G., Abeyou W. W., Haimanote K. B., Yohannes T. Y., Seifu A. T., Prasad D., Louise K., Raghavan S., 2018. Advances in water resources research in the Upper Blue Nile basin and the way forward: A review. Journal of Hydrology 560, 407–423

Yokoo, Y. and Sivapalan, M., 2011. Towards reconstruction of the flow duration curve: development of a conceptual framework with a physical basis. Hydrology and Earth System Sciences, 15(9), 2805–2819. https://doi.org/10.5194/hess-15-2805-2011

Yuan C., Guijun L., Yuan Y., Lixiao Z. and Chang Y., 2016. Quantifying the Water-Energy-Food Nexus: Current Status and Trends. Energies, 9(2), 65.

https://doi.org/10.3390/en9020065

Zegeye, F., Alamirew, B., & Tolossa, D., 2020. Analysis of Wheat Yield Gap and Variability in Ethiopia. International Journal of Agricultural Economics, 5(4), 89. https://doi.org/10.11648/j.ijae.20200504.11

Zhang, X., Jiang, C., Huang, J., Ni, Z., Sun, J., Li, Z., Wen, T., 2022. Spatiotemporal Evaluation of Blue and Green Water in Xinjiang River Basin Based on SWAT Model. Water, 14, 2429. https:// doi.org/10.3390/w14152429

Zuzanna, Z., Beatriz R.R., Peter S., Peter B., Feyera A.H., Hylke B., 2017. The impact of lake and reservoir parameterization on global stream flow simulation. Journal of Hydrology. https://doi.org/10.1016/j.jhydrol.2017.03.022

Appendixes

Appendix-A

Hyro-meteorological data analysis

Table A-1. list of Meteorological Stations used for ArcSWAT modeling.

St. Name	LAT	LONG	ELEV	St. Name	LAT	LONG	ELEV
D.markos	10.33	37.74	2446.00	D.Berhan	9.63	39.58	2636.00
Pawe	11.15	36.05	1119.00	Bahir Dar	11.36	37.21	1800.00
Bedele	8.45	36.33	2011.00	Gonder Airport	12.55	37.42	1973.00
Arjo	8.75	36.50	2565.00	D.tabor	11.85	38.01	2612.00
Mankush	11.28	35.28	860.00	Mota	11.08	37.87	2417.00
Ambo	8.98	37.84	2068.00	Dangila	11.43	36.85	2116.00
Assosa	10.20	34.58	1600.00	N.mewucha	11.73	38.47	3098.00
Begi	9.33	34.53	1650.00	Fiche	9.80	38.70	2784.00
Bulen	10.60	36.08	1659.00	Addis Zemen	12.12	37.77	1940.00
Gimbi	9.17	35.78	1970.00	Enjibara	11.00	36.92	2568.00
Nekemte	9.08	36.46	2080.00	Gorgora	12.25	37.30	1830.00
Chagni	10.97	36.50	1614.00	Gundo Beret	9.75	39.67	2600.00
Chancho	9.30	38.76	2632.00	Kabie	10.83	39.46	2879.00
Alibo	9.89	37.07	2513.00	Wetet Abay	11.37	37.04	1920.00
Dembecha	10.57	37.49	2117.00	Zege	11.69	37.31	1801.00
Dembi	8.07	36.45	1925.00	Mehal meda	10.31	39.66	3084.00
Fincha	9.57	37.37	2248.00	Mekane Selam	10.74	38.76	2605.00
Gedo	9.02	37.46	2520.00	Makesegnit	12.39	37.56	1912.00
Jarso	9.45	35.32	1750.00	Gundo weyn	10.93	38.09	2052.00
Kidamaja	11.00	36.68	1928.00	Tis Abay	11.49	37.58	2642.00
Mandura	11.50	36.50	1184.00	Woreta	11.92	37.70	1819.00
Mendi	9.78	35.10	1650.00	Debrezeit	11.81	38.58	3220.00
Yebu	7.68	36.82	1982.00	Amed Ber	11.91	37.89	2051.00
Yejube	10.15	37.75	2322.00	Combolcha	9.50	37.47	2341.00
Guder	8.96	39.75	2011.00				

Table A-2. Stations used for WEGN Statistics

OBJECT ID	STATION NAME	WLATITUDE	WLONGITUDE	WELEV
1	Debre Berhan	9.63	39.58	2636.00
2	Bahir Dar	11.36	37.21	1800.00
3	Gonder	12.55	37.42	1973.00
4	Debreb Tabor	11.85	38.01	2612.00
5	Motta	11.08	37.87	2417.00
6	Dangila	11.43	36.85	2116.00
7	Nefas Mewucha	11.73	38.47	3098.00
8	Fiche	9.80	38.70	2784.00
9	Debre Markos	10.33	37.74	2446.00
10	Pawe	11.15	36.05	1119.00
11	Bedele	8.45	36.33	2011.00
12	Arjo	8.75	36.50	2565.00
13	Mankush	11.28	35.28	860.00
14	Ambo	8.98	37.84	2068.00
15	Assosa	10.20	34.58	1600.00
16	Begi	9.33	34.53	1650.00
17	Bulen	10.60	36.08	1659.00
18	Gimbi	9.17	35.78	1970.00
19	Nekemte	9.08	36.46	2080.00

Appendix-B

Physical and operational data

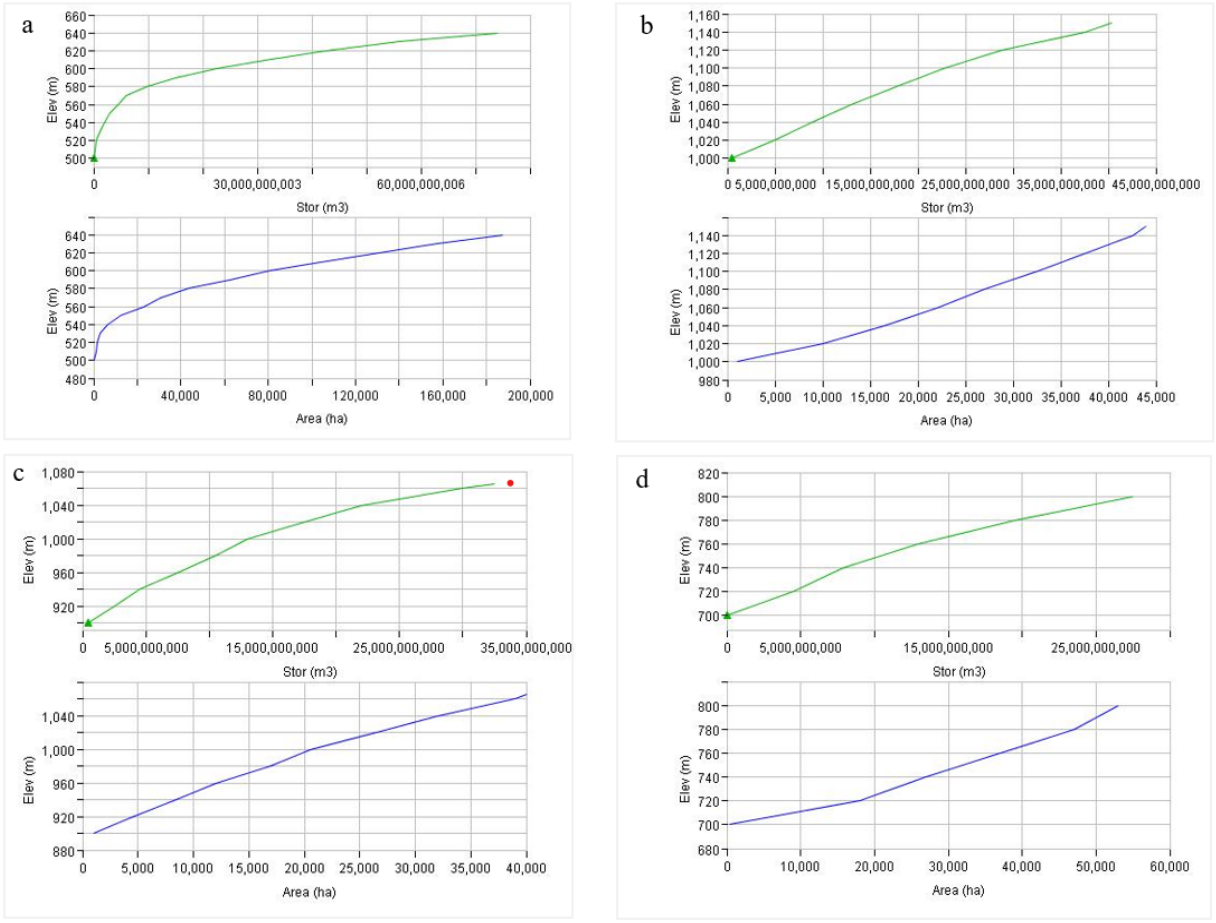

Figure B-1: Elevation_Area-Volume curve reservpoirs. GERD (a), Karadobi (b), Bekoabo (c) and Mandaya (d)

Table B-2: Properties of existed and proposed hydropower dams and reservoirs over Abbay river basin

	Karadobi	**Bekoabo**	**Mandaya**	**GERD**
Catchment Area (km^2)	82237	95390	110410	176918
Average Inflow (m^3/s)	565	679	825	1551
Average Turbine discharge (m^3/s)	532	648	729	1547
Installed capacity (MW)	1600	2400	2000	5150
Full supply level (masl)	1146	1062	800	640
Dam Height (m)	250	270	175	145
Reservoir surface area (km^2)	445	403	521	1874
Reservoir capacity (MCM	40400	32000	27700	74000
Minimum operating level (masl)	1100	1020	760	590

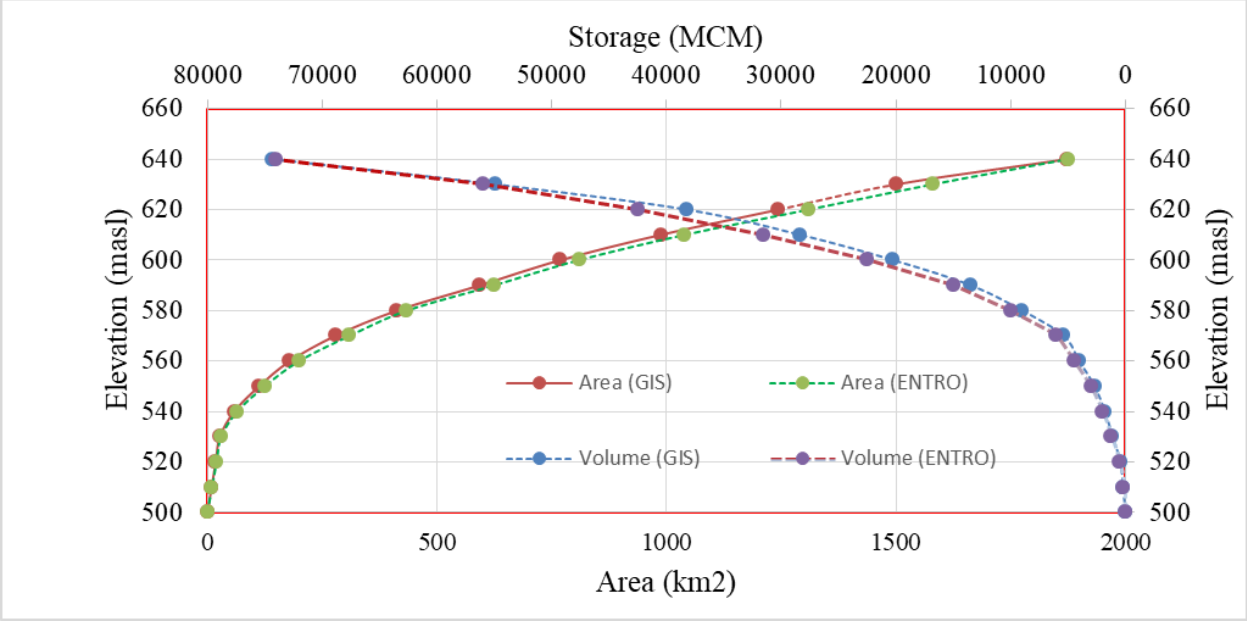

Figure B-3: GERD Elevation- Area-Volume relation estimated by GIS. Area (ENTRO) and volume (ENTRO): Elevation-area-volume data collected from Eastern Nile Technical Regional Office

Appendix-C

Interpolated rainfall

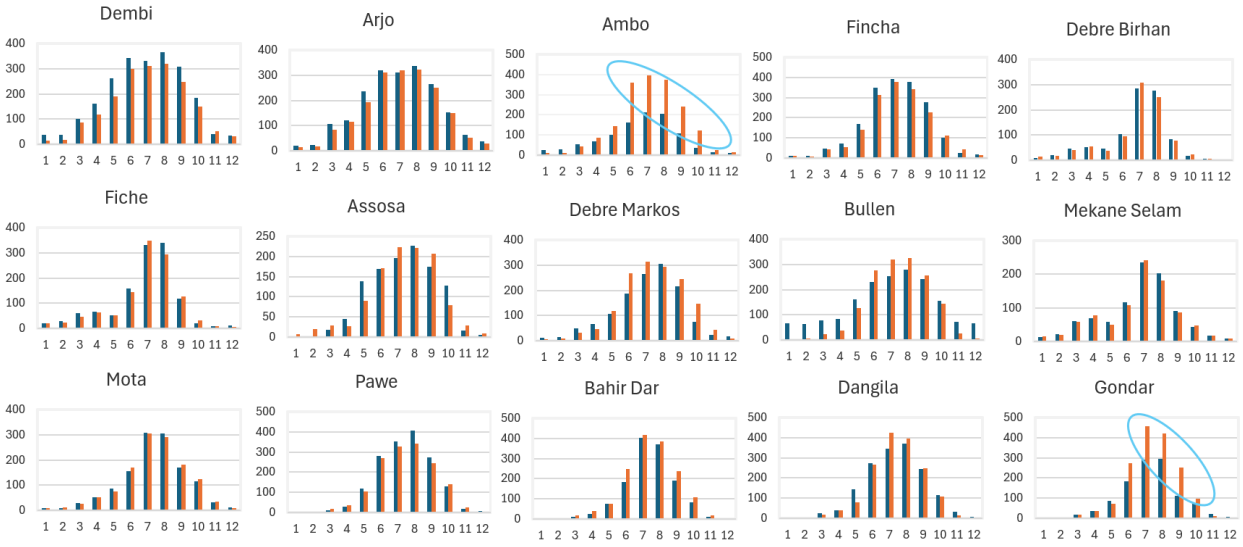

Figure C-1. Measured and interpolated rainfall at selected stations using kiging/Co-kriging

Appendix-D

Irrigation Site

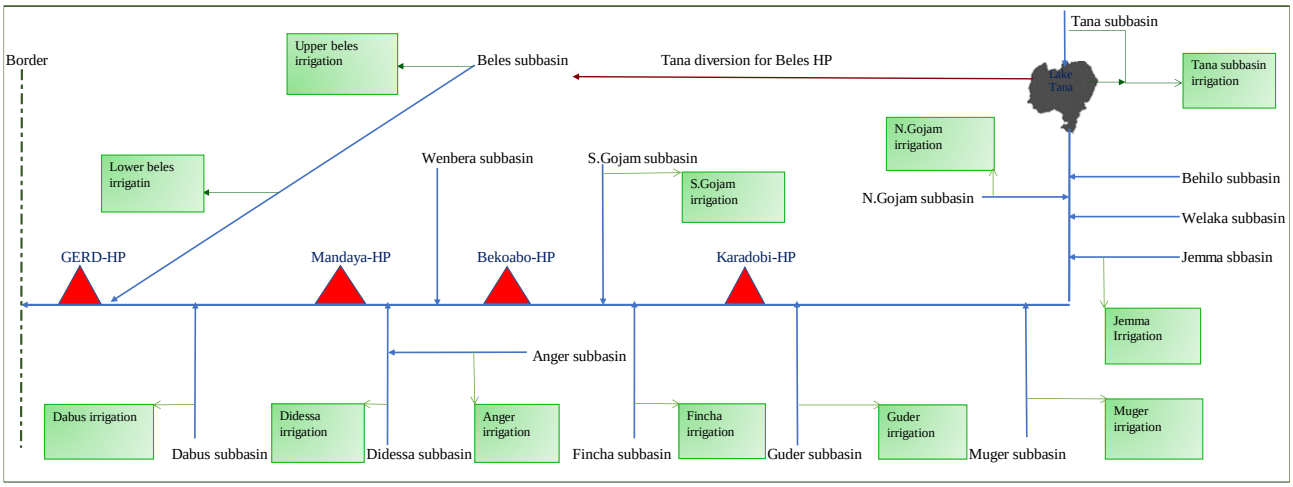

Figure D-1. Potential irrigation Site and Hydropower Project

Appendix-E

HEC-ResSim output graphs

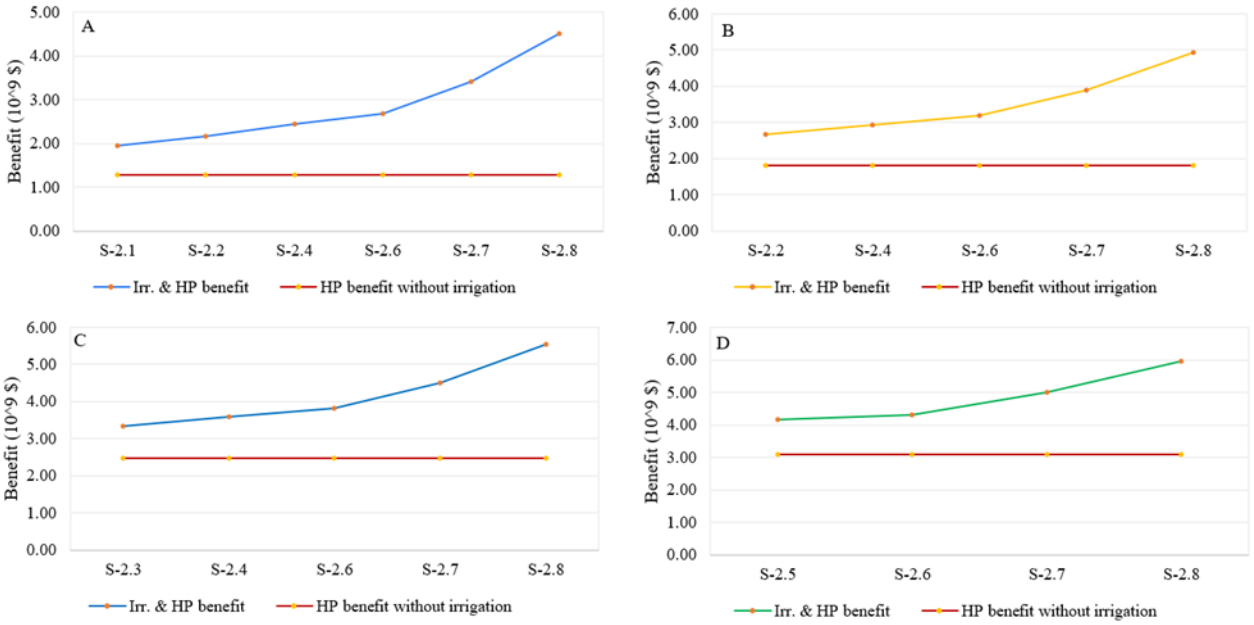

Figure E-1: Detail Hydro-economic benefit of hydropower and irrigation development (P1). A) GERD plus six irrigation scenarios, B) GERD and Karadobi plus five irrigation scenarios, C) GERD, Karadobi and Bekoabo plus five irrigation Considering the present value (P1)

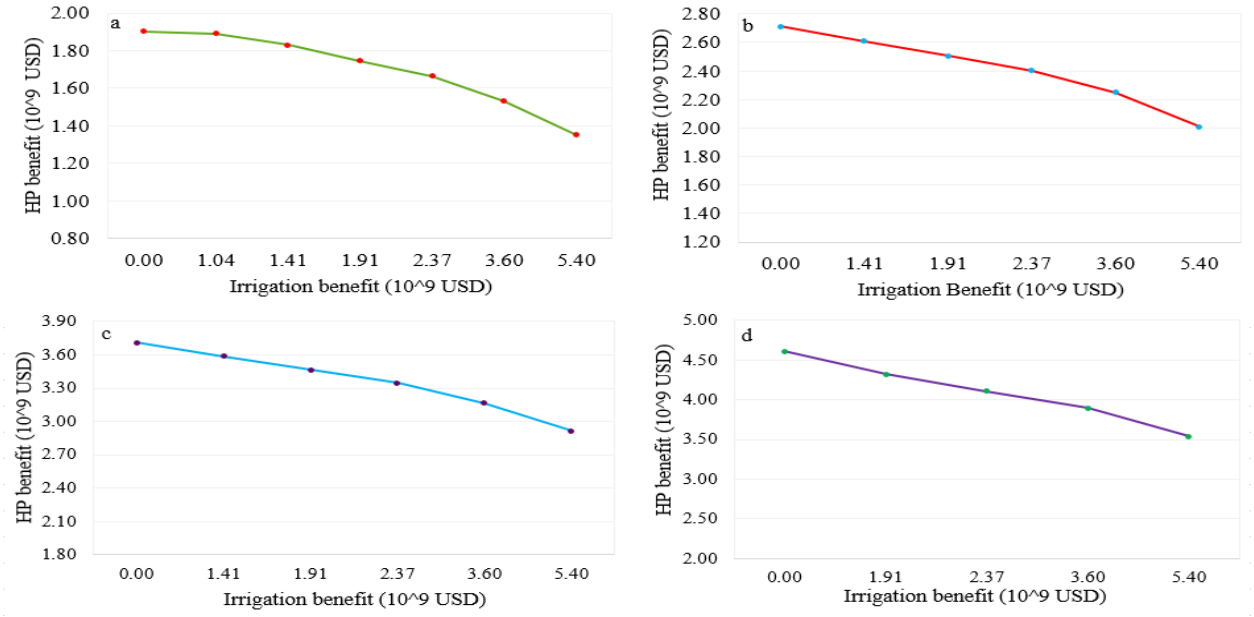

Figure E-2: Hydro-economic trade-off between hydropower and irrigation development (P2). a) GERD plus six irrigation scenarios, b) GERD and Karadobi plus five irrigation scenarios, c) GERD, Karadobi and Bekoabo plus five irrigation scenarios, d) GERD, Karadobi, Bekoabo and Mandaya plus four irrigation Scenarios (as shown in Table 3.2)

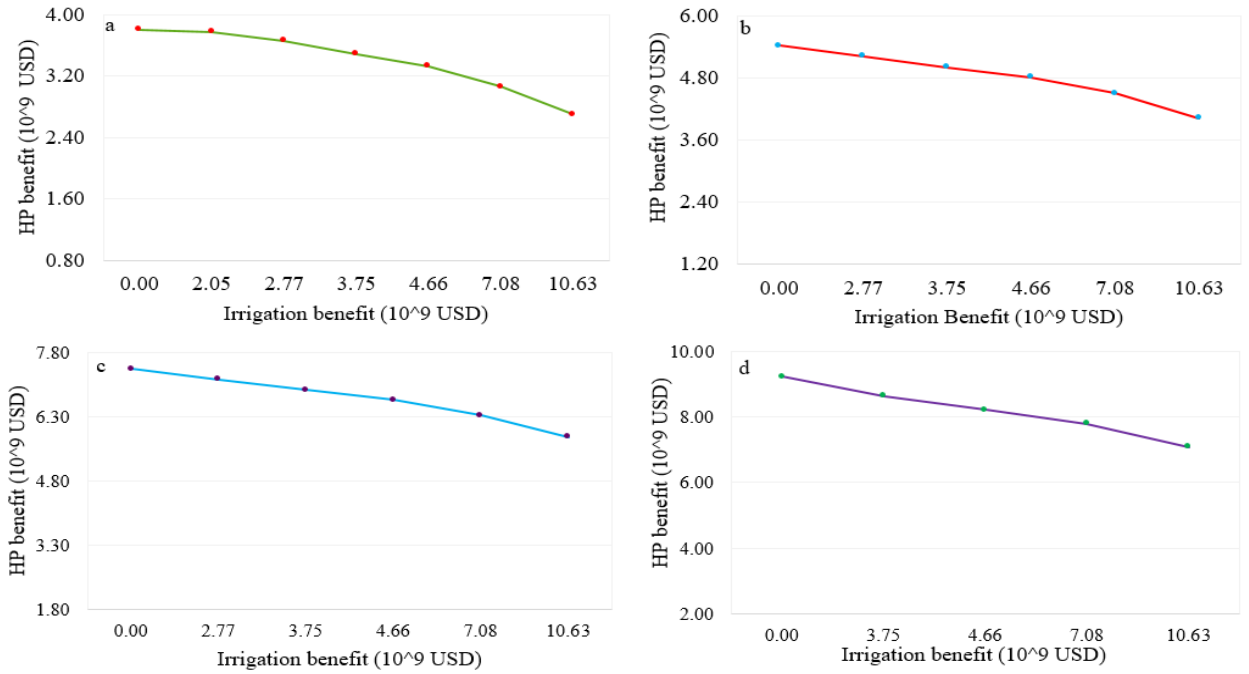

Figure E-3: Hydro-economic trade-off between hydropower and irrigation development (P3). a) GERD plus six irrigation scenarios, b) GERD and Karadobi plus five irrigation scenarios, c) GERD, Karadobi and Bekoabo plus five irrigation scenarios, d) GERD, Karadobi, Bekoabo and Mandaya plus four irrigation Scenarios (as shown in Table 3.2)

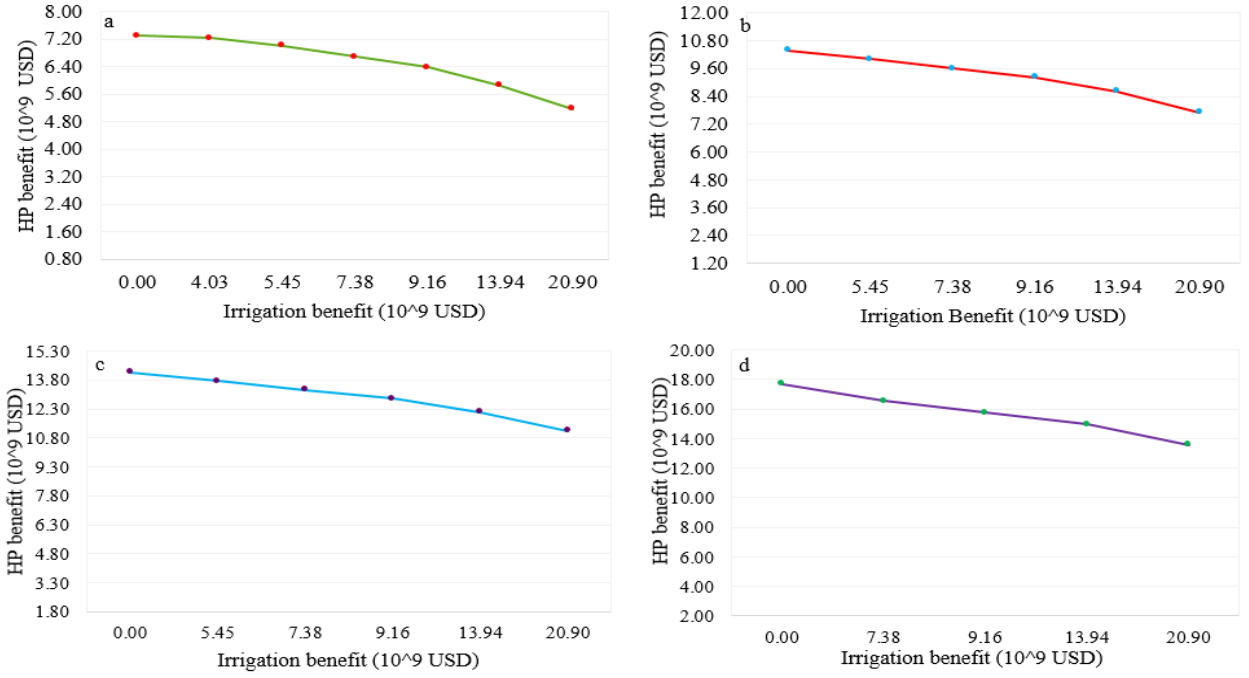

Figure E-4: Hydro-economic trade-off between hydropower and irrigation development (P3). a) GERD plus six irrigation scenarios, b) GERD and Karadobi plus five irrigation scenarios, c)

GERD, Karadobi and Bekoabo plus five irrigation scenarios, d) GERD, Karadobi, Bekoabo and Mandaya plus four irrigation Scenarios (as shown in Table 3.2)

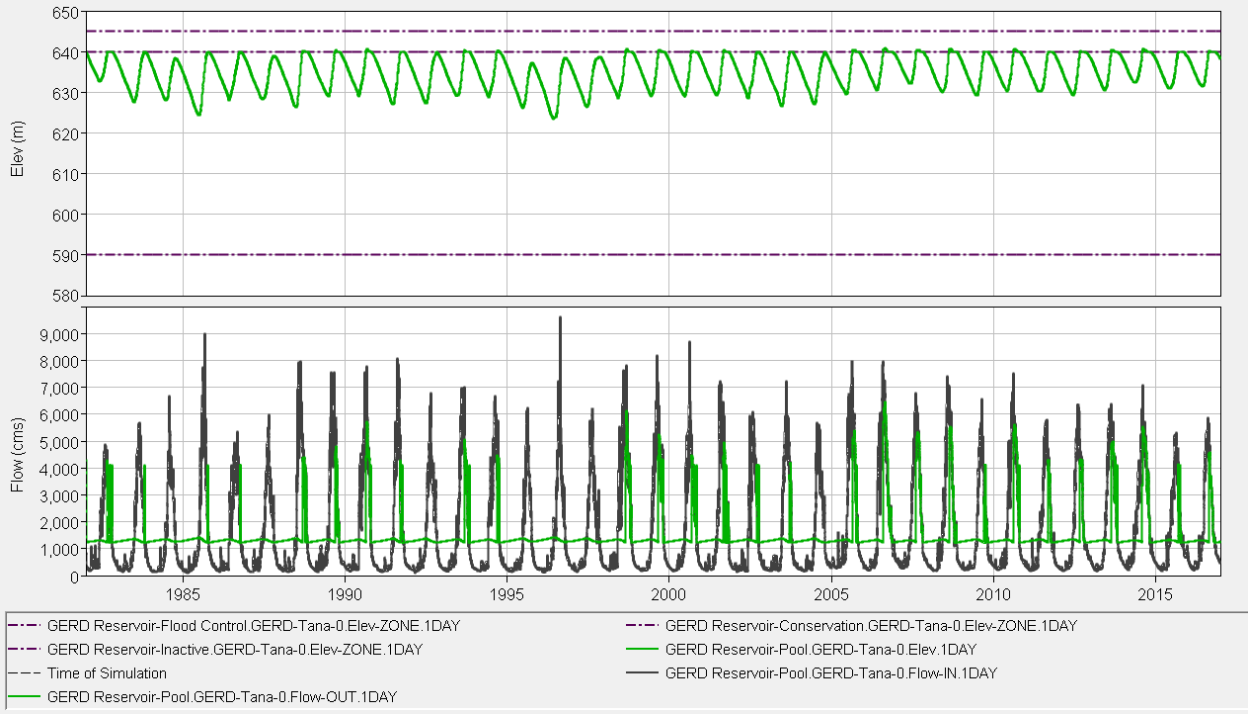

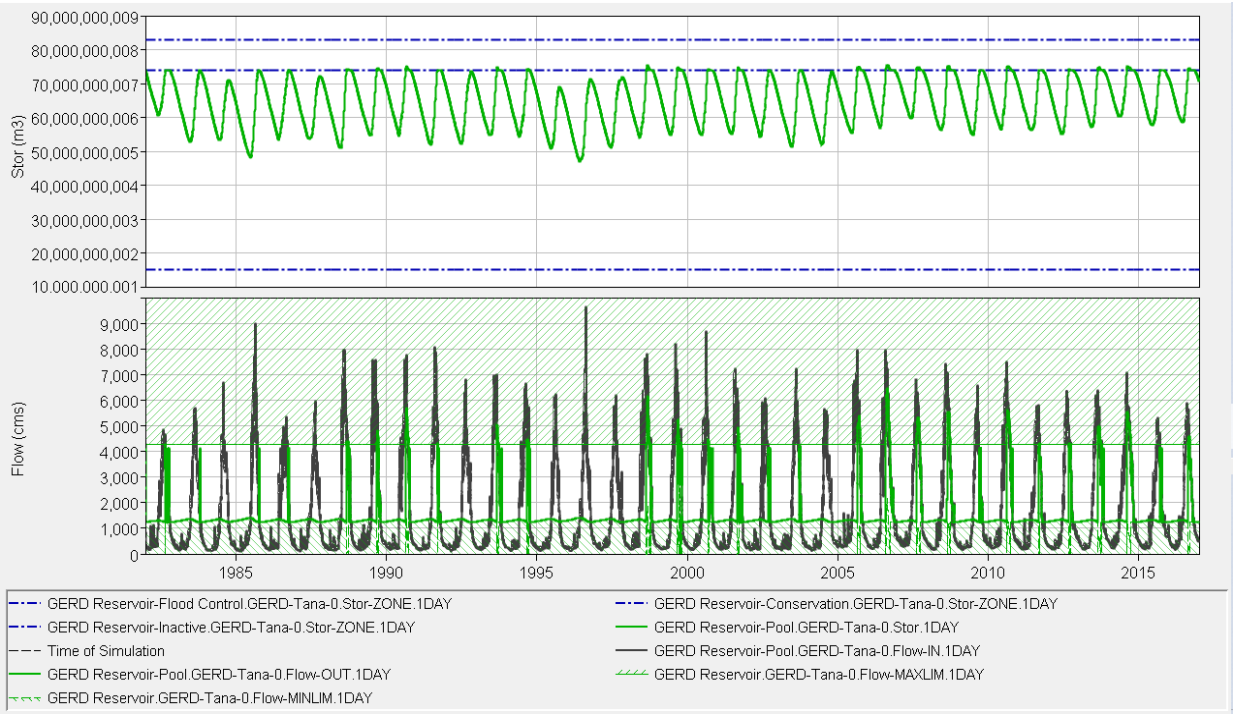

Figure E-5: GERD reservoir level and storage (Power guide curve rule)

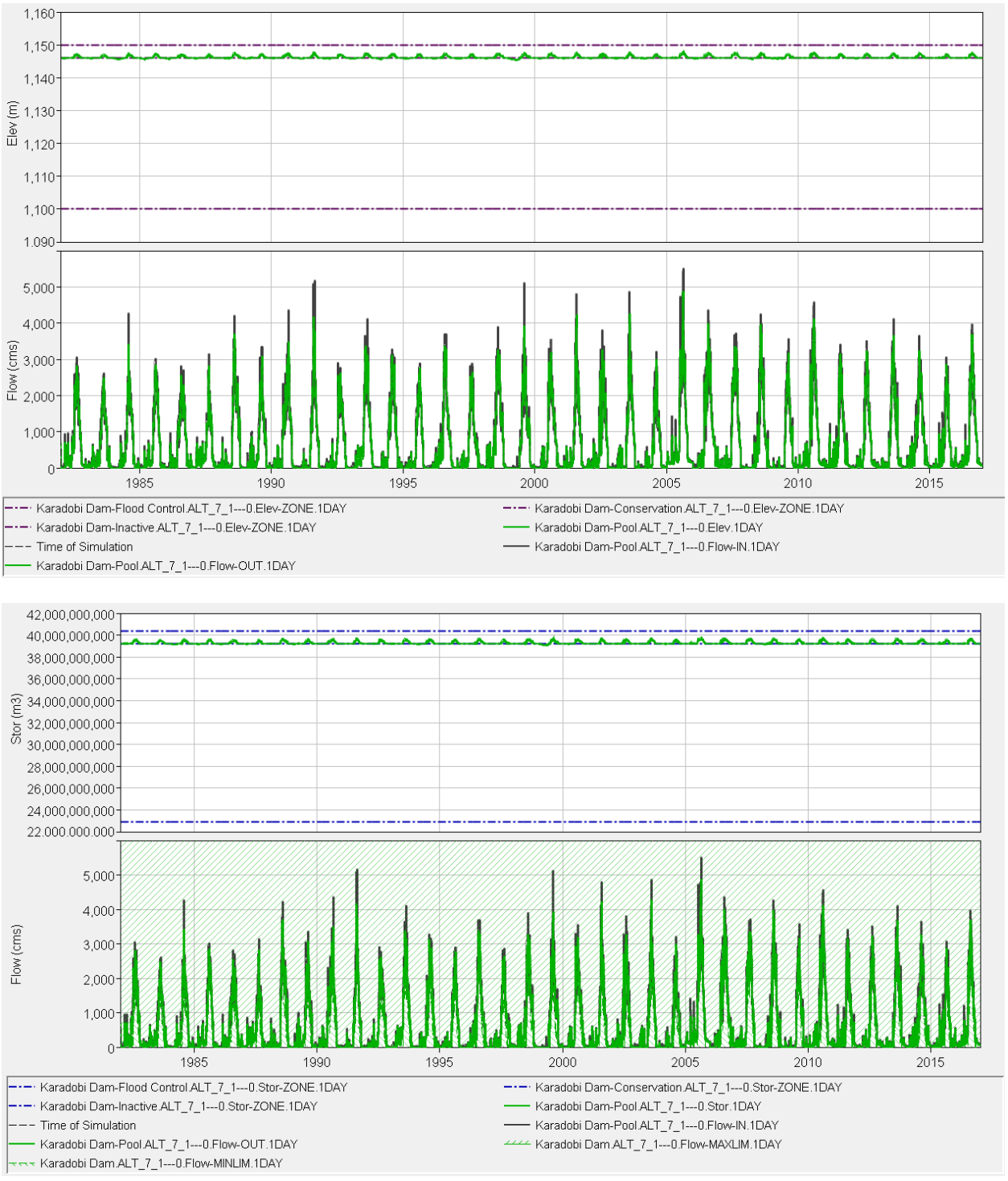

Figure E-6: Karadobi Tandem operation rule (scenario_1.2)

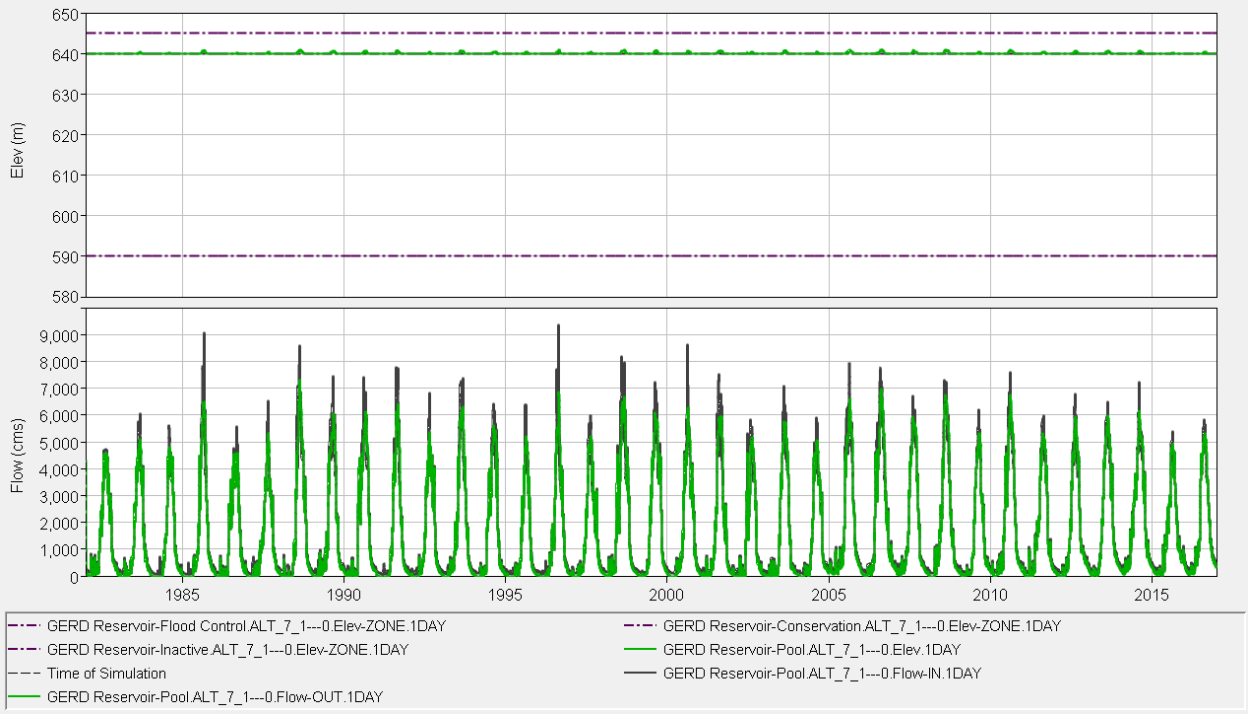

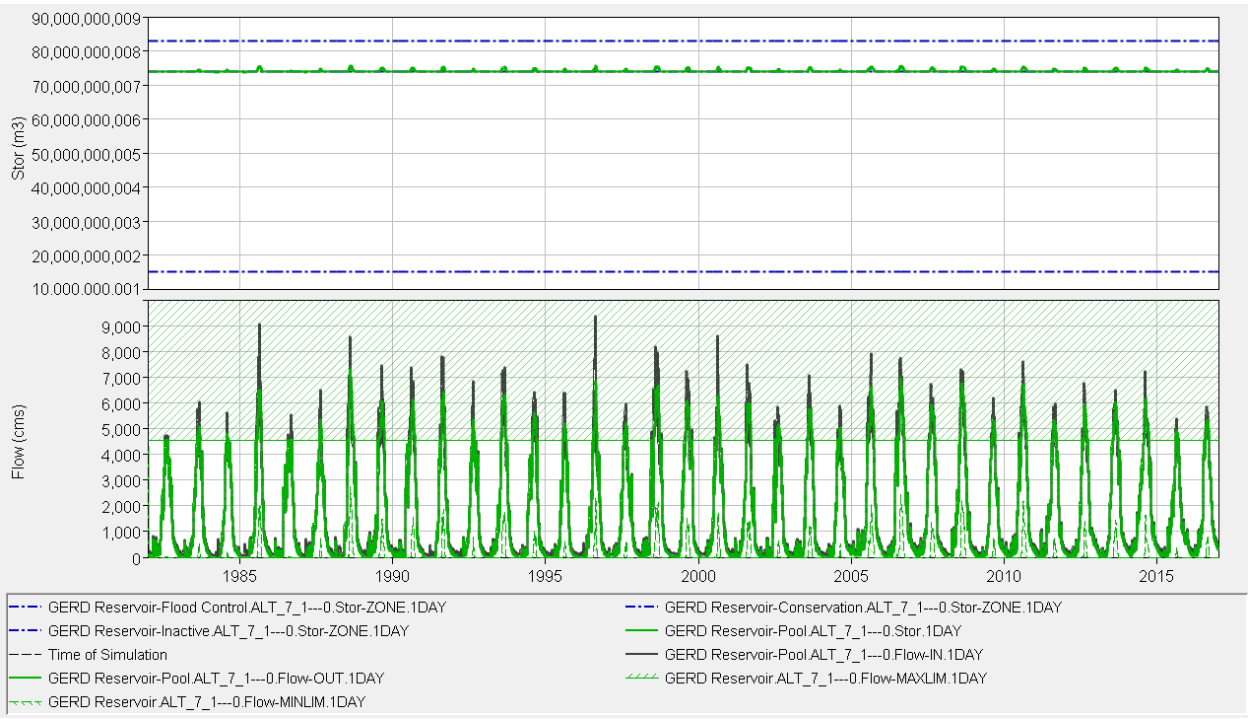

Figure E-7: GERD tandem operation rule (scenario_1.2)

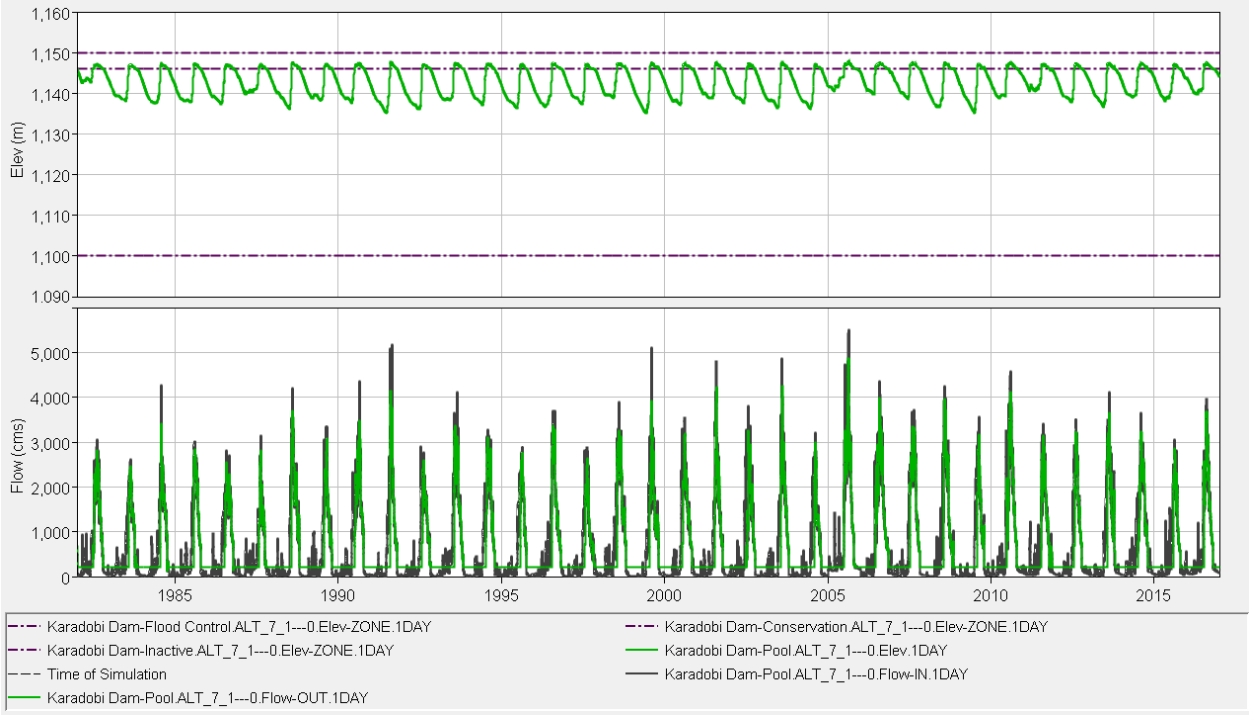
Elev (m)
1,160
1,150
1,140
1,130
1,120
1,110
1,100
1,090
Flow (cms)
5,000
4,000
3,000
2,000
1,000
0
1985
1990
1995
2000
2005
2010
2015
Karadobi Dam-Flood Control.ALT_7_1---0.Elev-ZONE.1DAY
Karadobi Dam-Conservation.ALT_7_1---0.Elev-ZONE.1DAY
Karadobi Dam-Inactive.ALT_7_1---0.Elev-ZONE.1DAY
Karadobi Dam-Pool.ALT_7_1---0.Elev.1DAY
Time of Simulation
Karadobi Dam-Pool.ALT_7_1---0.Flow-IN.1DAY
Karadobi Dam-Pool.ALT_7_1---0.Flow-OUT.1DAY

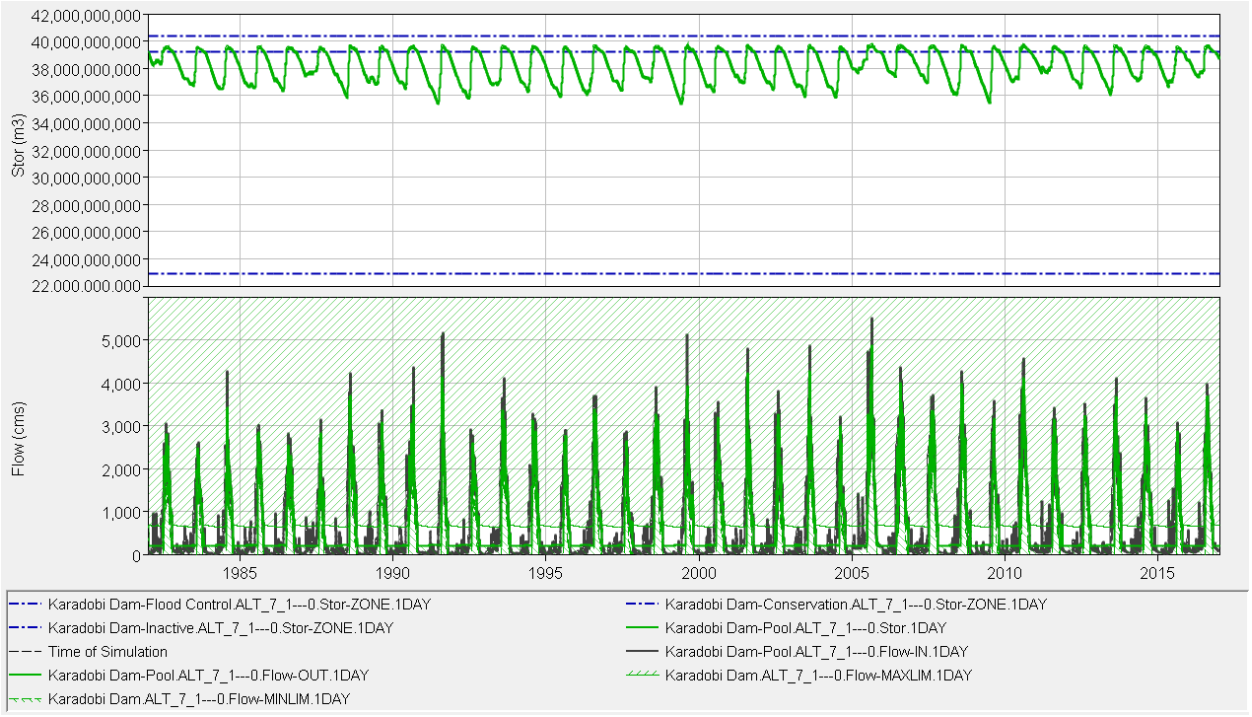
Stor (m3)
42,000,000,000
40,000,000,000
38,000,000,000
36,000,000,000
34,000,000,000
32,000,000,000
30,000,000,000
28,000,000,000
26,000,000,000
24,000,000,000
22.000.000.000
Flow (cms)
5,000
4,000
3,000
2,000
1,000
0
1985
1990
1995
2000
2005
2010
2015
Karadobi Dam-Flood Control.ALT_7_1---0.Stor-ZONE.1DAY
Karadobi Dam-Conservation.ALT_7_1---0.Stor-ZONE.1DAY
Karadobi Dam-Inactive.ALT_7_1---0.Stor-ZONE.1DAY
Karadobi Dam-Pool.ALT_7_1---0.Stor.1DAY
Time of Simulation
Karadobi Dam-Pool.ALT_7_1---0.Flow-IN.1DAY
Karadobi Dam-Pool.ALT_7_1---0.Flow-OUT.1DAY
Karadobi Dam.ALT_7_1---0.Flow-MAXLIM.1DAY
Karadobi Dam.ALT_7_1---0.Flow-MINLIM.1DAY

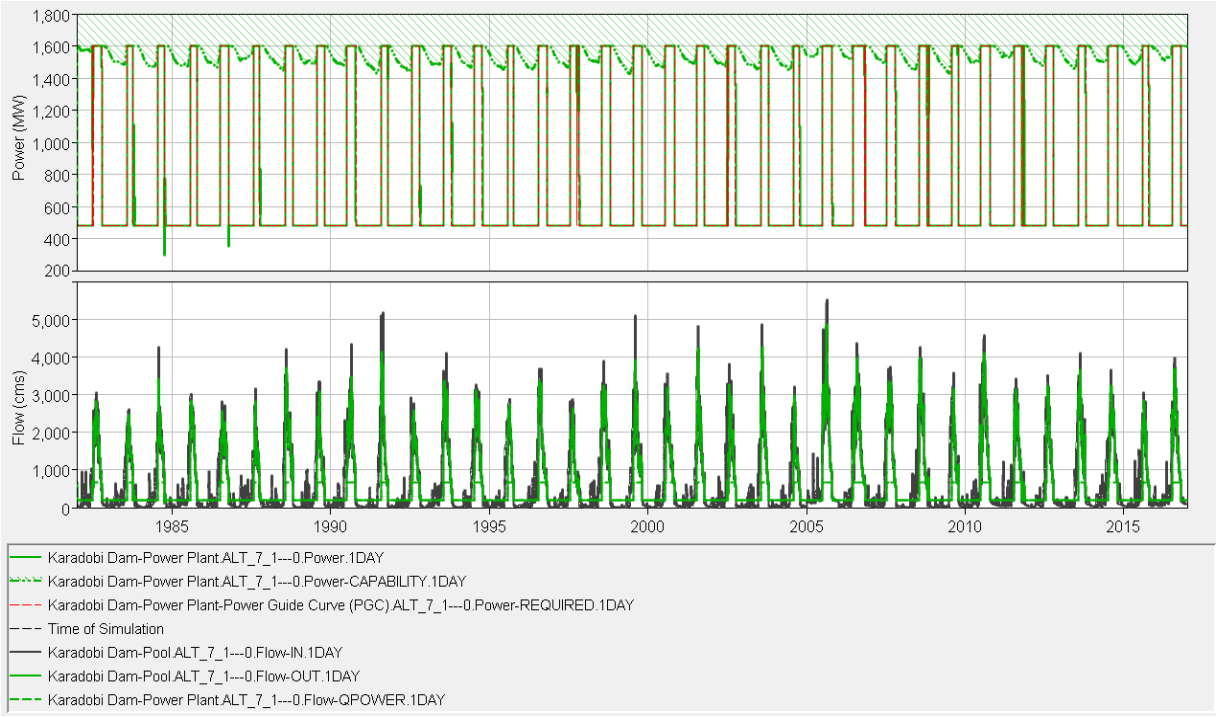

Figure E-8: Karadobi Hydropower guide curve rule (Scenario_1.2)

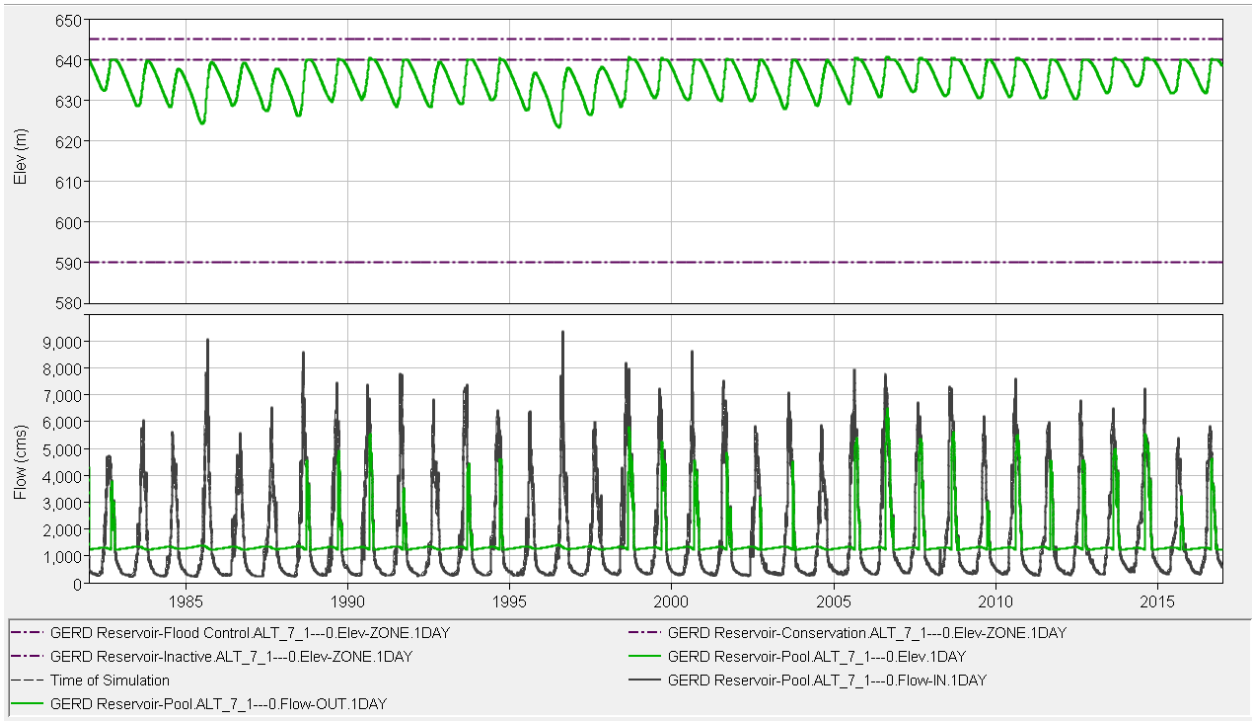

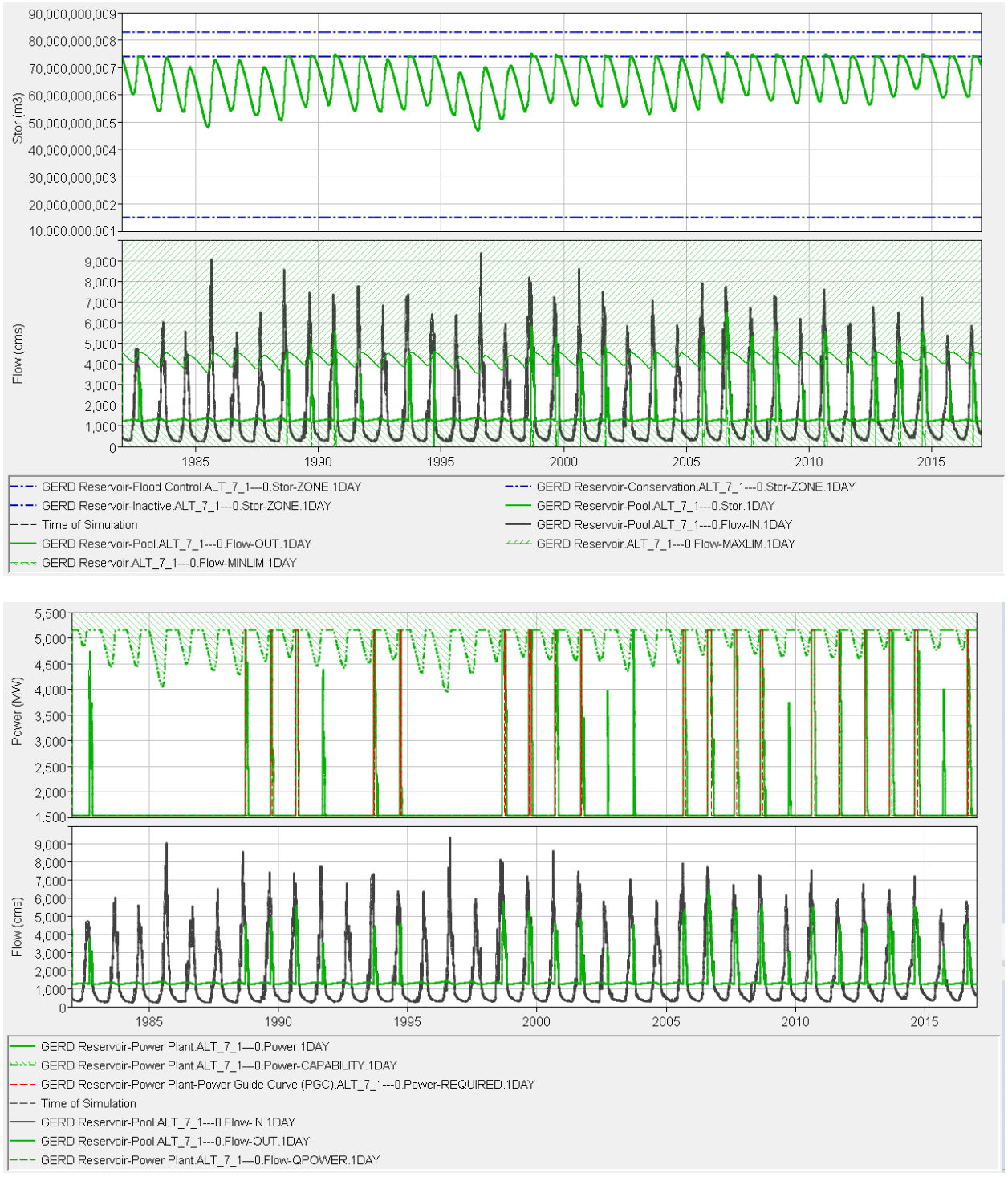

Figure E-9: GERD hydropower guide curve rule (Scenario_1.2)

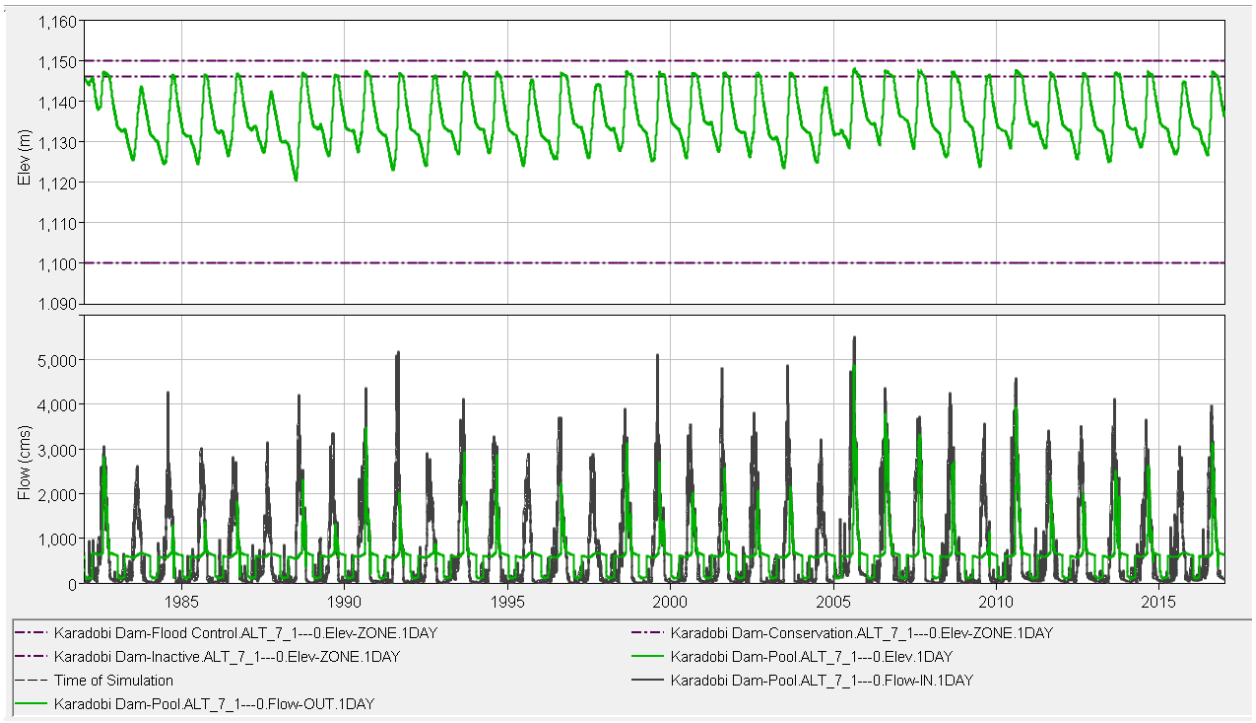
Elev (m)
1,160
1,150
1,140
1,130
1,120
1,110
1,100
1,090
Flow (cms)
5,000
4,000
3,000
2,000
1,000
0
1985
1990
1995
2000
2005
2010
2015
Karadobi Dam-Flood Control.ALT_7_1---0.Elev-ZONE.1DAY
Karadobi Dam-Conservation.ALT_7_1---0.Elev-ZONE.1DAY
Karadobi Dam-Inactive.ALT_7_1---0.Elev-ZONE.1DAY
Karadobi Dam-Pool.ALT_7_1---0.Elev.1DAY
Time of Simulation
Karadobi Dam-Pool.ALT_7_1---0.Flow-IN.1DAY
Karadobi Dam-Pool.ALT_7_1---0.Flow-OUT.1DAY

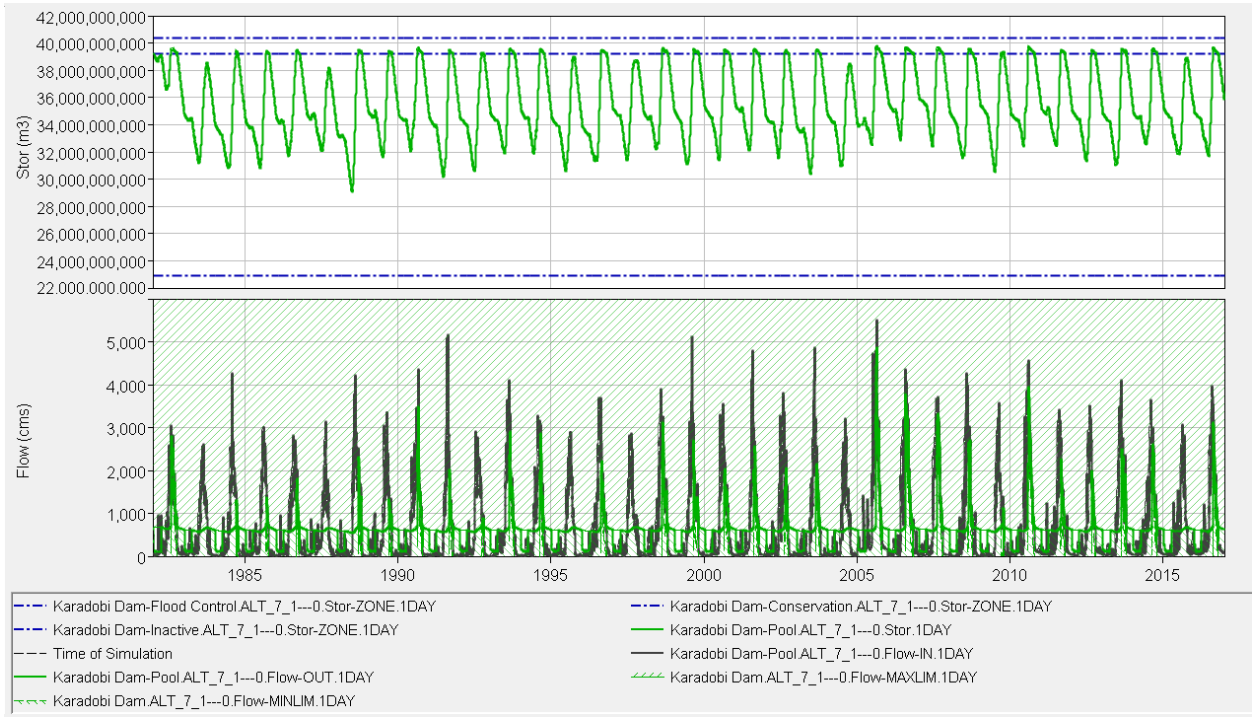
Stor (m3)
42,000,000,000
40,000,000,000
38,000,000,000
36,000,000,000
34,000,000,000
32,000,000,000
30,000,000,000
28,000,000,000
26,000,000,000
24,000,000,000
22.000.000.000
Flow (cms)
5,000
4,000
3,000
2,000
1,000
0
1985
1990
1995
2000
2005
2010
2015
Karadobi Dam-Flood Control.ALT_7_1---0.Stor-ZONE.1DAY
Karadobi Dam-Conservation.ALT_7_1---0.Stor-ZONE.1DAY
Karadobi Dam-Inactive.ALT_7_1---0.Stor-ZONE.1DAY
Karadobi Dam-Pool.ALT_7_1---0.Stor.1DAY
Time of Simulation
Karadobi Dam-Pool.ALT_7_1---0.Flow-IN.1DAY
Karadobi Dam-Pool.ALT_7_1---0.Flow-OUT.1DAY
Karadobi Dam.ALT_7_1---0.Flow-MAXLIM.1DAY
Karadobi Dam.ALT_7_1---0.Flow-MINLIM.1DAY

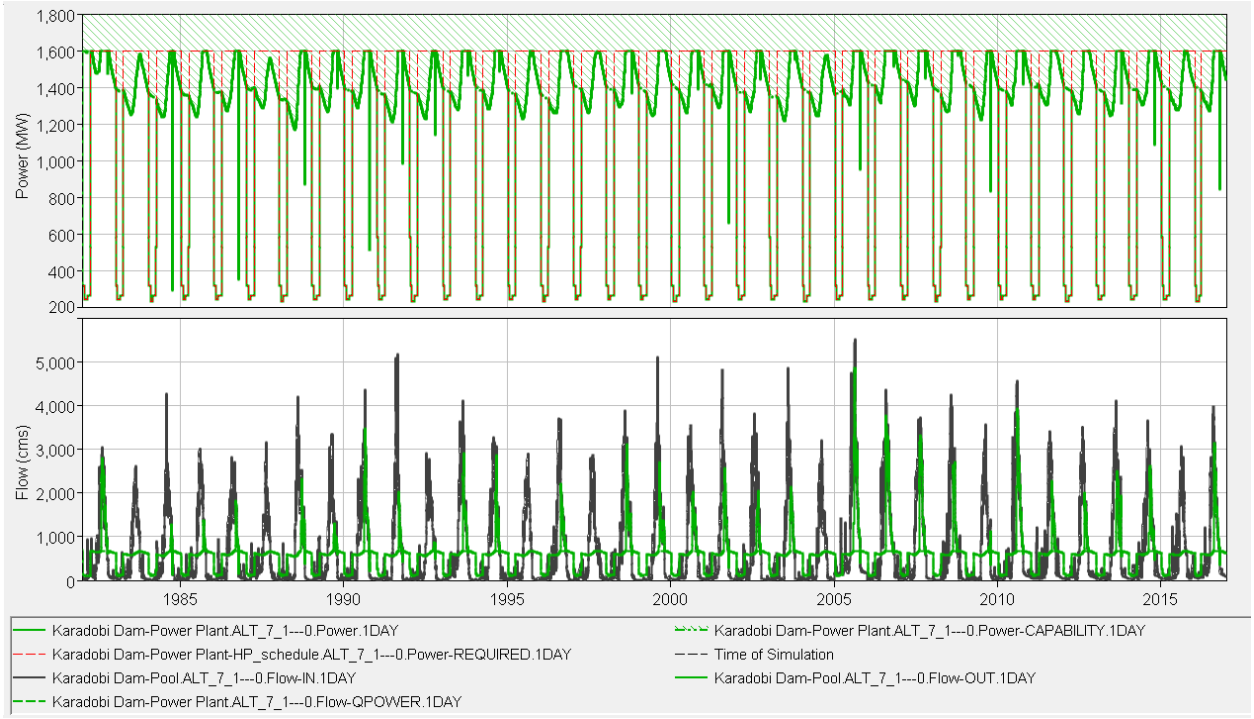

Figure E-10: Karadobi Hydropower schedule rule (scenario_1.2)

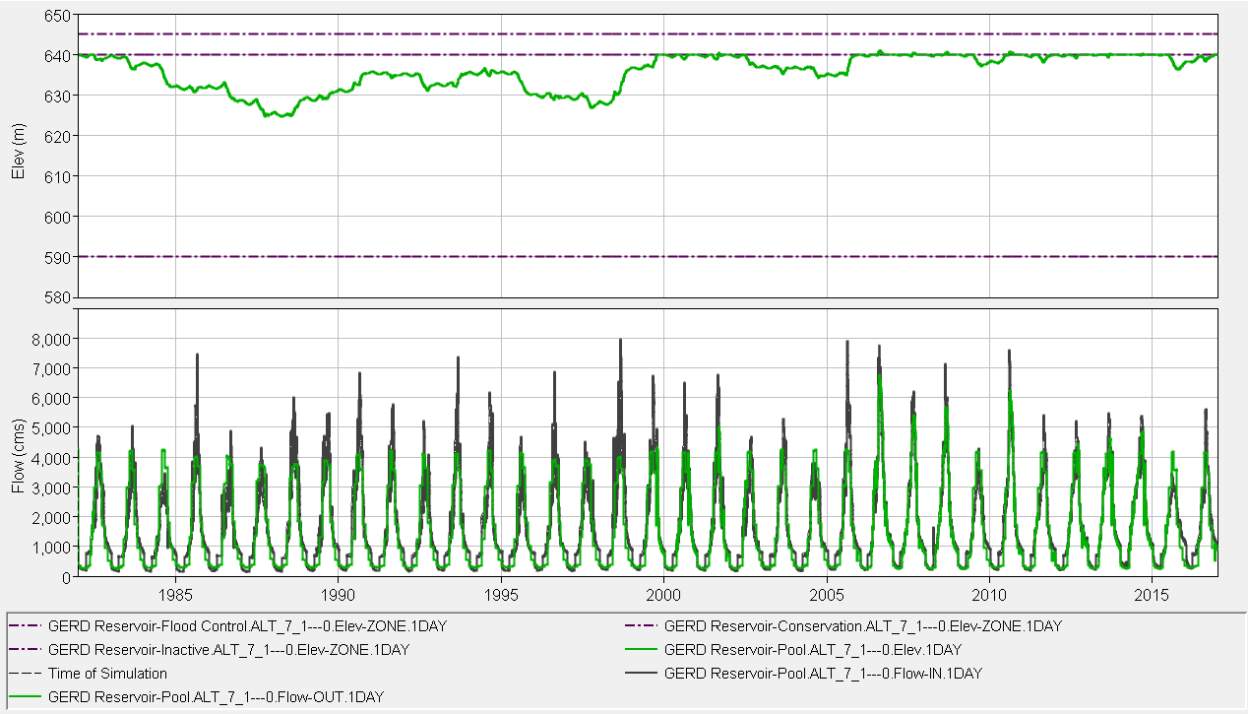

Figure E-11: GERD Hydropower schedule rule (scenario_1.2)

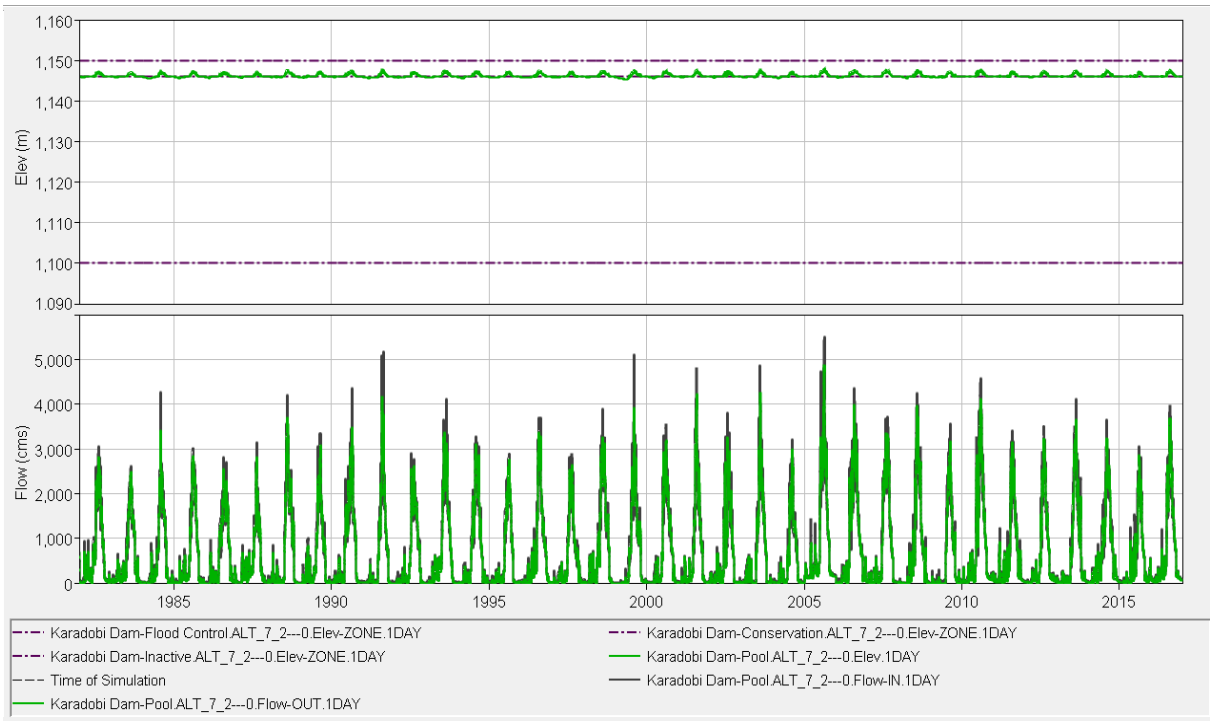
Elev (m)
1,160
1,150
1,140
1,130
1,120
1,110
1,100
1,090
Flow (cms)
5,000
4,000
3,000
2,000
1,000
0
1985
1990
1995
2000
2005
2010
2015
Karadobi Dam-Flood Control.ALT_7_2---0.Elev-ZONE.1DAY
Karadobi Dam-Conservation.ALT_7_2---0.Elev-ZONE.1DAY
Karadobi Dam-Inactive.ALT_7_2---0.Elev-ZONE.1DAY
Karadobi Dam-Pool.ALT_7_2---0.Elev.1DAY
Time of Simulation
Karadobi Dam-Pool.ALT_7_2---0.Flow-IN.1DAY
Karadobi Dam-Pool.ALT_7_2---0.Flow-OUT.1DAY

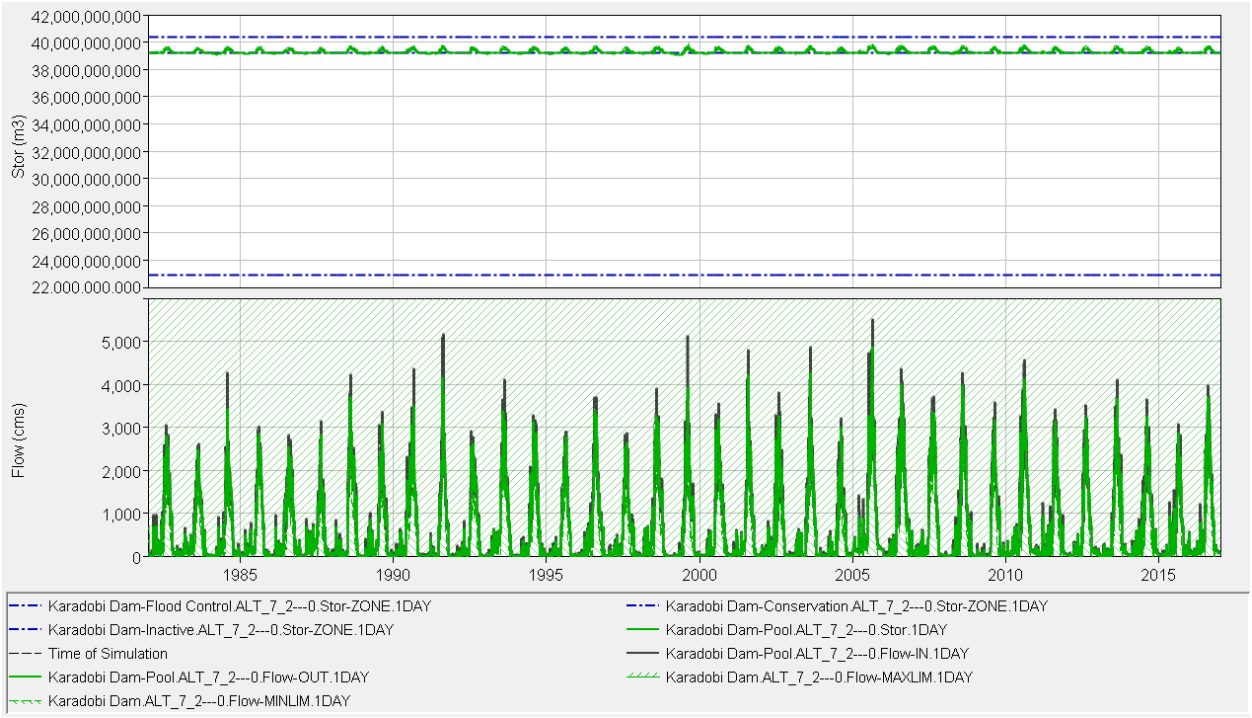
Stor (m3)
42,000,000,000
40,000,000,000
38,000,000,000
36,000,000,000
34,000,000,000
32,000,000,000
30,000,000,000
28,000,000,000
26,000,000,000
24,000,000,000
22.000.000.000
Flow (cms)
5,000
4,000
3,000
2,000
1,000
0
1985
1990
1995
2000
2005
2010
2015
Karadobi Dam-Flood Control.ALT_7_2---0.Stor-ZONE.1DAY
Karadobi Dam-Conservation.ALT_7_2---0.Stor-ZONE.1DAY
Karadobi Dam-Inactive.ALT_7_2---0.Stor-ZONE.1DAY
Karadobi Dam-Pool.ALT_7_2---0.Stor.1DAY
Time of Simulation
Karadobi Dam-Pool.ALT_7_2---0.Flow-IN.1DAY
Karadobi Dam-Pool.ALT_7_2---0.Flow-OUT.1DAY
Karadobi Dam.ALT_7_2---0.Flow-MAXLIM.1DAY
Karadobi Dam.ALT_7_2---0.Flow-MINLIM.1DAY

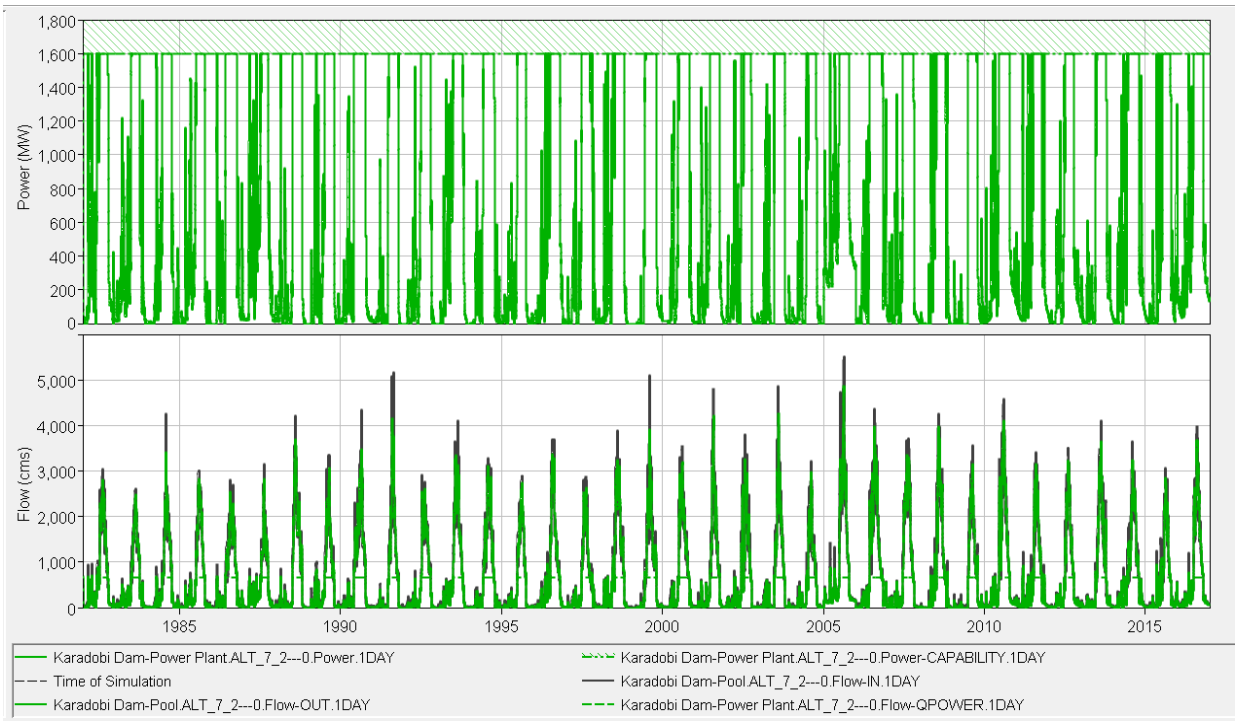

Figure E-12: Karadobi Tandem operation (scenario_1.3)

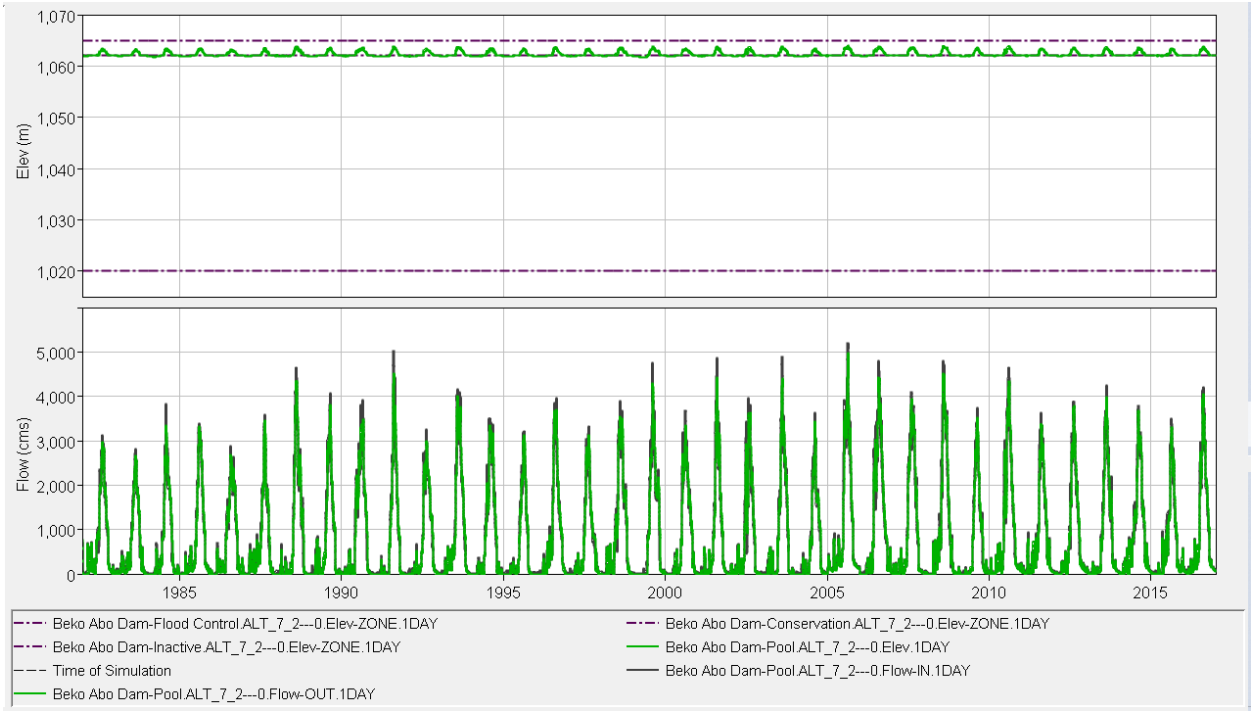

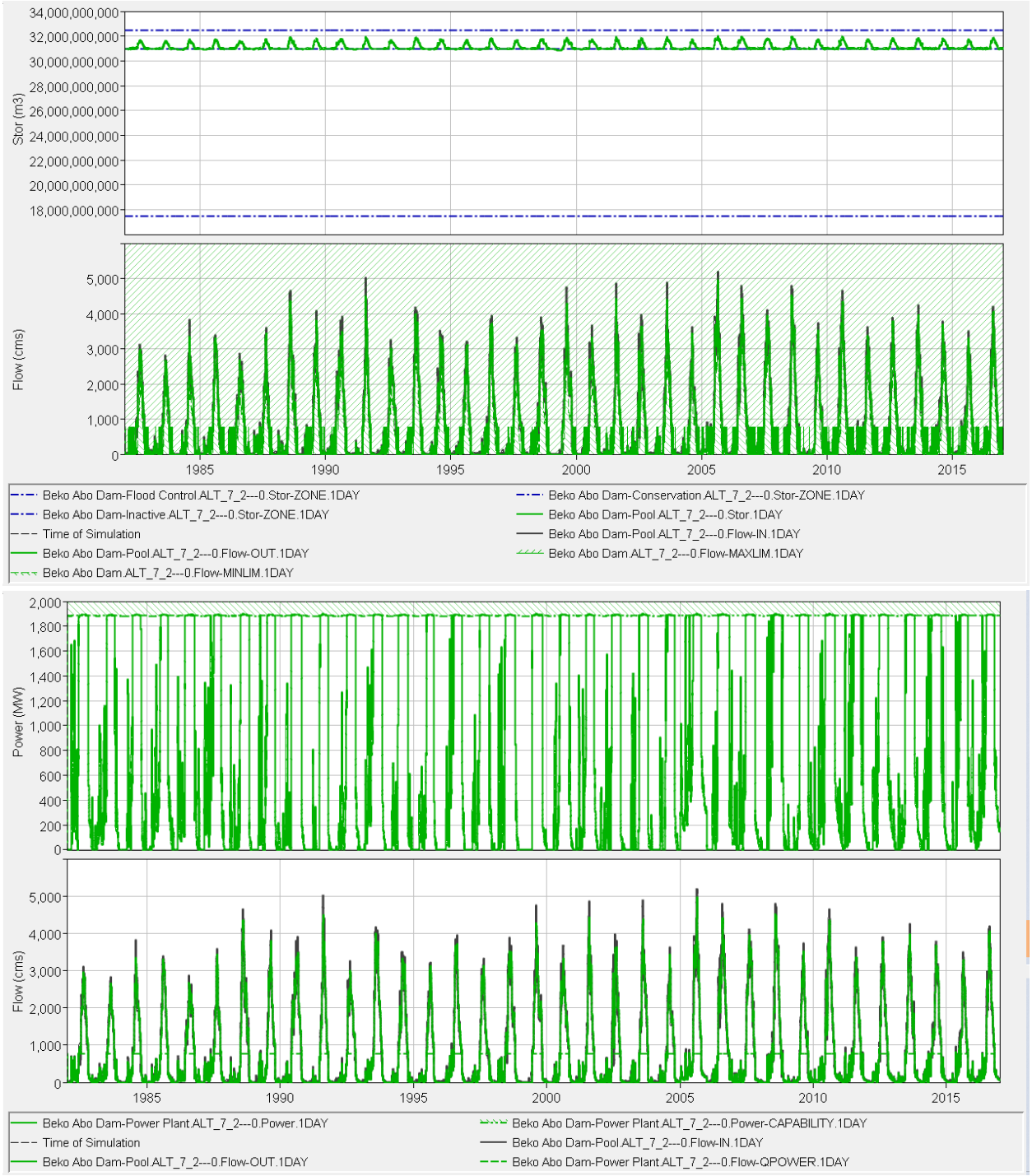

Figure E-13: Bekoabo Tandem operation (scenario_1.3)

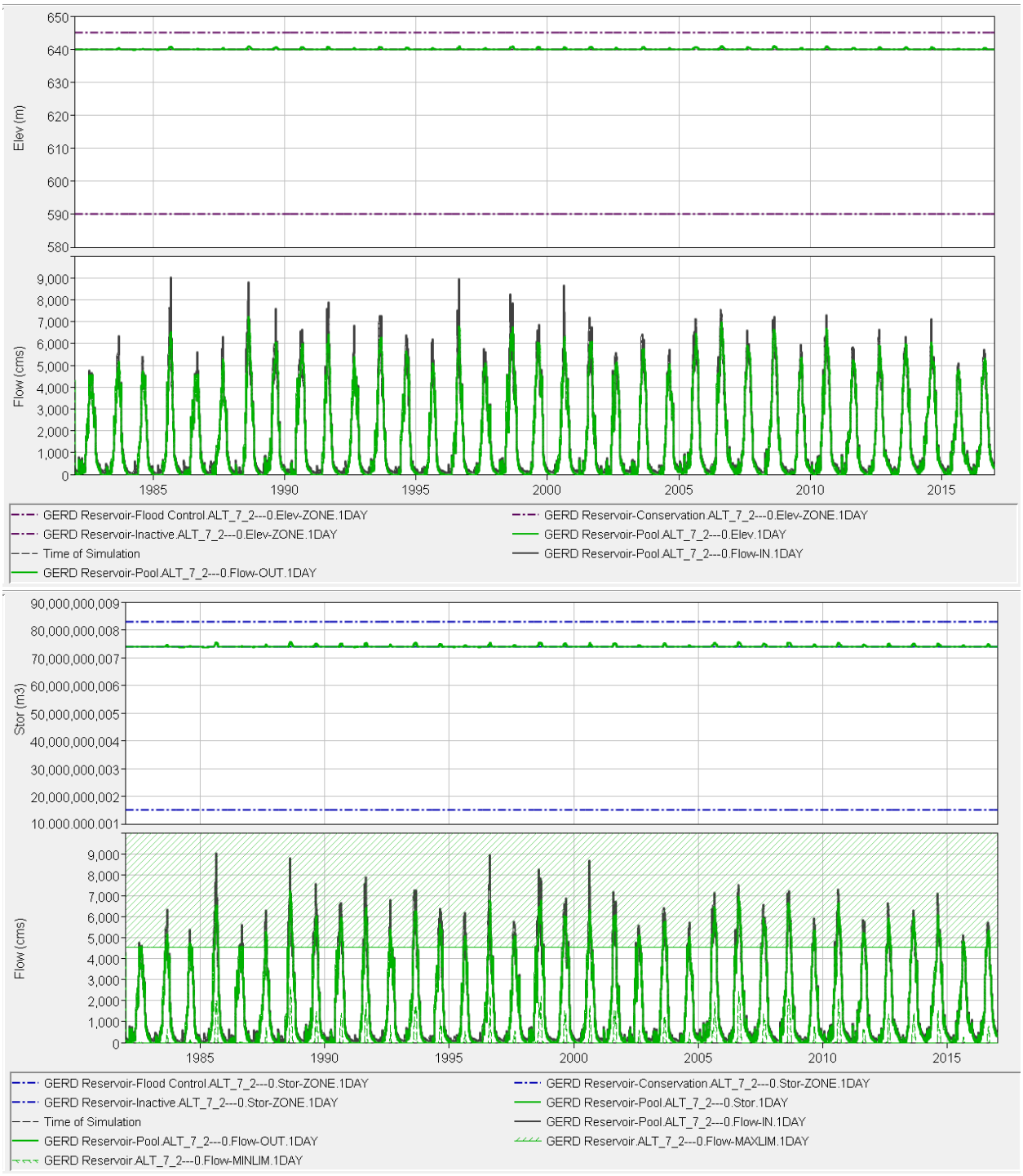
Elev (m)
650
640
630
620
610
600
590
580
Flow (cms)
9,000
8,000
7,000
6,000
5,000
4,000
3,000
2,000
1,000
0
1985
1990
1995
2000
2005
2010
2015
GERD Reservoir-Flood Control.ALT_7_2---0.Elev-ZONE.1DAY
GERD Reservoir-Conservation.ALT_7_2---0.Elev-ZONE.1DAY
GERD Reservoir-Inactive.ALT_7_2---0.Elev-ZONE.1DAY
GERD Reservoir-Pool.ALT_7_2---0.Elev.1DAY
Time of Simulation
GERD Reservoir-Pool.ALT_7_2---0.Flow-IN.1DAY
GERD Reservoir-Pool.ALT_7_2---0.Flow-OUT.1DAY
Stor (m3)
90,000,000,009
80,000,000,008
70,000,000,007
60,000,000,006
50,000,000,005
40,000,000,004
30,000,000,003
20,000,000,002
10.000.000.001
Flow (cms)
9,000
8,000
7,000
6,000
5,000
4,000
3,000
2,000
1,000
0
1985
1990
1995
2000
2005
2010
2015
GERD Reservoir-Flood Control.ALT_7_2---0.Stor-ZONE.1DAY
GERD Reservoir-Conservation.ALT_7_2---0.Stor-ZONE.1DAY
GERD Reservoir-Inactive.ALT_7_2---0.Stor-ZONE.1DAY
GERD Reservoir-Pool.ALT_7_2---0.Stor.1DAY
Time of Simulation
GERD Reservoir-Pool.ALT_7_2---0.Flow-IN.1DAY
GERD Reservoir-Pool.ALT_7_2---0.Flow-OUT.1DAY
GERD Reservoir.ALT_7_2---0.Flow-MAXLIM.1DAY
GERD Reservoir.ALT_7_2---0.Flow-MINLIM.1DAY

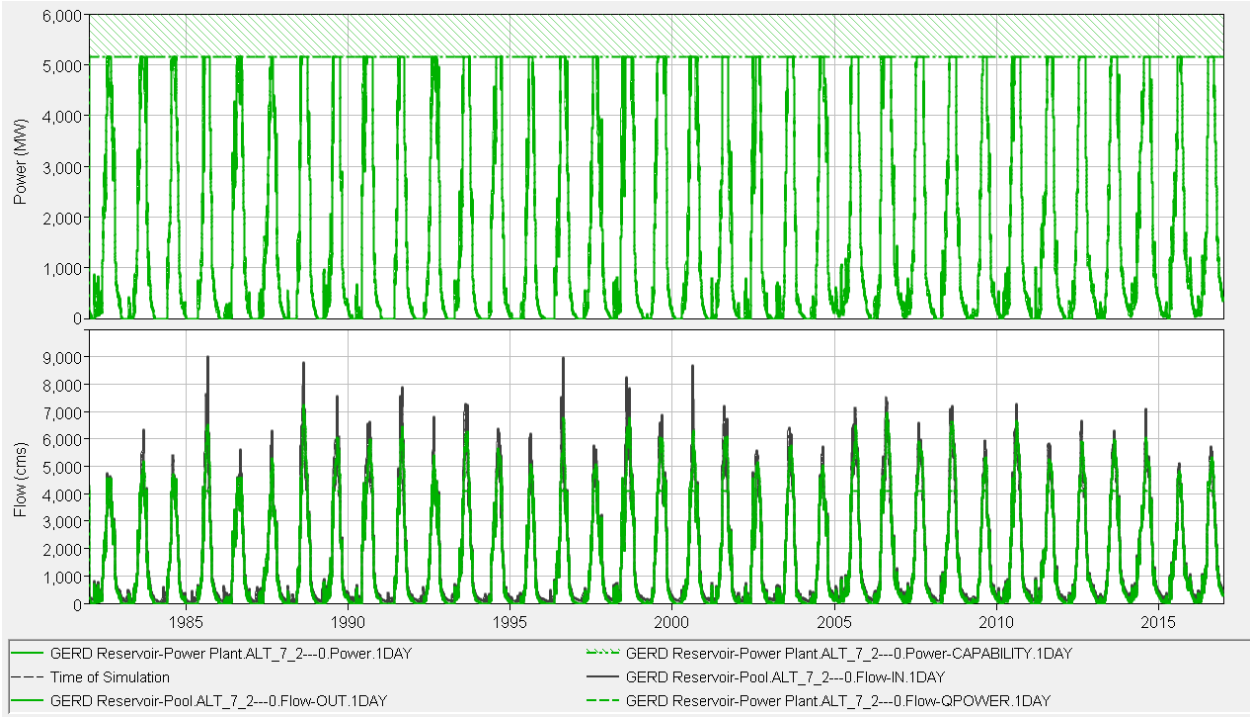

Figure E-14: GERD Tandem operation (scenario_1.3)

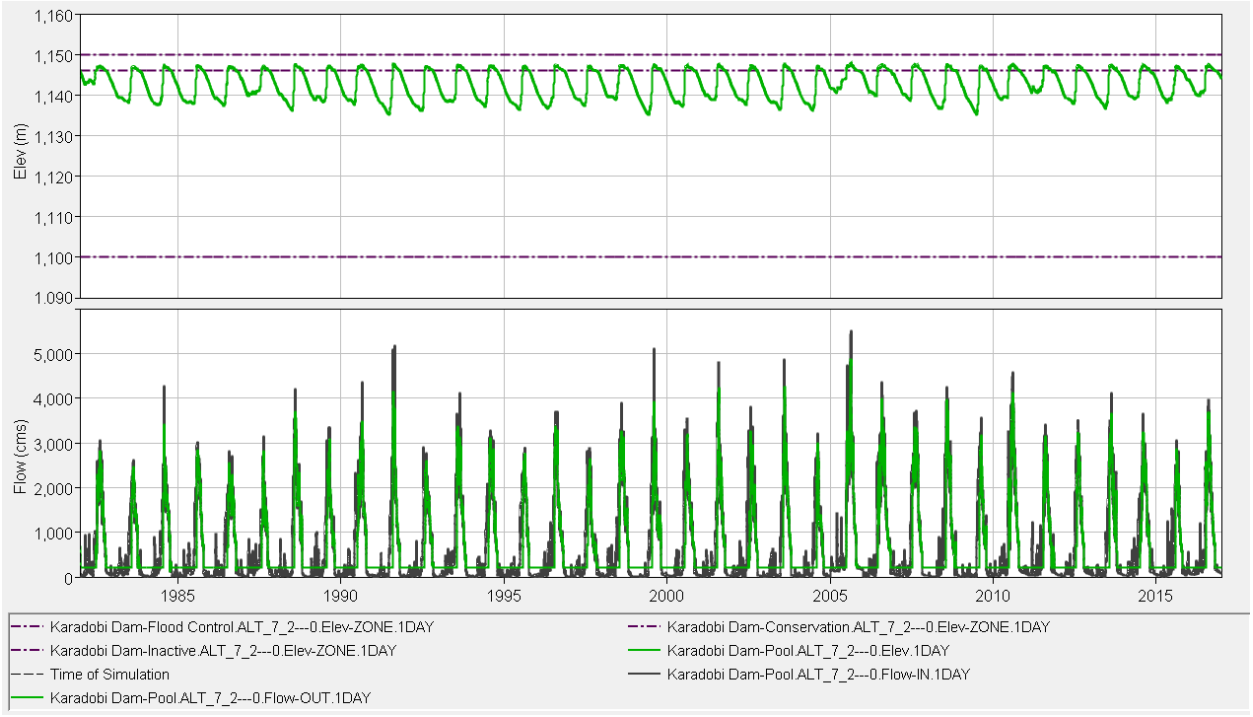

Figure E-15: Karadobi hydropower guide curve (scenario_1.3)

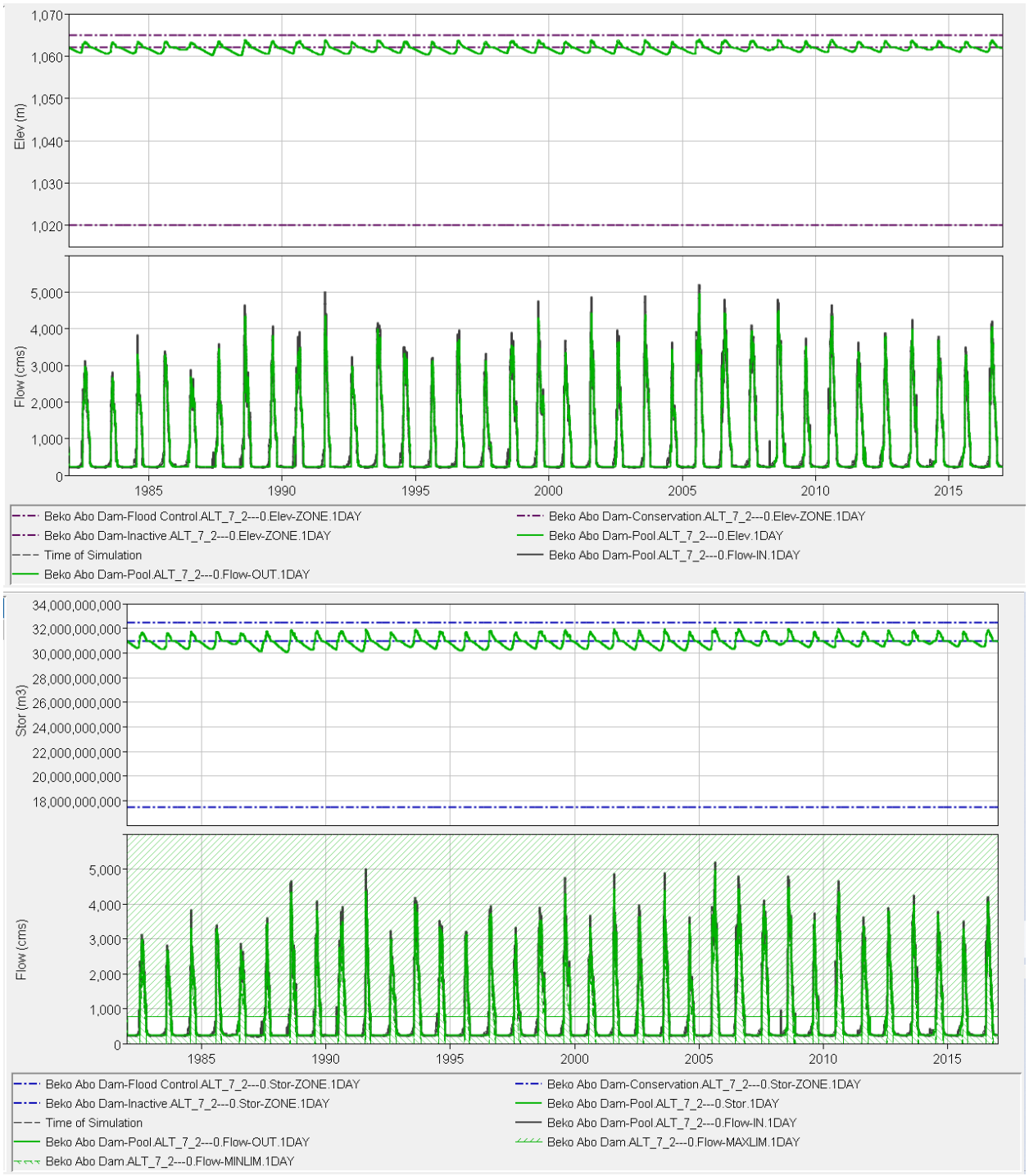
Elev (m)
1,070
1,060
1,050
1,040
1,030
1,020
Flow (cms)
5,000
4,000
3,000
2,000
1,000
0
1985
1990
1995
2000
2005
2010
2015
Beko Abo Dam-Flood Control.ALT_7_2---0.Elev-ZONE.1DAY
Beko Abo Dam-Conservation.ALT_7_2---0.Elev-ZONE.1DAY
Beko Abo Dam-Inactive.ALT_7_2---0.Elev-ZONE.1DAY
Beko Abo Dam-Pool.ALT_7_2---0.Elev.1DAY
Time of Simulation
Beko Abo Dam-Pool.ALT_7_2---0.Flow-IN.1DAY
Beko Abo Dam-Pool.ALT_7_2---0.Flow-OUT.1DAY
Stor (m3)
34,000,000,000
32,000,000,000
30,000,000,000
28,000,000,000
26,000,000,000
24,000,000,000
22,000,000,000
20,000,000,000
18,000,000,000
Flow (cms)
5,000
4,000
3,000
2,000
1,000
0
1985
1990
1995
2000
2005
2010
2015
Beko Abo Dam-Flood Control.ALT_7_2---0.Stor-ZONE.1DAY
Beko Abo Dam-Conservation.ALT_7_2---0.Stor-ZONE.1DAY
Beko Abo Dam-Inactive.ALT_7_2---0.Stor-ZONE.1DAY
Beko Abo Dam-Pool.ALT_7_2---0.Stor.1DAY
Time of Simulation
Beko Abo Dam-Pool.ALT_7_2---0.Flow-IN.1DAY
Beko Abo Dam-Pool.ALT_7_2---0.Flow-OUT.1DAY
Beko Abo Dam.ALT_7_2---0.Flow-MAXLIM.1DAY
Beko Abo Dam.ALT_7_2---0.Flow-MINLIM.1DAY

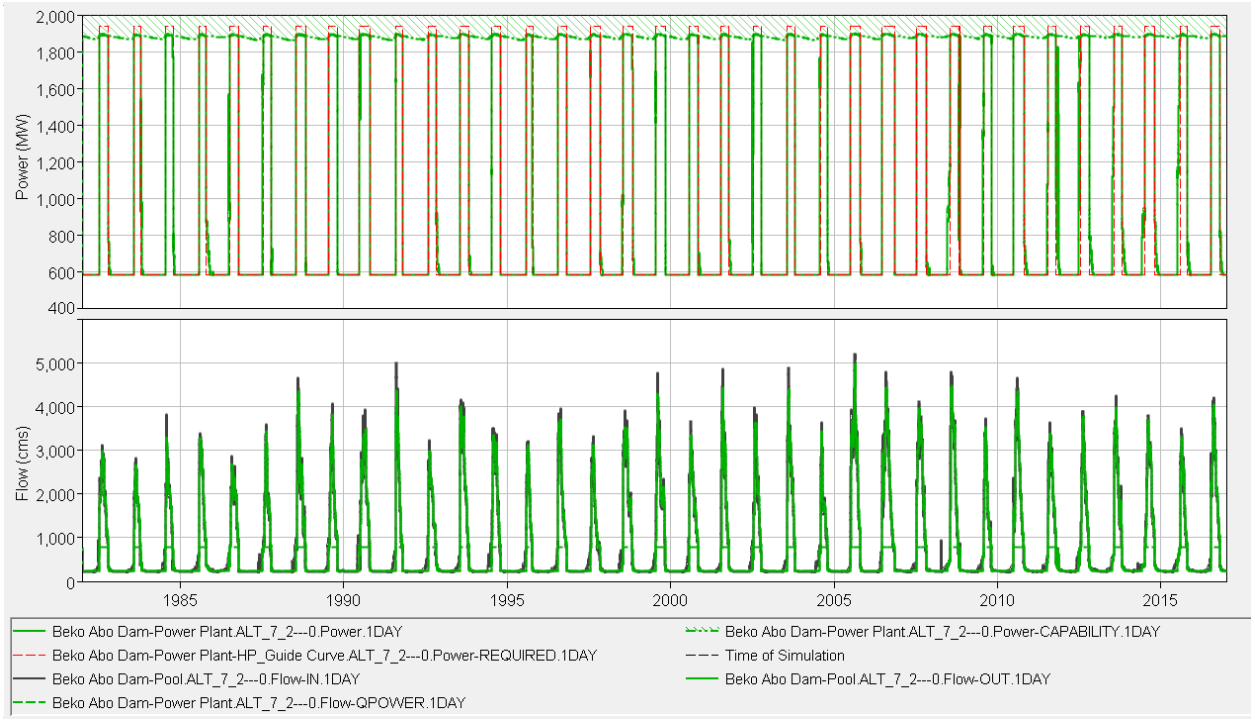

Figure E-16: Bekoabo hydropower guide curve (scenario_1.3)

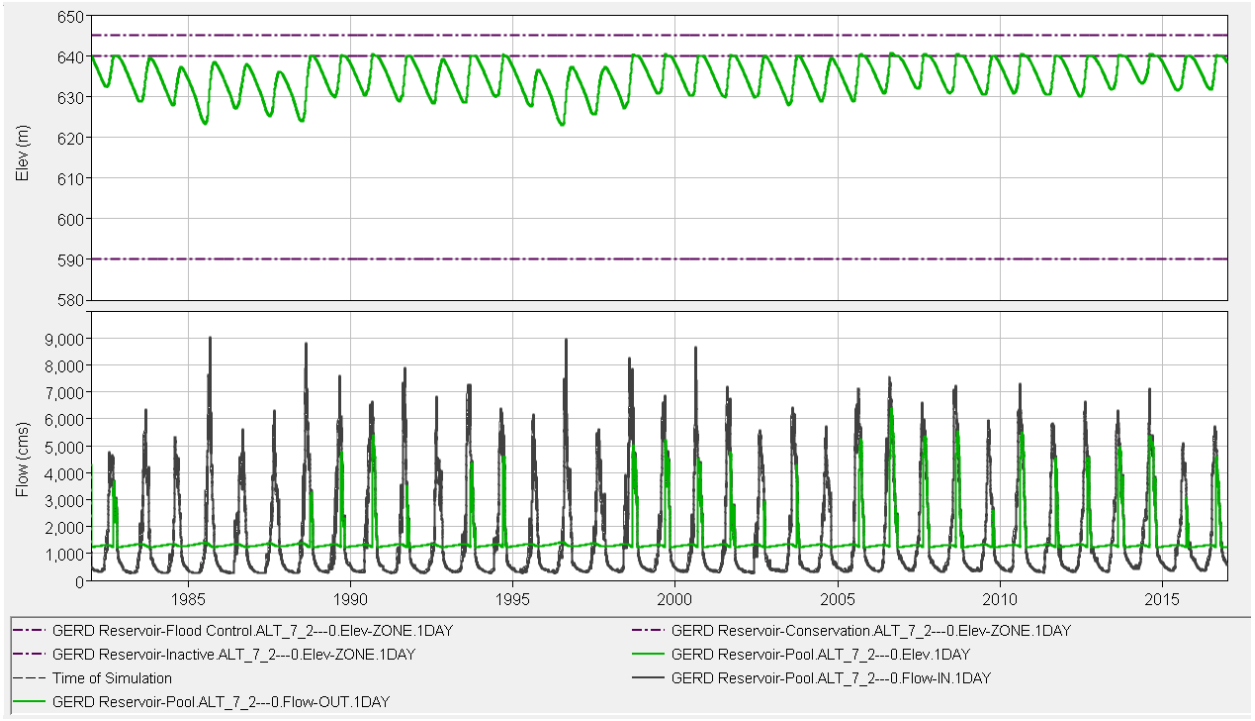

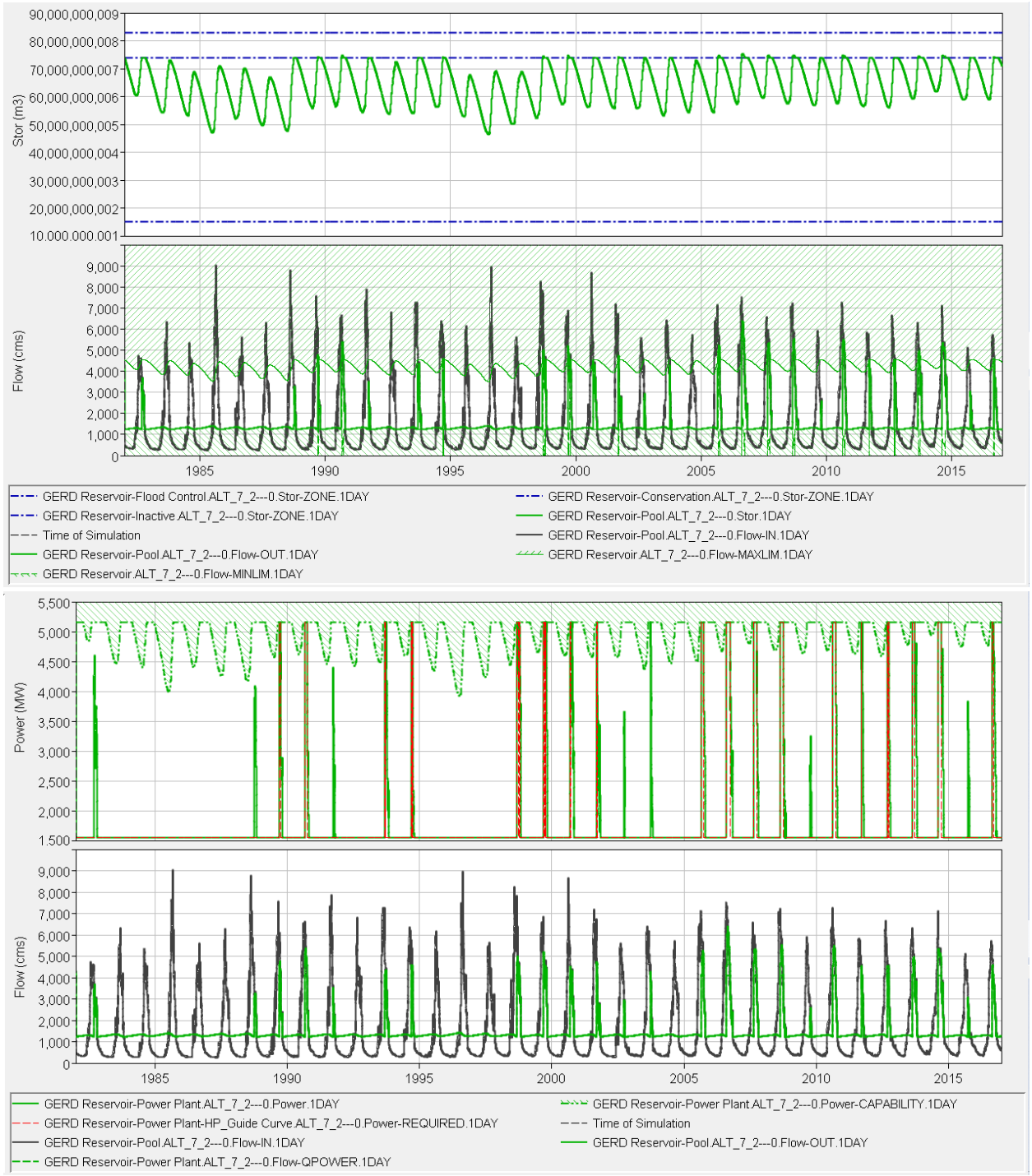

Figure E-17: GERD hydropower guide curve (scenario_1.3)

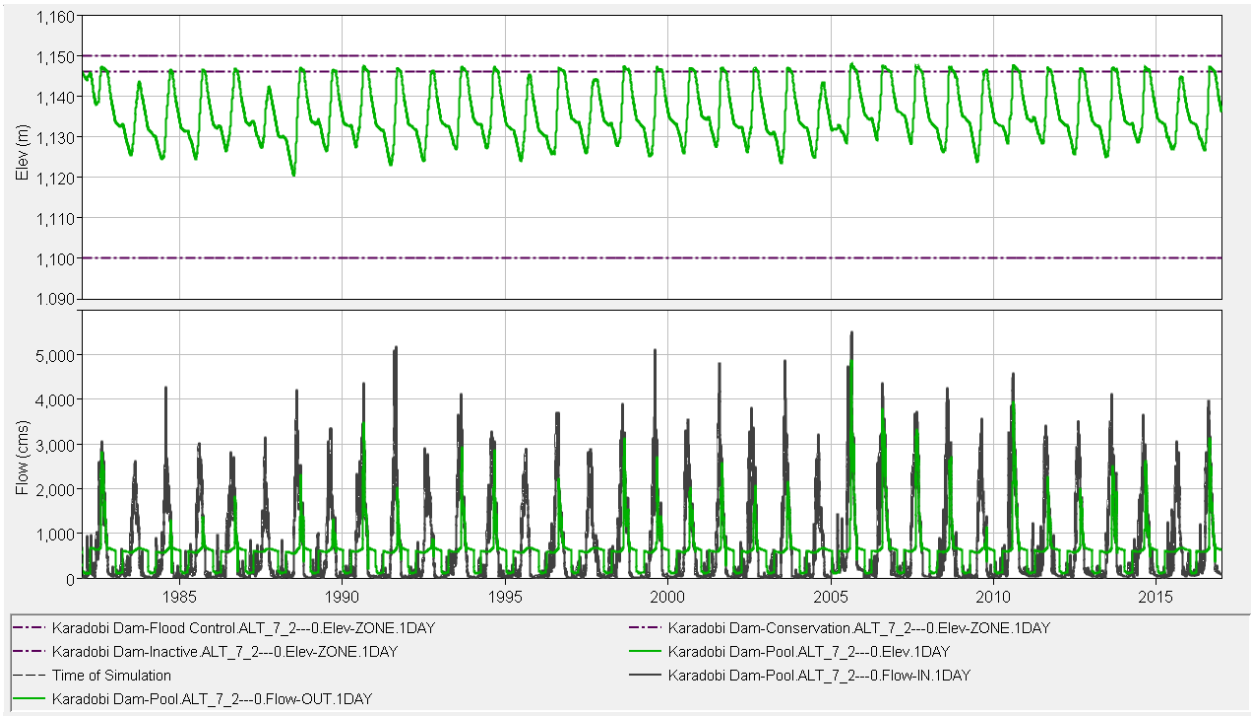
Elev (m)
1,160
1,150
1,140
1,130
1,120
1,110
1,100
1,090
Flow (cms)
5,000
4,000
3,000
2,000
1,000
0
1985
1990
1995
2000
2005
2010
2015
Karadobi Dam-Flood Control.ALT_7_2---0.Elev-ZONE.1DAY
Karadobi Dam-Conservation.ALT_7_2---0.Elev-ZONE.1DAY
Karadobi Dam-Inactive.ALT_7_2---0.Elev-ZONE.1DAY
Karadobi Dam-Pool.ALT_7_2---0.Elev.1DAY
Time of Simulation
Karadobi Dam-Pool.ALT_7_2---0.Flow-IN.1DAY
Karadobi Dam-Pool.ALT_7_2---0.Flow-OUT.1DAY

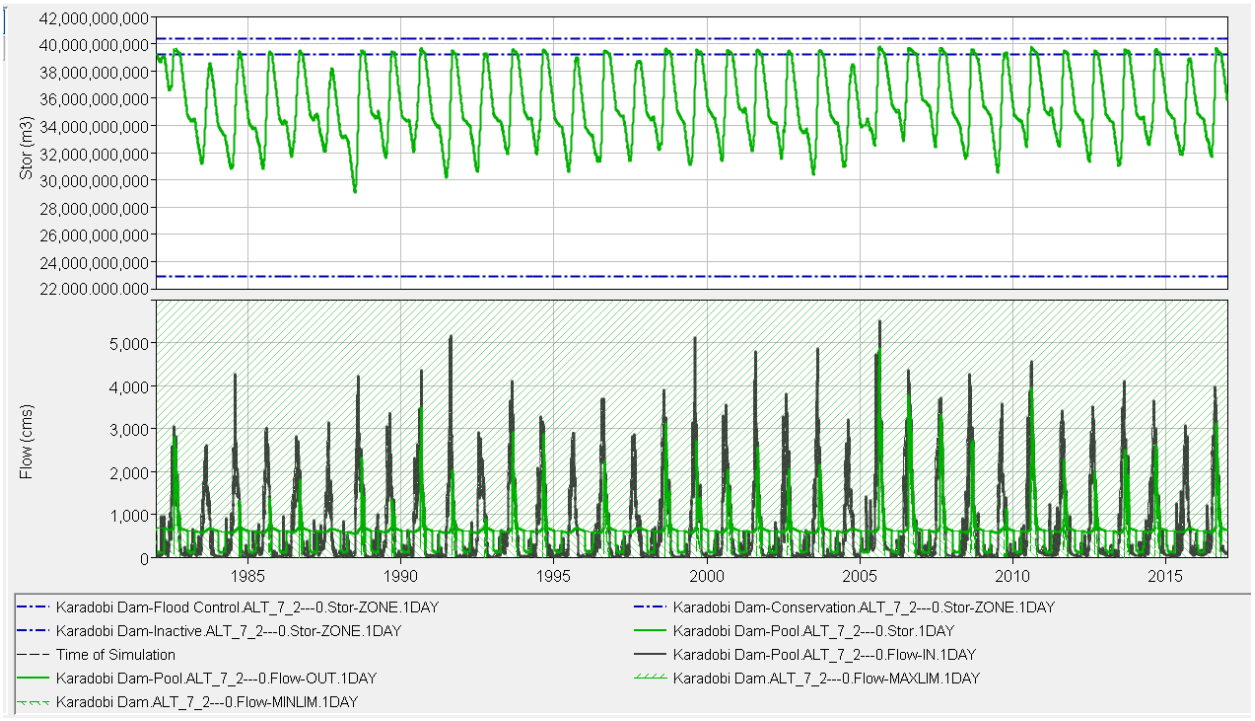
Stor (m3)
42,000,000,000
40,000,000,000
38,000,000,000
36,000,000,000
34,000,000,000
32,000,000,000
30,000,000,000
28,000,000,000
26,000,000,000
24,000,000,000
22.000.000.000
Flow (cms)
5,000
4,000
3,000
2,000
1,000
0
1985
1990
1995
2000
2005
2010
2015
Karadobi Dam-Flood Control.ALT_7_2---0.Stor-ZONE.1DAY
Karadobi Dam-Conservation.ALT_7_2---0.Stor-ZONE.1DAY
Karadobi Dam-Inactive.ALT_7_2---0.Stor-ZONE.1DAY
Karadobi Dam-Pool.ALT_7_2---0.Stor.1DAY
Time of Simulation
Karadobi Dam-Pool.ALT_7_2---0.Flow-IN.1DAY
Karadobi Dam-Pool.ALT_7_2---0.Flow-OUT.1DAY
Karadobi Dam.ALT_7_2---0.Flow-MAXLIM.1DAY
Karadobi Dam.ALT_7_2---0.Flow-MINLIM.1DAY

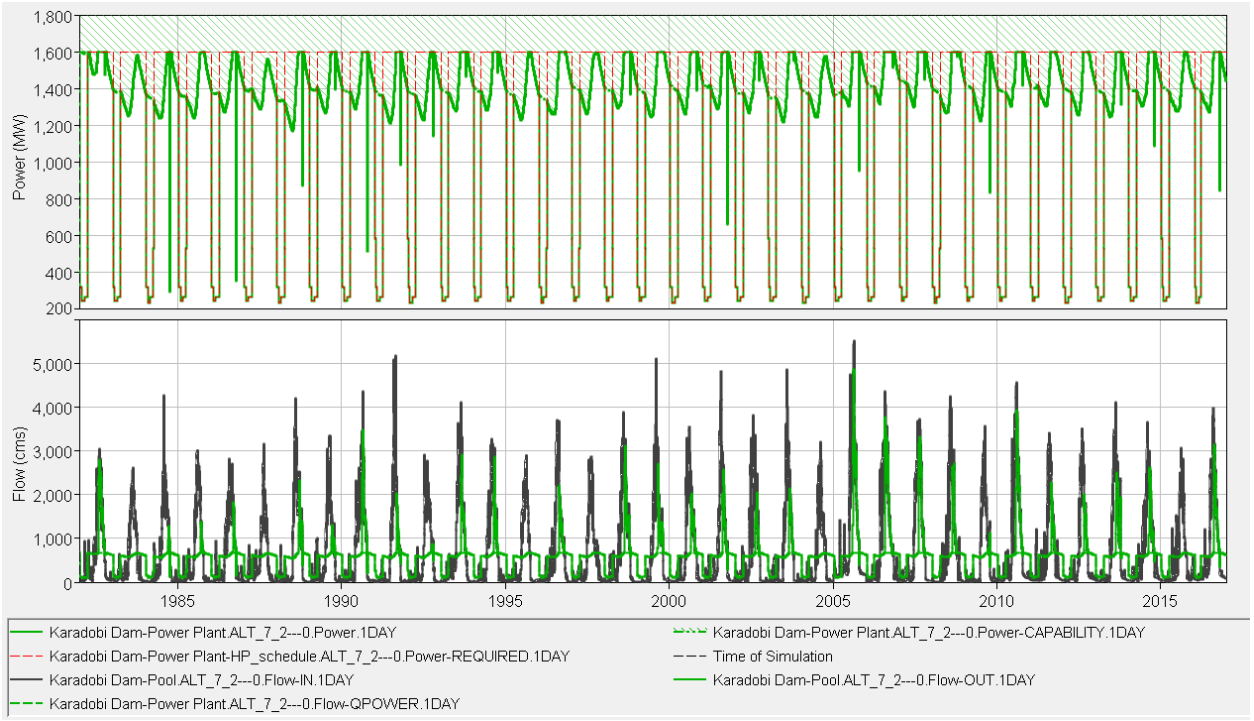

Figure E-18: Karadobi hydropower schedule (scenario_1.3)

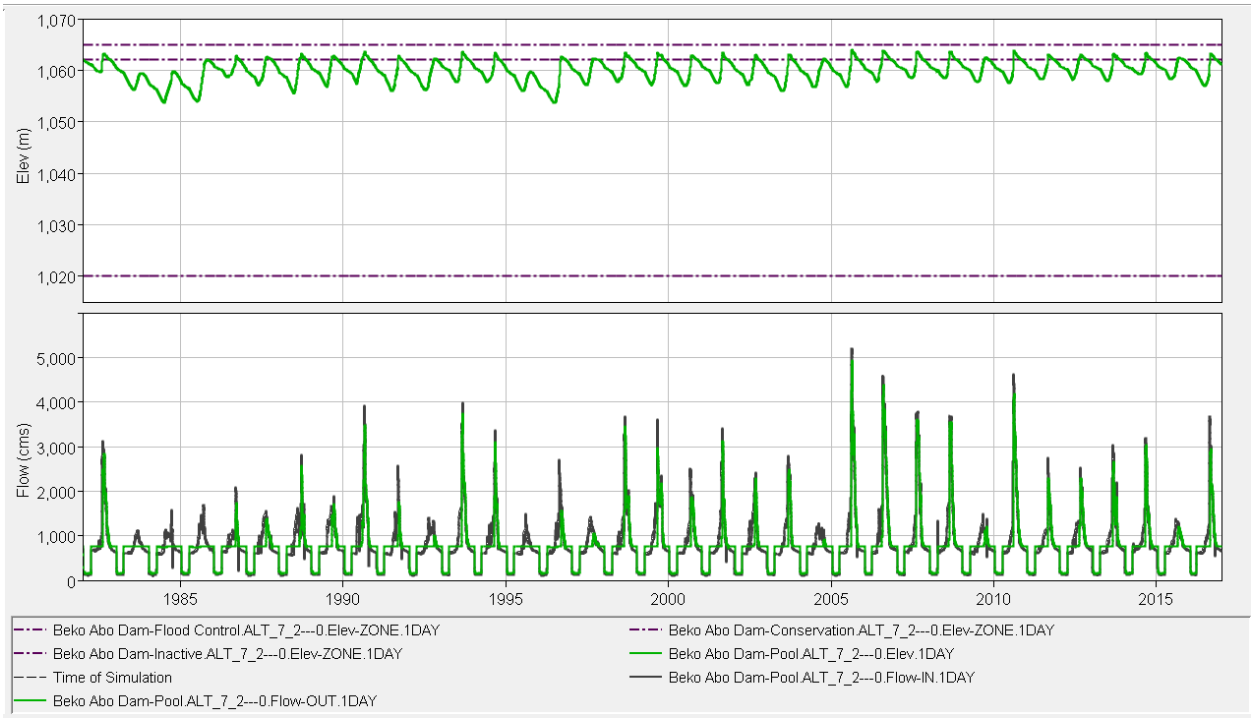

Figure E-19: Bekoabo hydropower schedule rule (scenario_1.3)

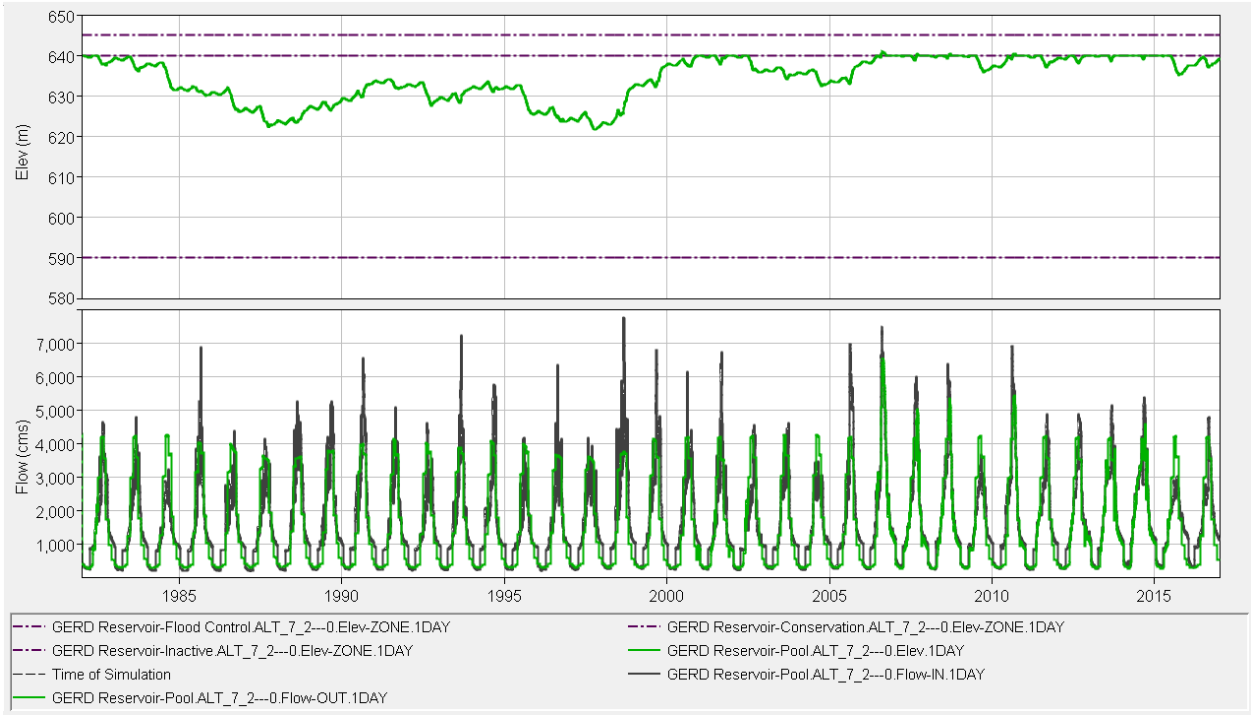
Elev (m)
650
640
630
620
610
600
590
580
Flow (cms)
7,000
6,000
5,000
4,000
3,000
2,000
1,000
1985
1990
1995
2000
2005
2010
2015
GERD Reservoir-Flood Control.ALT_7_2---0.Elev-ZONE.1DAY
GERD Reservoir-Conservation.ALT_7_2---0.Elev-ZONE.1DAY
GERD Reservoir-Inactive.ALT_7_2---0.Elev-ZONE.1DAY
GERD Reservoir-Pool.ALT_7_2---0.Elev.1DAY
Time of Simulation
GERD Reservoir-Pool.ALT_7_2---0.Flow-IN.1DAY
GERD Reservoir-Pool.ALT_7_2---0.Flow-OUT.1DAY

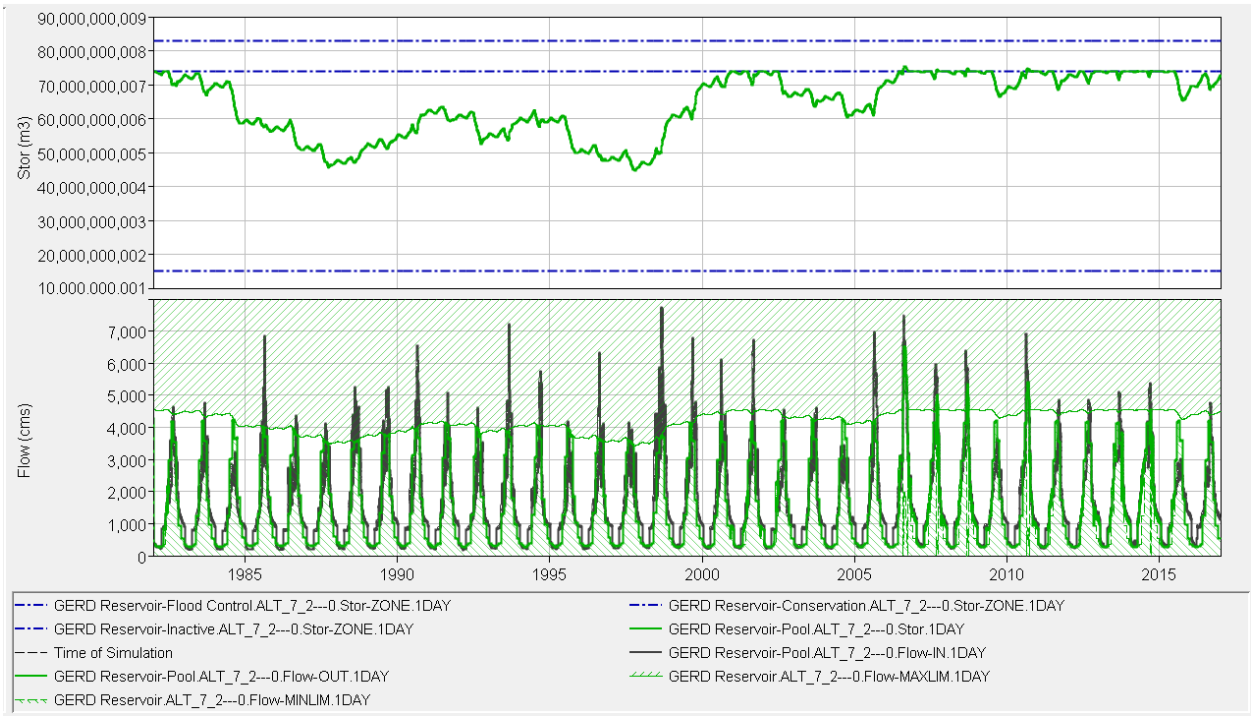
Stor (m3)
90,000,000,009
80,000,000,008
70,000,000,007
60,000,000,006
50,000,000,005
40,000,000,004
30,000,000,003
20,000,000,002
10.000.000.001
Flow (cms)
7,000
6,000
5,000
4,000
3,000
2,000
1,000
0
1985
1990
1995
2000
2005
2010
2015
GERD Reservoir-Flood Control.ALT_7_2---0.Stor-ZONE.1DAY
GERD Reservoir-Conservation.ALT_7_2---0.Stor-ZONE.1DAY
GERD Reservoir-Inactive.ALT_7_2---0.Stor-ZONE.1DAY
GERD Reservoir-Pool.ALT_7_2---0.Stor.1DAY
Time of Simulation
GERD Reservoir-Pool.ALT_7_2---0.Flow-IN.1DAY
GERD Reservoir-Pool.ALT_7_2---0.Flow-OUT.1DAY
GERD Reservoir.ALT_7_2---0.Flow-MAXLIM.1DAY
GERD Reservoir.ALT_7_2---0.Flow-MINLIM.1DAY

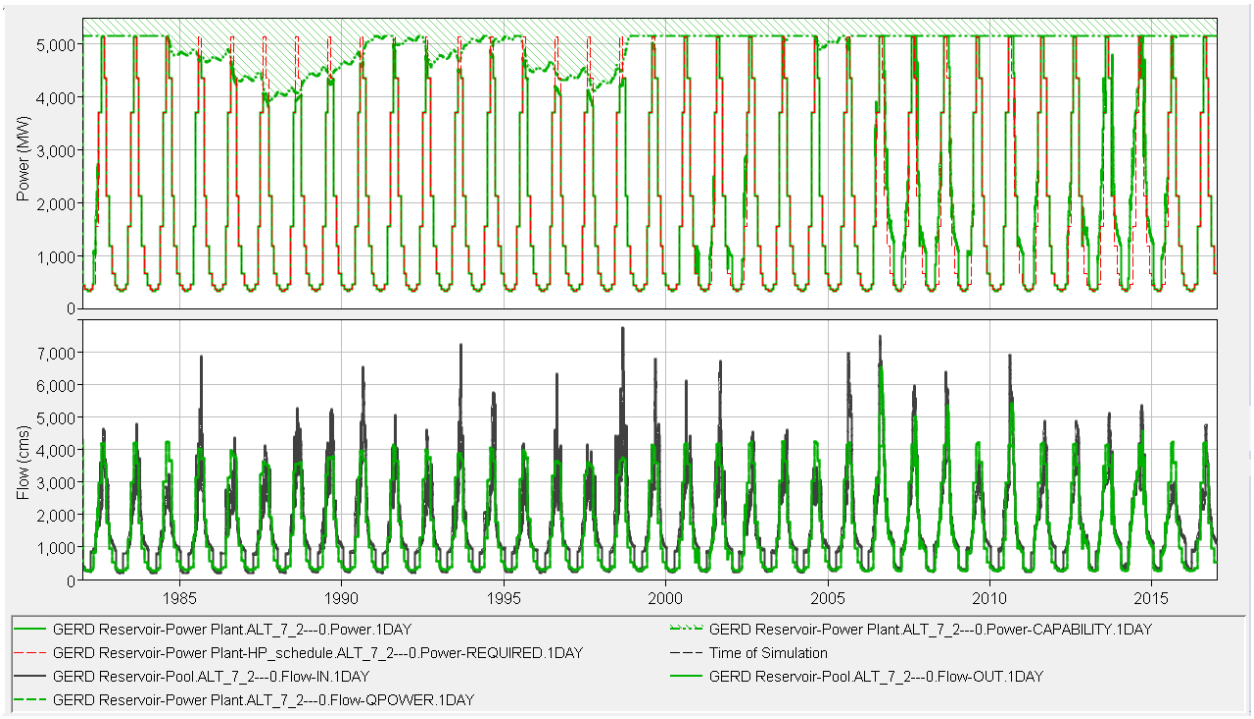

Figure E-20: GERD hydropower schedule rule (scenario_1.3)

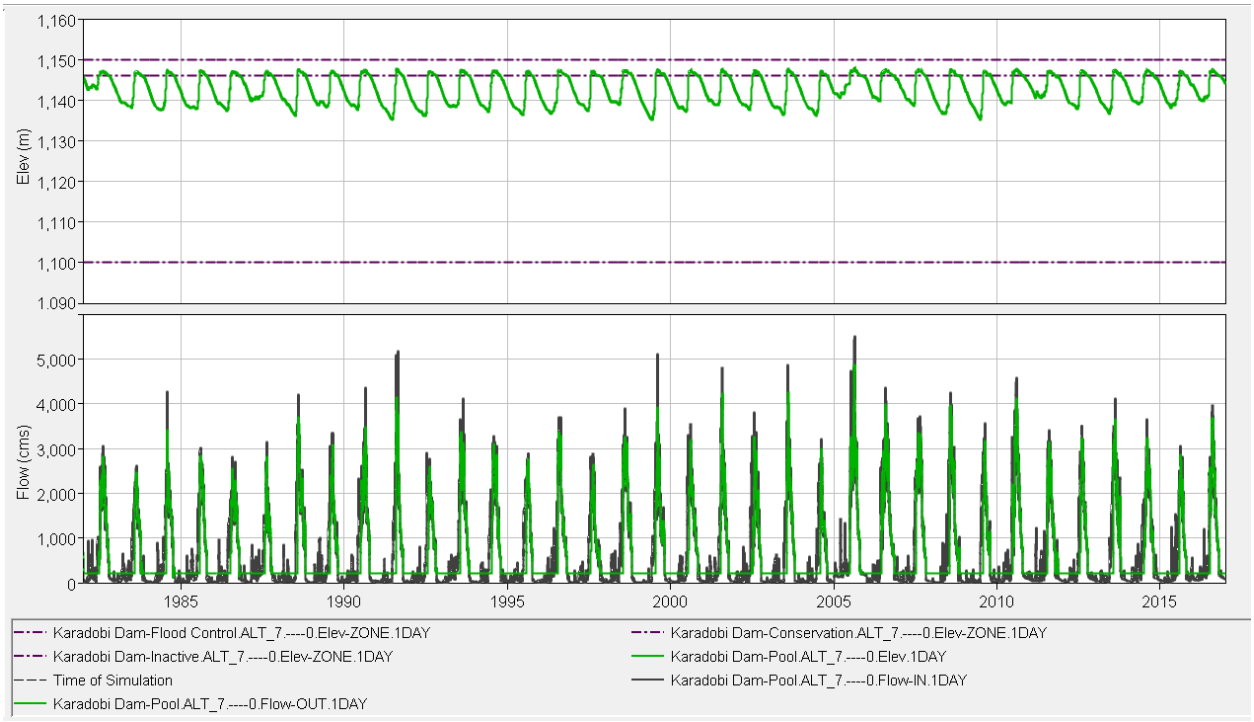

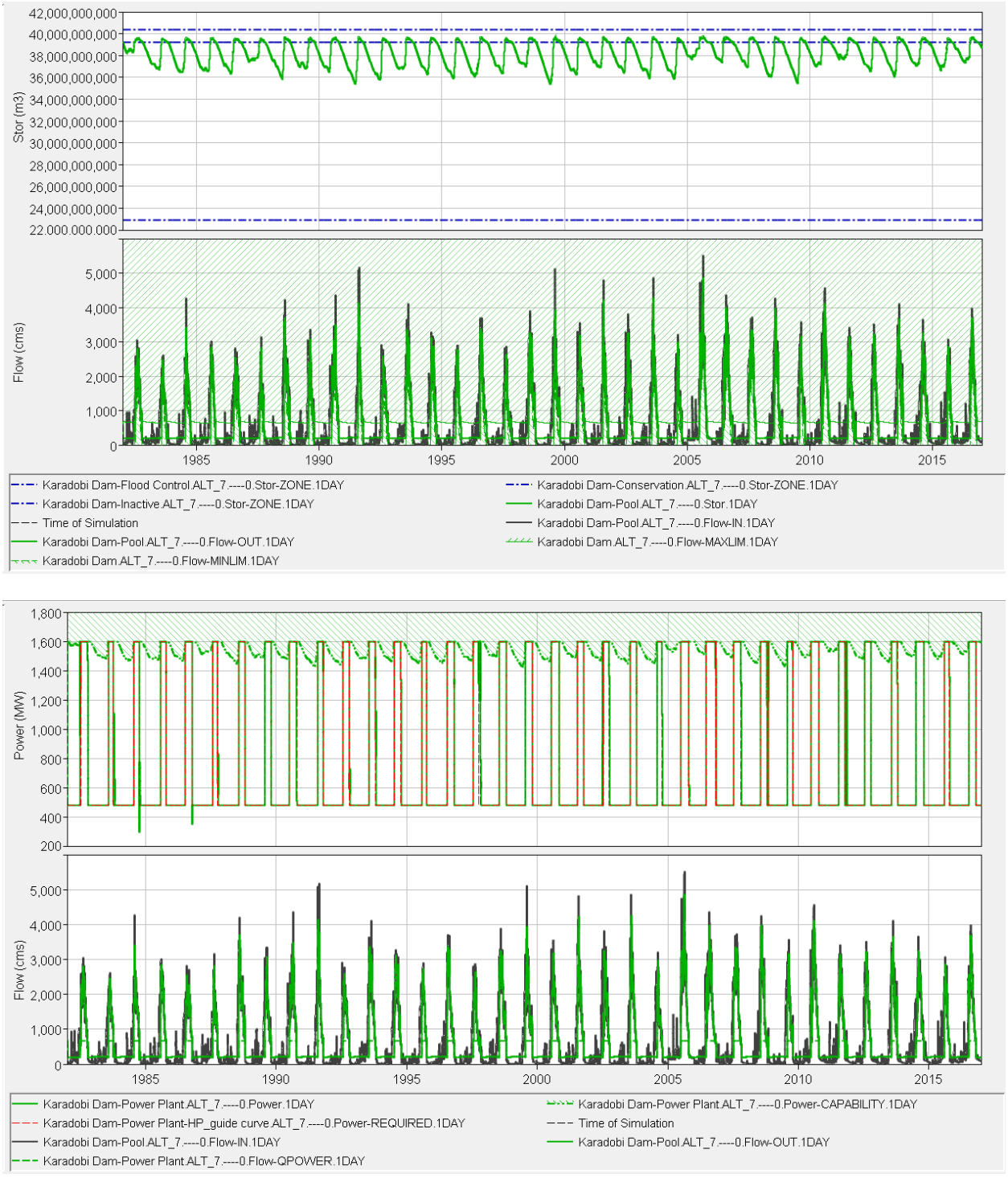

Figure E-21: Karadobi hydropower guide curve (scenario_1.4)

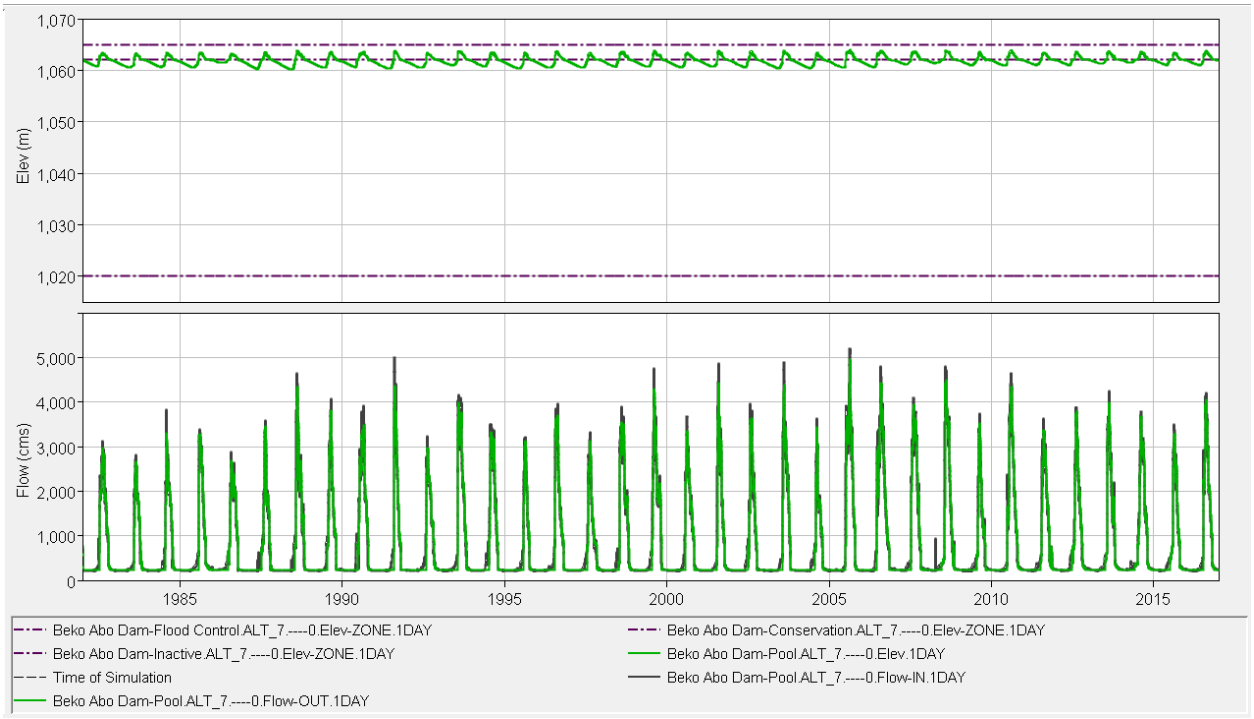
Elev (m)
1,070
1,060
1,050
1,040
1,030
1,020
Flow (cms)
5,000
4,000
3,000
2,000
1,000
0
1985
1990
1995
2000
2005
2010
2015
Beko Abo Dam-Flood Control.ALT_7.----0.Elev-ZONE.1DAY
Beko Abo Dam-Conservation.ALT_7.----0.Elev-ZONE.1DAY
Beko Abo Dam-Inactive.ALT_7.----0.Elev-ZONE.1DAY
Beko Abo Dam-Pool.ALT_7.----0.Elev.1DAY
Time of Simulation
Beko Abo Dam-Pool.ALT_7.----0.Flow-IN.1DAY
Beko Abo Dam-Pool.ALT_7.----0.Flow-OUT.1DAY

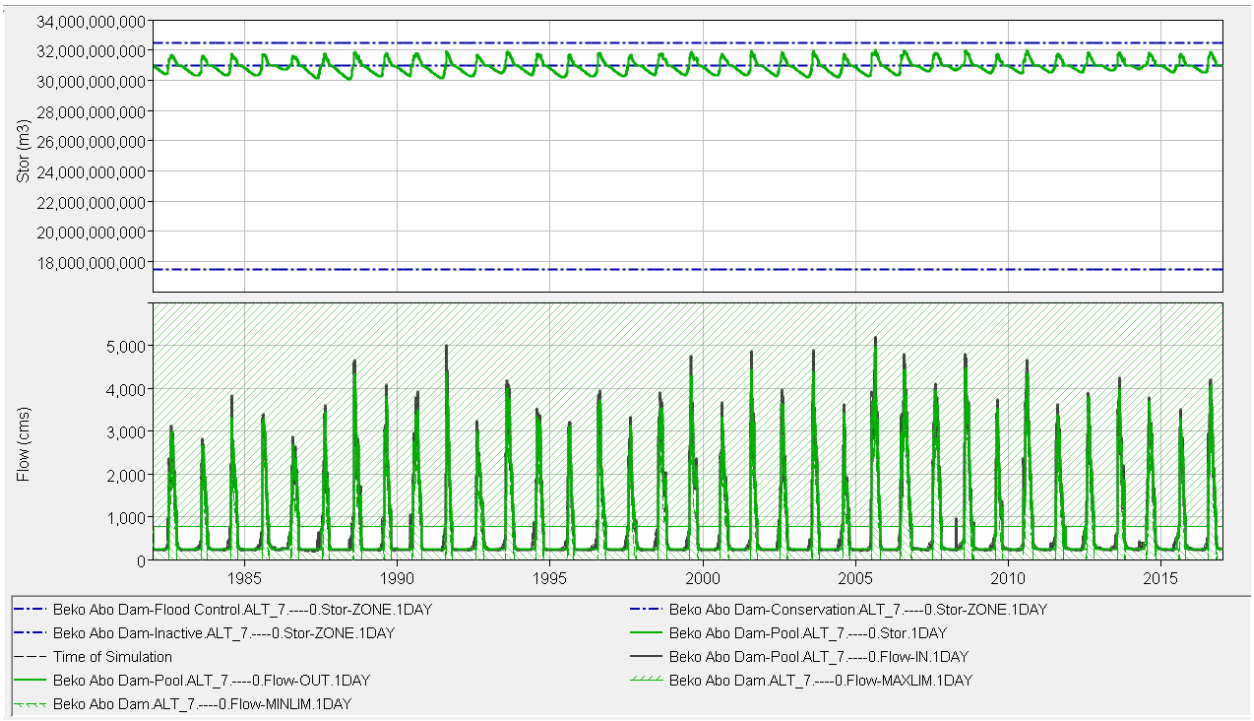
Stor (m3)
34,000,000,000
32,000,000,000
30,000,000,000
28,000,000,000
26,000,000,000
24,000,000,000
22,000,000,000
20,000,000,000
18,000,000,000
Flow (cms)
5,000
4,000
3,000
2,000
1,000
0
1985
1990
1995
2000
2005
2010
2015
Beko Abo Dam-Flood Control.ALT_7.----0.Stor-ZONE.1DAY
Beko Abo Dam-Conservation.ALT_7.----0.Stor-ZONE.1DAY
Beko Abo Dam-Inactive.ALT_7.----0.Stor-ZONE.1DAY
Beko Abo Dam-Pool.ALT_7.----0.Stor.1DAY
Time of Simulation
Beko Abo Dam-Pool.ALT_7.----0.Flow-IN.1DAY
Beko Abo Dam-Pool.ALT_7.----0.Flow-OUT.1DAY
Beko Abo Dam.ALT_7.----0.Flow-MAXLIM.1DAY
Beko Abo Dam.ALT_7.----0.Flow-MINLIM.1DAY

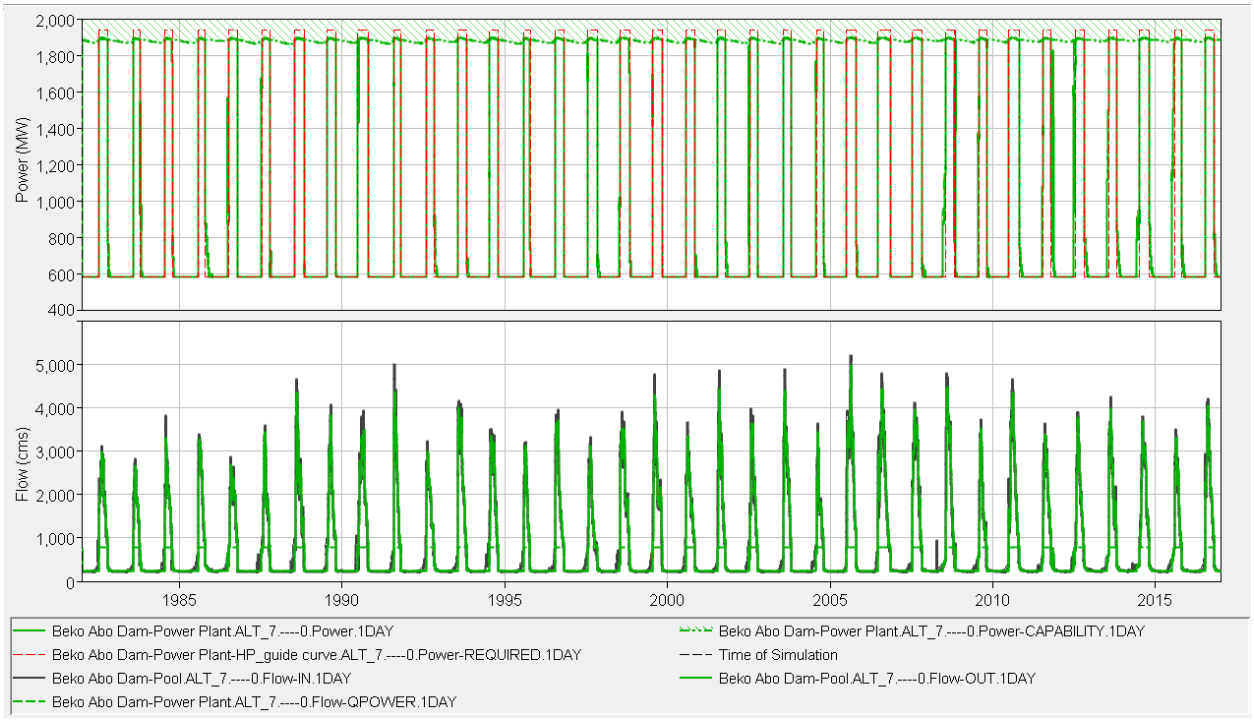

Figure E-22: Beko Abo hydropower guide curve (scenario_1.4)

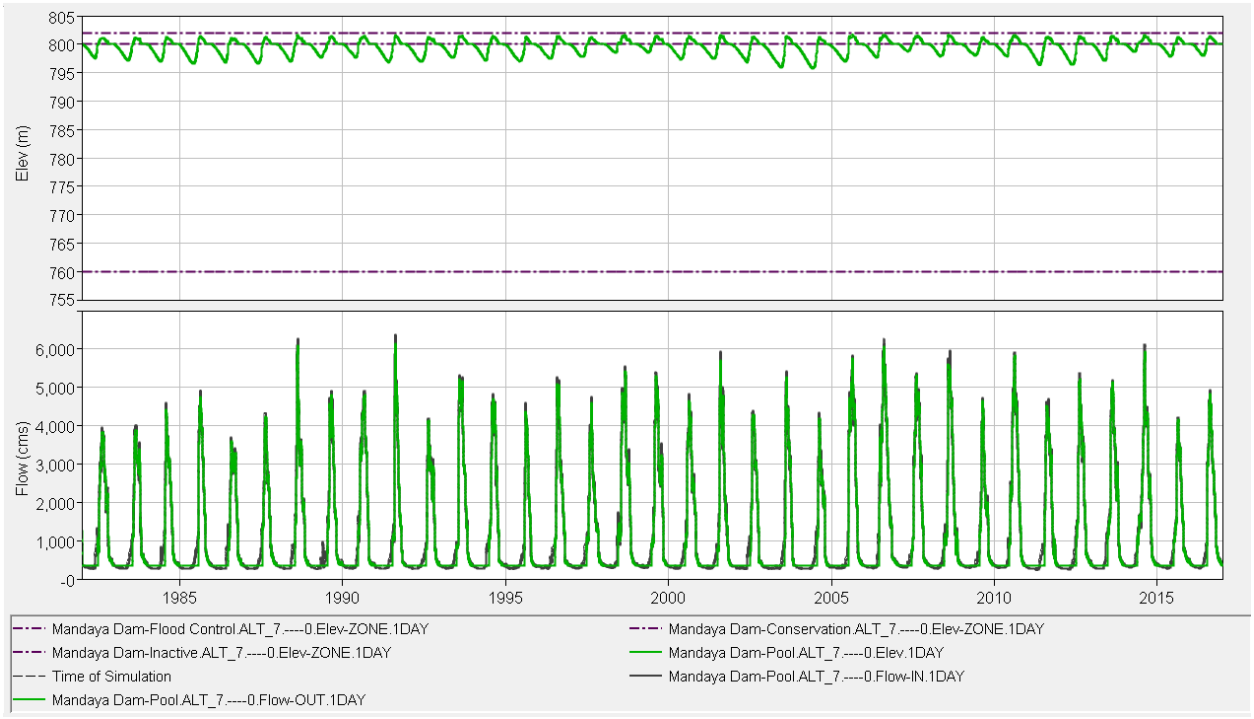

Figure E-23: Mandaya hydropower guide curve (scenario_1.4)

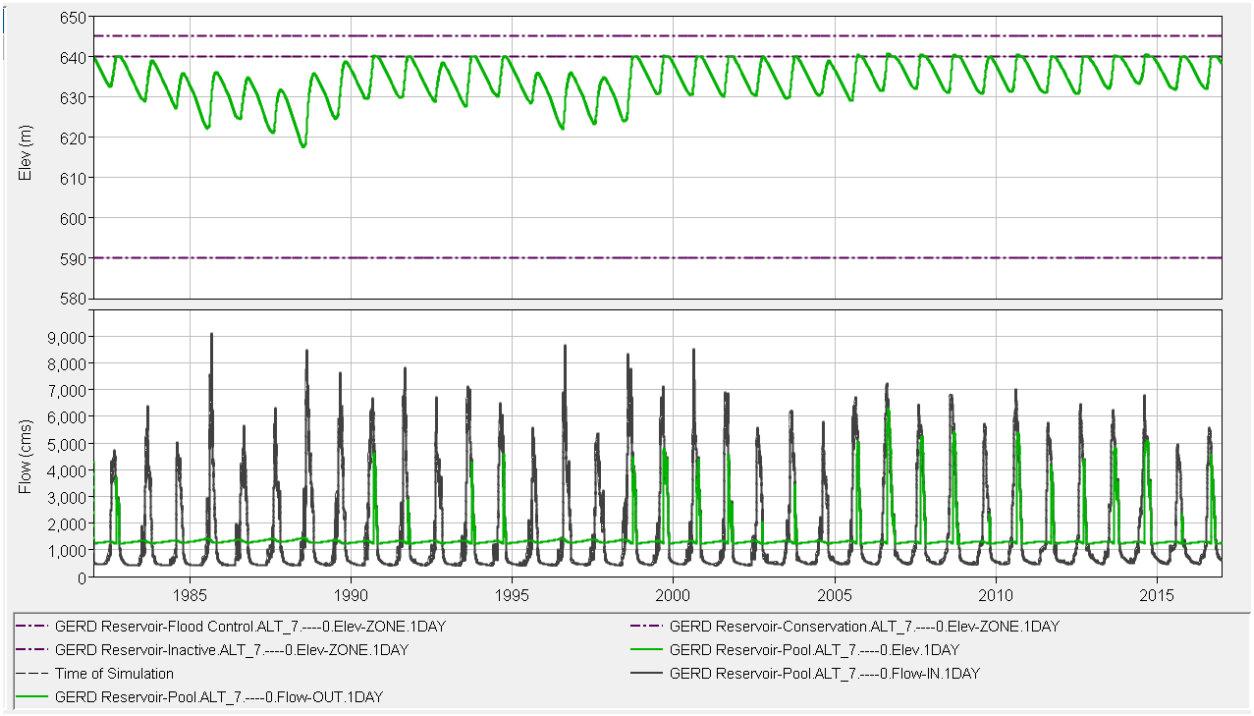
Elev (m)
650
640
630
620
610
600
590
580
Flow (cms)
9,000
8,000
7,000
6,000
5,000
4,000
3,000
2,000
1,000
0
1985
1990
1995
2000
2005
2010
2015
GERD Reservoir-Flood Control.ALT_7.----0.Elev-ZONE.1DAY
GERD Reservoir-Conservation.ALT_7.----0.Elev-ZONE.1DAY
GERD Reservoir-Inactive.ALT_7.----0.Elev-ZONE.1DAY
GERD Reservoir-Pool.ALT_7.----0.Elev.1DAY
Time of Simulation
GERD Reservoir-Pool.ALT_7.----0.Flow-IN.1DAY
GERD Reservoir-Pool.ALT_7.----0.Flow-OUT.1DAY

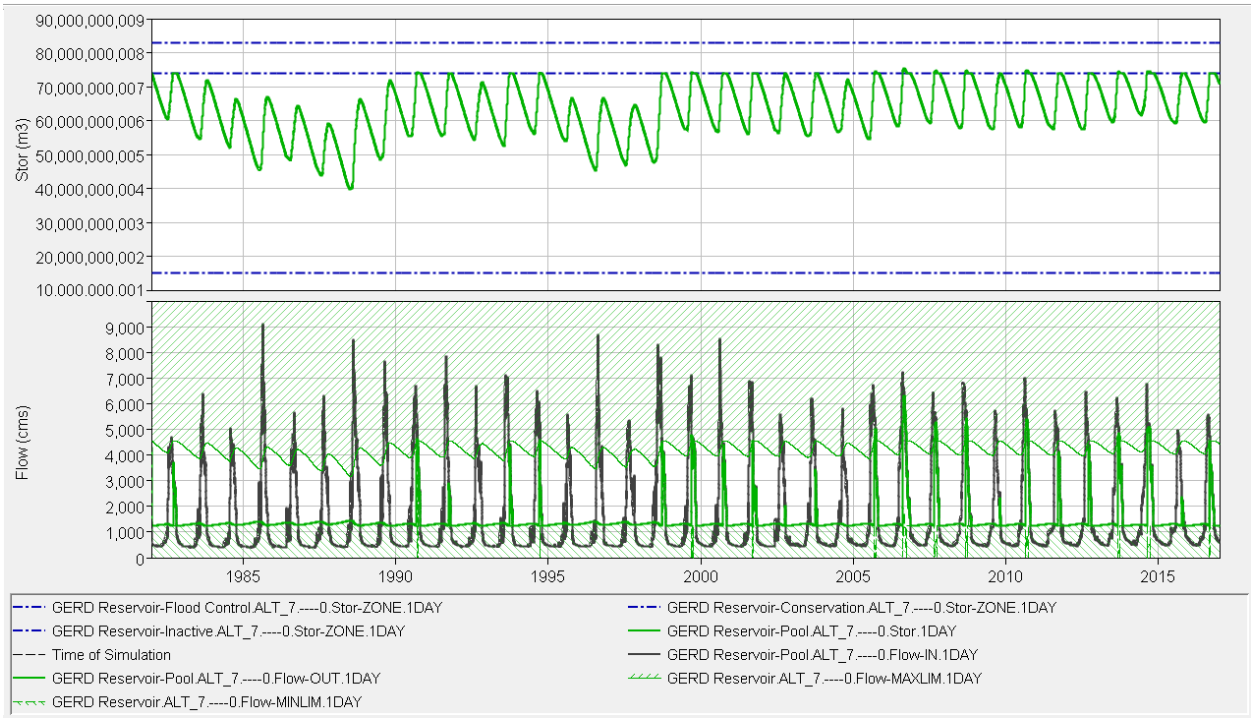
Stor (m3)
90,000,000,009
80,000,000,008
70,000,000,007
60,000,000,006
50,000,000,005
40,000,000,004
30,000,000,003
20,000,000,002
10.000.000.001
Flow (cms)
9,000
8,000
7,000
6,000
5,000
4,000
3,000
2,000
1,000
0
1985
1990
1995
2000
2005
2010
2015
GERD Reservoir-Flood Control.ALT_7.----0.Stor-ZONE.1DAY
GERD Reservoir-Conservation.ALT_7.----0.Stor-ZONE.1DAY
GERD Reservoir-Inactive.ALT_7.----0.Stor-ZONE.1DAY
GERD Reservoir-Pool.ALT_7.----0.Stor.1DAY
Time of Simulation
GERD Reservoir-Pool.ALT_7.----0.Flow-IN.1DAY
GERD Reservoir-Pool.ALT_7.----0.Flow-OUT.1DAY
GERD Reservoir.ALT_7.----0.Flow-MAXLIM.1DAY
GERD Reservoir.ALT_7.----0.Flow-MINLIM.1DAY

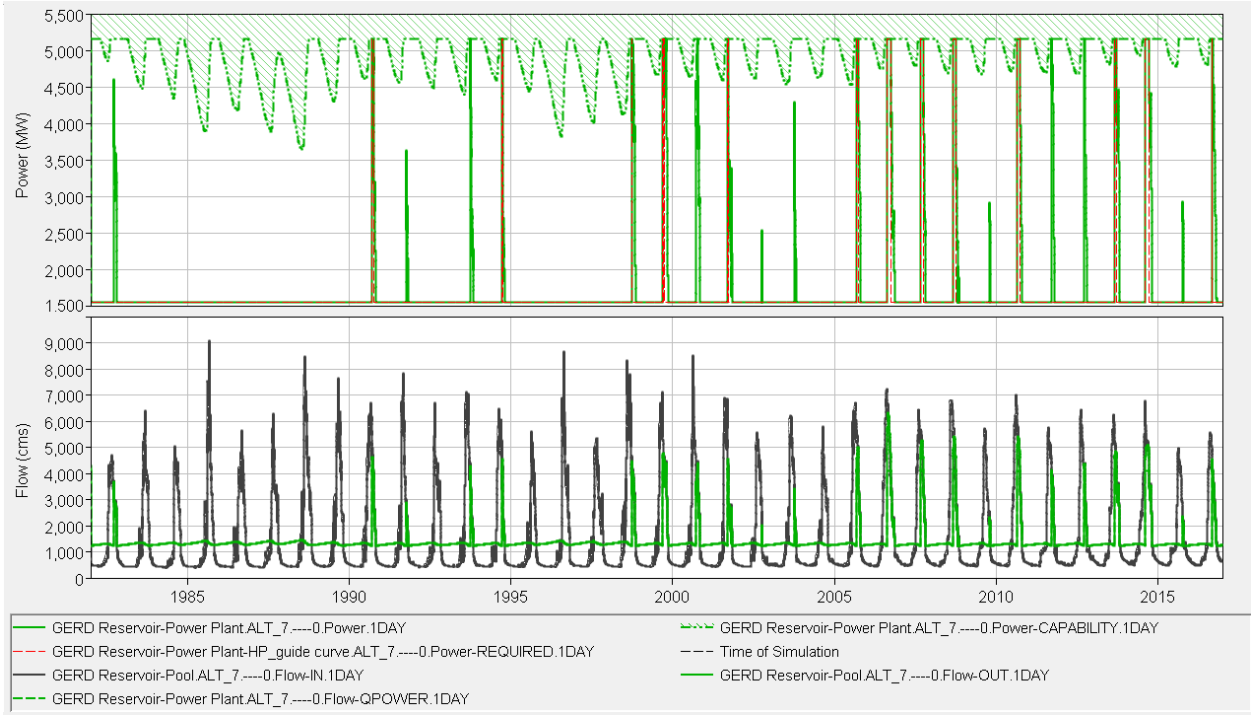

Figure E-24: GERD hydropower guide curve (scenario_1.4)

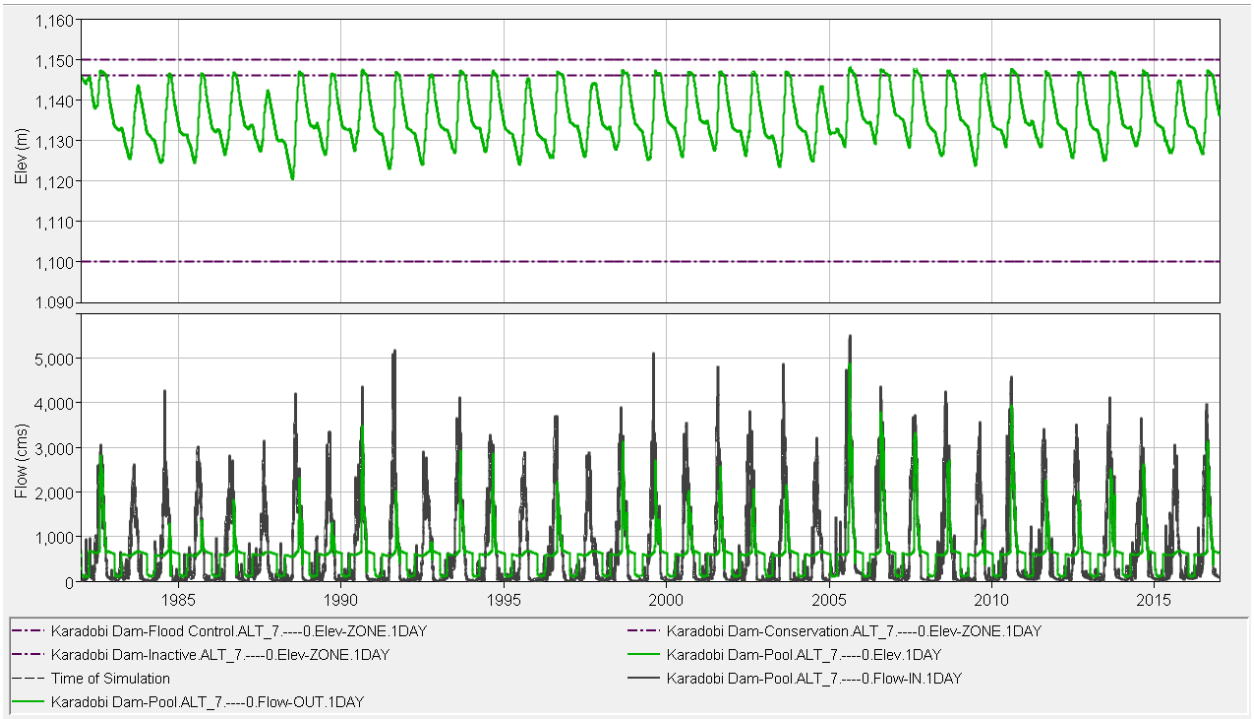

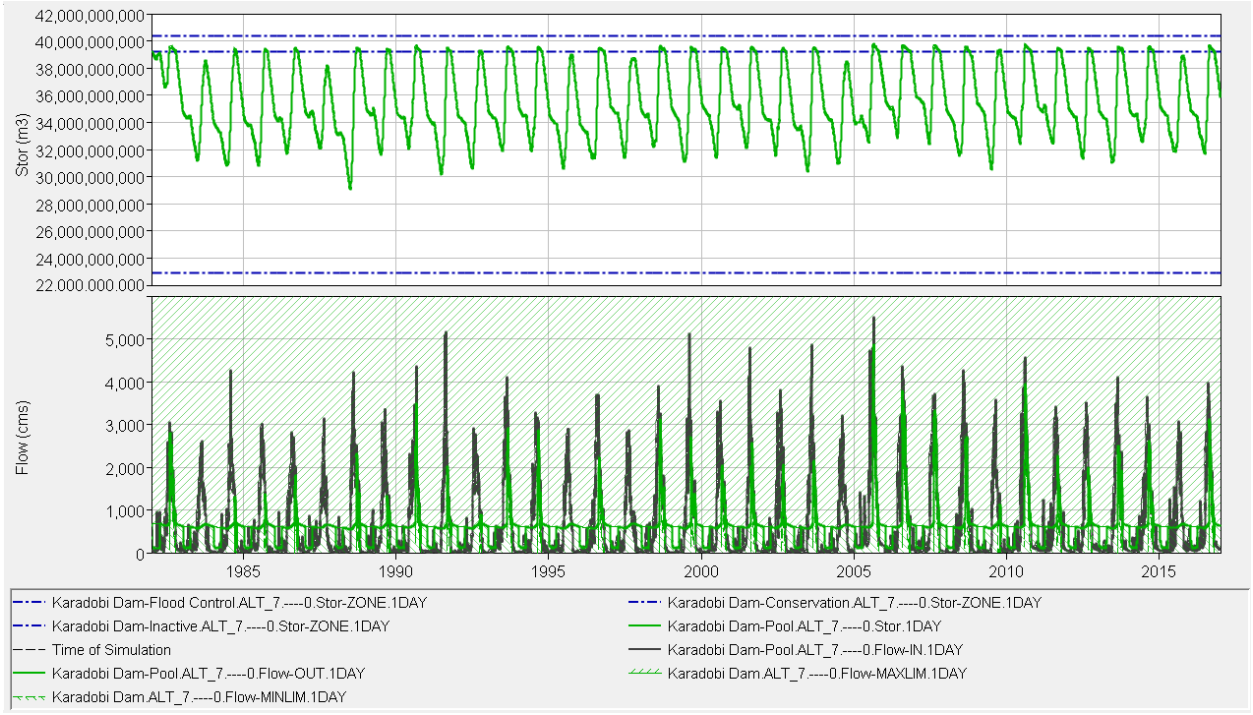

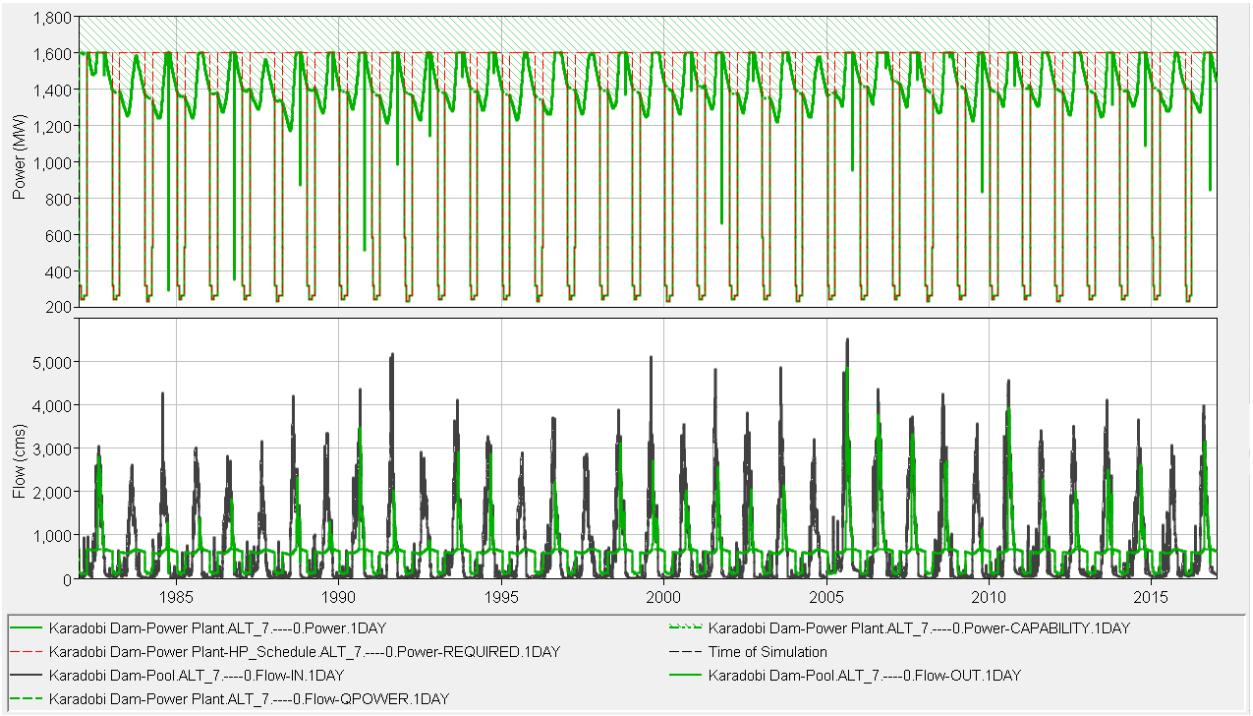

Figure E-25: Karadobi Hydropower schedule (scenario_1.4)

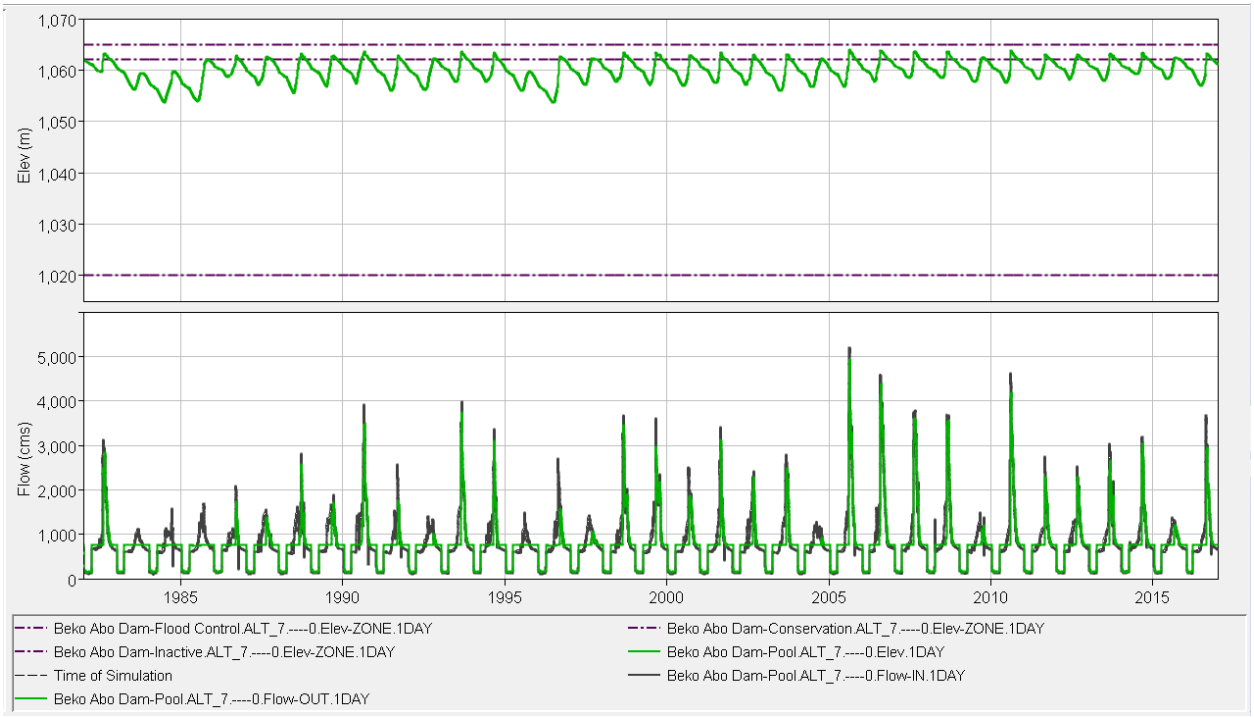
Elev (m)
1,070
1,060
1,050
1,040
1,030
1,020
Flow (cms)
5,000
4,000
3,000
2,000
1,000
0
1985
1990
1995
2000
2005
2010
2015
Beko Abo Dam-Flood Control.ALT_7.----0.Elev-ZONE.1DAY
Beko Abo Dam-Conservation.ALT_7.----0.Elev-ZONE.1DAY
Beko Abo Dam-Inactive.ALT_7.----0.Elev-ZONE.1DAY
Beko Abo Dam-Pool.ALT_7.----0.Elev.1DAY
Time of Simulation
Beko Abo Dam-Pool.ALT_7.----0.Flow-IN.1DAY
Beko Abo Dam-Pool.ALT_7.----0.Flow-OUT.1DAY

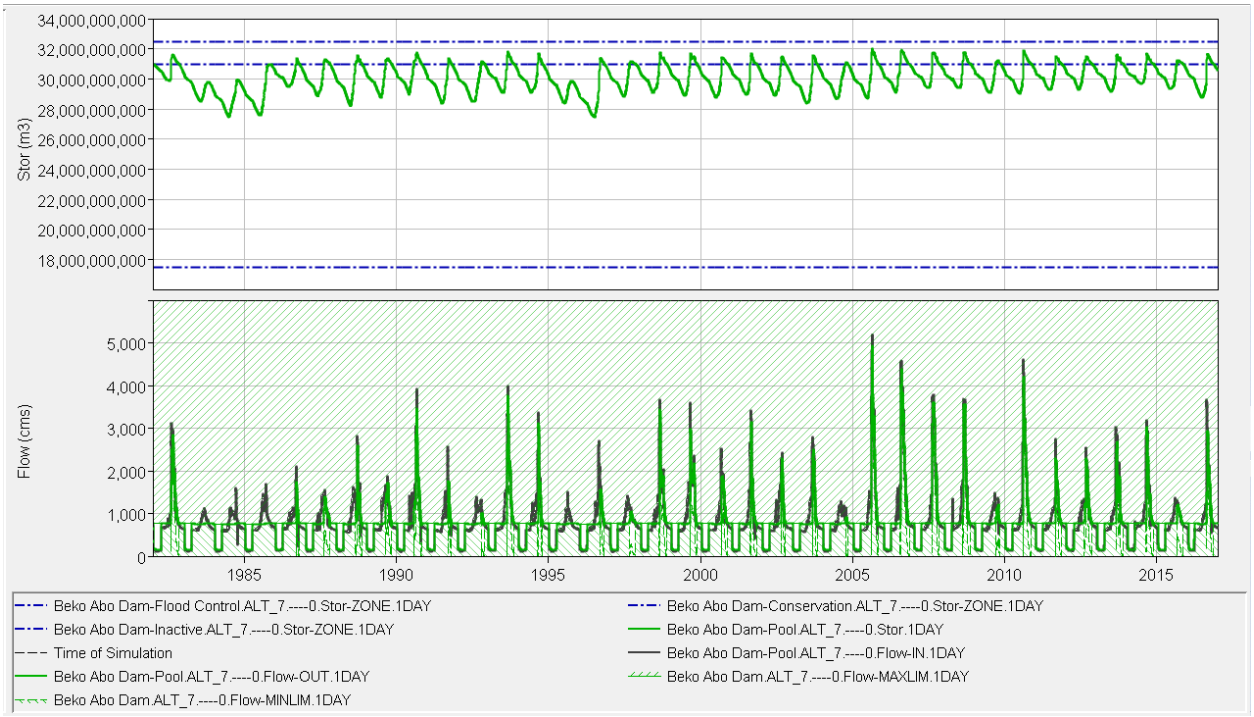
Stor (m3)
34,000,000,000
32,000,000,000
30,000,000,000
28,000,000,000
26,000,000,000
24,000,000,000
22,000,000,000
20,000,000,000
18,000,000,000
Flow (cms)
5,000
4,000
3,000
2,000
1,000
0
1985
1990
1995
2000
2005
2010
2015
Beko Abo Dam-Flood Control.ALT_7.----0.Stor-ZONE.1DAY
Beko Abo Dam-Conservation.ALT_7.----0.Stor-ZONE.1DAY
Beko Abo Dam-Inactive.ALT_7.----0.Stor-ZONE.1DAY
Beko Abo Dam-Pool.ALT_7.----0.Stor.1DAY
Time of Simulation
Beko Abo Dam-Pool.ALT_7.----0.Flow-IN.1DAY
Beko Abo Dam-Pool.ALT_7.----0.Flow-OUT.1DAY
Beko Abo Dam.ALT_7.----0.Flow-MAXLIM.1DAY
Beko Abo Dam.ALT_7.----0.Flow-MINLIM.1DAY

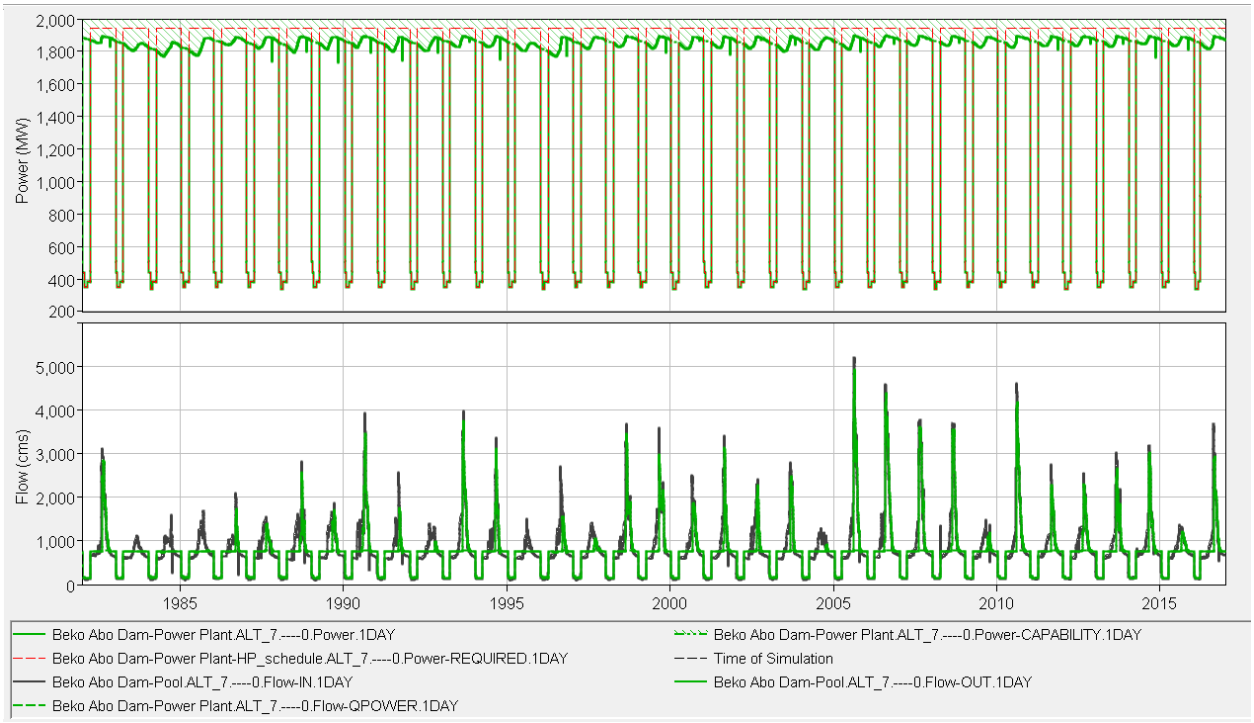

Figure E-26: Beko Abo Hydropower schedule (scenario_1.4)

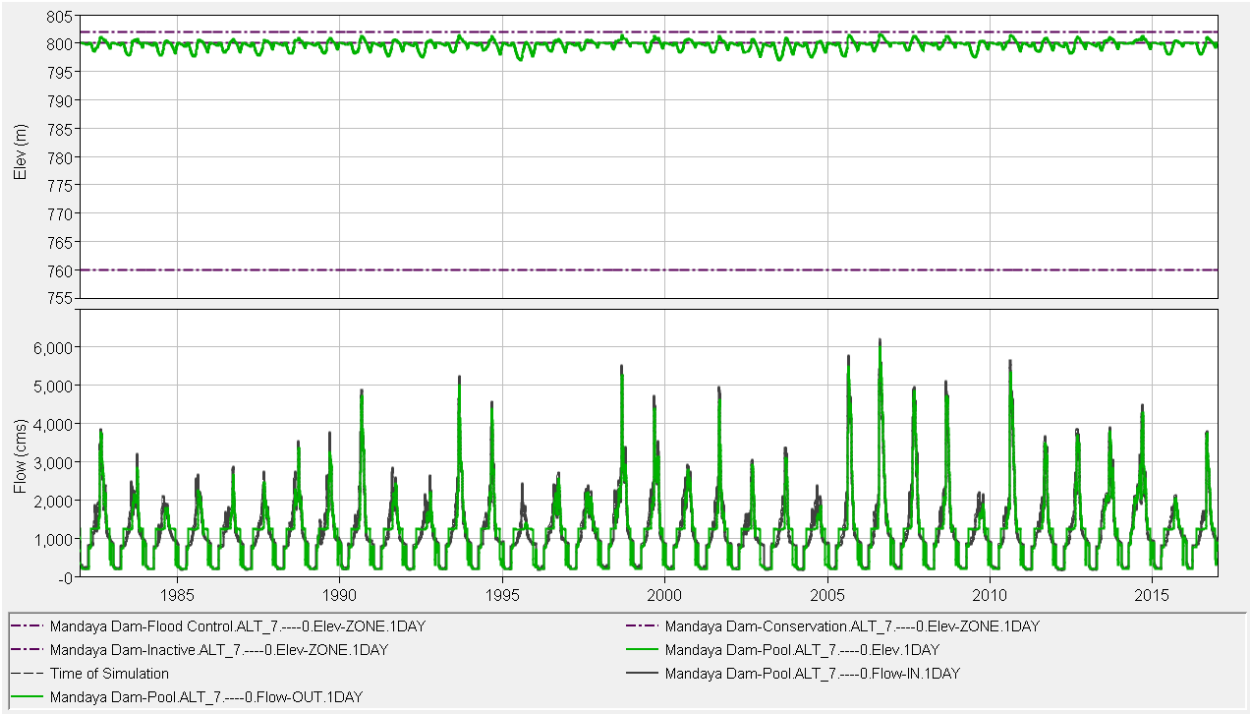

Figure E-27: Mandaya Hydropower schedule (scenario_1.4)

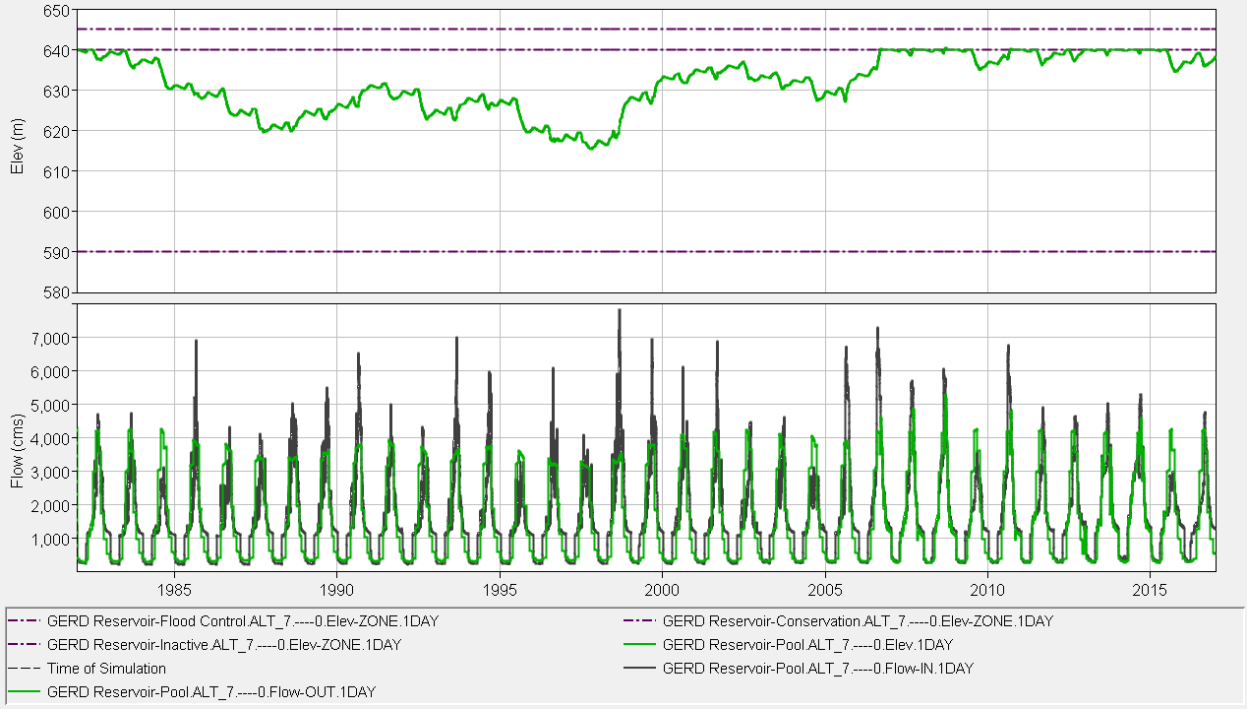
Elev (m)
650
640
630
620
610
600
590
580
Flow (cms)
7,000
6,000
5,000
4,000
3,000
2,000
1,000
1985
1990
1995
2000
2005
2010
2015
GERD Reservoir-Flood Control.ALT_7.----0.Elev-ZONE.1DAY
GERD Reservoir-Conservation.ALT_7.----0.Elev-ZONE.1DAY
GERD Reservoir-Inactive.ALT_7.----0.Elev-ZONE.1DAY
GERD Reservoir-Pool.ALT_7.----0.Elev.1DAY
Time of Simulation
GERD Reservoir-Pool.ALT_7.----0.Flow-IN.1DAY
GERD Reservoir-Pool.ALT_7.----0.Flow-OUT.1DAY

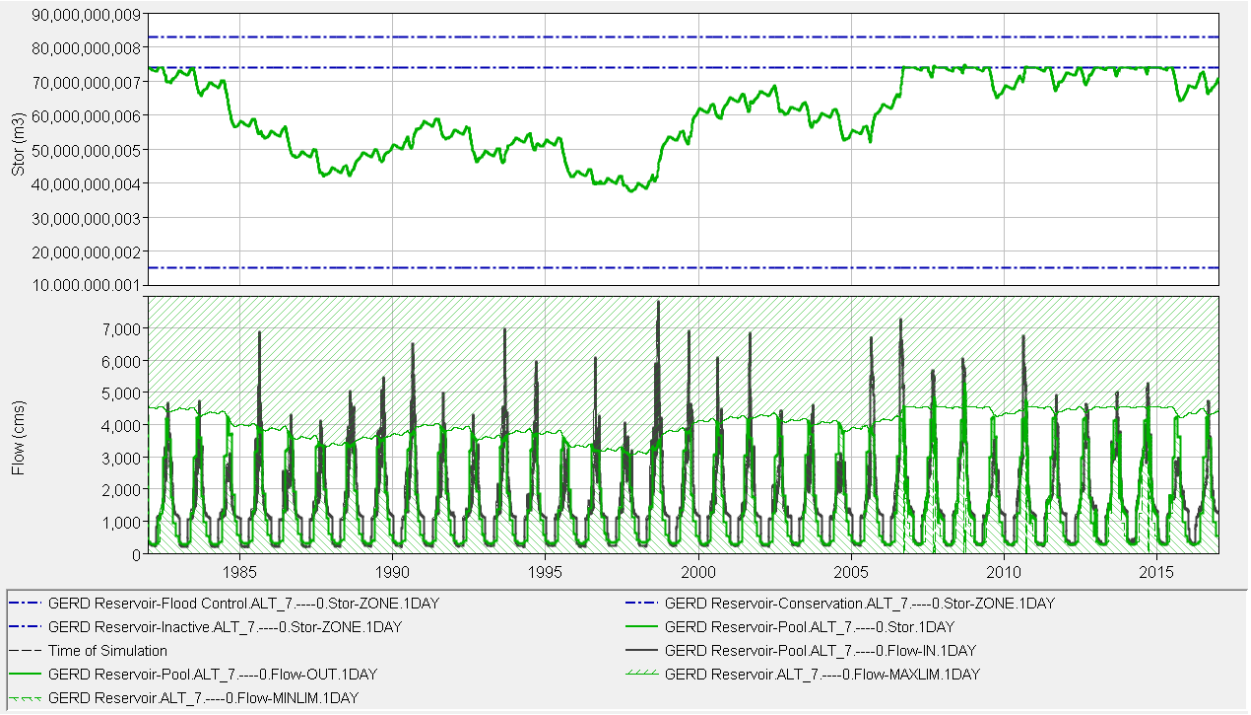
Stor (m3)
90,000,000,009
80,000,000,008
70,000,000,007
60,000,000,006
50,000,000,005
40,000,000,004
30,000,000,003
20,000,000,002
10.000.000.001
Flow (cms)
7,000
6,000
5,000
4,000
3,000
2,000
1,000
0
1985
1990
1995
2000
2005
2010
2015
GERD Reservoir-Flood Control.ALT_7.----0.Stor-ZONE.1DAY
GERD Reservoir-Conservation.ALT_7.----0.Stor-ZONE.1DAY
GERD Reservoir-Inactive.ALT_7.----0.Stor-ZONE.1DAY
GERD Reservoir-Pool.ALT_7.----0.Stor.1DAY
Time of Simulation
GERD Reservoir-Pool.ALT_7.----0.Flow-IN.1DAY
GERD Reservoir-Pool.ALT_7.----0.Flow-OUT.1DAY
GERD Reservoir.ALT_7.----0.Flow-MAXLIM.1DAY
GERD Reservoir.ALT_7.----0.Flow-MINLIM.1DAY

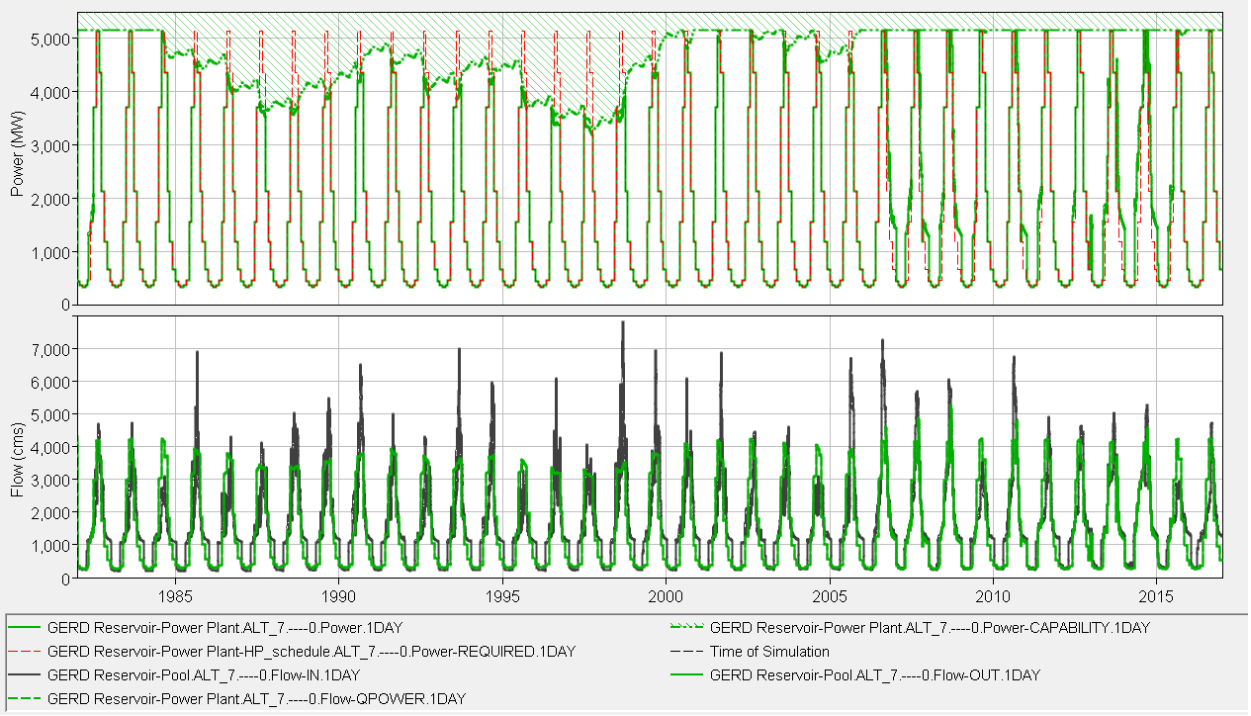

Figure E-28: GERD Hydropower schedule (scenario_1.4)